

STEREOCHEMISTRY AND ABSOLUTE CONFIGURATION

OF COMPLEXES OF

Co(III) AND Cr(III) WITH TRIDENTATE LIGANDS

by

Malcolm Stanley Bilton

A thesis submitted in partial  
fulfilment of the requirements  
for the degree of

Doctor of Philosophy

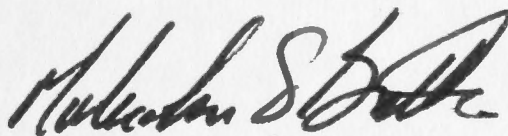
at

The Australian National University

Department of Chemistry  
School of General Studies  
November 1976



No part of the work described  
in this thesis has been  
submitted in support of  
an application for another  
degree. The work is the  
author's own except where  
otherwise stated.



Malcolm S. Bilton



## ACKNOWLEDGEMENTS

I should like to thank:

Drs N. Gill and M. Sterns for encouragement and many patient discussions throughout this work.

Mr T. Benson for providing the compounds which were the basis for the work.

Dr G. Robertson for diffractometer facilities at A.N.U.

Drs B. Anderson, D. Taylor and P. Whimp for help in using the ANUCRYS system of programs.

Mr G. McLaughlin who instructed me in the use of the Picker FACS-I diffractometer at A.N.U.

Dr B. Hoskins for laboratory, diffractometer and data processing facilities at Melbourne University.

The staff of the Univac U-1108 computer centre.

The technical staff of the chemistry department, S.G.S., in particular Mr B. Dowhy (Photography) and Mr B. Machan (Electronics).

This work was financed by an A.N.U. Scholarship for which I am sincerely grateful.

## ABSTRACT

The crystal structure of five complexes and the absolute configuration of four complexes has been determined.

The crystal and molecular structure of  $(+)_486\text{-S-}[\text{Co}(\text{sal}(\text{R})\text{pn}(2\text{-Me}))_2]\text{I}\cdot 3\text{H}_2\text{O}$  has been determined from diffractometer data by three-dimensional Patterson and Fourier methods and refined by block-diagonal least-squares to  $R = 0.102$  for a total of 621 independent reflections (487; 78.4% observed). The crystals are orthorhombic, space group  $\text{C}222_1$ , with  $a = 10.570(2)$ ,  $b = 16.052(3)$ ,  $c = 15.220(7)$  Å and  $Z = 4$ . Co and I atoms induce mmm pseudo-symmetry. The cobalt atom is octahedrally coordinated by two tridentate Schiff-base ligands in the meridional arrangement and the complex has S absolute configuration. Hydrogen bonding connects symmetry related cations along the ab cell diagonal.

The crystal and molecular structure of  $(+)_489\text{-S-}[\text{Co}(\text{sal}(\text{R})\text{pn}(1\text{-Me}))(\text{sal}(\text{R})\text{pn}(2\text{-Me}))]\text{ClO}_4\cdot 0.75\text{EtOH}$  has been determined from diffractometer data by three-dimensional Patterson and Fourier methods and refined by block-diagonal least-squares to  $R = 0.068$  for 2205 independent non-zero reflections. The crystals are monoclinic, space group  $\text{P}2_1$ , with  $a = 10.683(4)$ ,  $b = 7.672(3)$ ,  $c = 15.565(6)$  Å,  $\beta = 92.40(3)^\circ$  and  $Z = 2$ . The cobalt atom is octahedrally coordinated by two tridentate Schiff-base ligands in the meridional arrangement and the complex has S absolute configuration. The ligands differ only in the position of the methyl group in the (R)pn moieties. Disorder of the solvent molecule is present and an occupancy of 0.75 is suggested.

The crystal and molecular structure of  $\text{Co}(\text{sal en})_2\text{I}\cdot \text{H}_2\text{O}$  has been determined from diffractometer data by three-dimensional Patterson and Fourier methods and refined by block-diagonal least-squares to



$R = 0.098$  for a total of 4493 independent reflections (2850; 63.5% observed). The crystals are monoclinic, space group  $P2_1/c$ , with  $a = 18.368(1)$ ,  $b = 10.216(1)$ ,  $c = 12.004(1)$  Å,  $\beta = 109.87(2)^\circ$  and  $Z = 4$ . The cobalt atom is octahedrally coordinated by two tridentate Schiff-base ligands in the meridional arrangement. The complex is analogous to  $\text{Cr}(\text{sal en})_2\text{I}$  differing only in the geometry of the metal environment.

The crystal and molecular structure of  $(-)_409\text{-R,S-}[\text{Cr}(\text{sal}(\text{R})\text{pn}(2\text{-Me}))_2]\text{ClO}_4$  was determined from diffractometer data by three-dimensional Patterson and Fourier methods and refined by block-diagonal least-squares to  $R = 0.044$  for 4466 independent non-zero reflections. The crystals are triclinic, with  $a = 8.626(1)$ ,  $b = 12.729(2)$ ,  $c = 12.580(2)$  Å,  $\alpha = 113.01(3)$ ,  $\beta = 105.16(3)$ ,  $\gamma = 103.15(3)^\circ$  and  $Z = 2$ . The complex is a pseudo-racemate in which the chromium atoms are each octahedrally coordinated by two tridentate Schiff-base ligands in a meridional arrangement.

The crystal and molecular structure of  $(+)_366\text{-S-}[\text{Cr}(\text{sal en})_2]\text{bz}_2\text{-(R,R)-Htart,}3\text{H}_2\text{O}$  has been determined from diffractometer data by the tangent formula and three-dimensional Fourier methods and refined by block-diagonal least-squares to  $R = 0.038$  for 4735 independent non-zero reflections. The crystals are monoclinic, space group  $P2_1$ , with  $a = 15.552(1)$ ,  $b = 7.791(1)$ ,  $c = 17.445(1)$  Å,  $\beta = 109.30(1)^\circ$  and  $Z = 2$ . The chromium atom is octahedrally coordinated by two tridentate Schiff-base ligands in the meridional arrangement and the complex has S absolute configuration. Extensive hydrogen bonding is present.

Bond angles and bond lengths for the five structures are compared and features which are characteristic of the tridentate ligands are



discussed. The conformations of the chelate rings are discussed and compared with previously reported data. Distortions of donor atoms from ideal octahedral arrangement are noted. The geometry of each complex is found to be very dependent upon non-bonded interactions. The C.D. of the solid complexes in KBr discs is found to be similar to that reported for the complexes in ethanolic solution.

The  $\text{Cr}(\text{sal}(\text{R})\text{pn})_2\text{ClO}_4$  system has been investigated by column chromatography and a method for the resolution of  $\text{R,S-}[\text{Cr}(\text{sal}(\text{R})\text{pn}(\text{2-Me}))_2]\text{ClO}_4$  is proposed.

(R)pn

py

sal

sal(R)pn

sal(R)pn(1-Me)

sal(R)pn(2-Me)

sal

sal(R)pn

57.5 M

5-pro

trien

\* Note onomenclature:

Traditional names are used for ligands in order to be consistent with existing literature. The I.U.P.A.C. system of nomenclature of the trifluoromethane ligands, sal and sal(R)pn, requires that these be named as substituted phenols.

## ABBREVIATIONS

$\text{\AA}$	angstrom; ( $10^{-10}\text{m}$ )
B.D.L.S.	block-diagonal least-squares
$\text{bz}_2\text{-(R,R)-Htart}$	hydrogen-0-dibenzoyl-(R,R)-tartrate
C.D.	circular dichroism
C.M.C.	carboxymethyl cellulose chromatography
en	ethylenediamine
Et	ethyl
Me	methyl
O.R.D.	optical rotatory dispersion
pn	racemic 1,2-diaminopropane
(R)pn	(-) $_{589}$ -1,2-diaminopropane
py	pyridine
sal en	N-(2-aminoethyl)salicylaldiminate ion; * 2-(aminoethyliminomethyl)phenol
sal (R)pn	N-aminopropylsalicylaldiminate ion; * 2-(R-aminopropyliminomethyl)phenol
sal (R)pn(1-Me)	R-N-[(2-amino-1-methyl)ethyl]salicylaldiminate ion; * 2-(amino-2-R-methyl-ethyliminomethyl)phenol
sal (R)pn(2-Me)	R-N-(2-aminopropyl)salicylaldiminate ion; * 2-(R-2-amino-propyliminomethyl)phenol
salen	N,N'-bis(salicylidene)ethylenediamine; * bis-2-(methyleneiminomethylphenol)
sal(R)pn	R-N,N'-bis(salicylidene)propylenediamine; * bis-2-(R-aminopropyliminomethylphenol)
SP.S.C.	SP-Sephadex C-25 chromatography
S-pro	S-prolinate ion
trien	triethylenetetramine

\* Note on nomenclature:

Traditional names are used for ligands in order to be consistent with existing literature. The I.U.P.A.C. system of nomenclature of the tridentate ligands, sal en and sal (R)pn, requires that these be named as substituted phenols.

## CONTENTS

	Page
CHAPTER 1	
INTRODUCTION	1
1.1 PERSPECTIVE	1
1.2 STEREOCHEMISTRY AND NOMENCLATURE	3
1.3 DETERMINATION OF ABSOLUTE CONFIGURATION	6
1.3.1 Friedel's law and anomalous scattering	7
1.3.1.a The "Bijvoet" technique	8
1.3.1.b The "lowest R-factor" technique	9
1.4 THE COMPLEXES STUDIED IN THIS WORK	9
1.4.1 The sal en system	9
1.4.2 The sal (R)pn system	13
CHAPTER 2	
CRYSTAL AND MOLECULAR STRUCTURE OF (+) <sub>486</sub> -S-BIS-[R-N-(2-AMINO(R)PROPYL)SALICYLALDIMINATO - COBALT(III)] IODIDE, TRI-HYDRATE	15
2.1 UNIT CELL AND DIFFRACTION SYMMETRY	15
2.2 DATA COLLECTION AND REDUCTION	16
2.2.1 Unit cell refinement	16
2.2.2 Data collection	17
2.2.3 Data reduction	19
2.3 DETERMINATION OF THE POSITIONS OF IODINE AND COBALT ATOMS	21
2.4 DETERMINATION OF LIGHT ATOM POSITIONS	25
2.5 DETERMINATION OF A WEIGHTING SCHEME FOR B.D.L.S. REFINEMENT	27
2.6 LEAST-SQUARES REFINEMENT	29
2.7 DETERMINATION OF THE ABSOLUTE CONFIGURATION	34
2.8 DESCRIPTION OF THE STRUCTURE	34
CHAPTER 3	
CRYSTAL AND MOLECULAR STRUCTURE OF (+) <sub>489</sub> -S-[(R-N-(2-AMINOPROPYL)SALICYLALDIMINATO)- (R-N-((2-AMINO-1-METHYL)ETHYL)SALICYLALDIMINATO) COBALT(III)] PERCHLORATE, 0.75 ETHANOL	44
3.1 UNIT CELL AND DIFFRACTION SYMMETRY	44



	Page
3.2 DATA COLLECTION AND REDUCTION	45
3.2.1 Unit cell refinement	45
3.2.2 Data collection	45
3.2.3 Data reduction	47
3.3 DETERMINATION OF COBALT AND CHLORINE ATOM POSITIONS	48
3.4 DETERMINATION OF LIGHT ATOM POSITIONS	50
3.5 ABSORPTION CORRECTION AND LEAST-SQUARES REFINEMENT	54
3.5.1 Absorption correction and isotropic refinement	54
3.5.2 Initial anisotropic refinement and calculation of hydrogen atom positions	55
3.5.3 Re-examination of composition and final anisotropic refinement	55
3.6 DETERMINATION OF THE ABSOLUTE CONFIGURATION	60
3.7 DESCRIPTION OF THE STRUCTURE	60
CHAPTER 4	
CRYSTAL AND MOLECULAR STRUCTURE OF BIS-(N-(2-AMINOETHYL)SALICYLALDIMINATO)COBALT(III) IODIDE, MONOHYDRATE	74
4.1 UNIT CELL AND DIFFRACTION SYMMETRY	74
4.2 DATA COLLECTION AND REDUCTION	75
4.2.1 Refinement of unit cell dimensions	75
4.2.2 Data collection and reduction	75
4.3 DETERMINATION OF THE POSITIONS OF IODINE AND COBALT ATOMS	76
4.4 DETERMINATION OF LIGHT ATOM POSITIONS	81
4.5 LEAST-SQUARES REFINEMENT	83
4.5.1 Weighting scheme analysis	83
4.5.2 Isotropic refinement and absorption correction	83
4.5.3 Anisotropic refinement	85
4.6 DESCRIPTION OF THE STRUCTURE	86
CHAPTER 5	
CRYSTAL AND MOLECULAR STRUCTURE OF (-) <sub>409</sub> -R,S-[(R-N(2-AMINOPROPYL)SALICYLALDIMINATO) CHROMIUM(III)]PERCHLORATE	99
5.1 UNIT CELL AND DIFFRACTION SYMMETRY	99
5.2 DATA COLLECTION AND REDUCTION	100
5.2.1 Unit cell refinement	100

	Page
5.2.2 Data collection and reduction	101
5.3 DETERMINATION OF CHROMIUM ATOM POSITIONS	102
5.4 DETERMINATION OF LIGHT ATOM POSITIONS	104
5.5 LEAST-SQUARES REFINEMENT AND ABSORPTION CORRECTION	108
5.5.1 Initial least-squares refinement	108
5.5.2 Absorption correction and final anisotropic refinement	109
5.6 DETERMINATION OF THE ABSOLUTE CONFIGURATION	110
5.7 DESCRIPTION OF THE STRUCTURE	115
CHAPTER 6	
CRYSTAL AND MOLECULAR STRUCTURE OF (+) <sub>366</sub> S- [BIS(N-(2-AMINOETHYL)SALICYLALDIMINATO) CHROMIUM(III)]HYDROGEN-O-DIBENZOYL-(R,R)-TARTRATE TRIHYDRATE	132
6.1 UNIT CELL AND DIFFRACTION SYMMETRY	132
6.2 DATA COLLECTION AND REDUCTION	133
6.2.1 Refinement of unit cell dimensions	133
6.2.2 Data collection and reduction	134
6.3 INITIAL ANALYSIS BY DIRECT METHODS	134
6.4 DIFFERENCE FOURIER ANALYSIS	142
6.5 LEAST-SQUARES REFINEMENT AND DETERMINATION OF THE ABSOLUTE CONFIGURATION	145
6.5.1 Isotropic refinement and determination of absolute configuration	145
6.5.2 Absorption correction and anisotropic refinement	146
6.6 DESCRIPTION OF THE STRUCTURE	152
CHAPTER 7	
THE STRUCTURAL AND CONFORMATIONAL ASPECTS OF COMPLEXES OF COBALT(III) AND CHROMIUM(III) WITH TRIDENTATE SCHIFF-BASE LIGANDS	169
7.1 STATISTICAL PARAMETERS	169
7.2 BOND LENGTHS AND ANGLES	170
7.2.1 Bond lengths and bond angles of the ligands	172
7.2.2 Metal-ligand bond lengths and angles	182
7.3 ANALYSIS OF ASYMMETRY IN THE COMPLEXES	182
7.3.1 Absolute configuration	183
7.3.2 Conformation of the ligands	184



	Page
7.3.2.a Five-membered chelate rings	184
7.3.2.b Six-membered chelate rings	190
7.3.2.c The overall conformation of the ligands	194
7.3.3 Distortions of the donor atoms	196
7.4 THE CIRCULAR DICHROISM OF THE CRYSTALLINE COMPLEXES	197
7.5 CONCLUSION	199
CHAPTER 8	
SEPARATION OF THE ISOMERS OF BIS-(N-AMINO(R)PROPYLSALICYLALDIMINATO)CHROMIUM(III)	200
8.1 PREPARATION OF $\text{Cr}(\text{sal}(\text{R})\text{pn})_2\text{ClO}_4$	200
8.2 COLUMN CHROMATOGRAPHY OF $\text{R,S-}[\text{Cr}(\text{sal}(\text{R})\text{pn})_2]\text{ClO}_4$	200
8.2.1 Carboxymethyl cellulose chromatography	200
8.2.2 SP-Sephadex C-25 chromatography	203
8.3 CONCLUSIONS	208
APPENDIX A	
STRUCTURE FACTORS FOR $\text{S-}[\text{Co}(\text{sal}(\text{R})\text{pn}(2\text{-Me}))]\text{I}, 3\text{H}_2\text{O}$	210
APPENDIX B	
STRUCTURE FACTORS FOR $\text{S-}[\text{Co}(\text{sal}(\text{R})\text{pn}(1\text{-Me}))(\text{sal}(\text{R})\text{pn}(2\text{-Me}))]\text{ClO}_4,$ $0.75\text{EtOH}$	212
APPENDIX C	
STRUCTURE FACTORS FOR $\text{Co}(\text{sal en})_2\text{I}, \text{H}_2\text{O}$	215
APPENDIX D	
STRUCTURE FACTORS FOR $\text{R,S-}[\text{Cr}(\text{sal}(\text{R})\text{pn}(2\text{-Me}))_2]\text{ClO}_4$	219
APPENDIX E	
STRUCTURE FACTORS FOR $\text{S-}[\text{Cr}(\text{sal en})_2]\text{bz}_2\text{-(R,R)-Htart}, 3\text{H}_2\text{O}$	224
REFERENCES	228



## CHAPTER 1

## INTRODUCTION

## 1.1 PERSPECTIVE

In recent years increasing emphasis has been placed on studies which involve the conformational aspects of chelate rings and absolute configuration in relation to the O.R.D. and C.D. of transition metal complexes (Ciardelli & Salvadori, 1973). Sector rules and molecular orbital models which would allow the prediction of absolute configuration from the Cotton effect associated with d-d transitions, have been sought for some time (Hawkins & Larsen, 1965; Mason, 1971; Bosnich & Harrowfield, 1972; Richardson, 1972; Gillard, 1971; Strickland & Richardson, 1973: (and references therein)).

Optical activity may be regarded as a second-order effect, which is extremely sensitive to the details of asymmetry in metal complexes. Unfortunately, in the absence of a detailed structure analysis, the fact that the precise nature of the asymmetry is unknown prevents any real application of the proposed rules and theories to such systems. Indeed, the importance of accurate structural data has been emphasised by Saito (1974), who also points out the need for more extensive work on the absolute configuration of complexes of metals other than cobalt.

A large amount of work has been devoted to the study of metal complexes of Schiff-bases. Structural studies have involved mainly bidentate ligands, such as salicylaldimines (Lingafelter & Braun, 1966), and tetradentate ligands, such as N,N'-bis-(salicylidene)ethylenediamines (Calligaris, Nardin & Randaccio, 1972), of bivalent metals. In recent

publications (Dey & Ray, 1974; Finney & Everett, 1974; Benson, 1976; O'Connor & West, 1968) several trivalent metal complexes have been reported and earlier work has been the subject of several reviews (Holm, Everett & Chakrovorty, 1966; Yamada, 1966; Sacconi, 1966; West, 1968; Calligaris, Nardin & Randaccio, 1972; Hobday & Smith, 1972; Dey, 1974; Lingafelter & Braun, 1966).

The only structural study on a bis-tridentate Schiff-base complex of a trivalent metal,  $\text{Cr}(\text{sal en})_2\text{I}$ , is due to Gardner, Gatehouse and White (1971). Earlier work involved N-substituted tridentate ligands, usually complexed to bivalent metals (Kistenmacher, Szalda & Marzilli, 1974; Mangia, Nardelli, Pelizzi & Plelizzi, 1973; Chieh & Palenik, 1972; Orioli, Vaira & Sacconi, 1966; Vaira & Orioli, 1967). Recently, the first x-ray structure analysis of a tridentate sulphur-Schiff-base complex, bis(2-aminoethylthiosalicylideneiminato)iron(III) chloride, has been determined (Fallon & Gatehouse, 1975).

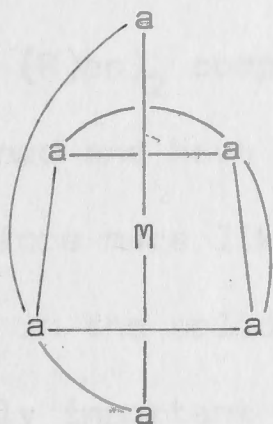
Benson (1976) has reported the resolution of N-(2-aminoethyl) salicylaldiminato derivatives of chromium(III) and cobalt(III), together with the synthesis of a series of analogous chromium(III) and cobalt(III) complexes of the tridentate Schiff-bases containing a (R)-propanediamine moiety. These complexes are the subject of this study.

The object of the present work is the determination of the absolute configuration and confirmation of the structures postulated by Benson (1976). And also to provide detailed information for, and to explore the possibility of finding the general geometrical features of, some bis-tridentate Schiff-base complexes. It is hoped that the theorist will use such data in his endeavours to predict the C.D. and preferred structure of these and analogous complexes.

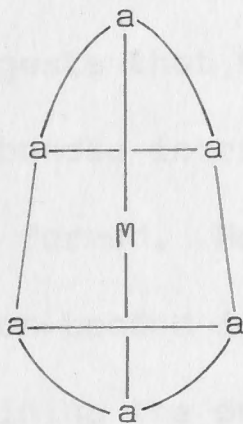


## 1.2 STEREOCHEMISTRY AND NOMENCLATURE

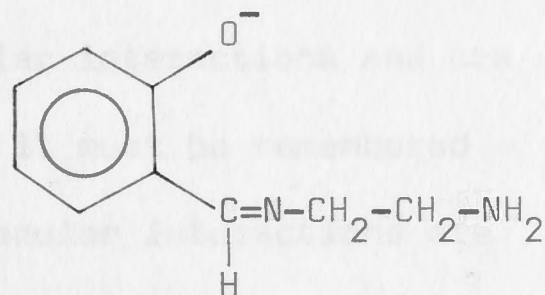
In octahedral complexes, tridentate ligands can adopt either meridional, (1), or facial, (2), arrangements. With the tridentate



(1)



(2)



(3)

ligands sal en, (3), and sal (R)pn, which contain a central imine linkage, a meridional distribution of the donor atoms involves a lower strain energy than the facial arrangement. In agreement with this the meridional arrangement is found in the majority of complexes containing tridentate ligands of this type (Black & Hartshorn, 1972). However, octahedral Ni(II) N-substituted aminopropylsalicylaldiminates with facial ligands have been synthesised (Sacconi, Nardin & Zanobini, 1966). The crystal structures of bis-N- $\gamma$ -dimethylaminopropylsalicylaldiminato Ni(II) (Vaira & Orioli, 1967) and bis-N- $\beta$ -dimethylaminoethylsalicylaldiminato Cu(II) (pseudo trigonal bipyramidal, Chieh & Palenik, 1972) have been reported and the ligands were found to be in the non-planar arrangement.

The quadridentate ligand, salen, is also generally bonded in a planar arrangement about the metal ion (Calligaris, Nardin & Randaccio, 1972). However, a non-planar arrangement of this ligand has been proposed in several cases (Cozens & Murray, 1972) and has been confirmed for two complexes (Bailey, Higson & McKenzie, 1972; Calligaris, Manzini, Nardin & Randaccio, 1972). In these compounds a bidentate ligand is also bonded to the metal ion and thus the quadridentate is forced to take up the non-planar arrangement.



A total of six geometrical isomers are possible for octahedral complexes containing two unsymmetrical tridentate ligands if both meridional and facial configurations are allowed. Five of these have optical isomers. Examination of space-filling models of  $M(\text{sal en})_2$  and  $M(\text{sal (R)pn})_2$  complexes suggests that the meridional isomers are less strained and have less non-bonded intramolecular interactions and are therefore more likely to be formed. However, it must be remembered that, in the solid state, non-bonded intermolecular interactions are equally important in determining the overall energy of a particular isomer and, considering the ideal geometry given to space-filling models, the facial arrangement must not be dismissed out of hand.

Flexibility in sal en and sal (R)pn ligands exists in the diamine moiety, where two skew conformations are possible,  $\lambda$  and  $\delta$  (Figure 1.1).

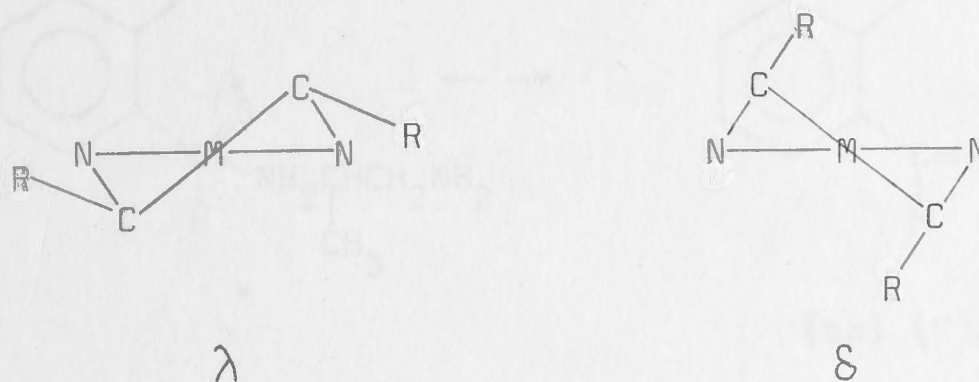
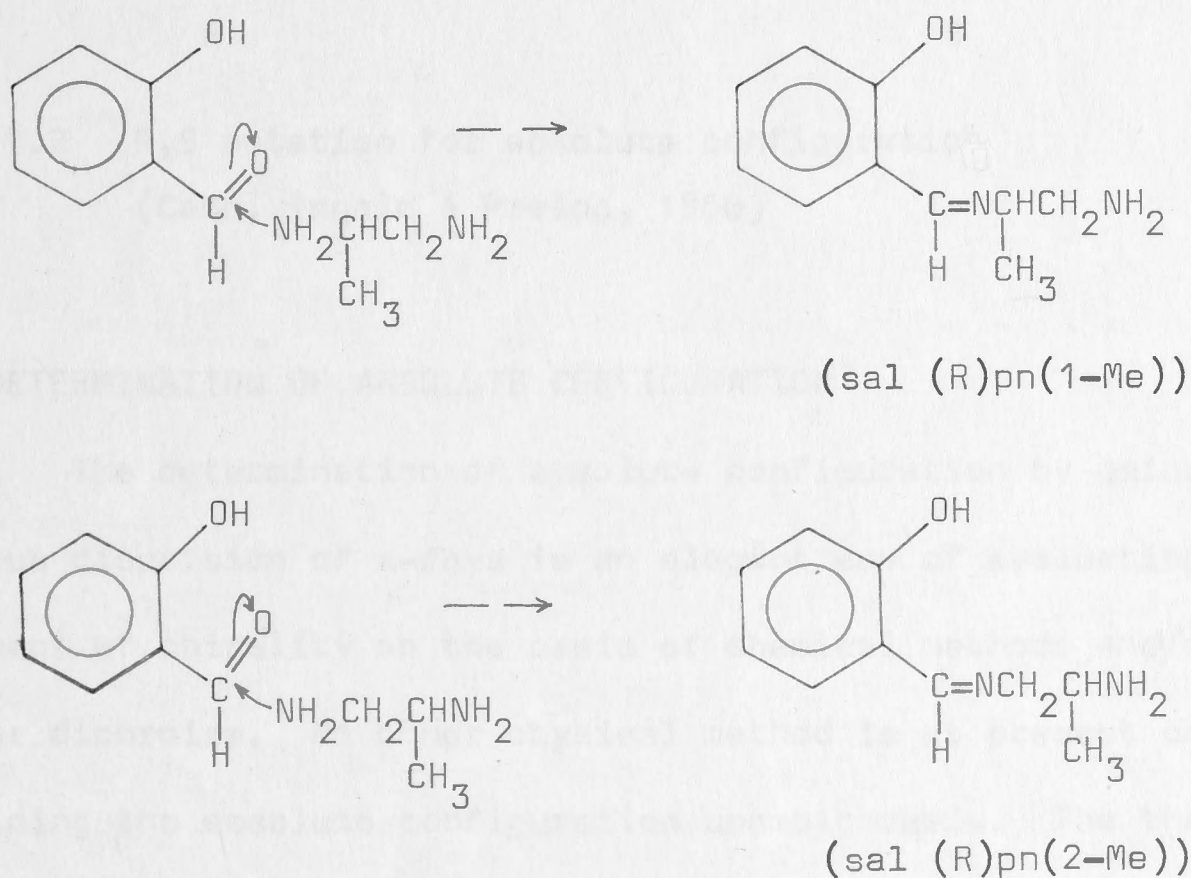


Figure 1.1 Nomenclature for the conformation of five-membered chelate rings

For sal en, the conformations  $\lambda$  and  $\delta$  are equally likely given that non-bonded interactions are of minor importance. However, for sal (R)pn ligands stereospecificity arises from the conformational requirements of the methyl group. Corey & Bailar (1959) have calculated the energy difference between the two conformations to be  $\sim 2 \text{ k cal mol}^{-1}$  in favour of  $\lambda$ , in which the methyl group is equatorial to the chelate ring. However, from theoretical calculations on the trans-diamine

complexes  $\text{Co(R)pn}_2\text{Cl}_2$  and  $\text{Co(R)pn}_2(\text{NH}_3)_2$  (Gollogly & Hawkins, 1969) it has been concluded that (a) the conformations of the rings with the methyl group equatorial ( $\lambda$ ) and axial ( $\delta$ ) are not enantiomeric, and (b) the difference in energy between the equatorial and axial conformations is between 0 and 3 kcal mol<sup>-1</sup>, in favour of the equatorial conformation, depending upon the model used for non-bonded interactions. In fact, only the  $\lambda$  conformation has been found in the metal complexes studied to date (Saito, 1974) with the exception of malononitrilato ( $\text{sal(R)pn}$ ), Py Co(III) which has been found to be disordered over the  $\lambda$  and  $\delta$  configurations (Bailey, Higson & McKenzie, 1975).

Two geometrical isomers, which differ only with respect to the position of the methyl group, are possible for the  $\text{sal(R)pn}$  ligand. This may be represented by the following:



(The above scheme is not meant to imply a mechanism or indicate that the ligands are isolable). Under equilibrium conditions both modes of condensation would be likely to occur since large differences in steric interactions would not be anticipated (Benson, 1976). Hence, three isomers are possible for each of the six geometrical isomers



noted above. Theoretically, 30 optical isomers are possible for the Co(III) and Cr(III) sal (R)pn complexes with respect to the metal.

Many schemes have been proposed for the nomenclature of the absolute configuration of metal complexes (Hawkins, 1971). To describe the absolute configuration of the complexes reported here, which have unsymmetric tridentate ligands, it is necessary to use the R,S notation of Cahn, Ingold and Prelog (1966) (Figure 1.2). This notation is used throughout this work.

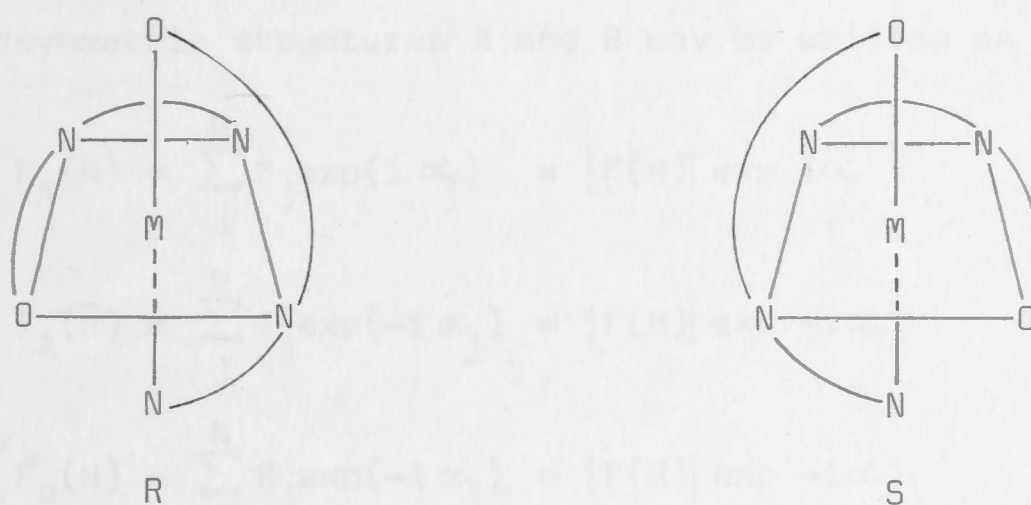


Figure 1.2 R,S notation for absolute configuration  
(Cahn, Ingold & Prelog, 1966)

### 1.3 DETERMINATION OF ABSOLUTE CONFIGURATION

The determination of absolute configuration by using the anomalous dispersion of x-rays is an elegant way of evaluating the assignment of chirality on the basis of chemical methods and/or circular dichroism. No other physical method is at present capable of determining the absolute configuration unambiguously. The theory of the method has been reviewed by several workers (Saito, 1974; Hawkins, 1971; Ramaseshan, 1964; Ramachandran & Srinivasan, 1970). However, for the sake of completeness, a brief outline of the theory is given below.

Peerdeman, van Bommel and Bijvoet (1951) were the first to

determine the absolute configuration of a metal complex by means of anomalous scattering of x-rays.

### 1.3.1 Friedel's law and anomalous scattering

If two structures A and B are enantiomers and if

$$A = (x_j, y_j, z_j) \quad ; \quad j = 1, \dots, N$$

then

$$B = (\bar{x}_j, \bar{y}_j, \bar{z}_j) \quad ; \quad j = 1, \dots, N.$$

For normal scattering, the structure factors for the non-centrosymmetric structures A and B may be written as

$$F_A(H) = \sum_j^N f_j \exp(i\alpha_j) = |F(H)| \exp i\alpha$$

$$F_A(\bar{H}) = \sum_j^N f_j \exp(-i\alpha_j) = |F(H)| \exp -i\alpha$$

$$F_B(H) = \sum_j^N f_j \exp(-i\alpha_j) = |F(H)| \exp -i\alpha$$

$$F_B(\bar{H}) = \sum_j^N f_j \exp(i\alpha_j) = |F(H)| \exp i\alpha$$

where  $\alpha_j = 2\pi(hx_j + ky_j + lz_j)$ .

Hence for normal scattering of x-rays

$$|F_A(H)| = |F_B(H)| = |F_A(\bar{H})| = |F_B(\bar{H})|$$

$$\alpha_A(H) = -\alpha_B(H) = -\alpha_A(\bar{H}) = \alpha_B(\bar{H})$$

$$\text{and} \quad I_A(H) = I_A(\bar{H}) = I_B(\bar{H}) = I_B(H).$$

This equality is known as Friedel's law, the implication of which is that when normal scattering occurs it is impossible to distinguish between  $I(\bar{H})_{\text{obs}}$  and  $I(H)_{\text{obs}}$  and hence between the enantiomers A and B.

However, if the structure contains two or more types of atom of which one or more show anomalous dispersion of the incident x-rays,



distinction between enantiomers A and B becomes possible. The anomalous scattering factors are represented by

$$f_j^{\text{anom}} = f_j + \Delta f'_j + i\Delta f''_j = f'_j + i\Delta f''_j$$

where  $\Delta f'$  and  $\Delta f''$  are small correction factors. The imaginary part,  $i\Delta f''$ , is always positive and  $\pi/2$  ahead of the real part,  $f'$ . This advance in phase is independent of the direction of the incident radiation and the position of the atoms in the structure.

When anomalous scattering occurs, say for atom m, the structure factors for structures A and B are given by

$$F_A(H) = \sum_j^N f_j \exp(i\alpha_j) + \Delta f'_m \exp(i\alpha_m) + \Delta f''_m \exp(i(\frac{\pi}{2} + \alpha_m))$$

$$F_A(\bar{H}) = \sum_j^N f_j \exp(-i\alpha_j) + \Delta f'_m \exp(-i\alpha_m) + \Delta f''_m \exp(i(\frac{\pi}{2} - \alpha_m))$$

$$F_B(H) = \sum_j^N f_j \exp(-i\alpha_j) + \Delta f'_m \exp(-i\alpha_m) + \Delta f''_m \exp(i(\frac{\pi}{2} - \alpha_m))$$

$$F_B(\bar{H}) = \sum_j^N f_j \exp(i\alpha_j) + \Delta f'_m \exp(i\alpha_m) + \Delta f''_m \exp(i(\frac{\pi}{2} + \alpha_m)).$$

Consequently

$$I_A(H) \gg I_A(\bar{H}) \text{ and } I_B(H) \ll I_B(\bar{H}).$$

Thus, when anomalous scattering is present, Friedel's law no longer holds and the inequality relations observed in one structure are the reverse of those found for the enantiomer. This is the basis of the determination of absolute configuration by anomalous scattering of x-rays.

Two methods of applying the above effect are commonly used.

#### 1.3.1.a The "Bijvoet" technique\*

This technique involves the comparison of the value of  $I(H)$

\* Bijvoet (1955)

and  $I(\bar{H})$  for several strong reflections. The technique is generally used when the intensity data are obtained by photographic means. The most important factor is the initial definition of the 'handedness' of the crystal axes (Peerdeman & Bijvoet, 1956; Ramaseshan, 1964) and the subsequent assignment of the correct sign to the Miller indices  $h$ ,  $k$  and  $l$ . Observed and calculated "Bijvoet differences" are compared for the structural model. Correspondence of these differences in sign and magnitude indicates the correct absolute configuration.

#### 1.3.1.b The "lowest R-factor" technique\*\*

This is an extension of the Bijvoet method. The absolute configuration is established by calculating the structure factors for both configurations. The correct absolute configuration should give the lowest R value and the significance can be assessed by Hamilton's (1965) test. This method was used in the present work\*\*\*.

### 1.4 THE COMPLEXES STUDIED IN THIS WORK

Several solid products, obtained from the syntheses of Co(III) and Cr(III) complexes with sal en and sal (R)pn ligands (Table 1.1), were provided by Benson (1976).

#### 1.4.1 The sal en system

##### (a) Racemic compounds

X-ray powder diffraction patterns of  $M(\text{sal en})_2\text{I}$  complexes

---

\*\* Ibers & Hamilton (1964)

\*\*\* Hawkins (1971) has described what he calls the 'crystal-engineering' method. This involves normal x-ray analysis of a structure which includes a dissymmetric moiety of known absolute configuration. Clearly this method applies to the optically active complexes reported in this work. Both this method and the "lowest R-factor" technique gave the same absolute configuration.



Table 1.1

Summary of characteristics of crystals examined

(I) space group; (II) solvent of crystallization; (III) structure reported in this work; d - disordered; pw - powder; td - to dryness; tw - twinned; vp - very poor; XS - excess

Cation	Anion	Solvent*	Comments
$\text{Co}(\text{sal en})_2^+$	$\text{I}^-$	XS MeOH	(I) Pbac, $a=18.95$ , $b=30.12$ , $c=7.44 \text{ \AA}$ , $Z=8$
		XS EtOH	brown pw, not isostructural with other phases
		$\text{H}_2\text{O}$ or EtOH td	(I) $\text{P2}_1/\text{c}$ ; (II) $1\text{H}_2\text{O}$ (III)
		MeOH td	
$\text{Cr}(\text{sal en})_2^+$	$\text{I}^-$	$\text{H}_2\text{O}$ or EtOH	vp; d; tw; (I) $\text{P2}_1/\text{c}$ ?
		MeOH	(I) $\text{P}\bar{1}$ (Gardner, Gatehouse & White, 1971)
$(-)\text{Co}(\text{sal en})_2^+$	$\text{I}^-, \text{ClO}_4^-, \text{BF}_4^-, \text{PF}_6^-$	$\text{H}_2\text{O}$ ,	vp; pw; d; tw
		EtOH,	all combinations of anion
		MeOH	and solvent used
$(+)\text{Cr}(\text{sal en})_2^+$	DBT	$\text{H}_2\text{O}$	(I) $\text{P2}_1$ ; (II) $3\text{H}_2\text{O}$ ; (III)
DBT = $\text{bz}_2-(\text{R},\text{R})-\text{Htart}^-$			
$\text{Co}(\text{sal}(\text{R})\text{pn})_2^+$			
isomer (i)	$\text{I}^-$	$\text{H}_2\text{O}$	(I) $\text{C222}_1$ ; (II) $3\text{H}_2\text{O}$ ; (III)
isomer (ii)	$\text{I}^-$	$\text{H}_2\text{O}$ or EtOH or MeOH	vp; d; tw; pw; materials from solution were isostructural ?
		$\text{ClO}_4^-$	(I) $\text{C2}$ ?; (II) 1 or $1.5\text{H}_2\text{O}$ vp; tw; d
		EtOH	(I) $\text{P2}_1$ ; (II) $0.75\text{EtOH}$ or $0.75\text{EtOH}, 0.25\text{H}_2\text{O}$ ; (III)
$\text{Cr}(\text{sal}(\text{R})\text{pn})_2^-$			
isomer (i)	$\text{ClO}_4^-$	$\text{H}_2\text{O}$	(I) $\text{P1}$ ; pseudo-racemate, $Z=2$ ; (III)
isomer (ii)	$\text{ClO}_4^-$		non-crystalline powder

\* solvent used for crystallization

(M = Co(III) and Cr(III)), which were crystallized from water, ethanol and methanol, showed that the cobalt and chromium complexes were not isostructural (Table 1.2). Results of microanalysis of the cobalt compounds suggested two stoichiometries;  $\text{Co}(\text{sal en})_2\text{I}\cdot\text{H}_2\text{O}$  obtained from aqueous solution, and  $\text{Co}(\text{sal en})_2\text{I}$ , obtained from both excess methanol and ethanol. It was also found that the monohydrate crystallized from both ethanol and methanol if water was not excluded and the solution allowed to evaporate to dryness. Powder diffraction patterns also showed that the anhydrous compounds obtained from ethanol and methanol were not isostructural (Table 1.2), and repeated recrystallizations showed that the two phases were interconvertible. Two possibilities could account for this behaviour: (a) partial occupancy of one or more solvent sites and (b) a change in the conformation of the diamine chelate rings. Results of microanalysis of the chromium compounds suggested only one stoichiometry,  $\text{Cr}(\text{sal en})_2\text{I}$ , obtained from water, ethanol or methanol. However, powder diffraction data showed that the compounds obtained from both aqueous and ethanolic solutions were isostructural but different from that obtained from methanolic solution (Table 1.2). The latter corresponded to the previously published structure for  $\text{Cr}(\text{sal en})_2\text{I}$  (Gardner, Gatehouse & White, 1971).

The crystal structure determination of  $\text{Co}(\text{sal en})_2\text{I}\cdot\text{H}_2\text{O}$  was undertaken to confirm that the Co(III) complex was analogous to the Cr(III) complex and also to investigate the effect of the water molecule. It was intended to carry out structural studies to determine the nature of the anhydrous compounds, but all attempts to grow single crystals of  $\text{Co}(\text{sal en})_2\text{I}$  from ethanolic solution were fruitless.

#### (b) Optical isomers

Benson (1976) resolved the  $\text{M}(\text{sal en})_2\text{I}$  complexes and predicted their absolute configuration on the basis of C.D.



Table 1.2

Powder diffraction patterns of  $M(\text{sal en})_2\text{I}$  isomers\* $2\theta$  values (degrees), Cu  $K\alpha$  radiation, s - strong,

m - medium, w - weak, br - broad, sh - shoulder

$\text{Co}(\text{sal en})_2\text{I}$			$\text{Cr}(\text{sal en})_2\text{I}$	
$\text{H}_2\text{O}$	EtOH	MeOH	MeOH	EtOH/ $\text{H}_2\text{O}$
5.18 s		5.90 s	8.20 w	8.50 m
10.10 w	9.80 s	9.00 m	8.70 w	9.10 s
10.30 m	10.20 w,br	9.50 s	9.30 s	12.10 m
11.38 w	10.60 m	10.80 w	10.10 w	12.95 s
11.70 w,br	12.50 s	11.80 w	12.80 w	13.20 mw
13.50 w,br	15.40 w,br	12.60 w	13.25 m	15.00 mw,br
13.80 mw	16.50 mw	13.20 w	14.90 w	16.35 s
14.85 s	17.80 m,br	14.08 m	15.20 s	17.05 w
15.78 m	18.00 m,br	15.30 s	15.90 w	18.10 mw
17.18 w	18.90 w	16.10 w,br	17.25 m	18.90 w
17.42 m	19.10 w	16.80 w	18.55 m	19.60 m
17.95 mw	19.55 ms	17.40 m	19.20 w	19.80 w,sh
18.35 m	19.90 m	19.00 s	19.70 w	20.70 s
19.10 w	20.40 m	19.55 mw	20.40 mw,br	20.90 w,sh
21.30 m	20.90 m	20.18 mw	20.60 mw,br	21.20 m
21.50 s	21.20 m	21.40 m	21.05 m	21.70 w,br
22.40 m	21.50 w	21.90 s	22.40 w	23.20 w
22.90 s	22.30 ms	22.60 m	23.70 mw	24.20 w,br
23.60 w	22.40 w	23.40 s	23.90 m	25.70 m
24.10 w,br	22.60 ms	26.40 w	24.20 w,br	26.20 mw
25.10 mw,br	24.40 m,br	26.60 m	25.40 m,br	26.40 w,sh
25.80 m	25.50 m	26.80 w	25.70 w	26.80 w
27.10 m	25.75 w	27.25 m	26.35 m	27.25 w
28.30 w,br	27.60 w	27.55 m	27.60 mw	27.40 w
29.90 w	29.20 w,br	27.90 s	27.90 w	27.90 w,sh
30.30 m	30.50 m	29.70 m	28.30 w	28.10 w,sh
30.70 m		30.40 mw	29.00 mw	28.25 mw
		30.70 w	30.30 m	29.30 mw
		31.40 w		
		32.10 mw		

\* Instrumentation: Philips PW 1050/25 recording diffractometer

measurements. Repeated attempts were made to obtain suitable single crystals of these complexes, using different solvents and various anions; all of which were unsuccessful. However, excellent single crystals of  $(+)\text{}_{336}\text{Cr}(\text{sal en})_2\text{bz}_2-(R,R)\text{-Htart}, 3\text{H}_2\text{O}$  were available and it was decided to use these in order to determine the absolute configuration and substantiate Benson's (1976) predictions.

#### 1.4.2 The sal (R)pn system

##### (a) cobalt complexes

Four compounds were isolated from the synthesis of  $\text{Co}(\text{sal (R)pn})_2\text{I}$ , two of which (isomer (i) and (ii)) were major products and were shown to have different powder diffraction patterns. On the basis of p.m.r. measurements, Benson (1976) predicted that the complexes were: isomer (i),  $\text{Co}(\text{sal (R)pn}(2\text{-Me}))_2\text{I}$  and isomer (ii),  $\text{Co}(\text{sal (R)pn}(1\text{-Me}))(\text{sal (R)pn}(2\text{-Me}))\text{I}$ . Very small single crystals of isomer (i), were eventually grown, but efforts to obtain suitable single crystals of isomer (ii) were unsuccessful. Isomer (ii) was converted to the perchlorate which was crystallized successfully from ethanolic solution. Isomers (iii) and (iv) were isolated in small amounts only and single crystals were never obtained. Determination of the crystal structures of isomer (i), as iodide, and isomer (ii) as perchlorate, were undertaken in order to substantiate the predicted positions of the methyl groups and to determine the absolute configuration.

##### (b) chromium complexes

Two products were isolated from the synthesis of  $\text{Cr}(\text{sal (R)pn})_2\text{ClO}_4$  and microanalysis of the major product (isomer (i))



was consistent with the stoichiometry  $\text{Cr}(\text{sal}(\text{R})\text{pn})_2\text{ClO}_4$ . Isomer (ii) was never obtained in crystalline form (Benson, 1976). X-ray crystallographic studies were carried out to determine the nature of isomer (i) and to provide the absolute configuration.

## 2.1. UNIT CELL AND DIFFRACTION SYMMETRY

Specimens of acicular, submicron crystals were grown by slow evaporation of an aqueous solution of  $\text{Cr}(\text{sal}(\text{R})\text{pn})_2\text{ClO}_4 \cdot 1.5\text{H}_2\text{O}$ . Individual crystals showed a variety of habits of the form (1070) and had an average size of  $0.5 \times 0.2 \times 0.1$  mm. Several crystals were mounted without etching the surfaces and others were etched with dilute  $\text{HNO}_3$  for 10 min. The etching was done in a solution of  $\text{HNO}_3$  in water (1:1 v/v) at room temperature. The etching was stopped by rinsing the crystals in water and drying them in a vacuum oven at  $50^\circ\text{C}$  for 24 h.

Unit cell dimensions and diffraction symmetry were determined from single-crystal X-ray diffraction photographs. The crystals were found to belong to the orthorhombic system and the following unit cell dimensions:

$$\begin{aligned} a &= 10.36 \text{ \AA} & b &= 10.36 \text{ \AA} \\ c &= 10.36 \text{ \AA} & \beta &= 90^\circ \\ \alpha &= 90^\circ & \gamma &= 90^\circ \end{aligned}$$

Systematic absences were determined to be

$$\begin{aligned} h0l: h &= 2n+1 & h0l: l &= 2n+1 \\ 0kl: k &= 2n+1 & 0kl: l &= 2n+1 \\ h0l: h &= 2n+1 & 0kl: k &= 2n+1 \\ h0l: h &= 2n+1 & 0kl: l &= 2n+1 \end{aligned}$$

These absences are found with space group  $C2/c$  (No. 35) (International Tables, 1952) which is non-centrosymmetric, has no mirror planes and therefore conforms with the requirements of an optically active compound.

$\text{Cr}(\text{sal}(\text{R})\text{pn})_2\text{ClO}_4 \cdot 1.5\text{H}_2\text{O}$  for analysis

## CHAPTER 2

CRYSTAL AND MOLECULAR STRUCTURE OF  $(+)_486$ -S-BIS-[R-N-(2-AMINO(R)PROPYL) SALICYLALDIMINATO]-COBALT(III) IODIDE, TRI-HYDRATE\*

## 2.1 UNIT CELL AND DIFFRACTION SYMMETRY

Rosettes of acicular, euohedral crystals were grown by slow evaporation of an aqueous solution of  $S-[Co(sal(R)pn(2-Me))_2]I \cdot 3H_2O$ . Individual crystals showed pseudo-hexagonal symmetry of the form (1010) and had an average size of approximately  $0.1 \times 0.1 \times 2.00$  mm. Several crystals were selected and suitable lengths were cut (ca. 0.3 mm long) and mounted along their needle axis.

Unit cell dimensions and diffraction symmetry were determined from equi-inclination Weissenberg and precession photographs. The crystals were found to belong to the orthorhombic system and had the following unit cell dimensions

$$\begin{array}{ll} a = 10.56 \text{ \AA} & \alpha = \beta = \gamma = 90.0^\circ \\ b = 16.16 \text{ \AA} & V = 2567 \text{ \AA}^3 \\ c = 15.24 \text{ \AA} & \end{array}$$

Systematic absences were determined to be

$$\begin{array}{ll} hk1; h+k = 2n+1 & h00; (h = 2n+1) \\ 0k1; (k = 2n+1) & 0k0; (k = 2n+1) \\ h01; (h = 2n+1) & 001; l = 2n+1 \\ hk0; (h+k = 2n+1) & \end{array}$$

These absences are found with space group  $C222_1$  (No. 20) (International Tables, 1952) which is non-centrosymmetric, has no mirror planes and therefore complies with the requirements of an optically active compound.

\*  $S-[Co(sal(R)pn(2-Me))_2]I \cdot 3H_2O$  for brevity



Re-examination of the crystal morphology showed that the pseudo-hexagonal prism was due to the coincidence of the needle axis and the cell c-axis and the presence of the form (110) and the pinacoid (010). Fracture faces perpendicular to the c-axis were assumed to be the pinacoid (001).

The density of the crystals was determined to be  $1.56 \text{ g cm}^{-3}$  by the method of flotation using a mixture of carbon tetrachloride and ethyl bromide. This value for the density gave  $Z = 4$ , where  $Z$  is the number of formula units in the unit cell, this in turn gave a calculated density of  $1.53 \text{ g cm}^{-3}$ .

## 2.2 DATA COLLECTION AND REDUCTION

### 2.2.1 Unit cell refinement

One of the several crystals initially used for photographic experiments was remounted about the needle axis (Araldite Fast Set; glass capillary) and placed on a Siemens automatic four-circle diffractometer. The crystal was oriented so that the c-axis was coincident with the  $\phi$ -axis of the diffractometer.

Unit cell parameters were refined using the method of least-squares (Busing, Ellison, Levy, King & Rosebury, 1968). Nine prominent reflections were chosen to give the widest range of non-axial  $h$ ,  $k$  and  $l$  with the greatest  $2\theta$  values using Ni-filtered Cu-K $\alpha$  radiation (Table 2.1). The  $2\theta$  values were refined by scanning in  $\phi$ ,  $\chi$ , and  $\theta$  individually. The original settings of these arcs for a given  $hkl$  were calculated from the photographically obtained cell dimensions. Each scan consisted of a number ( $> 10$ ) of stationary counts which spanned either side of the manually optimised maximum intensity for each arc individually. Three cycles of least-squares refinement gave the

Table 2.1

Unit cell refinement data for  $S-[Co(sal(R)pn(2-Me))_2]I \cdot 3H_2O$ 

h	k	l	$2\theta$	h	k	l	$2\theta$
1	11	1	64.80	4	2	4	43.22
6	6	1	63.52	5	11	2	81.04
3	3	2	32.66	2	10	4	65.56
3	7	2	48.90	5	9	3	71.70
5	7	1	59.82				

parameters listed below.

$$a = 10.570(2) \text{ \AA}$$

$$\alpha = \beta = \gamma = 90.0^\circ$$

$$b = 16.052(3) \text{ \AA}$$

$$V = 2574.3 \text{ \AA}^3$$

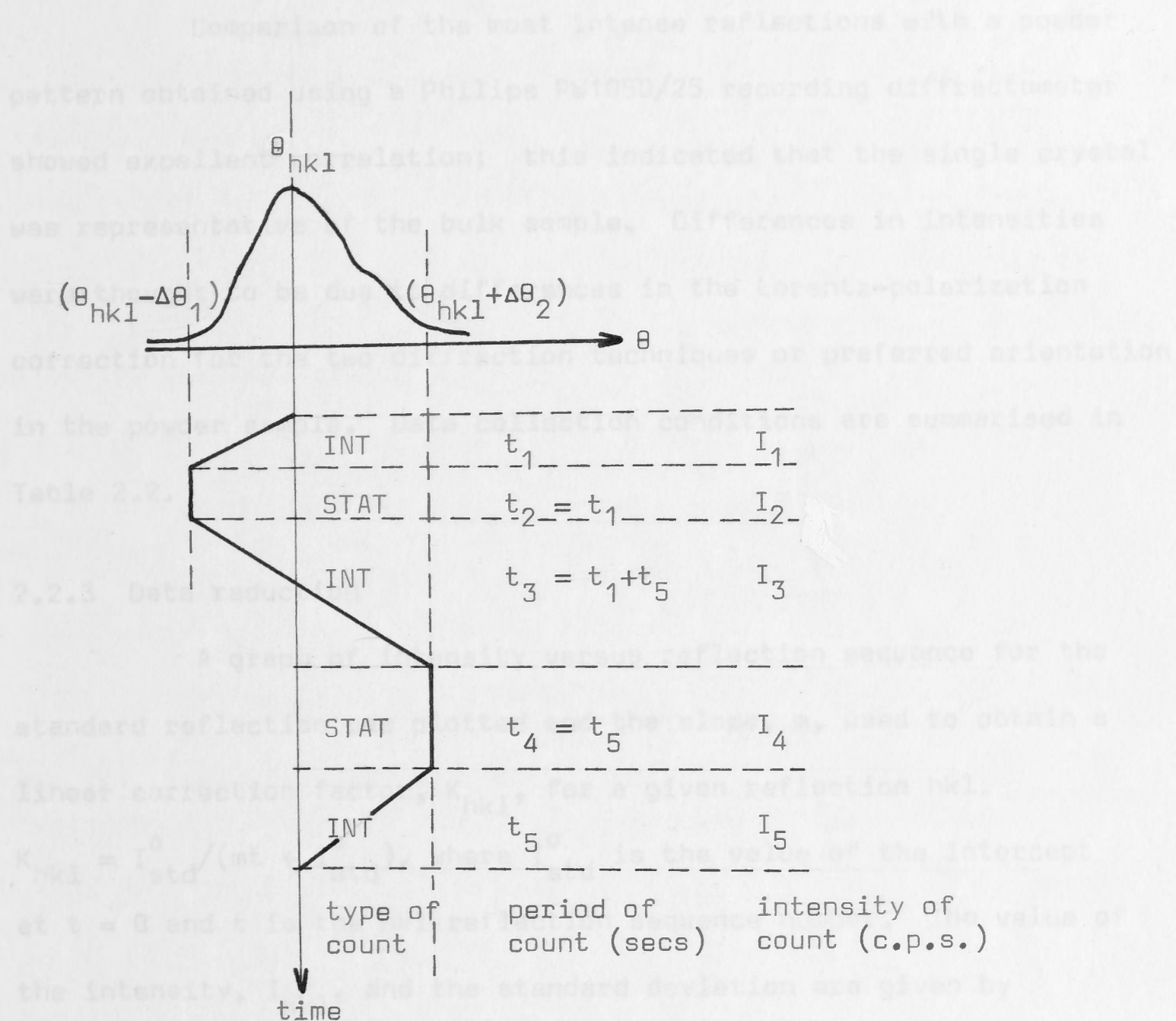
$$c = 15.220(7) \text{ \AA}$$

### 2.2.2 Data collection

HKL data were collected, at room temperature, using Ni-filtered Cu-K $\alpha$  radiation and a maximum value of  $45^\circ$  for  $\theta$ . This restriction in the value of  $\theta$  was due to the small size of the crystal. Intensities were measured by the 'five-point' method (Hoppe, 1965) (Figure 2.1). If the count rate exceeded 5000 counts per second a nickel foil attenuator was automatically introduced. A single standard reflection was monitored after every twenty reflections.

During the data collection the collimator was changed in order to give a greater count rate for the weaker reflections. This change was allowed for in the following way. The standard reflection must be constant throughout the data collection. This was achieved by multiplying the values,  $I_{obs}$ , prior to the collimator change by the ratio  $I'_{std}/I_{std}$ , where  $I'_{std}$  is the average value of the standard intensity after collimator change and  $I_{std}$  the average value before such a change.





INT - integrated      STAT - static

$$I_{hk1}^{obs} = \frac{1}{2} (I_1 + I_3 + I_5) - 2(I_2 + I_4)$$

$$\sigma(I_{hk1}^{obs}) = (I_1 + I_2 + I_3 + I_4 + I_5)^{\frac{1}{2}}$$

$$s(I_{hk1}^{obs}) = [\sigma(I_{hk1}^{obs})]^2$$

Figure 2.1 Five-point counting method (Hoppe, 1965).

Comparison of the most intense reflections with a powder pattern obtained using a Philips PW1050/25 recording diffractometer showed excellent correlation; this indicated that the single crystal was representative of the bulk sample. Differences in intensities were thought to be due to differences in the Lorentz-polarization correction for the two diffraction techniques or preferred orientation in the powder sample. Data collection conditions are summarised in Table 2.2.

### 2.2.3 Data reduction

A graph of intensity versus reflection sequence for the standard reflection was plotted and the slope,  $m$ , used to obtain a linear correction factor,  $K_{hkl}$ , for a given reflection  $hkl$ .

$K_{hkl} = I_{std}^0 / (mt + I_{std}^0)$ , where  $I_{std}^0$  is the value of the intercept at  $t = 0$  and  $t$  is the  $hkl$  reflection sequence number. The value of the intensity,  $I_{hkl}$ , and the standard deviation are given by

$$I_{hkl} = I_{hkl}^{obs} \cdot K_{hkl} \cdot AF$$

$$\sigma_1(I_{hkl}) = (AF \cdot S(I_{hkl}^{obs}))^{\frac{1}{2}}$$

where  $AF$  is the attenuator factor.

A total of 621 reflections were measured, of which 134 (21.6%) were considered unobserved, using the criteria  $I < 3\sigma_1$ . This assumes Gaussian distribution of random errors in the value of  $I$ ; the probability that the error in  $I$  exceeds  $3\sigma_1$  is less than 1:1000 (Lipson & Cochran, 1966). Unobserved reflections were given a value of  $I = 1.5\sigma_1(I)$  and included in the data.



Table 2.2

Summary of crystal data and data collection S-[Co(sal (R)pn(2-Me))<sub>2</sub>] I, 3H<sub>2</sub>O

Chemical formula	C <sub>20</sub> H <sub>26</sub> N <sub>4</sub> O <sub>2</sub> CoI, 3H <sub>2</sub> O																																
Formula weight	594.42																																
Space group	C222 <sub>1</sub> (No. 20)																																
Boundary faces of crystal; (mm from internal origin in parentheses)	<table><tr><td>1</td><td>1</td><td>0</td><td>(.036)</td><td>1</td><td>-1</td><td>0</td><td>(.040)</td></tr><tr><td>-1</td><td>-1</td><td>0</td><td>(.036)</td><td>-1</td><td>1</td><td>0</td><td>(.040)</td></tr><tr><td>0</td><td>1</td><td>0</td><td>(.060)</td><td>0</td><td>-1</td><td>0</td><td>(.050)</td></tr><tr><td>0</td><td>0</td><td>1</td><td>(.160)</td><td>0</td><td>0</td><td>-1</td><td>(.160)</td></tr></table>	1	1	0	(.036)	1	-1	0	(.040)	-1	-1	0	(.036)	-1	1	0	(.040)	0	1	0	(.060)	0	-1	0	(.050)	0	0	1	(.160)	0	0	-1	(.160)
1	1	0	(.036)	1	-1	0	(.040)																										
-1	-1	0	(.036)	-1	1	0	(.040)																										
0	1	0	(.060)	0	-1	0	(.050)																										
0	0	1	(.160)	0	0	-1	(.160)																										
Unit cell parameters	<table><tr><td>a</td><td>=</td><td>10.570(2)</td><td>Å</td></tr><tr><td>b</td><td>=</td><td>16.052(3)</td><td>Å</td></tr><tr><td>c</td><td>=</td><td>15.220(7)</td><td>Å</td></tr><tr><td colspan="4">α = β = γ = 90.0°</td></tr><tr><td>V</td><td>=</td><td>2574.3</td><td>Å<sup>3</sup></td></tr></table>	a	=	10.570(2)	Å	b	=	16.052(3)	Å	c	=	15.220(7)	Å	α = β = γ = 90.0°				V	=	2574.3	Å <sup>3</sup>												
a	=	10.570(2)	Å																														
b	=	16.052(3)	Å																														
c	=	15.220(7)	Å																														
α = β = γ = 90.0°																																	
V	=	2574.3	Å <sup>3</sup>																														
Radiation for unit cell refinement	Cu-Kα = 1.5418 Å																																
Density	1.56 ± 0.04 g cm <sup>-3</sup>																																
D <sub>m</sub>																																	
D <sub>c</sub>	1.53 g cm <sup>-3</sup>																																
Z	4																																
Linear absorption coefficients	<table><tr><td>μ(Cu-Kα)</td><td>=</td><td>153.1</td><td>cm<sup>-1</sup></td></tr><tr><td>μ(Mo-Kα)</td><td>=</td><td>19.8</td><td>cm<sup>-1</sup></td></tr></table>	μ(Cu-Kα)	=	153.1	cm <sup>-1</sup>	μ(Mo-Kα)	=	19.8	cm <sup>-1</sup>																								
μ(Cu-Kα)	=	153.1	cm <sup>-1</sup>																														
μ(Mo-Kα)	=	19.8	cm <sup>-1</sup>																														
Radiation used for data collection	Cu-Kα																																
Scan type/mode	'Five-point'/θ - 2θ																																
Standard reflection	3 3 2																																
Standard average range	± 8.8%																																
Standard slope with sequence	-0.069																																
Standard frequency	20																																
Data collected (2θ limit)	HKL (90°)																																
Number of observed reflections (%)	487 (78.4)																																

The observed structure factors and their standard deviations were calculated using the following formulae

$$|F_o| = (I/L_p)^{\frac{1}{2}}$$

$$\sigma_1(|F_o|) = \sigma_1(I)/(L_p \cdot 2 |F_o|)$$

where  $L_p = (1 + \cos^2 2\theta)/2\sin 2\theta$  (Stout & Jensen, 1968).

Linear absorption coefficients for both Cu-K $\alpha$  and Mo-K $\alpha$  radiation were calculated from available data (International Tables, 1962) as  $153.1 \text{ cm}^{-1}$  and  $19.8 \text{ cm}^{-1}$  respectively.

### 2.3 DETERMINATION OF THE POSITIONS OF IODINE AND COBALT ATOMS

The ratio  $\sum Z_h^2 / \sum Z_l^2$  (where  $Z_h$  represents the atomic number of a designated heavy atom and  $Z_l$  that of a light atom) was calculated as 1.41 with iodine as the only heavy atom and 2.79 with both iodine and cobalt as heavy atoms. Hence, the determination of the correct position of the iodine and cobalt atoms in turn determines most (>80% (Sim, 1961)) of the phases and allows a preliminary Fourier synthesis to be carried out. Since  $S-[Co(sal(R)pn(2-Me))_2]I \cdot 3H_2O$  crystallizes in space group  $C222_1$  and  $Z = 4$ , both the iodine and cobalt atoms must each occupy one of the four-fold special positions

$$\text{i) } 0, y, \frac{1}{4} \quad \text{ii) } x, 0, 0$$

Atoms in these positions give rise to the Patterson peaks listed in Table 2.3.

To a good approximation the volume under a Patterson peak is proportional to the peak height,  $H_{ij}$ , the magnitude of which is



given by

$$H_{ij} = \sum \frac{m \cdot H_{ii}}{z_i} \cdot z_i z_j$$

where  $H_{ii}$  is the height of the origin peak,  $z_i$  is the atomic number of the various atoms and  $m$  is the vector multiplicity.

Table 2.3

Patterson peaks for atoms in special positions in space group  $C222_1$   
(No. 20)

i)	$0, y, \frac{1}{4}$	$0, -y, \frac{3}{4}$	$\frac{1}{2}, \frac{1}{2} + y, \frac{1}{4}$	$\frac{1}{2}, \frac{1}{2} - y, \frac{3}{4}$
$0, y, \frac{1}{4}$	-	$0, -2y, \frac{1}{2}$	$\frac{1}{2}, \frac{1}{2}, 0$	$\frac{1}{2}, \frac{1}{2} - 2y, \frac{1}{2}$
$0, -y, \frac{3}{4}$	$0, 2y, -\frac{1}{2}$	-	$\frac{1}{2}, \frac{1}{2} + 2y, -\frac{1}{2}$	$\frac{1}{2}, \frac{1}{2}, 0$
$\frac{1}{2}, \frac{1}{2} + y, \frac{1}{4}$	$-\frac{1}{2}, -\frac{1}{2}, 0$	$-\frac{1}{2}, -\frac{1}{2} - 2y, \frac{1}{2}$	-	$0, -2y, \frac{1}{2}$
$\frac{1}{2}, \frac{1}{2} - y, \frac{3}{4}$	$-\frac{1}{2}, -\frac{1}{2} + 2y, -\frac{1}{2}$	$-\frac{1}{2}, -\frac{1}{2}, 0$	$0, 2y, -\frac{1}{2}$	-
ii)	$x, 0, 0$	$-x, 0, \frac{1}{2}$	$\frac{1}{2} + x, \frac{1}{2}, 0$	$\frac{1}{2} - x, \frac{1}{2}, \frac{1}{2}$
$x, 0, 0$	-	$-2x, 0, \frac{1}{2}$	$\frac{1}{2}, \frac{1}{2}, 0$	$\frac{1}{2} - 2x, \frac{1}{2}, \frac{1}{2}$
$-x, 0, \frac{1}{2}$	$2x, 0, -\frac{1}{2}$	-	$\frac{1}{2} + 2x, \frac{1}{2}, -\frac{1}{2}$	$\frac{1}{2}, \frac{1}{2}, 0$
$\frac{1}{2} + x, \frac{1}{2}, 0$	$-\frac{1}{2}, \frac{1}{2}, 0$	$-\frac{1}{2} - 2x, -\frac{1}{2}, \frac{1}{2}$	-	$-2x, 0, \frac{1}{2}$
$\frac{1}{2} - x, \frac{1}{2}, \frac{1}{2}$	$-\frac{1}{2} + 2x, -\frac{1}{2}, -\frac{1}{2}$	$-\frac{1}{2}, -\frac{1}{2}, 0$	$2x, 0, -\frac{1}{2}$	-

In this case the origin peak was normalized to a value of 999 so that iodine-iodine and cobalt-cobalt vectors would have anticipated heights of 612 and 121 respectively. The largest peaks in the unsharpened three-dimensional Patterson are listed in Table 2.4. Examination of the Harker line  $(U, 0, \frac{1}{2})$  and Harker section  $(U, \frac{1}{2}, \frac{1}{2})$  enabled the calculation of the iodine and cobalt positions as shown in Table 2.5.

Positions 'A'  $(\frac{1}{2}, 0, 0)$  and 'B'  $(0, 0, \frac{1}{4})$  of Table 2.5 were chosen for iodine (I(10)) and cobalt (Co(10)) respectively. This

Table 2.4

Patterson peaks for  $S-[Co(sal(R)pn(2-Me))_2]I, 3H_2O$ 

U	V	W	H	U	V	W	H
0	0	0	999	0	0	5	438
.5	.5	.5	438	.5	.5	0	999
.5	0	.25	483	0	.5	.25	483
.5	.231	.5	127	0	.269	.5	127
0	.238	.25	80	.5	.269	.25	80

Table 2.5

Calculation of iodine and cobalt atom positions for

 $S-[Co(sal(R)pn(2-Me))_2]I, 3H_2O$ 

Vector	U	V	W	Comments
$2x, 0, \frac{1}{2}$	0	0	$\frac{1}{2}$	$x = \frac{1}{2}$
$\frac{1}{2}, \frac{1}{2}, \frac{1}{2}$	$\frac{1}{2}$	$\frac{1}{2}$	$\frac{1}{2}$	'A' = $(\frac{1}{2}, 0, 0)$
$\frac{1}{2} - 2x, \frac{1}{2}, \frac{1}{2}$	$\frac{1}{2}$	$\frac{1}{2}$	$\frac{1}{2}$	All vectors found for
$\frac{1}{2}, \frac{1}{2}, 0$	$\frac{1}{2}$	$\frac{1}{2}$	0	this position
$0, 2y, \frac{1}{2}$	0	0	$\frac{1}{2}$	$y = 0$ or $\frac{1}{2}$
$\frac{1}{2}, \frac{1}{2} + 2y, \frac{1}{2}$	$\frac{1}{2}$	$\frac{1}{2}$	$\frac{1}{2}$	'B' = $(0, 0, \frac{1}{4})$
$\frac{1}{2}, \frac{1}{2}, \frac{1}{2}$	$\frac{1}{2}$	$\frac{1}{2}$	$\frac{1}{2}$	'C' = $(0, \frac{1}{2}, \frac{1}{4})$
$\frac{1}{2}, \frac{1}{2}, 0$	$\frac{1}{2}$	$\frac{1}{2}$	0	All vectors found for
				these positions

Cross vectors: 'A'-'B'

$\frac{1}{2}, 0, \frac{1}{4}$	$\frac{1}{2}$	0	$\frac{1}{4}$
$0, \frac{1}{2}, \frac{1}{4}$	0	$\frac{1}{2}$	$\frac{1}{4}$

'A' and 'B' are possible

Cross vectors: 'B'-'C'

$0, \frac{1}{2}, 0$	None
$0, \frac{1}{2}, \frac{1}{2}$	None
$\frac{1}{2}, 0, 0$	None
$\frac{1}{2}, 0, \frac{1}{2}$	None

'B'+'C' not possible

Cross vectors: 'A'-'C'

$\frac{1}{2}, \frac{1}{2}, \frac{1}{4}$	None
$0, 0, \frac{1}{4}$	None

'A'+'C' not possible



arbitrary choice is justified since interchange of atom types only results in a re-defined origin for the space group.

Both cobalt and iodine atoms were given initial isotropic temperature factors of  $3.5 \text{ \AA}^2$  and the scale factor was set equal to unity. Scattering factors were those for neutral atoms (Cromer & Waber, 1965). Anomalous dispersion terms  $\Delta F'$  and  $\Delta F''$  were included (International Tables, 1962), although no allowance was made for their dependence on  $\sin \theta$ .

One cycle of block diagonal least-squares (B.D.L.S. for brevity) was carried out with I(10) (.5,0,0) (isotropic temperature factor and scale factor) and the resulting data used to phase a difference Fourier synthesis. The value of  $R^*$  was 0.732. This synthesis showed pseudo-symmetry of the form  $(x,y,z) \rightarrow (x,y,z+\frac{1}{2})$  and examination of a model for the heavy atoms showed higher pseudo-symmetry - both mirror planes and a centre.

In order to remove the pseudo-symmetry the iodine position was moved arbitrarily to (.48,0,0) and three cycles of B.D.L.S. were carried out on the scale factor and x-coordinate of I(10). The position of I(10) was then (.475,0,0) and the value of  $R$  was .442. Several calculations were made with the I(10) x-coordinate less than .475 and these refined to a value of  $x = .475$ . Similarly, calculations were made with the I(10) x-coordinate greater than .5. These calculations gave the position of I(10) as (.525,0,0). The alternative positions for the iodine atom were related by a centre at (.5,0,0).

---

\* the reliability index used in this thesis is defined by

$$R = \frac{\sum_H (|F_{oH}| - K |F_{cH}|)}{\sum_H |F_{oH}|}$$

The model I(10) (.475,0,0) plus Co(10) (0,0,.25) was arbitrarily chosen and subjected to four cycles of B.D.L.S. (scale factor, atom coordinates and isotropic temperature factors) which gave a reduction in the value of R from .543 to .283. The initial increase in the value of R was thought to be due to a large error in the scale factor. The new atom coordinates were, I(10) (.475,0,0) and Co(10) (0,-.0145,.25). Identical calculations were carried out with I(10) (.525,0,0) plus Co(10) (0,0,.25) and the final parameters were I(10) (.525,0,0) and Co(10) (0,+.0145,.25) with a value for R of .283. By using the model I(10) (.475,0,0) plus Co(10) (0,+.0145,.25) the value of R was .545, hence this model was discarded.

The model I(10) (.475,0,0) plus Co(10) (0,-.0145,.25) was used in the subsequent analysis and proved to be correct.

#### 2.4 DETERMINATION OF LIGHT ATOM POSITIONS

A difference Fourier synthesis phased on (I(10) + Co(10)) gave the positions of the atoms in the coordination octahedron of the cobalt atom (Table 2.6). These atoms were arbitrarily given the designations O(10), N(10) and N(20) since at this stage oxygen and nitrogen could not be differentiated. Initial isotropic temperature factors were set equal to  $3.5 \text{ \AA}^2$ .

One cycle of B.D.L.S. was used to recalculate the scale factor and the model was then used to phase a second difference Fourier synthesis. This gave the positions of the carbon atoms in the aromatic ring (Table 2.6). At this stage the value of R was .281. Isotropic temperature factors of these carbon atoms were set equal to  $3.5 \text{ \AA}^2$ . From the position of the aromatic ring it was possible to determine that the correct oxygen and nitrogen designations had already been made.



Table 2.6

Initial atom positions for  $S-[Co(sal(R)pn(2-Me))_2]I \cdot 3H_2O$  obtained from difference Fourier syntheses

Atom	x	y	z	Interatomic distances (Å)
O(10)	.431	.577	.327	Co(10) - O(10): 2.01 cf 2.13 <sup>a</sup>
N(10)	.656	.490	.327	Co(10) - N(10): 2.02 cf 1.99 <sup>b</sup>
N(20)	.434	.413	.317	Co(10) - N(20): 1.72
C(10)	.519	.731	.000	C(10) - C(30): 1.37 cf 1.40 <sup>a</sup>
C(20)	.403	.719	.980	C(10) - C(20): 1.28
C(30)	.584	.678	.048	C(30) - C(50): 1.59
C(40)	.342	.644	.010	C(40) - C(60): 1.52
C(50)	.516	.612	.115	C(50) - C(60): 1.35
C(60)	.397	.596	.087	C(60) - C(70): 1.37
C(70)	.681	.538	.375	C(70) - N(10): 1.09 cf 1.33 <sup>a</sup>
C(80)	.260	.413	.201	
C(90)	.722	.404	.204	
C(100)	.175	.400	.304	
OH(21)	.000	.739	.250	(special position $0, y, \frac{1}{4}$ )
OH(22)	.154	.623	.322	

<sup>a</sup> International Tables (1962)

<sup>b</sup> Saito (1968)

The scale factor was again recalculated and a difference Fourier synthesis carried out. The value of R was now .224. From this difference synthesis it was possible to determine the position of two other carbon atoms and one oxygen atom from one of the three molecules of water of crystallization. This oxygen atom was in the special position (.0,.739,.25) (Table 2.6). Initial isotropic temperature

factors were set equal to  $3.5 \text{ \AA}^2$  for carbon atoms and  $5.5 \text{ \AA}^2$  for the water oxygen atom.

One cycle of B.D.L.S. (scale factor only) was carried out and a difference Fourier synthesis phased on the model so far. R at this stage was .205. From this synthesis the positions of the two remaining carbon atoms were determined (Table 2.6). These atoms were given isotropic temperature factors equal to  $3.5 \text{ \AA}^2$ .

The scale factor was again updated and a final difference Fourier synthesis phased on the model. The value of R was .187. The position of the remaining oxygen atom was easily recognised and this atom was given an isotropic temperature factor equal to  $3.5 \text{ \AA}^2$ . One cycle of B.D.L.S. refinement of the scale factor alone gave a value of .151 for R.

## 2.5 DETERMINATION OF A WEIGHTING SCHEME FOR B.D.L.S. REFINEMENT

Since the positions of all atoms were now determined, a suitable weighting scheme was needed in order to continue refinement by the B.D.L.S. method.

It has been pointed out (Cruickshank, 1961; Cruickshank, 1965) that in the least-squares method the weights applied to observations must reflect the accuracy of those observations if the final analysis is to be correct. In the absolute case<sup>a</sup> the weight,  $w = 1/\sigma^2$ , and in the relative case<sup>b</sup>,  $w \propto 1/\sigma^2$ , where  $\sigma$  is the standard deviation of

---

<sup>a</sup> That is where  $\sigma(x)$  is estimated by a large number of repeated measurements of the same quantity x.

<sup>b</sup> Where only one measurement of each observation is made and the weight reflects the magnitude of the observation relative to other observations in the same population.



the observation (or e.s.d.). Hence, the weight applied to an observation is inversely proportional to the variance of that observation. If the weighting scheme is correct, then the average  $w\Delta F^2$  should be constant when the set of  $w\Delta F^2$  values are analysed in a systematic way. In most structure analyses,  $w$  depends mainly upon  $|F_o|$ . Several schemes have been suggested to derive weights to apply to least-squares analyses; these will now be briefly discussed.

Hughes (1941) suggested that  $w = 1$  for  $|F_o| < 4F_{\min}$  and that  $w = 4F_{\min}/|F_o|$  for  $|F_o| > 4F_{\min}$ . This scheme has been used with success for photographic data and is certainly better than unit weights (Stout & Jensen, 1968). However, this scheme is likely to place too small a weight on the more intense reflections.

The analytical method (Cruickshank, 1961; Cruickshank, 1965) requires that  $w = 1/(a + b|F_o| + c|F_o|^2 + \dots)$ . Initially it was suggested that  $a$ ,  $b$  and  $c$  should be of the order of  $2F_{\min}$ , unity and  $2/F_{\max}$ , respectively. It is important to note that this analysis must include unobserved reflections.

The third, and most commonly used, for diffractometer data utilizes an estimate of the variance of the observation (Stout & Jensen, 1968; Busing & Levy, 1957a; Corfield et al., 1967). The variance is given by one of the following,

$$\sigma_2^2 = \sigma_1^2 + (aN_p^2)$$

where  $a \approx 0.01$  and  $N_p$  is the peak count (Stout & Jensen, 1968);

$$\sigma_2^2 = (\sigma_1^2 + 0.02 \cdot N_p^2) + (0.1E)^2$$

where  $E$  is the extinction coefficient (Busing & Levy, 1957a)

$$\sigma_2^2 = N_p + 0.5(t_p/t_B) \cdot (B_1 + B_2) + (aI)^2$$

where  $t$  refers to either peak or background time,  $B_1$  and  $B_2$  are background counts,  $I$  is the intensity of the observation, after taking

background into account, and a (ca 0.03) is termed the 'ignorance factor', which takes into account all non-isotropic effects, extinction etc. (Corfield et al., 1967).

Assuming that the value of  $w$  depends primarily upon  $|F_o|$  and since unobserved reflections were included in the data, it was decided to use an analytical weighting scheme. The values of  $\overline{w\Delta F^2}$  were determined using a sample width of 11.0 for  $|F_o|$  and unit weights (Fig. 2.2). The equation  $w = 1/(3.2 + 0.001 F_o^2)$ , deduced by trial and error, was used in further B.D.L.S. refinement cycles.

The dependence of  $w$  upon  $\sin \theta / \lambda$  was ignored at this stage since the model used had isotropic temperature factors and the hydrogen atom positions were not determined (Cruickshank, 1961). Application of this weighting scheme gave values of  $\overline{w\Delta F^2}$  in the range 2.0 to 5.0

## 2.6 LEAST-SQUARES REFINEMENT

Srinivasan (1961) points out that B.D.L.S. breaks down for non-centric space groups, due to the increased importance of the off-diagonal terms of the normal equations of least-squares, when there are either a) centrosymmetric groups of atoms which contribute predominantly to the structure factor or b) pseudo-centrosymmetric groups of heavy atoms related by 'super' special positions, in this case I(10) (.5,0,0) and Co(10) (0,0,.25). However, it was decided to utilize B.D.L.S. until either a suitably low R value had been reached or abnormalities in parameters were suspected, when full matrix least-squares would be needed.

After five cycles of B.D.L.S. the residual was reduced to a value of .135 (63 parameters; atom positional and thermal parameters). Iodine, cobalt, water, oxygen and the methyl carbon atoms were now



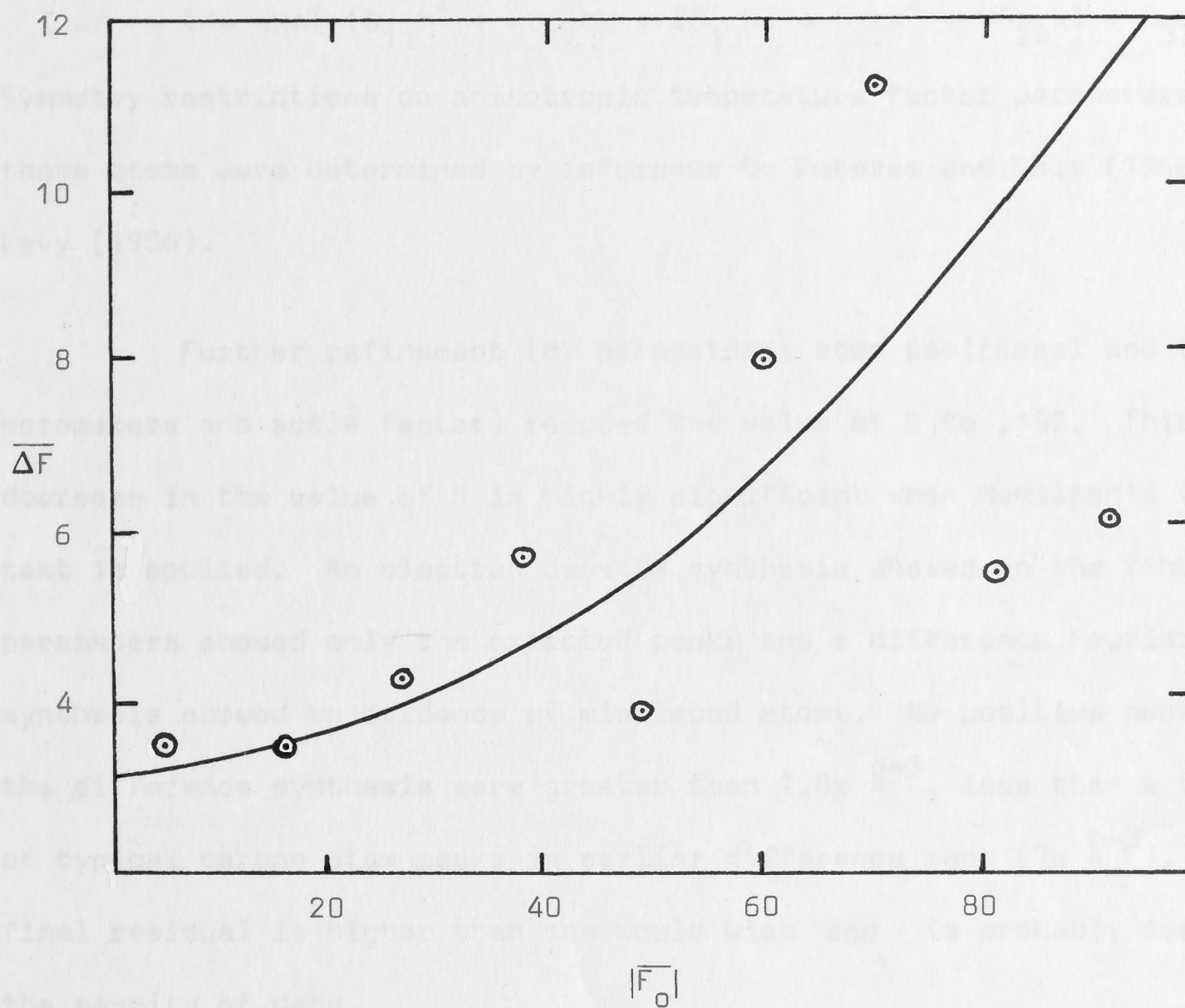


Figure 2.2 Empirical weighting scheme for  
 $S-[Co(sal(R)pn(2-Me))_2]I \cdot 3H_2O$ .

⊙ Experimental data;

—  $\Delta \bar{F} = 3.2 + 0.001 |F_0|$

given anisotropic temperature factors of the form

$$T = \exp(-(B_{11}h^2 + 2B_{12}hk + 2B_{13}hl + B_{22}k^2 + 2B_{23}kl + B_{33}l^2))$$

Symmetry restrictions on anisotropic temperature factor parameters for these atoms were determined by reference to Peterse and Palm (1966) and Levy (1956).

Further refinement (82 parameters; atom positional and thermal parameters and scale factor) reduced the value of R to .102. This decrease in the value of R is highly significant when Hamilton's (1965) test is applied. An electron density synthesis phased on the final parameters showed only the expected peaks and a difference Fourier synthesis showed no evidence of misplaced atoms. No positive peaks in the difference synthesis were greater than  $1.8e \text{ \AA}^{-3}$ , less than a third of typical carbon atom peaks in earlier difference maps ( $7e \text{ \AA}^{-3}$ ). The final residual is higher than one would wish and is probably due to the paucity of data.

On the final cycle of B.D.L.S. no individual parameter shift was greater than 0.1 of the parameter e.s.d. (estimated standard deviations were derived from inversion of the block-diagonal matrices). The standard deviation of an observation of unit weight, defined as

$$\left[ \sum w (|F_o| - |F_c|)^2 / (M-n) \right]^{1/2}$$

where M (= 621) is the number of observations and n (= 82) is the number of parameters varied, was .988; the expected value for ideal weighting is unity. The final positional and thermal parameters, together with their estimated standard deviations, where appropriate, are listed in Table 2.7. Structure factors are listed in Appendix A.

An absorption correction was not carried out.

Difference between the maximum and minimum transmission coefficients

was only 4.5%. No hydrogen atoms were included in this analysis. A



Table 2.7  
 Fractional coordinates ( $\times 10^4$ )<sup>(a)</sup>, with estimated standard deviations in parentheses

Atoms	x/a	y/b	z/c
I(10)	4757(3)	0	0
Co(10)	5000	4869(4)	2500
O(10)	4230(20)	5710(10)	3240(10)
N(10)	6530(20)	4280(20)	3160(20)
N(20)	4210(20)	4000(10)	3260(20)
C(10)	5240(30)	7330(20)	150(30)
C(20)	4030(30)	7110(20)	-140(20)
C(30)	5870(30)	6830(20)	820(20)
C(40)	3320(30)	6440(20)	170(20)
C(50)	5020(40)	6160(10)	1170(20)
C(60)	3910(30)	5970(20)	880(20)
C(70)	6890(30)	5320(20)	3800(20)
C(80)	2610(40)	4140(20)	2090(20)
C(90)	7210(30)	4040(20)	1860(20)
C(100)	2134(47)	3246(23)	3434(25)
OH(21)	0	7386(14)	2500
OH(22)	1618(27)	6160(17)	3104(18)

Table 2.7 continued  
(b)

Anisotropic temperature factors of the form

$$T = \exp(-(B_{11}h^2 + 2B_{12}hk + 2B_{13}hl + B_{22}k^2 + 2B_{23}kl + B_{33}l^2)) \quad (\times 10^4)$$

and isotropic temperature factors of the form  $T = \exp(-4B_{\text{iso}}(\sin \theta / \lambda)^2)$  ( $\text{\AA}^2$ ), with estimated standard deviations in parentheses

Atom	$B_{11}$	$B_{22}$	$B_{33}$	$B_{12}$	$B_{13}$	$B_{23}$
I(10)	125(4)	77(2)	65(3)	0	0	-3(3)
Co(10)	122(9)	33(3)	38(4)	0	-31(7)	0
C(100)	253(74)	63(20)	66(21)	-61(34)	-32(36)	29(18)
OH(21)	233(61)	38(11)	86(24)	0	-122(40)	0
OH(22)	180(38)	103(18)	76(16)	45(22)	17(24)	3(14)

Atom	$B_{\text{iso}} (\text{\AA}^2)$	Atom	$B_{\text{iso}} (\text{\AA}^2)$	Atom	$B_{\text{iso}} (\text{\AA}^2)$
O(10)	5.6(5)	C(20)	3.9(6)	C(60)	3.5(6)
N(10)	5.2(6)	C(30)	4.4(7)	C(70)	3.5(6)
N(20)	4.3(5)	C(40)	4.6(7)	C(80)	5.2(7)
C(10)	6.3(8)	C(50)	3.9(6)	C(90)	5.0(7)



summary of the analysis is given in Table 2.8.

## 2.7 DETERMINATION OF THE ABSOLUTE CONFIGURATION

In order to establish the correct absolute configuration, structure factors for both possible configurations are calculated and compared with the observed data (Stout & Jensen, 1968; Ibers & Hamilton, 1964). The correct configuration should give the lower R value and the significance of the R-factor ratio can be tested (Hamilton, 1965).

For the enantiomorphous absolute configuration (obtained by reversing the sign of all z-coordinates) the refinement converged to an R value of .125, while the standard deviation of an observation of unit weight was 1.179. Application of Hamilton's test showed that this increase in the value of R, in comparison with that obtained for the enantiomorph, to be highly significant and that, by chance, the correct enantiomorph had been chosen for the analysis. Furthermore, the presence of a chiral centre in the R-1,2-diaminopropane moiety provided an immediate indication of the chirality of the cation since the original R configuration of the diamine is preserved throughout the preparation. Both the R-ratio test and examination of the chiral carbon were in agreement.

All diagrams are presented with respect to a right-handed set of crystal axes and show the correct absolute configuration for  $S-[Co(sal(R)pn(2-Me))_2]I \cdot 3H_2O$ .

## 2.8 DESCRIPTION OF THE STRUCTURE

A perspective view of the  $S-[Co(sal(R)pn(2-Me))_2]^+$  ion, together with atom numbering scheme, is shown in Figure 2.3. Thermal ellipsoids have been drawn to include 50% of the probability distribution.

Table 2.8

Summary of crystal structure analysis of  $S-[Co(sal(R)pn(2-Me))_2]I \cdot 3H_2O$ 

Solution method	Heavy atom
Least-squares method	Block-diagonal
Atom scattering factors (neutral atoms)	Cromer & Waber, 1965
Absorption correction	Not applied
Anomalous dispersion (source)	Included (International Tables, 1962)
Co	$\Delta F' = -2.2$ $\Delta F'' = 3.8$
I	$\Delta F' = -1.2$ $\Delta F'' = 6.9$
O	$\Delta F' = 0.0$ $\Delta F'' = 0.1$
Weighting scheme	Empirical; $w = 1.0/(3.2 + 0.001 F_o^2)$
Range of transmission factors	4.5%
Data for final refinement	All data used
Final model	Anisotropic: I, Co, Methyl-C, $H_2O-O$  Isotropic: All other atoms  No hydrogen atoms
Largest parameter shift on final cycle (average)	0.03 (0.01)
Summary of R values:	
end of isotropic refinement	0.135
final R	0.102
Final difference Fourier peaks	$2.8e \text{ \AA}^{-3}$



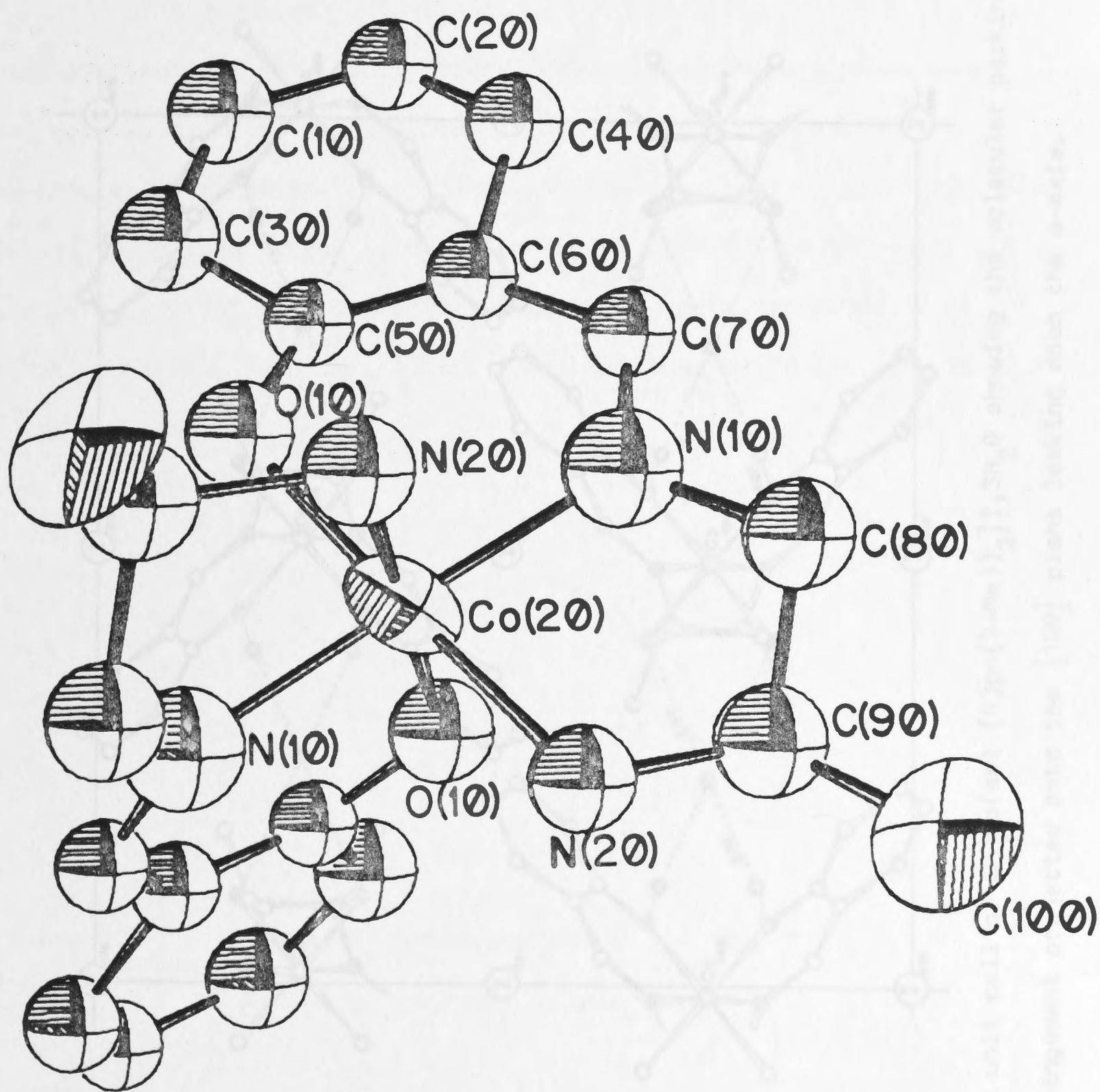


Figure 2.3 Overall stereochemistry of the  $S\text{-[Co(sal(R)pn(2-Me))}_2\text{]}^+$  ion and atom numbering scheme.

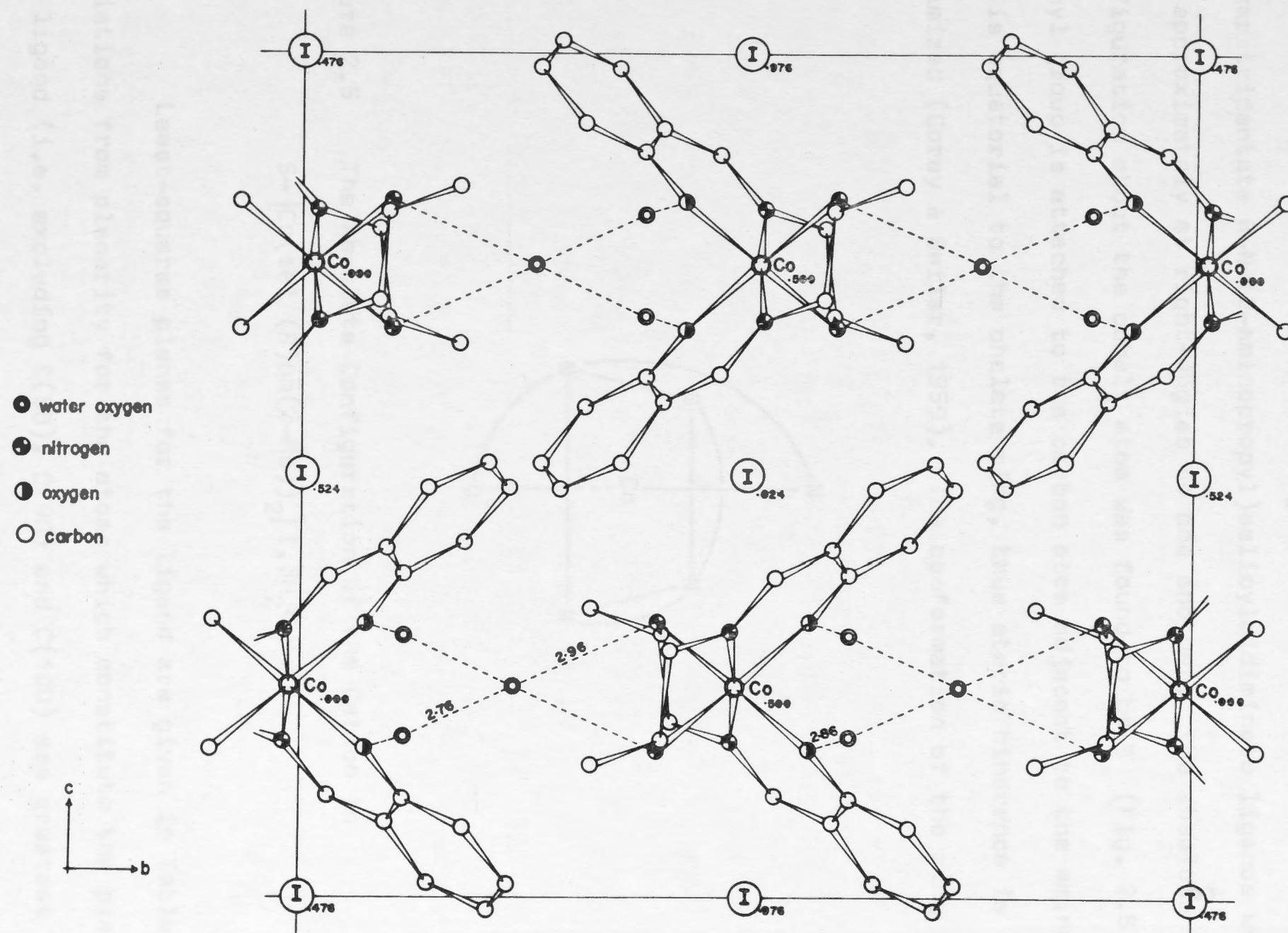


Figure 2.4 The unit cell of  $S-[Co(sal(R)pn(2-Me))_2]I \cdot 3H_2O$  showing the molecular packing arrangement projected onto the  $[100]$  plane looking down the  $a$ -axis.



The unit cell, showing the molecular packing arrangement, is shown in Figure 2.4. The crystal structure consists, as expected, of discrete ions. The cations have true  $C_2$  symmetry.

The  $S-[Co(sal(R)pn(2-Me))_2]^+$  ion consists of two essentially planar tridentate  $R-N-(2-aminopropyl)salicylaldiminato$  ligands which are approximately at right-angles to one another. The absolute configuration about the cobalt atom was found to be  $S$  (Fig. 2.5). The methyl group is attached to the carbon atom adjacent to the amine group and is equatorial to the chelate ring, thus steric hindrance is minimized (Corey & Bailar, 1959). The conformation of the ring is  $\lambda$ .

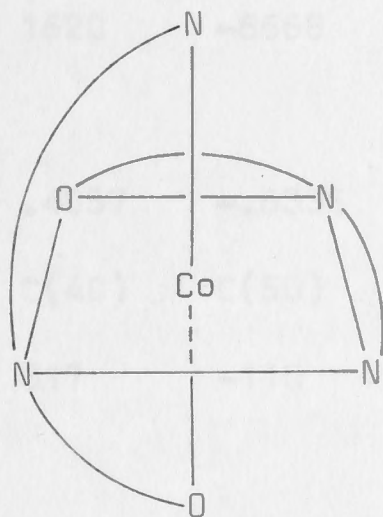
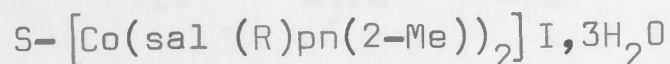


Figure 2.5 The Absolute Configuration of the Cation in

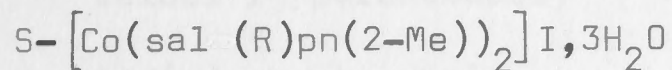


Least-squares planes for the ligand are given in Table 2.9. Deviations from planarity for the atoms which constitute the plane of the ligand (i.e. excluding C(80), C(90) and C(100) are greatest for N(20) and O(10).

Bond angles and bond lengths, given in Table 2.10 and Figure 2.6, are in no way unusual when compared with related structures, with the exception of the C(50) - C(60) bond. In this analysis the average

Table 2.9

Mean planes for the R-N-(2-aminopropyl)salicylaldiminato ligand in



Equations are of the form  $Ax + By + Cz + D = 0$  where  $x$ ,  $y$  and  $z$  refer to the unit cell axes. The coefficients for each plane are given, followed by the atoms defining the plane and their distances from that plane ( $\text{\AA} \times 10^4$ ).

				A	B	C	D
Plane (1)				.3870	-.6457	-.6582	5.4948
Co(10)	N(10)	N(20)	O(10)	C(10)	C(20)	C(30)	C(40)
4	842	-1523	1916	-680	-419	-302	322
C(50)	C(60)	C(70)	C(80)	C(90)	C(100)		
-378	-191	409	1620	-6668	-3533		
Plane (2)				.4057	-.6335	-.6589	5.3031
C(10)	C(20)	C(30)	C(40)	C(50)	C(60)		
-137	-159	264	317	-110	-175		
Plane (3)				.3709	-.6367	-.6761	5.5890
Co(10)	N(10)	O(10)	C(50)	C(60)	C(70)		
-879	402	1227	-724	-301	276		
Plane (4)				.3874	.6483	-.6556	-4.6384

this plane is symmetry related to plane (1) by a  $C_2$  axis.

#### Dihedral angles (degrees)

Plane (1) - Plane (2)	1.3	Plane (2) - Plane (3)	2.2
Plane (1) - Plane (3)	1.5	Plane (2) - Plane (4)	79.7
Plane (1) - Plane (4)	80.6	Plane (3) - Plane (4)	79.9



Table 2.10

Bond lengths and angles for  $S-[Co(sal(R)pn(2-Me))_2]I \cdot 3H_2O$  (e.s.d. values in parentheses)

## (a) about cobalt

Atoms	Bond lengths (Å)	Atoms	Bond angles (degrees)
Co(10)-O(10)	1.93(2)	N(10)-Co(10)-O(10)	95(1)
Co(10)-N(10)	1.91(2)	N(10)-Co(10)-N(20)	85(1)
Co(10)-N(20)	1.99(2)	N(10)-Co(10)-N(20) <sup>'</sup>	91(1)
		N(10)-Co(10)-O(10) <sup>'</sup>	95(1)
		O(10)-Co(10)-O(10) <sup>'</sup>	91(1.3)
		O(10)-Co(10)-N(20) <sup>'</sup>	89(1)
		N(20)-Co(10)-N(20) <sup>'</sup>	91(1.4)
		N(10)-Co(10)-O(10) <sup>'</sup>	89(1)

' the superscript indicates atoms belong to the  $C_2$  symmetry related ligand attached to the same cobalt atoms

## (b) for (sal(R)pn(2-Me)) ligand

Atoms	Bond lengths (Å)	Atoms	Bond angles (degrees)
C(10)-C(20)	1.40(5)	C(10)-C(20)-C(40)	126(3)
C(20)-C(40)	1.41(4)	C(20)-C(40)-C(60)	115(3)
C(40)-C(60)	1.46(4)	C(40)-C(60)-C(50)	121(3)
C(60)-C(50)	1.30(5)	C(60)-C(50)-C(30)	127(3)
C(50)-C(30)	1.50(4)	C(50)-C(30)-C(10)	112(3)
C(30)-C(10)	1.44(5)	C(30)-C(10)-C(20)	120(3)
C(60)-C(70)	1.42(4)	C(50)-C(60)-C(70)	127(3)
C(70)-N(10)	1.31(4)	C(60)-C(70)-N(10)	122(3)
N(10)-C(80)	1.47(4)	C(70)-N(10)-Co(10)	127(2)
C(80)-C(90)	1.61(4)	C(80)-N(10)-Co(10)	115(2)
C(90)-C(100)	1.52(5)	C(90)-C(80)-N(10)	105(3)
C(90)-N(20)	1.51(4)	C(80)-C(90)-C(100)	109(3)
C(50)-O(10)	1.40(4)	C(80)-C(90)-N(20)	104(3)
		N(20)-C(90)-C(100)	112(3)
		C(90)-N(10)-Co(10)	108(2)
		C(50)-O(10)-Co(10)	120(2)
		O(10)-C(50)-C(60)	127(3)

aromatic carbon-carbon bond is 1.45(4) Å which is 0.14 Å longer than the C(50)-C(60) bond. This difference is greater than 3  $\sigma$ , where  $\sigma$  is the average s.d. No explanation is offered for the shortening of the C(50)-C(60) bond.

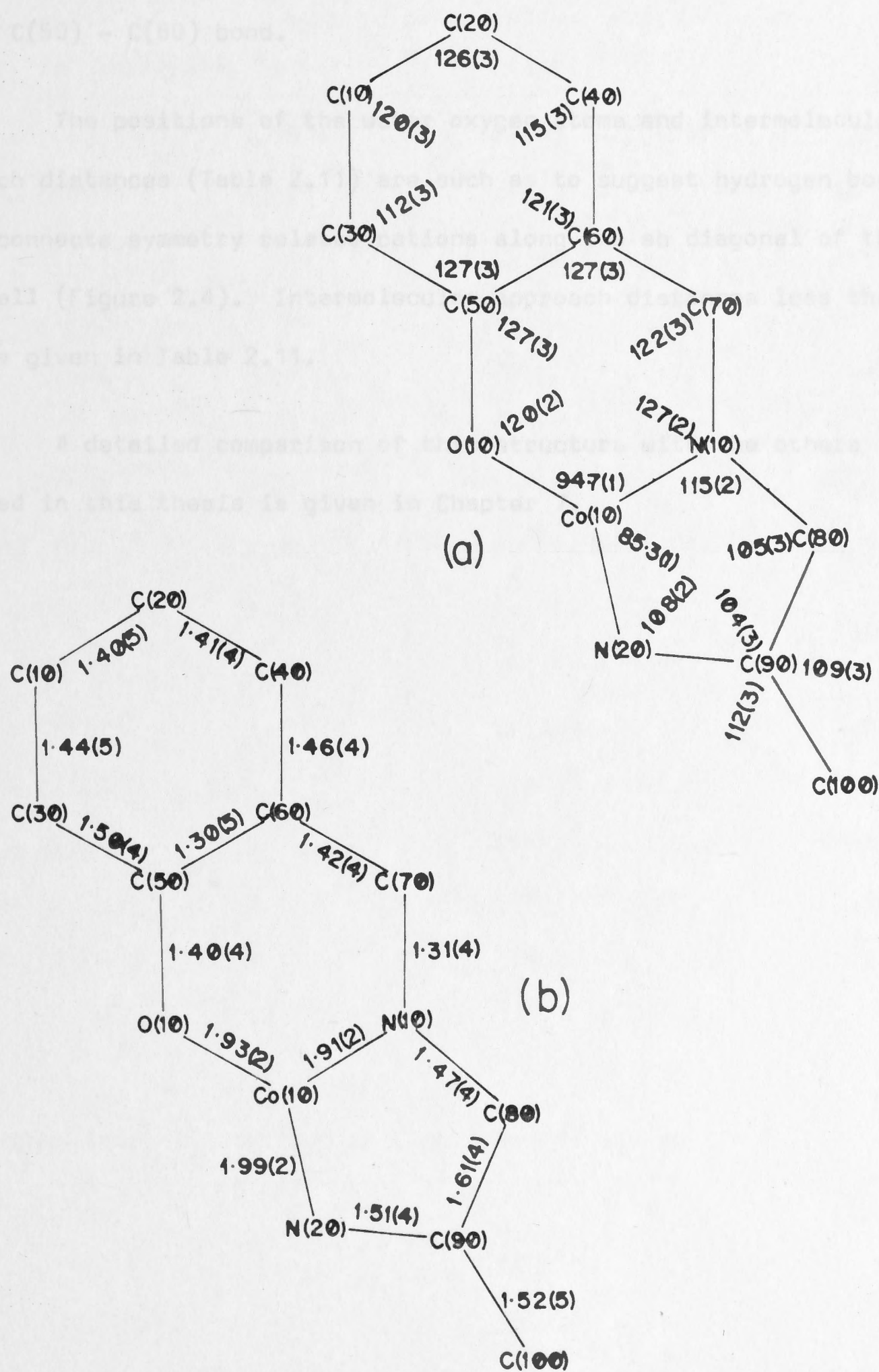


Figure 2.6 (a) Bond angles (degrees) and (b) bond lengths (Å) for  $S-[Co(sal(R)pn(2-Me))_2]I \cdot 3H_2O$  (estimated standard deviations in parentheses).



aromatic carbon - carbon bond is 1.45(4) Å which is 0.14 Å longer than the C(50) - C(60) bond. This difference is greater than  $3\sigma_{av}$ , where  $\sigma_{av}$  is the average e.s.d. No explanation is offered for the shortening of the C(50) - C(60) bond.

The positions of the water oxygen atoms and intermolecular approach distances (Table 2.11) are such as to suggest hydrogen bonding, which connects symmetry related cations along the ab diagonal of the unit cell (Figure 2.4). Intermolecular approach distances less than 4 Å are given in Table 2.11.

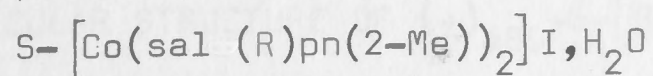
A detailed comparison of this structure with the others reported in this thesis is given in Chapter 7.

C(10) <sup>a</sup> - C(10) <sup>b</sup>	3.84	OH(21) - C(10)	3.87
C(20) <sup>a</sup> - OH(21)	3.91	C(21) - C(20)	3.83
OH(21) - OH(22)	2.75*	OH(21) - C(17)	3.42
C(20) - OH(22)	3.91	OH(22) - C(20)	3.91
C(70) <sup>a</sup> - C(80) <sup>b</sup>	3.91	C(10) <sup>a</sup> - C(10) <sup>b</sup>	3.84
C(40) <sup>a</sup> - C(70) <sup>b</sup>	3.94	C(10) <sup>a</sup> - C(10) <sup>b</sup>	3.84
C(40) <sup>a</sup> - C(100) <sup>b</sup>	4.03	OH(21) - C(20)	3.87
C(40) <sup>a</sup> - C(80) <sup>b</sup>	3.85	C(20) <sup>a</sup> - C(100) <sup>b</sup>	3.87

\* hydrogen bonds illustrated in Figure 2.4 as broken lines.

Table 2.11

Intermolecular approach distances less than 4 Å for



Transformations of the asymmetric unit are indicated by superscripts

a: 0, y,  $\frac{1}{4}$ ; b:  $\frac{1}{2}$ ,  $\frac{1}{2}+y$ ,  $\frac{1}{4}$ ; c: 0,  $\bar{y}$ ,  $\frac{3}{4}$ ; d:  $\frac{1}{2}$ ,  $\frac{1}{2}-y$ ,  $\frac{3}{4}$

I(10) - OH(22)	3.70	C(40) <sup>a</sup> - C(10) <sup>d</sup>	3.84
Co(10) - OH(21)	3.98	C(60) <sup>a</sup> - C(70) <sup>c</sup>	3.86
N(10) <sup>a</sup> - C(40) <sup>c</sup>	3.65	C(70) <sup>a</sup> - C(70) <sup>c</sup>	3.79
N(20) <sup>a</sup> - C(20) <sup>c</sup>	3.56	C(20) <sup>a</sup> - C(30) <sup>d</sup>	3.89
N(20) <sup>a</sup> - C(10) <sup>c</sup>	3.61	OH(22) - O(10)	2.86*
N(20) <sup>a</sup> - C(40) <sup>c</sup>	3.96	C(90) - OH(21)	3.67
C(10) <sup>a</sup> - C(100) <sup>b</sup>	3.61	OH(21) - C(100)	3.64
C(10) <sup>a</sup> - C(100) <sup>d</sup>	3.84	OH(21) - C(90)	3.67
C(20) <sup>a</sup> - OH(21)	3.81	OH(21) - C(20)	3.83
OH(21) - OH(22)	2.76*	OH(21) - C(80)	3.83
C(20) - OH(22)	3.91	OH(22) - C(20)	3.91
C(20) <sup>a</sup> - C(80) <sup>c</sup>	3.91	C(60) <sup>a</sup> - C(100) <sup>b</sup>	3.97
C(40) <sup>a</sup> - C(70) <sup>c</sup>	3.51	C(10) <sup>a</sup> - C(100) <sup>c</sup>	3.91
C(40) <sup>a</sup> - C(100) <sup>c</sup>	3.63	OH(21) - N(20)	2.96*
C(40) <sup>a</sup> - C(80) <sup>c</sup>	3.65	C(20) <sup>a</sup> - C(100) <sup>b</sup>	3.37

\* hydrogen bonds illustrated in Figure 2.4 as broken lines



## CHAPTER 3

CRYSTAL AND MOLECULAR STRUCTURE OF  $(+)_489$ -S-[R-N-(2-AMINOPROPYL) SALICYLALDIMINATO] - (R-N-((2-AMINO-1-METHYL)ETHYL) SALICYLALDIMINATO) COBALT (III)]PERCHLORATE, 0.75 ETHANOL\*

## 3.1 UNIT CELL AND DIFFRACTION SYMMETRY

Euhedral crystals were grown by slow evaporation of an ethanolic solution of S-[Co(sal (R)pn(1-Me))(sal (R)pn(2-Me))]ClO<sub>4</sub>, 0.75 EtOH. The crystals were generally twinned, as evidenced by re-entrant angles and appearance under crossed polarizers. One crystal was eventually found which proved to be a single individual. This crystal was mounted about the longest axis for photographic experiments.

Unit cell parameters and diffraction symmetry were determined from equi-inclination Weissenberg and precession photographs. The crystal was found to belong to the monoclinic system and had the unit cell dimensions

$$\begin{array}{ll} a = 10.60 \text{ \AA} & \alpha = \gamma = 90.0^\circ \\ b = 7.71 \text{ \AA} & \beta = 92^\circ 34' \\ c = 15.57 \text{ \AA} & V = 1272 \text{ \AA}^3 \end{array}$$

Systematic absences were determined to be

$$\begin{array}{ll} hkl; \text{ no conditions} & 0k0; k = 2n + 1 \\ h0l; \text{ no conditions} & \end{array}$$

These conditions establish the space group as either P2<sub>1</sub> (No. 4) or P2<sub>1</sub>/m (No. 11) (International Tables, 1952). Space group P2<sub>1</sub> was used in this analysis since the presence of a mirror plane, m, is not possible with an optically active compound.

\* S-[Co(sal (R)pn(1-Me))(sal (R)pn(2-Me))]ClO<sub>4</sub>, 0.75 EtOH for brevity

Re-examination of the crystal showed that the morphology was due to the presence of the pinacoids (001) and (010) and the hemi-orthodomes (101) and ( $\bar{1}01$ ).

The density of the crystals was determined to be  $1.41 \text{ g cm}^{-3}$  by the method of flotation using a mixture of carbon tetrachloride and ethyl bromide. This value of  $D_m$  gave  $Z = 2$ , corresponding to  $D_c = 1.39 \text{ g cm}^{-3}$ .

### 3.2 DATA COLLECTION AND REDUCTION

#### 3.2.1 Unit cell refinement

The crystal was mounted about the b-axis (Araldite Fast Set; glass capillary) and placed on a Picker FACS-I automatic four-circle diffractometer. The crystal was oriented so that the b-axis was coincident with the  $\phi$ -axis of the diffractometer.

Unit cell parameters were refined by the method of least-squares (Busing, Ellison, Levy, King & Rosebury, 1968). Twelve prominent reflections were chosen to give a wide range of h, k and l with large  $2\theta$  values (Table 3.1).  $2\theta$ ,  $\chi$ ,  $\phi$  and  $\omega$  values for each reflection were refined individually using  $\text{Cu-K}\alpha_1$  radiation, and the results used to produce a new orientation matrix and refined unit cell parameters which are listed below

$$a = 10.683(4) \text{ \AA}$$

$$\alpha = \gamma = 90.0^\circ$$

$$b = 7.672(3) \text{ \AA}$$

$$\beta = 92.40(4)^\circ$$

$$c = 15.565(6) \text{ \AA}$$

$$V = 1273.25 \text{ \AA}^3$$

#### 3.2.2 Data collection

Both  $\text{H}\bar{\text{K}}\text{L}$  and  $\text{HKL}$  data were collected using graphite monochromated  $\text{Cu-K}\alpha_1$  radiation and a maximum value for  $\theta$  of  $62.5^\circ$ .

Intensities were measured, at room temperature, in the bisecting



$\theta - 2\theta$  mode, where the  $\chi$  and  $\phi$  circles were set to make the scattering vector coincident with the horizontal plane and the plane of the  $\chi$  circle. The counter was moved so as to make an angle of  $(2\theta - w/2)^\circ$  with the incident radiation, where  $w$  is the scan range (here  $2.5^\circ$ ). In this way the  $\chi$  circle plane always bisects the angle between the incident and the diffracted beams. An integral count,  $I$ , was recorded as the counter was moved at constant speed ( $2^\circ \text{min}^{-1}$ ) to an angle  $(2\theta + w/2 + d)^\circ$ , where  $d$  is the dispersion correction. The crystal moved at a constant speed of  $1^\circ \text{min}^{-1}$ , thus maintaining bisecting geometry. Background counts,  $B_1$  and  $B_2$ , were made with the counter stationary at the initial and final scan positions for the same period (10 sec.).

Table 3.1

Unit cell refinement data for  $S\text{-}[\text{Co}(\text{sal}(\text{R})\text{pn}(1\text{-Me}))(\text{sal}(\text{R})\text{pn}(2\text{-Me}))]\text{ClO}_4$ ,  
0.75 EtOH

$h$	$k$	$l$	$2\theta$	$h$	$k$	$l$	$2\theta$
0	-4	0	47.356	0	0	-8	46.685
6	0	0	51.313	4	-4	4	64.994
-5	-3	-5	65.131	5	-3	5	65.131
1	-2	6	43.221	-4	-1	-11	78.863
-5	-2	-5	58.578	1	-2	8	53.832
3	-2	7	55.066	2	-1	9	57.996

If the count rate exceeded 5000 counts per second a nickel foil attenuator was automatically inserted. Five such attenuators were available. The discrimination levels were set to admit 95% of the  $\text{Cu-K}\alpha_1$  peak. Three standard reflections were each measured after every 97 reflections.

### 3.2.3. Data reduction

A graph of intensity versus reflection sequence number for each of the standard reflections was plotted. To each of the three graphs a least-squares fit was calculated to give the slope which was used to obtain anisotropic linear correction factors, these were

$$0 \quad -4 \quad 0 \quad .1001 \times 10^{-4}; \quad 0 \quad 0 \quad 5 \quad .1096 \times 10^{-4}; \quad 6 \quad 0 \quad 0 \quad .7975 \times 10^{-4}$$

The mean fractional drop (degradation factor,  $D_t$ ) of intensity during data collection was corrected using the method of Churchill & Kalra (1974). The degradation factor is given by

$$D_t = (p_1^2 + p_2^2 + p_3^2) / (p_1^2/k_1^2 + p_2^2/k_2^2 + p_3^2/k_3^2)^{-\frac{1}{2}}$$

where  $k_i$  is the fraction of the  $i^{\text{th}}$  standard at the  $t^{\text{th}}$  point in the data collection sequence and  $p_i$  is the cosine of the angle between the reciprocal lattice vector of the reflection being corrected and that of the  $i^{\text{th}}$  standard.

The values of the observed intensity,  $I$  and  $\sigma_1(I)$  were calculated as follows

$$I = AF \cdot D_t (I^{\text{obs}} - (t_p/t_b)(B_1 + B_2))$$

where  $AF$  is the attenuator factor used for that reflection,  $t_p$  is the time for the integrated peak count and  $t_b$  is the background count time and

$$\sigma_1(I) = (AF \cdot D_t \cdot (I^{\text{obs}} + (t_p/t_b)(B_1 + B_2)))^{\frac{1}{2}}$$

The observed structure factors,  $F_o$ , and the estimated standard deviation,  $\sigma_1(F_o)$ , were calculated as follows

$$F_o = (I/L_p)$$

$$\text{and } \sigma_1(F_o) = \sigma_1(I) / (L_p \cdot 2 F_o)$$

where the Lorentz-polarization factor,  $L_p$ , is given by



$$L_p = (\cos^2 2\theta + \cos^2 2\theta_m) / (\sin 2\theta (1 + \cos^2 2\theta_m))$$

where  $\theta_m$  refers to the Bragg angle for the monochromator ( $26.5^\circ$ ).

Backgrounds were checked for equivalence. If  $\Delta B > 6.00 \sigma_1(B)$ , where  $\Delta B = |B_1 - B_2|$  and  $\sigma_1(B) = (B_1 + B_2)^{\frac{1}{2}}$ , the backgrounds were considered uneven and the reflection was rejected. Only 15 such reflections were present in the data. Furthermore, if  $I_{hkl} < 3.0 \sigma_1(I_{hkl})$  the reflection was rejected as unobserved. A total of 2205 observed data were collected (1568 unobserved reflections; 41.6%). The high number of unobserved data was probably due to the use of a high value for  $2\theta$  and a rapid cut off of intensity where  $2\theta > \text{ca } 60.0^\circ$ .

A second estimated standard deviation,  $\sigma_2$ , was calculated for each  $F_o$  using the relation

$$\sigma_2(F_o) = ((\sigma_1(F_o))^2 + (p^2 F_o^4))^{1/2}$$

where  $p^2 (= .002)$  is the "instrumental uncertainty factor" (Busing & Levy, 1957a; Corfield, Doedens & Ibers, 1967). The values of  $\sigma_2$  were used to provide a weighting scheme throughout the analysis, ( $w = 1/\sigma_2^2$ ).

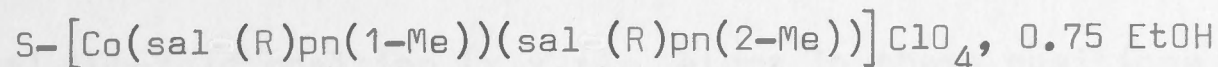
Comparison of the  $2\theta$  values of reflections with a powder pattern obtained using a Philips PW1050/25 recording diffractometer and Ni-filtered Cu-K $\alpha$  radiation showed excellent agreement indicating that the crystal used for data collection was representative of the bulk sample. Data collection conditions are summarised in Table 3.2.

### 3.3 DETERMINATION OF COBALT AND CHLORINE ATOM POSITIONS

The ratio  $\Sigma z_h^2 / \Sigma z_l^2$  was calculated as 0.44 with cobalt as the only heavy atom and 0.73 with cobalt and chlorine as the heavy atoms. Hence, it was decided to utilize normal heavy atom techniques.

Table 3.2

Summary of crystal data and data collection for



Chemical formula	$C_{22}H_{26}N_4O_2CoClO_4, 0.75(C_2H_5OH)$
Formula weight	571.5
Space group	$P2_1$ (No. 4)
Boundary faces of crystal; (mm from internal origin in parentheses)	$\begin{array}{cccccc} 0 & 0 & 1 & (.045) & 0 & 0 & -1 & (.044) \\ 1 & 0 & 1 & (.083) & -1 & 0 & -1 & (.080) \\ -1 & 0 & 1 & (.114) & 0 & 1 & 0 & (.315) \\ 0 & -1 & 0 & (.315) & & & & \end{array}$
Unit cell parameters	$a = 10.683(4) \text{ \AA}$ $b = 7.672(3) \text{ \AA}$ $c = 15.565(6) \text{ \AA}$ $\alpha = \gamma = 90^\circ$ $\beta = 92.40(4)^\circ$ $V = 1273.25 \text{ \AA}^3$
Radiation for unit cell refinement	$Cu-K\alpha_1 = 1.5405 \text{ \AA}$
Density	$1.41 \pm 0.04 \text{ g cm}^{-3}$
$D_m$	
$D_c$	$1.39 \text{ g cm}^{-3}$
Z	2
Linear absorption coefficients	$\mu(Cu-K\alpha) = 66.67 \text{ cm}^{-1}$ $\mu(Mo-K\alpha) = 10.27 \text{ cm}^{-1}$
Radiation used for data collection (monochromator; $2\theta$ )	$Cu-K\alpha_1$ (graphite; $26.50^\circ$ )
Scan width; speed; dispersion	$(2.5 + \Delta)^\circ$ ; $2^\circ \text{ min}^{-1}$ ; 0.285
Scan mode	$\theta - 2\theta$
Background times	10 sec
Standard reflections	0 -4 0; 6 0 0; 0 0 5
Standard linear correction factors ( $\times 10^4$ )	0.1001; 0.7975; 0.1096
Standard frequency	97
Data collected ( $2\theta$ limit)	$\overline{HKL}$ and $\overline{HKL}$ ( $125.0^\circ$ )
Number of observed data (%)	2205 (58.4)



Since  $S-[Co(sal(R)pn(1-Me))(sal(R)pn(2-Me))]ClO_4 \cdot 0.75 EtOH$  crystallizes in space group  $P2_1$  and  $Z = 2$ , cobalt and chlorine must each occupy the general two-fold position  $(x,y,z)$ . Atoms in these positions give rise to the Patterson vectors

$$\pm 2x, \frac{1}{2}, \pm 2z$$

Hence, either the cobalt or chlorine  $y$ -coordinate must be set equal to zero to define the cell origin (it was decided to set the cobalt  $y = 0$ ). Prominent Patterson peaks are listed and their subsequent analysis is given in Table 3.3.

Both cobalt and chlorine atoms were given initial isotropic temperature factors of  $3.5 \text{ \AA}^2$  and the scale factor was set equal to unity. Scattering factors used were those for neutral atoms (Cromer & Waber, 1965). Anomalous dispersion terms  $\Delta F'$  and  $\Delta F''$  were included (International Tables, 1962), although no allowance was made for their dependence upon  $\sin \theta$ .

One cycle of B.D.L.S. was carried out on the scale factor only and the resulting data was used to phase a difference Fourier synthesis. The value of  $R$  was .386.

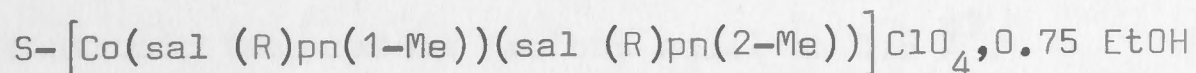
### 3.4 DETERMINATION OF LIGHT ATOM POSITIONS

The position of the atoms in the cobalt coordination octahedron were determined from the above difference Fourier synthesis (Table 3.4) and give the arbitrary designations N(10) to N(40), O(10) and O(20). These atoms were given individual isotropic temperature factors equal to  $3.5 \text{ \AA}^2$ .

The model was subjected to one cycle of B.D.L.S. (scale factor, atom positional and thermal parameters) reducing the value of  $R$  to .330. A difference Fourier synthesis was phased on the recalculated

Table 3.3

Analysis of Patterson peaks for



N	U	V	W	H	D(000)Å	Comments
1	0	0	0	999		
2	.534	.500	.408	201	9.19	Co - Co?
3	.170	0	.036	169	1.88	Co - O/N? proved to be Co - N(10) and Co - N(20)
4	.120	.500	.879	110	14.22	
5	.501	.674	.497	82		
6	.502	.327	.496	85		
7	.608	.217	.123	85	6.89	Co - Cl?
8	.352	0	.415	81	7.33	Co - Cl?
9	.625	0	.174	76	7.100	Co - Cl?
10	.308	$\frac{1}{2}$	.158	58		

## Analysis:

Cross vectors for atoms which result from peaks 2 and 4 were not present in the map.

- (i) assume peak 2 is a Co - Co vector; assume position .767,0,.204
- (ii) assume Co - Cl distance is in the range 6 - 8 Å; peak 7 corresponds to such a vector.

Hence:

Cl position: .159, .784, .081

Cl - Cl vector: .318,  $\frac{1}{2}$ , .162 i.e. peak 10

B.D.L.S. with Co(10) + Cl(10) gave an R value of .386 and the positions subsequently proved to be correct.



structure factors and this gave the position of the perchlorate oxygen atoms (O(30) to O(60); Table 3.4). These oxygen atoms were given individual isotropic temperature factors equal to  $3.5 \text{ \AA}^2$ .

One cycle of B.D.L.S. (scale factor, atom positional and thermal parameters) gave a value for R equal to .319. A difference Fourier synthesis phased on the model gave the position of one aromatic ring and the carbon atoms of the associated ethylenediamine bridge (C(10) to C(90); Table 3.4). Also the re-designations N(40)  $\rightarrow$  O(140) and O(20)  $\rightarrow$  N(120) were now made. The carbon atoms were given individual isotropic temperature factors equal to  $3.5 \text{ \AA}^2$ .

The model was subjected to one cycle of B.D.L.S., refining scale factor, atom thermal and positional parameters, and the resulting phases were used to calculate a difference Fourier synthesis. R was equal to .270. This Fourier gave the position of the atoms in the second aromatic ring and the methyl carbon atom of the first salpn ligand (C(110) to C(170) and C(100) respectively; Table 3.4). The new carbon atoms were given individual isotropic temperature factors equal to  $3.5 \text{ \AA}^2$ .

One cycle of B.D.L.S. (parameters as before) was followed by a difference Fourier synthesis, the R value was .228 at this stage. The positions of the remaining carbon atoms were now determined (Table 3.4) and these atoms were given individual isotropic temperature factors equal to  $3.5 \text{ \AA}^2$ .

One cycle of B.D.L.S. on the model (scale factor, atom positional and thermal parameters) gave a value for R equal to .212. Examination of a difference Fourier synthesis calculated after this cycle of B.D.L.S. gave the position of what was assumed to be the oxygen atom of one

Table 3.4

Initial atom positions for  $S-[Co(sal(R)pn(1-Me))(sal(R)pn(2-Me))]ClO_4 \cdot 0.75 EtOH$  obtained from difference Fourier syntheses

Atom	X	Y	Z	Interatomic distances (Å)	
N(10)	.404	.495	.831	Co(10) - N(10)	1.92 cf 1.99 <sup>a</sup>
N(20)	.063	.551	.766	- N(20)	1.96
N(30)	.219	.721	.851	- N(20)	1.94
N(40)	.234	.265	.745	- N(40)	1.98 (O(140))
O(10)	.281	.618	.681	- O(10)	2.01 cf 2.13 <sup>b</sup>
O(20)	.188	.397	.903	- O(20)	1.92 (N(120))
O(30)	.906	.397	.979	Cl(10) - O(30)	1.46 cf 1.44 <sup>a</sup>
O(40)	.809	.320	.848	- O(40)	1.20
O(50)	.750	.221	.957	- O(50)	1.40
O(60)	.938	.176	.872	- O(60)	1.46
C(10)	.500	.542	.702	C(10) - C(20)	1.39 cf 1.395 <sup>a</sup>
C(20)	.612	.523	.662	C(20) - C(30)	1.35
C(30)	.625	.618	.574	C(30) - C(40)	1.42
C(40)	.500	.640	.532	C(40) - C(50)	1.32
C(50)	.405	.649	.558	C(50) - C(60)	1.42
C(60)	.375	.595	.649	C(10) - C(70)	1.26 ?
C(70)	.495	.496	.785	C(70) - N(10)	1.25
C(80)	.406	.397	.925	C(80) - C(90)	1.60
C(90)	.313	.309	.936	C(80) - N(10)	1.48
C(100)	.313	.265	.043	C(90) - O(20)	1.50 (N(120))
C(110)	.031	.574	.447	C(110) - C(120)	1.58
C(120)	.061	.752	.382	C(120) - C(130)	1.42
C(130)	.031	.309	.669	C(130) - C(140)	1.57
C(140)	.156	.228	.681	C(140) - C(150)	1.39
C(150)	.187	.074	.638	C(150) - C(160)	1.36
C(160)	.094	.985	.585	C(170) - C(130)	1.43
C(170)	.969	.507	.702	C(180) - C(190)	1.56
C(180)	.000	.721	.808	C(180) - N(20)	1.50
C(190)	.125	.808	.809	C(190) - N(30)	1.49
C(200)	.102	.277	.227	C(200) - C(190)	
OH(20)	.413	.013	.790	OH(20) - CET(1)	1.45 cf 1.43 <sup>a</sup>
CET(1)	.543	.001	.772	CET(1) - CET(2)	1.49 cf 1.54 <sup>a</sup>
CET(2)	.590	.036	.682	OH(20) - CET(1) - CET(2)	118°

a International Tables (1962)

b Saito (1968)



molecule of water of crystallization (see section 3.5.3). Adjacent to this position were two smaller peaks (designated CET(1) and CET(2)), which were within bonding distance of the oxygen. These peaks were initially thought to be satellites due to anisotropy of the thermal motion. The oxygen atom was given an isotropic temperature factor equal to  $3.5 \text{ \AA}^2$ .

The model was subjected to six cycles of B.D.L.S. (scale factor, atom positional and thermal parameters refined) and a difference Fourier synthesis phased on the resulting data; R was now equal to .132. Examination of the difference Fourier still showed the presence of the two small peaks noted above. Anisotropic temperature factors (see section 3.5.2) were introduced in order to investigate the reality of the small peaks. Four cycles of B.D.L.S. (scale factor, atom thermal and positional parameters) gave a residual of .111 and a difference Fourier map phased on the refined model showed the persistence of the two peaks CET(1) and CET(2).

### 3.5 ABSORPTION CORRECTION AND LEAST-SQUARES REFINEMENT

#### 3.5.1. Absorption correction and isotropic refinement

The data were corrected for absorption (de Meulenaer & Tompa, 1965) using a linear absorption coefficient for Cu-K $\alpha$  radiation equal to  $66.67 \text{ cm}^{-1}$ , which was obtained from available data (International Tables, 1962) and the following crystal dimensions

0	0	1	(.045 mm)	0	0	-1	(.044 mm)
1	0	1	(.083 mm)	-1	0	-1	(.080 mm)
-1	0	1	(.114 mm)	0	1	0	(.315 mm)
0	-1	0	(.315 mm)				

where the perpendicular to the face is measured to an arbitrary internal origin. Absorption corrections ranged from .452 to .769 in value.

A  $\sigma_2$  weighting scheme was recalculated and applied to eight cycles of B.D.L.S. (132 parameters; scale factor, atom positional and thermal parameters), which gave a final value for R equal to .127.

### 3.5.2. Initial anisotropic refinement and calculation of hydrogen atom positions

The temperature factors of all non-hydrogen atoms were now converted to the anisotropic form

$$T = \exp(-(B_{11}h^2 + 2B_{12}hk + 2B_{13}hl + B_{22}k^2 + 2B_{23}kl + B_{33}l^2))$$

Nine cycles of B.D.L.S. (297 parameters; scale factor, atom positional and thermal parameters) gave a final value for R equal to .097. This decrease in the value of R when anisotropic thermal parameters were introduced is highly significant (Hamilton, 1965).

The position of all the hydrogen atoms with the exception of those attached to the methyl carbon atoms were calculated (Churchill, 1973) and added to the model. The positions of the hydrogen atoms were calculated using an average bond length of 1.0 Å. These atoms were given individual isotropic thermal parameters equal to 1.1 times the equivalent isotropic B of the attached non-hydrogen atom. The hydrogen scattering factors used were those for a neutral atom (Stewart, Davidson & Simpson, 1965).

Three cycles of B.D.L.S. (297 parameters; scale factor, positional and thermal parameters of non-hydrogen atoms) reduced the value of R to .095. A difference Fourier synthesis phased on the resulting model still showed the presence of peaks CET(1) and CET(2).

### 3.5.3. Re-examination of composition and final anisotropic refinement

On the basis of microanalytical data it was initially thought that one molecule of water was present in the asymmetric unit. As



noted above, examination of several difference Fourier syntheses showed the persistence of two small peaks (CET(1) and CET(2)). In the final Fourier map the heights of these peaks were 3.11 and  $1.95e \text{ \AA}^{-3}$  respectively. The two peaks were in such a position as to suggest the presence of ethanol (Table 3.4); the solvent from which the crystal was obtained.

A bulk sample was heated on a thermal balance and the resulting weight loss suggested the presence of 0.75 moles of ethanol per stoichiometric unit. Furthermore, a low temperature mass spectrum of the sample confirmed the presence of ethanol (Budzikiewicz, Djerassi & Williams, 1967). Hence, the refinement of the structure was continued with a fixed occupancy of 0.75 for a molecule of ethanol of crystallization.

The ethanol carbon atoms were given individual isotropic temperature factors of  $3.5 \text{ \AA}^2$  which were immediately converted to the anisotropic form for subsequent least-squares refinement. The model, including the solvent molecule, was subjected to two cycles of B.D.L.S. (scale factor, positional and thermal parameters of all atoms). The resulting value for R was .068; a highly significant drop.

Several other models for the solvent molecule(s) were tried (Table 3.5). Occupancy of the oxygen position always refined to a greater value than those for CET(1) and CET(2). Using ethanol for the solvent molecule produced an occupancy for the carbon atoms between .706 and .785, which is in good agreement with that suggested by the thermal balance data, namely 0.75.

Since the oxygen occupancy refined to a value near unity, it is suggested that this site could be partially occupied by water oxygen.

Table 3.5

Models for occupancy of solvent site for  $S-[Co(sal(R)pn(1-Me))(sal(R)pn(2-Me))]ClO_4 \cdot 0.75 EtOH$ 

Solvent	Occupancies			Bonds (Å)		R	X,Y,Z refined	Comments
	OH(20)	CET(1)	CET(2)	OH(20)-CET(1)	CET(1)-CET(2)			
H <sub>2</sub> O only	1.0	0.0	0.0	-	-	.095	yes	Hydrogens included
H <sub>2</sub> O disordered	1.02	0.71	0.84	1.44	1.22	.063	yes	Occupancies refined, hydrogens included
Ethanol	1.0	1.0	1.0	1.40	1.37	.078	yes	1.0 mole EtOH, no hydrogens
Ethanol	1.0	1.0	1.0	1.41	1.22	.065	yes	1.0 mole EtOH, hydrogens included
Ethanol	0.99	0.76	0.76	1.47	1.39	.078	yes	Occupancy refined, no hydrogens
Ethanol	0.98	0.71	0.79	1.43	1.21	.066	yes	Occupancy refined, hydrogens included
Ethanol	0.75	0.75	0.75	1.33	1.19	.067	yes	Fixed occupancy, hydrogens included
Ethanol	0.75	0.75	0.75	1.45	1.49	.068	no	Fixed occupancy, X,Y,Z from Fourier, hydrogens included



Corresponding to a stoichiometry of  $0.25(\text{H}_2\text{O}), 0.75(\text{C}_2\text{H}_5\text{OH})$ . This would involve disorder in the structure at either sub- or super-cell level, a state of affairs which cannot be resolved by x-ray crystallographic studies.

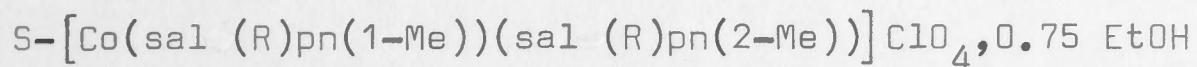
From Table 3.5 it can be seen that refinement of the ethanol positions leads to a very short carbon-carbon bond, in the range 1.39 to 1.19 Å, depending upon the overall model used. However, choosing the atom positions from a difference Fourier synthesis and not refining these positions, preserves a more reasonable bond length of 1.49 Å. This is still shorter than the value of 1.54 Å given in International Tables (1962).

Seven cycles of B.D.L.S. (306 parameters; scale factor non-hydrogen atom positional and thermal parameters; the ethanol atom positional parameters not refined and an occupancy of 0.75 for ethanol) gave a final R value of .068. This reduction in the value of R compared to that obtained using an anisotropic model and 1.0  $\text{H}_2\text{O}$  as the solvent, i.e., .095, is highly significant (Hamilton, 1965).

On the final cycle of least-squares refinement, no parameter shift was greater than 0.2 e.s.d. (e.s.d. values were derived from inversion of the block diagonal matrices). An electron density synthesis phased on the final model showed only the expected peaks and a difference Fourier synthesis showed no evidence of misplaced atoms. The difference map showed no positive peaks greater than  $0.9\text{e Å}^{-3}$ , less than one fifth of the value of typical carbon atom peaks in earlier difference maps (i.e., ca  $5\text{e Å}^{-3}$ ). The standard deviation of an observation of unit weight ( $m = 2205$ ,  $n = 306$ ; see section 2.6) was 2.63. A summary of the analysis is given in Table 3.6. The final positional and thermal parameters, together with their estimated

Table 3.6

Summary of crystal structure analysis for



Solution method	Heavy atom
Least-squares method	Block-diagonal
Atom scattering factors (neutral atoms)	Non-hydrogen: Cromer & Waber, 1965 Hydrogen: Stewart, Davidson & Simpson, 1965
Absorption correction	Applied (de Meuleneear & Tompa, 1965)
Anomalous dispersion (source)	Included (International Tables, 1962)
Co	$\Delta F' = -2.2$ $\Delta F'' = 3.8$
Cl	$\Delta F' = 0.3$ $\Delta F'' = 0.7$
O	$\Delta F' = 0.0$ $\Delta F'' = 0.1$
Weighting scheme	$w = 1/\sigma_2^2$
Range of transmission factors	0.452 to 0.769
Data for final refinement	'Observed' data only
Final model	All non-hydrogen atoms anisotropic; calculated hydrogens isotropic and not refined
Largest parameter shift on final cycle (average)	0.21 (0.1)
Final R value	0.068 (see also Table 3.5)
Final difference Fourier peaks	$0.9e \text{ \AA}^{-3}$
Disorder	Present: 0.75 ( $\text{C}_2\text{H}_5\text{OH}$ ) position of atoms not refined



standard deviations, where appropriate, are listed in Table 3.7.

Structure factors are listed in Appendix B.

### 3.6 DETERMINATION OF THE ABSOLUTE CONFIGURATION

The sign of the y-coordinates of all atoms was reversed (Stout & Jensen, 1968) and the enantiomorphic structure subjected to four cycles of B.D.L.S (306 parameters; scale factor, non-hydrogen atom positional and thermal parameters with the exception of ethanol atom positional parameters). The final value of R was equal to .137, this increase is highly significant (Ibers & Hamilton, 1964; Hamilton, 1965) when compared with .068 for the original configuration. Examination of the individual sal pn ligands showed that in the original model (R = .068) the R-pn moiety was present, this is in agreement with the R-ratio test.

All diagrams are presented with respect to a right-handed set of crystal axes and show the correct absolute configuration for  $S-[Co(sal(R)pn(1-Me))(sal(R)pn(2-Me))]ClO_4 \cdot 0.75 EtOH$ .

### 3.7 DESCRIPTION OF THE STRUCTURE

The crystal structure consists, as expected, of discrete ions. The cation has  $C_1$  symmetry and consists of two essentially planar tridentate sal pn ligands, which are approximately at right-angles to one another, surrounding the central cobalt atom. A perspective view of the  $S-[Co(sal(R)pn(1-Me))(sal(R)pn(2-Me))]^+$  ion, together with the atom numbering scheme, is shown in Figure 3.1. Thermal ellipsoids have been drawn to include 50% of the probability distribution. The unit cell, showing the molecular packing arrangement, is illustrated in Figure 3.2.

Table 3.7

(a)

Atom positional and anisotropic temperature factors of the form

$$T = \exp(-B_{11}h^2 + 2B_{12}hk + 2B_{13}hl + B_{22}k^2 + 2B_{23}kl + B_{33}l^2)$$

for S - [Co(sal (R)pn(1-Me))(sal (R)pn(2-Me))]ClO<sub>4</sub>·0.75(C<sub>2</sub>H<sub>5</sub>OH).

ATOM	X/A	Y/B	Z/C	BETA11	BETA22	BETA33	BETA12	BETA13	BETA23
CO(10)	0.2341(1)	0.5	0.7942(1)	0.0083(1)	0.0088(3)	0.0044(1)	0.0008(2)	0.0006(1)	-0.0001(2)
CL(10)	-0.1542(2)	0.2747(5)	0.9176(2)	0.0129(3)	0.0195(7)	0.0055(1)	-0.0011(4)	-0.0003(2)	0.0022(3)
N(10)	0.4035(6)	0.4603(10)	0.8307(4)	0.0098(8)	0.0049(19)	0.0042(3)	-0.0014(10)	-0.0002(4)	-0.0014(7)
N(20)	0.0635(6)	0.5404(10)	0.7653(4)	0.0068(7)	0.0115(21)	0.0043(3)	0.0004(10)	0.0008(4)	-0.0001(7)
N(30)	0.2360(7)	0.7384(12)	0.8433(5)	0.0113(9)	0.0124(22)	0.0061(4)	0.0016(12)	0.0012(5)	-0.0010(9)
O(140)	0.2377(5)	0.2760(9)	0.7423(4)	0.0098(7)	0.0088(15)	0.0057(3)	-0.0008(9)	-0.0007(4)	-0.0009(7)
O(10)	0.2745(5)	0.6046(10)	0.6897(3)	0.0086(7)	0.0134(16)	0.0051(3)	0.0020(9)	0.0019(4)	0.0019(6)
N(120)	0.1910(7)	0.3894(12)	0.9026(5)	0.0105(9)	0.0145(21)	0.0059(4)	-0.0005(12)	0.0013(5)	0.0006(8)
O(30)	-0.0853(8)	0.3888(18)	0.9767(5)	0.0247(15)	0.0700(47)	0.0097(6)	-0.0174(23)	-0.0028(8)	-0.0059(14)
O(40)	-0.2052(8)	0.3595(18)	0.8445(6)	0.0183(11)	0.0710(48)	0.0125(6)	-0.0037(21)	-0.0062(7)	0.0135(15)
O(50)	-0.2512(9)	0.1926(16)	0.9623(4)	0.0285(15)	0.0621(44)	0.0061(4)	-0.0260(22)	0.0004(7)	0.0058(11)
O(60)	-0.0586(11)	0.1639(17)	0.8872(9)	0.0316(19)	0.0347(36)	0.0270(13)	0.0181(21)	-0.0050(13)	-0.0150(19)
C(10)	0.4964(7)	0.5348(14)	0.6995(6)	0.0055(8)	0.0133(29)	0.0065(5)	-0.0003(13)	0.0017(5)	-0.0020(10)
C(20)	0.6028(9)	0.5378(17)	0.6565(6)	0.0089(11)	0.0178(35)	0.0120(8)	-0.0018(16)	0.0001(8)	-0.0035(15)
C(30)	0.6106(10)	0.6035(19)	0.5697(7)	0.0139(13)	0.0276(37)	0.0077(7)	-0.0005(21)	0.0056(8)	-0.0004(14)
C(40)	0.5044(11)	0.6614(18)	0.5319(6)	0.0154(14)	0.0250(38)	0.0069(7)	0.0005(20)	0.0032(9)	-0.0007(13)
C(50)	0.3955(9)	0.6595(17)	0.5699(6)	0.0129(13)	0.0209(31)	0.0048(5)	0.0016(17)	0.0033(7)	-0.0003(11)
C(60)	0.3868(8)	0.5952(13)	0.6552(6)	0.0091(10)	0.0078(23)	0.0063(5)	-0.0011(14)	0.0032(6)	-0.0030(10)
C(70)	0.4971(8)	0.4720(15)	0.7847(5)	0.0088(9)	0.0128(26)	0.0053(5)	0.0016(16)	-0.0002(6)	-0.0022(11)
C(80)	0.4174(9)	0.4015(16)	0.9237(7)	0.0110(12)	0.0160(28)	0.0077(7)	0.0013(16)	0.0007(7)	0.0000(12)
C(90)	0.3059(10)	0.2920(17)	0.9401(6)	0.0169(14)	0.0140(28)	0.0057(5)	0.0047(19)	-0.0007(7)	0.0023(11)
C(110)	-0.0238(10)	0.0818(18)	0.5625(6)	0.0144(13)	0.0265(37)	0.0055(5)	0.0027(20)	-0.0020(7)	-0.0030(13)
C(120)	-0.0534(9)	0.2233(17)	0.6108(6)	0.0133(13)	0.0189(32)	0.0057(5)	0.0022(17)	0.0001(7)	0.0021(11)
C(130)	0.0330(8)	0.3022(16)	0.6711(5)	0.0072(9)	0.0179(28)	0.0041(4)	-0.0016(15)	-0.0002(5)	0.0016(10)
C(140)	0.1513(8)	0.2256(13)	0.6830(5)	0.0114(11)	0.0105(25)	0.0035(4)	0.0020(14)	0.0011(6)	0.0016(9)
C(150)	0.1826(9)	0.0836(16)	0.6317(6)	0.0124(12)	0.0167(28)	0.0045(5)	0.0008(16)	-0.0013(6)	-0.0004(10)
C(160)	0.0947(10)	0.0148(18)	0.5741(6)	0.0180(14)	0.0215(33)	0.0047(5)	0.0040(22)	0.0004(7)	0.0012(13)
C(170)	-0.0057(7)	0.4553(13)	0.7167(5)	0.0073(9)	0.0120(29)	0.0046(4)	0.0023(13)	0.0010(5)	0.0006(9)
C(180)	0.2970(12)	0.2455(20)	1.0342(6)	0.0265(21)	0.0272(41)	0.0054(6)	0.0108(25)	0.0003(9)	0.0018(14)
C(190)	0.0129(8)	0.6973(14)	0.8073(6)	0.0089(10)	0.0125(26)	0.0065(6)	-0.0001(15)	0.0022(6)	-0.0001(11)
C(190)	0.1214(9)	0.8278(16)	0.8127(6)	0.0102(11)	0.0181(31)	0.0064(6)	0.0034(17)	0.0008(7)	-0.0008(12)
C(200)	-0.1042(8)	0.7871(19)	0.7656(7)	0.0082(11)	0.0257(36)	0.0085(7)	0.0039(18)	-0.0006(7)	0.0002(15)
OH(20)	0.4104	0.0077	0.7888	0.0068(7)	0.0081(18)	0.0062(4)	-0.0013(12)	0.0005(5)	-0.0004(10)
CET(1)	0.5431	0.0009	0.7722	0.0234(26)	0.0163(42)	0.0128(12)	-0.0071(36)	-0.0001(15)	-0.0006(27)
CET(2)	0.59	0.0357	0.685	0.0521(59)	0.0287(80)	0.0223(24)	0.0065(59)	-0.0072(33)	-0.0070(39)



Table 3.7 continued

(b)

Calculated hydrogen positional and isotropic thermal parameters

Atom	x/a	y/b	z/c	B( $\text{\AA}^2$ )
H(50)	0.318	0.705	0.539	5.3
H(40)	0.509	0.710	0.473	6.6
H(30)	0.693	0.603	0.544	6.9
H(20)	0.682	0.487	0.685	6.1
H(70)	0.580	0.434	0.811	4.2
H(150)	0.269	0.031	0.636	4.6
H(160)	0.120	-0.089	0.539	5.9
H(110)	-0.084	0.028	0.521	6.0
H(120)	-0.139	0.276	0.603	5.2
H(170)	-0.094	0.496	0.706	3.7
H(80)	0.415	0.505	0.961	5.3
H(81)	0.495	0.335	0.932	5.3
H(190)	0.101	0.925	0.853	4.8
H(191)	0.133	0.876	0.754	4.8
H(90)	0.310	0.171	0.908	5.4
H(180)	-0.016	0.662	0.866	4.4
HN(12)	0.169	0.480	0.945	4.6
HN(13)	0.119	0.307	0.892	4.6
HN(30)	0.239	0.730	0.908	4.5
HN(31)	0.312	0.802	0.825	4.5

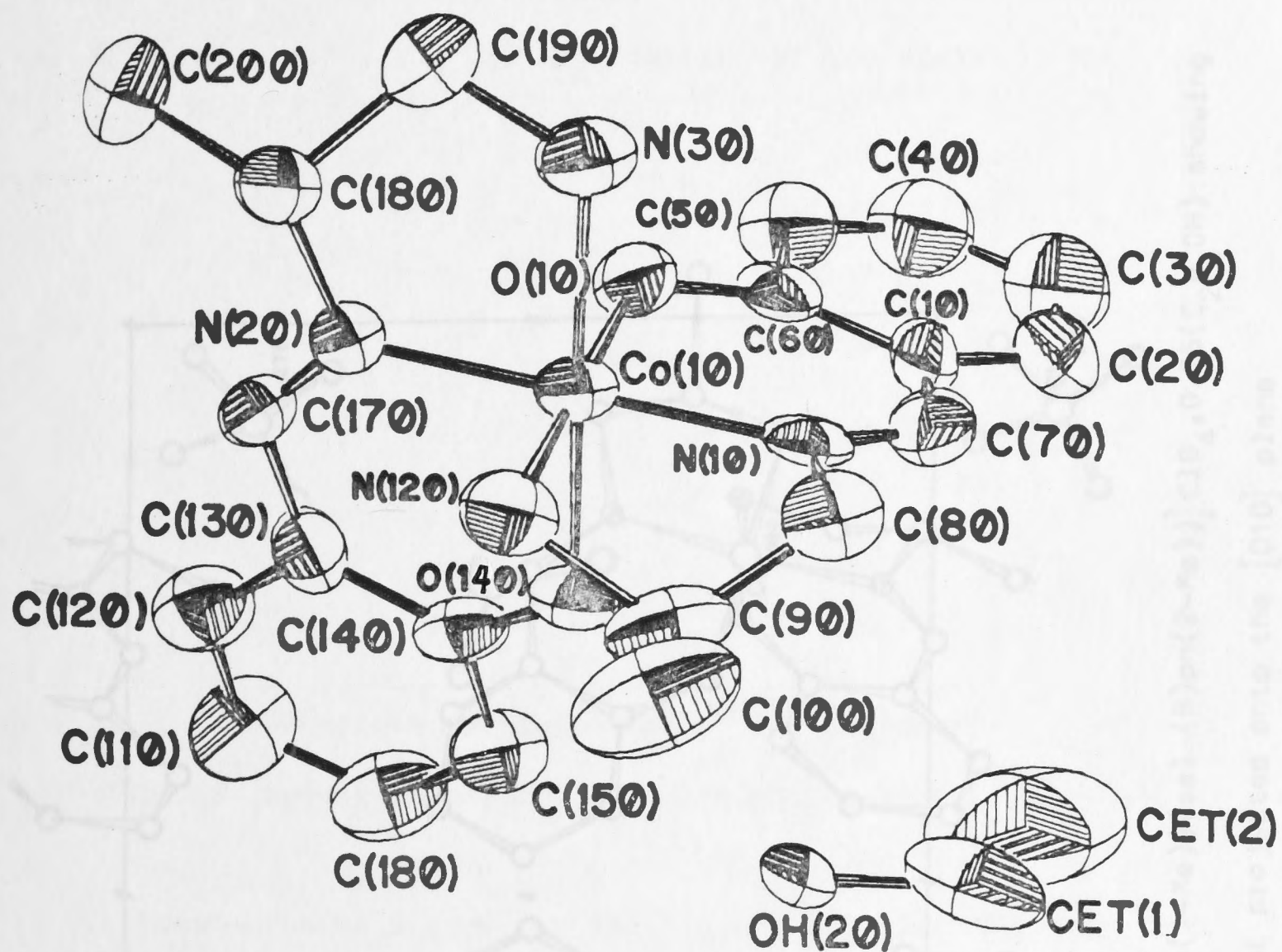


Figure 3.1 Overall stereochemistry of the  $S$ -[Co(sal(R)pn(1-Me))(sal(R)pn(2-Me))]⁺ ion and atom numbering scheme.



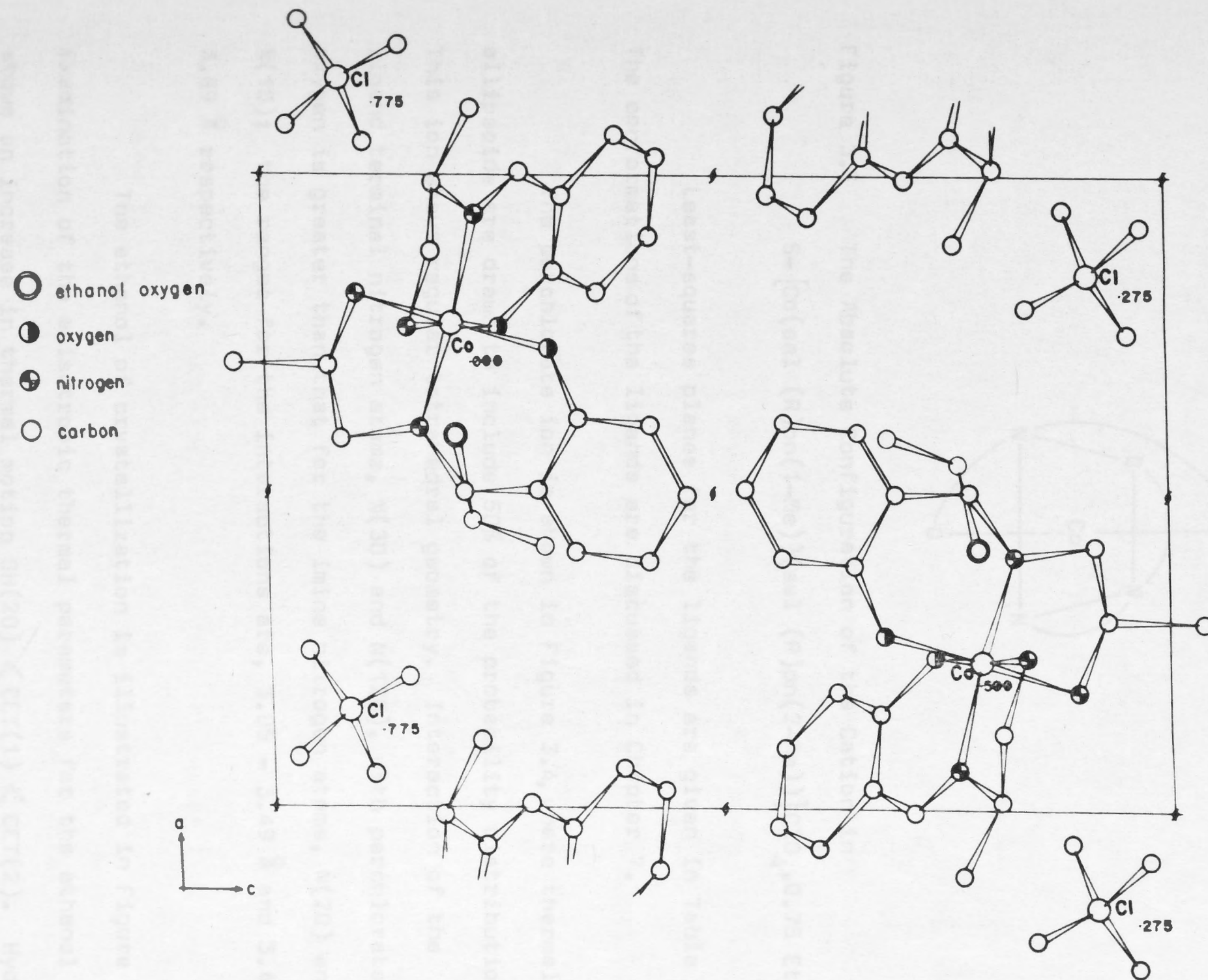


Figure 3.2 The unit cell of  $S\text{-}[\text{Co}(\text{sal}(\text{R})\text{pn}(1\text{-Me}))(\text{sal}(\text{R})\text{pn}(2\text{-Me}))]\text{ClO}_4 \cdot 0.75(\text{C}_2\text{H}_5\text{OH})$  showing the molecular packing arrangement projected onto the  $[010]$  plane

The absolute configuration of the complex ion was determined to be S (Figure 3.3). The methyl group in both ligands is equatorial to the diamine-cobalt chelate ring, thus minimising steric hindrance (Corey & Bailer, 1959), and the conformation of the rings is  $\lambda$ .

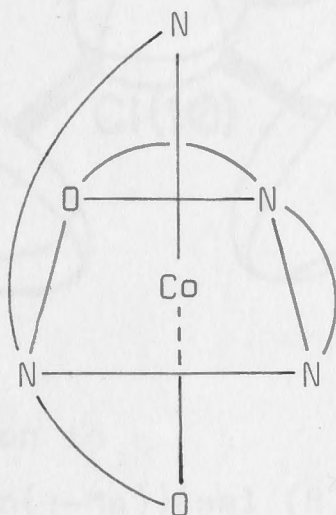


Figure 3.3 The Absolute Configuration of the Cation in  
 $S-[Co(sal(R)pn(1-Me))(sal(R)pn(2-Me))]ClO_4 \cdot 0.75 EtOH$

Least-squares planes for the ligands are given in Table 3.8. The conformations of the ligands are discussed in Chapter 7.

The perchlorate ion is shown in Figure 3.4, where thermal ellipsoids are drawn to include 50% of the probability distribution. This ion shows regular tetrahedral geometry. Interaction of the ligand terminal nitrogen atoms, N(30) and N(120), with perchlorate oxygen is greater than that for the imine nitrogen atoms, N(20) and N(10); the ranges for the interactions are, 3.05 – 3.49 Å and 3.46 – 3.89 Å respectively.

The ethanol of crystallization is illustrated in Figure 3.1. Examination of the anisotropic thermal parameters for the ethanol atoms shows an increase in thermal motion  $OH(20) < CET(1) < CET(2)$ . Hydrogen bonding is present between ethanol oxygen and N(30) (2.93 Å) and



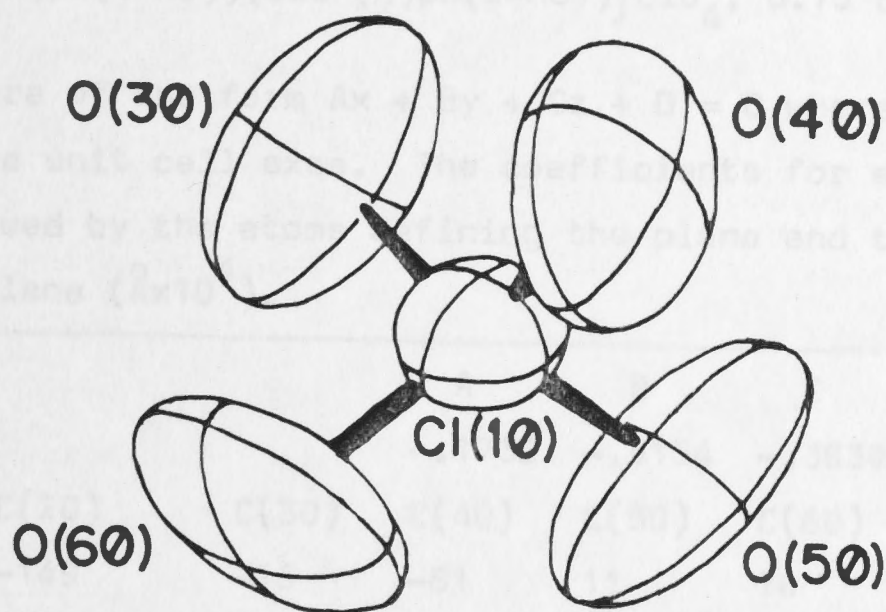
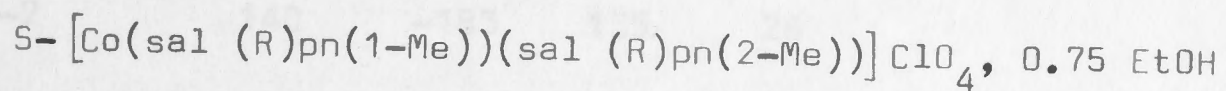


Figure 3.4 Perchlorate ion in



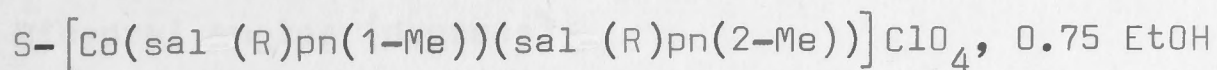
O(140) (2.84 Å). This hydrogen bonding probably lengthens the Co(10)-N(30) bond compared to the Co(10)-N(120) bond and also decreases the Co(10)-O(140)-C(140) angle,  $122.0^\circ$ , cf  $124.5^\circ$  for the ligand B. This interaction would account for the much lower thermal parameters for the oxygen, OH(20). However, as noted earlier, the possibility of  $0.75\text{C}_2\text{H}_5\text{OH}, 0.25\text{H}_2\text{O}$  must also be considered. The smaller value for the OH(20) thermal parameters may then be explained as follows. With an occupancy of 0.75 for OH(20) the thermal parameters will refine to smaller values if there were in fact a whole oxygen atom at the site.

The bond lengths and bond angles, given in Table 3.9 and Figures 3.5 and 3.6, are in no way unusual when compared with those in related structures. Intermolecular approach distances less than 4 Å are given in Table 3.10.

A detailed discussion of this structure together with others reported in this thesis is given in Chapter 7.

Table 3.8

Mean planes for the ligands in



Equations are of the form  $Ax + By + Cz + D = 0$  where  $x$ ,  $y$  and  $z$  refer to the unit cell axes. The coefficients for each plane are given followed by the atoms defining the plane and their distances from that plane ( $\text{\AA} \times 10^4$ ).

			A	B	C	D		
Plane (1)			-.1732	-.9154	-.3634	8.5188		
C(10)	C(20)	C(30)	C(40)	C(50)	C(60)			
-135	-149	-16	-81	11	74			
Plane (2)			.3572	.6068	-.7101	6.0413		
C(110)	C(120)	C(130)	C(140)	C(150)	C(160)			
-126	-2	140	-183	135	26			
Plane (3)			-.1113	-.9182	-.3802	8.4415		
Co(10)	N(10)	O(10)	C(10)	C(20)	C(30)	C(40)	C(50)	
61	-1353	-1554	138	1280	1393	733	-16	
C(60)	C(70)							
-265	-554							
Plane (4)			.3432	.5400	-.7685	6.7522		
Co(10)	N(20)	O(140)	C(110)	C(120)	C(130)	C(140)	C(150)	
76	-957	-2590	1532	546	-363	-595	872	
C(160)	C(170)							
1752	-937							
Plane (5)			-.1186	-.9106	-.3958	8.6161		
Co(10)	N(10)	O(10)	N(120)	C(10)	C(20)	C(30)	C(40)	
19	-1638	-1316	1758	142	1300	1642	1199	
C(50)	C(60)	C(70)	C(80)	C(90)	C(100)			
443	-38	-796	-3231	5314	2059			
Plane (6)			.3656	.5141	-.7759	6.8912		
Co(10)	N(20)	N(30)	O(140)	C(110)	C(120)	C(130)	C(140)	
-4	-1488	3322	-2145	1973	567	-362	-177	
C(150)	C(160)	C(170)	C(180)	C(190)	C(200)			
1715	2597	-1401	-2530	6231	1495			



Table 3.8 continued

## Dihedral angles (degrees)

Plane (2) - Plane (1) 68.9	Plane (1) - Plane (5) 3.7
Plane (2) - Plane (3) 70.8	Plane (3) - Plane (4) 76.0
Plane (2) - Plane (4) 5.2	Plane (3) - Plane (6) 77.4
Plane (2) - Plane (6) 6.6	Plane (3) - Plane (5) 1.1
Plane (2) - Plane (5) 71.7	Plane (4) - Plane (6) 2.0
Plane (1) - Plane (3) 3.7	Plane (4) - Plane (5) 76.8
Plane (1) - Plane (4) 73.1	Plane (6) - Plane (5) 78.2
Plane (1) - Plane (6) 75.4	

Table 3.9

(a)

Bond lengths and angles about cobalt in

 $S-[Co(sal(R)pn(1-Me))(sal(R)pn(2-Me))]ClO_4$ , 0.75 EtOH (e.s.d. values in parentheses)

Atoms	Bond lengths (Å)	Atoms	Bond angles (degrees)
Co(10)-O(10)	1.880(6)	O(10)-Co(10)-N(10)	94.4(3)
Co(10)-O(140)	1.898(7)	N(10)-Co(10)-N(120)	85.9(3)
Co(10)-N(10)	1.899(7)	N(120)-Co(10)-N(20)	91.0(3)
Co(10)-N(20)	1.884(6)	N(20)-Co(10)-O(10)	88.7(3)
Co(10)-N(30)	1.980(9)	O(10)-Co(10)-N(30)	86.6(3)
Co(10)-N(120)	1.959(8)	N(30)-Co(10)-N(120)	93.8(4)
		N(120)-Co(10)-O(140)	89.1(3)
		O(140)-Co(10)-O(10)	90.4(3)
		N(20)-Co(10)-N(30)	86.3(3)
		N(30)-Co(10)-N(10)	92.2(3)
		N(10)-Co(10)-O(140)	86.9(3)
		O(140)-Co(10)-N(20)	94.8(3)

69.  
Table 3.9 continued

(b)

Bond lengths and angles for ligands in  
S-[Co(sal (R)pn(1-Me))(sal (R)pn(2-Me))]ClO<sub>4</sub>, 0.75 EtOH (e.s.d. values  
in parentheses)

Atoms	Bond lengths (Å)	Atoms	Bond angles (degrees)
C(10)-C(20)	1.342(13)	C(10)-C(20)-C(30)	123.6(9)
C(20)-C(30)	1.448(16)	C(20)-C(30)-C(40)	116.5(10)
C(30)-C(40)	1.332(16)	C(30)-C(40)-C(50)	123.0(10)
C(40)-C(50)	1.328(15)	C(40)-C(50)-C(60)	120.9(9)
C(50)-C(60)	1.423(14)	C(50)-C(60)-C(10)	118.9(8)
C(60)-C(10)	1.412(12)	C(60)-C(10)-C(20)	117.0(9)
C(10)-C(70)	1.412(12)	Co(10)-O(10)-C(60)	124.6(6)
C(70)-N(10)	1.256(11)	O(10)-C(60)-C(10)	124.2(8)
N(10)-C(80)	1.517(12)	C(60)-C(10)-C(70)	122.8(8)
C(80)-C(90)	1.488(16)	C(10)-C(70)-N(10)	126.0(8)
C(90)-N(120)	1.532(14)	C(70)-N(10)-Co(10)	126.1(8)
C(90)-C(100)	1.515(15)	Co(10)-N(10)-C(80)	112.8(5)
C(60)-O(10)	1.337(10)	N(10)-C(80)-C(90)	106.6(8)
		C(80)-C(90)-N(120)	107.1(9)
		C(80)-C(90)-C(100)	112.5(9)
		C(100)-C(90)-N(120)	113.7(9)
		C(90)-N(120)-Co(10)	109.0(6)
C(110)-C(120)	1.364(17)	C(120)-C(110)-C(160)	117.4(10)
C(120)-C(130)	1.424(14)	C(110)-C(120)-C(130)	122.8(10)
C(130)-C(140)	1.398(13)	C(120)-C(130)-C(140)	117.8(10)
C(140)-C(150)	1.399(15)	C(130)-C(140)-C(150)	119.2(8)
C(150)-C(160)	1.376(14)	C(140)-C(150)-C(160)	119.8(9)
C(160)-C(110)	1.371(16)	C(150)-C(160)-C(110)	117.4(10)
C(140)-O(140)	1.336(10)	Co(10)-N(20)-C(170)	127.9(7)
C(130)-C(170)	1.404(14)	N(20)-C(170)-C(130)	124.0(8)
C(170)-N(20)	1.224(11)	C(170)-C(130)-C(140)	123.6(8)
N(20)-C(180)	1.482(13)	C(130)-C(140)-O(140)	124.4(9)
C(180)-C(200)	1.547(14)	C(140)-O(140)-Co(10)	122.0(6)
C(180)-C(190)	1.531(15)	Co(10)-N(20)-C(180)	113.4(5)
C(190)-N(30)	1.464(13)	N(20)-C(180)-C(200)	118.7(8)
		N(20)-C(180)-C(190)	105.3(8)
		C(200)-C(180)-C(190)	109.3(9)
		C(180)-C(190)-N(30)	109.5(9)
		C(190)-N(30)-Co(10)	108.2(6)



Table 3.9 continued

(c)

Bond lengths and angles for the perchlorate ion (e.s.d. values in parentheses)

Atoms	Bond lengths (Å)	Atoms	Bond angles (degrees)
Cl(10)-O(30)	1.45(1)	O(30)-Cl(10)-O(40)	114.0(7)
Cl(10)-O(40)	1.40(1)	O(30)-Cl(10)-O(50)	105.6(5)
Cl(10)-O(50)	1.42(1)	O(30)-Cl(10)-O(60)	102.7(7)
Cl(10)-O(60)	1.42(1)	O(40)-Cl(10)-O(50)	109.7(5)
		O(40)-Cl(10)-O(60)	105.4(7)
		O(50)-Cl(10)-O(60)	116.5(7)

(d)

Bond lengths and angles for ethanol of crystallization (atom positions were not refined)

Atoms	Bond lengths (Å)	Atoms	Bond angles (degrees)
OH(20)-CET(1)	1.45	OH(20)-CET(1)-CET(2)	122
CET(1)-CET(2)	1.49		

(e)

Bond lengths involving calculated hydrogen atoms (e.s.d. values in parentheses)

Atoms	Bond lengths (Å)	Atoms	Bond length (Å)
N(120)-HN(12)	0.994(9)	N(120)-HN(13)	1.000(8)
N(30)-HN(30)	0.995(8)	N(30)-HN(31)	1.010(8)
C(20)-H(20)	1.019(10)	C(30)-H(30)	0.983(11)
C(40)-H(40)	0.996(11)	C(50)-H(50)	1.003(10)
C(70)-H(70)	1.004(8)	C(80)-H(80)	0.991(12)
C(80)-H(81)	0.973(11)	C(90)-H(90)	1.053(12)
C(110)-H(110)	0.983(10)	C(120)-H(120)	0.999(11)
C(150)-H(150)	1.007(10)	C(160)-H(160)	1.010(12)
C(170)-H(170)	1.005(8)	C(180)-H(180)	1.013(10)
C(190)-H(190)	1.000(11)	C(190)-H(191)	1.002(10)

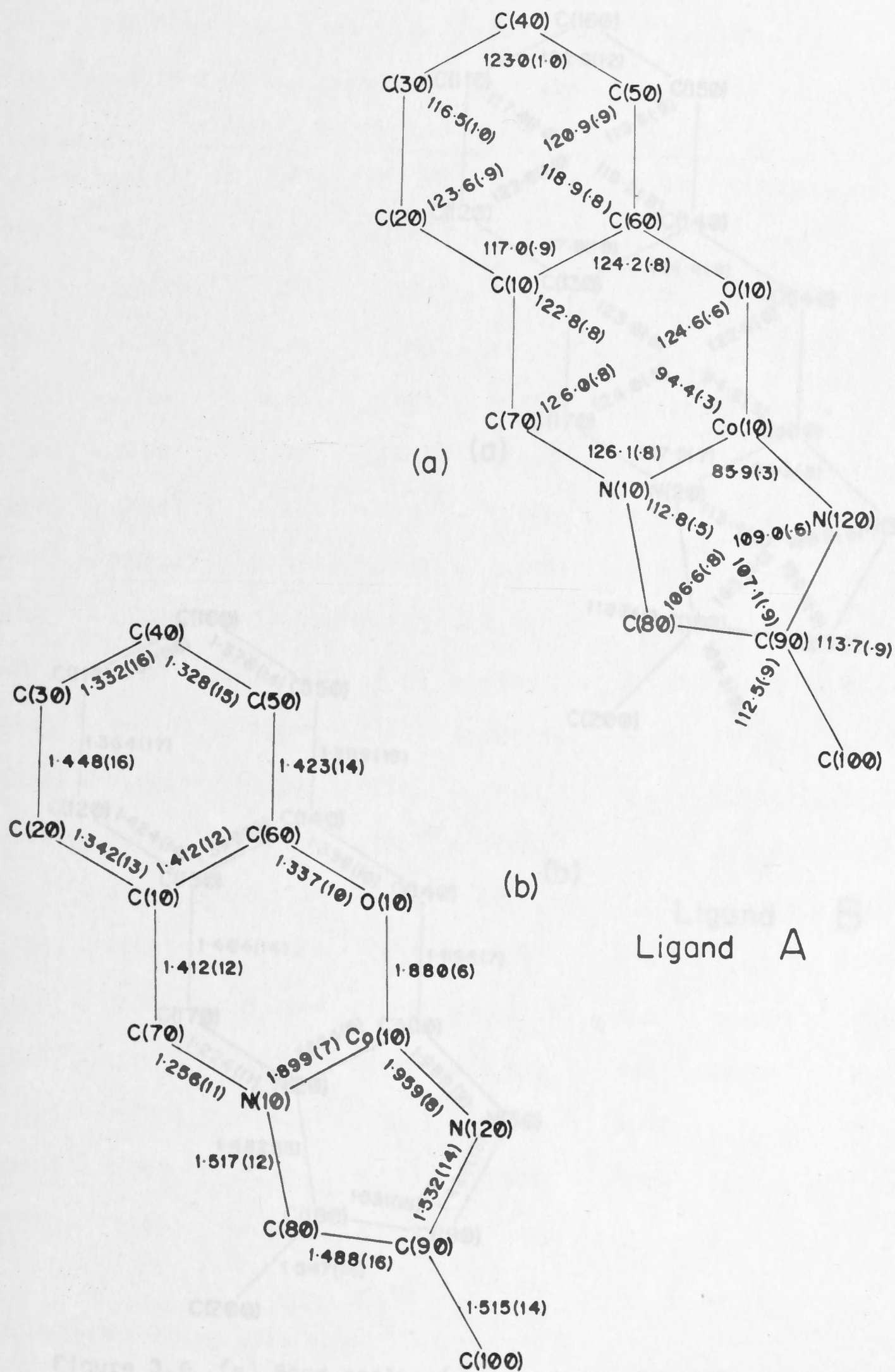


Figure 3.5 (a) Bond angles (degrees) and (b) bond lengths ( $\text{\AA}$ ) for  $\text{S-}[\text{Co}(\text{sal}(\text{R})\text{pn}(1\text{-Me}))(\text{sal}(\text{R})\text{pn}(2\text{-Me}))]\text{ClO}_4 \cdot 0.75(\text{C}_2\text{H}_5\text{OH})$  (estimated standard deviations in parentheses).



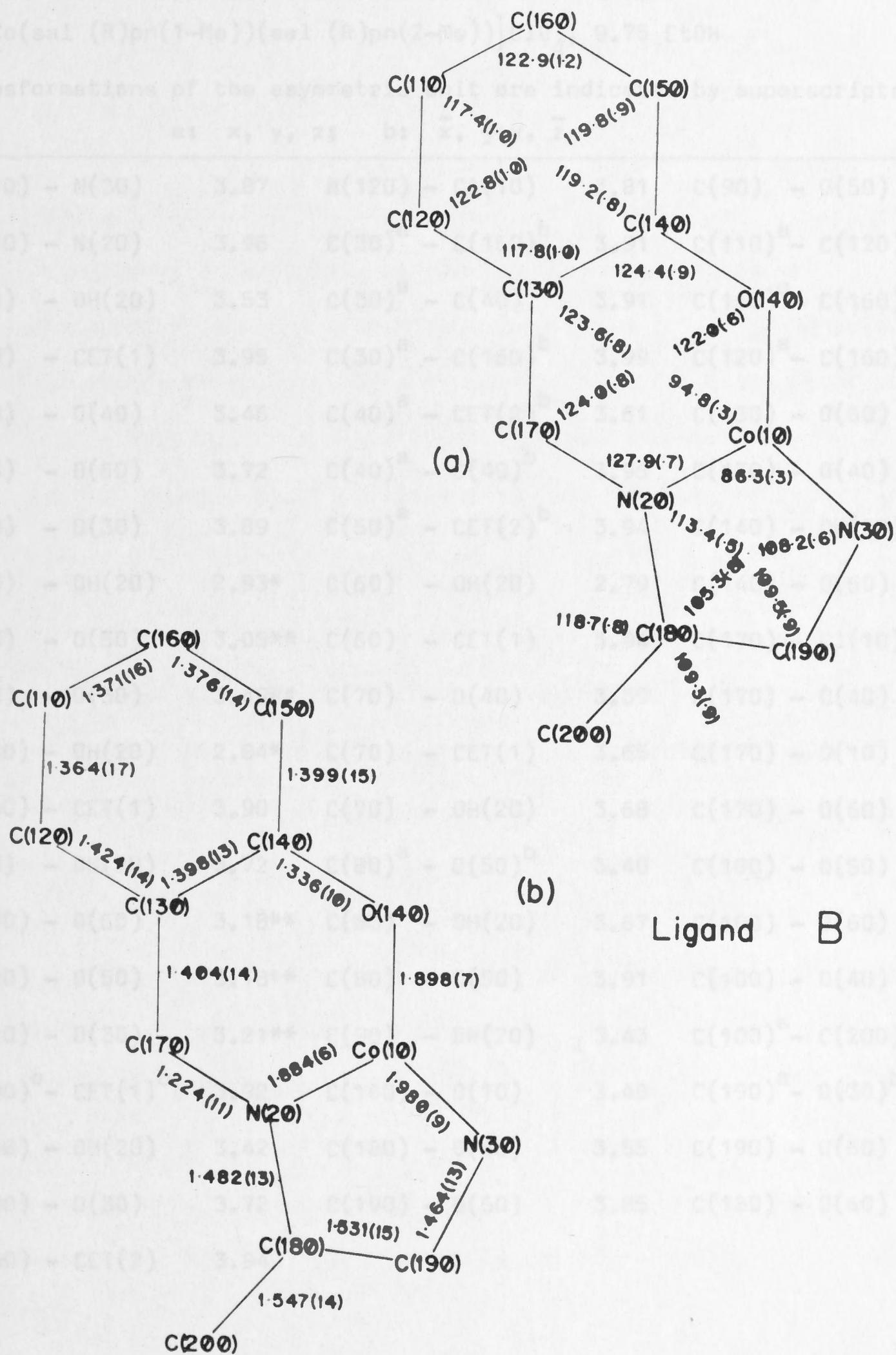


Figure 3.6 (a) Bond angles (degrees) and (b) bond lengths (Å) for  $S-[Co(sal(R)pn(1-Me))(sal(R)pn(2-Me))]ClO_4 \cdot 0.75(C_2H_5OH)$  (estimated standard deviations in parentheses).

Table 3.10

Intermolecular approach distances less than 4 Å for  
 $S-[Co(sal(R)pn(1-Me))(sal(R)pn(2-Me))]ClO_4, 0.75 EtOH$

Transformations of the asymmetric unit are indicated by superscripts

a: x, y, z; b:  $\bar{x}$ ,  $\frac{1}{2}+y$ ,  $\bar{z}$

Cl(10) - N(30)	3.87	N(120) - Cl(10)	3.81	C(90) - O(50)	3.49
Cl(10) - N(20)	3.96	C(30) <sup>a</sup> - C(150) <sup>b</sup>	3.91	C(110) <sup>a</sup> - C(120) <sup>b</sup>	3.96
N(10) - OH(20)	3.53	C(30) <sup>a</sup> - C(40) <sup>b</sup>	3.91	C(110) <sup>a</sup> - C(160) <sup>b</sup>	3.99
N(10) - CET(1)	3.95	C(30) <sup>a</sup> - C(160) <sup>b</sup>	3.99	C(120) <sup>a</sup> - C(160) <sup>b</sup>	3.66
N(20) - O(40)	3.46	C(40) <sup>a</sup> - CET(2) <sup>b</sup>	3.61	C(130) - O(60)	3.70
N(20) - O(60)	3.72	C(40) <sup>a</sup> - C(40) <sup>b</sup>	3.96	C(130) - O(40)	3.81
N(20) - O(30)	3.89	C(50) <sup>a</sup> - CET(2) <sup>b</sup>	3.94	C(140) - OH(20)	3.58
N(30) - OH(20)	2.93*	C(60) - OH(20)	2.79	C(140) - O(60)	3.99
N(30) - O(50)	3.05**	C(60) - CET(1)	3.94	C(170) - Cl(10)	3.82
N(30) - O(30)	3.49**	C(70) - O(40)	3.39	C(170) - O(40)	3.06
O(140) - OH(20)	2.84*	C(70) - CET(1)	3.65	C(170) - O(10)	3.25
O(140) - CET(1)	3.90	C(70) - OH(20)	3.68	C(170) - O(60)	3.53
O(10) - OH(20)	3.72	C(80) <sup>a</sup> - O(50) <sup>b</sup>	3.40	C(100) - O(50)	3.46
N(120) - O(60)	3.18**	C(80) - OH(20)	3.67	C(100) - O(60)	3.55
N(120) - O(50)	3.18**	C(80) - O(50)	3.91	C(100) - O(40)	3.66
N(120) - O(30)	3.21**	C(90) - OH(20)	3.43	C(100) <sup>a</sup> - C(200) <sup>b</sup>	3.82
C(100) <sup>a</sup> - CET(1) <sup>b</sup>	3.92	C(180) - O(10)	3.48	C(190) <sup>a</sup> - O(30) <sup>b</sup>	3.35
C(190) - OH(20)	3.42	C(180) - O(40)	3.55	C(190) - O(60)	3.44
C(180) - O(30)	3.72	C(190) - O(50)	3.85	C(180) - O(60)	3.87
C(200) - CET(2)	3.94				

\* hydrogen bonding with ethanol oxygen

\*\* hydrogen bonding with perchlorate oxygen



## CHAPTER 4

CRYSTAL AND MOLECULAR STRUCTURE OF BIS-(N-(2-AMINOETHYL)SALICYLALDIMINATO)  
COBALT(III) IODIDE, MONOHYDRATE\*

## 4.1 UNIT CELL AND DIFFRACTION SYMMETRY

Groups of euhedral, tabular crystals were grown by evaporation of an ethanolic solution of  $\text{Co}(\text{sal en})_2\text{I}\cdot\text{H}_2\text{O}$ . Individual crystals showed monoclinic,  $2/m$ , symmetry due to the presence of the pinacoid forms (100), (010) and (001). Several crystals were selected and mounted about their largest direction and perpendicular to their  $C_2$  axis.

Unit cell parameters and diffraction symmetry were determined from equi-inclination Weissenberg and precession photographs. The crystals were found to belong to the monoclinic system and had the following unit cell dimensions

$$a = 18.38 \text{ \AA}$$

$$\alpha = \gamma = 90.0^\circ$$

$$b = 10.17 \text{ \AA}$$

$$\beta = 110^\circ$$

$$c = 12.00 \text{ \AA}$$

$$V = 2242 \text{ \AA}^3$$

Systematic absences were determined to be

$$hkl; \text{ no conditions}$$

$$h0l; l = 2n + 1$$

$$0k0; k = 2n + 1$$

$$00l; (l = 2n + 1)$$

These established the space group uniquely as  $P2_1/c$  (No. 14)

(International Tables, (1952)) and this was confirmed by the subsequent analysis.

Re-examination of the crystals showed that the morphology described above was correct.

\*  $\text{Co}(\text{sal en})_2\text{I}\cdot\text{H}_2\text{O}$  for brevity

The density of the crystals was determined to be  $1.64 \text{ g cm}^{-3}$  by the method of flotation using a mixture of carbon tetrachloride and ethyl bromide. The use of this value gave  $Z = 4$  and this in turn gave a calculated density of  $1.66 \text{ g cm}^{-3}$ .

## 4.2 DATA COLLECTION AND REDUCTION

### 4.2.1 Refinement of unit cell dimensions

A suitable crystal for data collection was selected from several crystals used for photographic experiments. The crystal was mounted about the b-axis (Araldite Fast Set; glass capillary) and placed on a Siemens automatic four-circle diffractometer. The crystal was oriented so that the b-axis was coincident with the  $\phi$ -axis of the diffractometer; this orientation was needed since the  $\chi$ -axis of the Siemens diffractometer is restricted to  $90^\circ$ .

The unit cell parameters were refined using the method of least-squares (Busing, Ellison, Levy, King & Rosebury, 1968) and Cu-K $\alpha$  radiation. Twelve prominent reflections were chosen to give a wide range of h, k and l with large  $2\theta$  values (Table 4.1). Values of  $2\theta$  were refined as described in section 2.2.1. Final unit cell parameters are listed below

$$\begin{array}{ll} a = 18.386(1) \text{ \AA} & \alpha = \gamma = 90.0^\circ \\ b = 10.216(1) \text{ \AA} & \beta = 109.87(2)^\circ \\ c = 12.004(1) \text{ \AA} & V = 2120.5 \text{ \AA}^3 \end{array}$$

### 4.2.2 Data collection and reduction

HKL and  $\bar{H}KL$  data were collected using nickel filtered Cu-K $\alpha$  radiation and a maximum value of  $\theta = 70^\circ$ . Intensities were measured at room temperature by the 'five-point' method (Hoppe, 1965)(Figure 2.1). Nickel foil attenuators were automatically inserted when the count rate



exceeded 5000 counts per second. A single standard reflection was monitored every twenty reflections.

A graph of intensity versus reflection sequence for the standard reflection was plotted and the slope,  $m$ , used to obtain a linear correction factor (see section 2.2.2).

A total of 4493 reflections were measured, of which 1643 (36.5%) were considered unobserved using the criterion  $I < 3\sigma_1$ . Unobserved data were given a value of  $I = 1.5\sigma_1$ . The observed structure factors and their standard deviations were calculated as described in section 2.2.2.

Linear absorption coefficients for both Cu-K $\alpha$  and Mo-K $\alpha$  radiation were calculated from available data (International Tables, 1962) as  $180.5 \text{ cm}^{-1}$  and  $23.4 \text{ cm}^{-1}$  respectively. Data collection conditions are summarised in Table 4.2.

Table 4.1

Unit cell refinement data for  $\text{Co}(\text{sal en})_2\text{I}\cdot\text{H}_2\text{O}$

h	k	l	$2\theta^\circ$	h	k	l	$2\theta^\circ$
-21	1	9	137.54	16	5	4	135.74
20	2	1	136.68	-19	6	7	138.70
-11	3	13	124.54	-5	7	12	138.76
16	3	4	122.36	-17	8	3	138.62
15	4	5	128.32	6	9	7	134.12
-21	4	3	139.32	-9	10	8	139.42

#### 4.3 DETERMINATION OF THE POSITIONS OF IODINE AND COBALT ATOMS

The ratio  $\sum z_h^2 / \sum z_l^2$  was calculated as 1.57 with iodine as the only heavy atom. Hence, the analysis was a typical heavy atom problem.

Table 4.2

Summary of crystal data and data collection for  $\text{Co}(\text{sal en})_2\text{I}\cdot\text{H}_2\text{O}$ 

Chemical formula	$\text{C}_{18}\text{H}_{20}\text{N}_4\text{O}_2\text{CoI}\cdot\text{H}_2\text{O}$
Formula weight	528.32
Space group	$P2_1/c$ (No. 14)
Boundary faces of crystal; (mm from internal origin in parentheses)	$\begin{array}{cccccc} 1 & 0 & 0 & (.05) & -1 & 0 & 0 & (.05) \\ 0 & 1 & 0 & (.12) & 0 & -1 & 0 & (.12) \\ 0 & 0 & 1 & (.18) & 0 & 0 & -1 & (.18) \end{array}$
Unit cell parameters	$a = 18.386(1) \text{ \AA}$ $b = 10.216(1) \text{ \AA}$ $c = 12.004(1) \text{ \AA}$ $\alpha = \gamma = 90.0^\circ$ $\beta = 109.87(2)^\circ$ $V = 2120.5 \text{ \AA}^3$
Radiation for unit cell refinement	$\text{Cu-K}\alpha = 1.5418 \text{ \AA}$
Density	$D_m = 1.64 \pm 0.4 \text{ g cm}^{-3}$ $D_c = 1.66 \text{ g cm}^{-3}$
Z	4
Linear absorption coefficients	$\mu(\text{Cu-K}\alpha) = 180.5 \text{ cm}^{-1}$ $\mu(\text{Mo-K}\alpha) = 23.4 \text{ cm}^{-1}$
Radiation used for data collection	$\text{Cu-K}\alpha$
Scan type/mode	'Five-point' / $\theta - 2\theta$
Standard reflection	2 3 1
Standard average range	$\pm 2.5\%$
Standard slope with sequence	$7.5 \times 10^{-4}$
Standard frequency	20
Data collected (2 $\theta$ limit)	HKL; $\bar{H}\text{KL}$ ( $140^\circ$ )
Number of observed reflections (%)	2850 (63.5)



Since the space group was  $P2_1/c$  and  $Z = 4$  the iodine and cobalt atoms must occupy general positions (this assumes that only one cation configuration exists in the unit cell). Atoms in general positions give rise to the Patterson peaks listed in Table 4.3. The origin peak was normalized to 999 so that iodine-iodine and cobalt-cobalt vectors would have anticipated heights of the order 600 and 120 respectively. The largest peaks in the unsharpened three dimensional Patterson map are listed in Table 4.4.

Examination of the Harker line  $(0, V, \frac{1}{2})$  and the corresponding general vector  $(U, V, W)$  enabled the determination of two alternative iodine positions (I(10) and I(20)). These atoms were given individual isotropic temperature factors equal to  $3.5 \text{ \AA}^2$ . Each atom in turn was subjected to one cycle of B.D.L.S. (refining the scale factor only, which was initially set equal to unity) and the data used to phase individual difference Fourier syntheses. Both cases produced an R value of .533.

Scattering factors used in this analysis were those for neutral atoms (Cromer & Waber, 1965). Anomalous dispersion terms  $\Delta F'$  and  $\Delta F''$  were included (International Tables, 1962), although no allowance was made for their dependence upon  $\sin \theta$ .

It was possible to identify a likely cobalt position in both of the difference Fourier syntheses. The two independent models were

- a) I(10) + Co(10) (.027, .56, .042)
- b) I(20) + Co(20) (.214, .44, .333)

Model (a) may be dismissed immediately since the Co(10)-Co(10) distance is  $3.23 \text{ \AA}$  - far too close (Figure 4.1). Model (b) however, gave vectors which were completely compatible with the Patterson synthesis (Table 4.4). Cobalt was given an isotropic temperature factor equal to  $3.5 \text{ \AA}^2$ . One cycle of B.D.L.S. was carried out using (b) and refinement of the scale

Table 4.3

Patterson peaks for general positions in space group  $P2_1/c$ 

	$x, y, z$	$-x, -y, -z$	$-x, \frac{1}{2}+y, \frac{1}{2}-z$	$x, \frac{1}{2}-y, \frac{1}{2}+z$
$x, y, z$	-	$-2x, -2y, -2z$	$-2x, \frac{1}{2}, \frac{1}{2}-2z$	$0, \frac{1}{2}-2y, \frac{1}{2}$
$-x, -y, -z$	$2x, 2y, 2z$	-	$0, \frac{1}{2}+2y, \frac{1}{2}$	$2x, \frac{1}{2}, \frac{1}{2}+2z$
$-x, \frac{1}{2}+y, \frac{1}{2}-z$	$2x, -\frac{1}{2}, 2z-\frac{1}{2}$	$0, -2y-\frac{1}{2}, -\frac{1}{2}$	-	$2x, -2y, 2z$
$x, \frac{1}{2}-y, \frac{1}{2}+z$	$0, 2y-\frac{1}{2}, -\frac{1}{2}$	$-2x, -\frac{1}{2}, -2z-\frac{1}{2}$	$-2x, 2y, -2z$	-

Table 4.4

Patterson peaks for  $\text{Co}(\text{sal en})_2\text{I}, \text{H}_2\text{O}$ 

Atom pair	U	V	W	Height	Comments
Origin	0	0	0	999	
I-I	0	.41	.5	406	I(20) $x = .054$
I-I	.107	.5	.0	291	$y = .050$
I-I	.107	.10	.5	151	$z = .250$
I-I	0	.41	.5	406	I(10) $x = .135$
I-I	.268	.5	.583	293	$y = .05$
I-I	.268	.10	.084	150	$z = .042$

NB: The cross vectors I(10)-I(20) were not found

Co-Co	.429	.492	.67	102	Co(20) $x = .214$
Co-Co	.268	.092	.083	150	$y = .44$
Co-Co	.429	.092	.667	53	$z = .333$
Co-Co	.0	.585	.5	395	
Co-I	.161	.0	.583	326	
Co-I	.268	.492	.583	293	
Co-I	.161	.585	.083	157	
Co-I	.161	.40	.083	152	
Co-I	.268	.092	.083	150	
Co-I	.250	.492	.167	66	



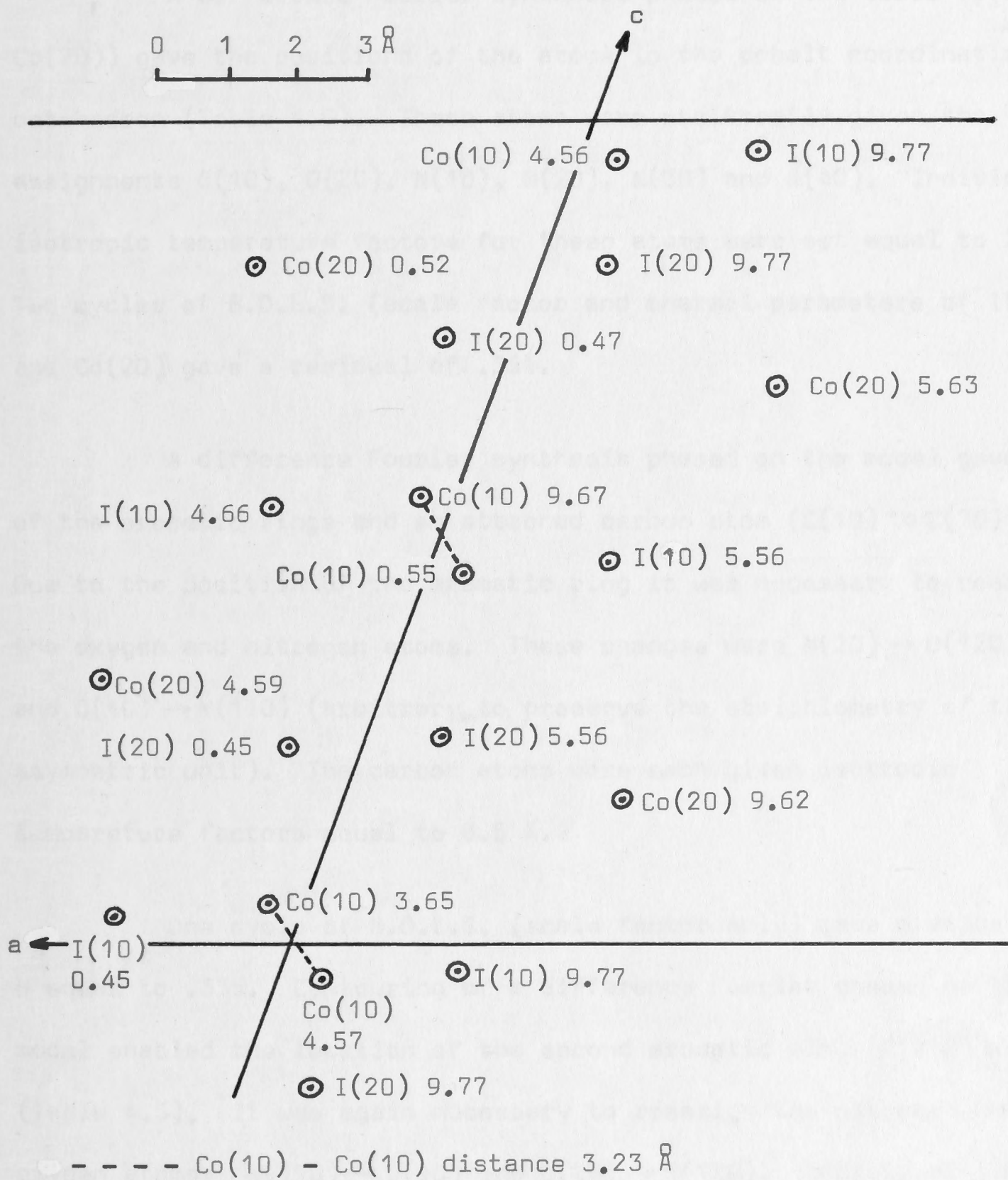


Figure 4.1 Alternative models for heavy atoms in  $\text{Co}(\text{sal en})_2\text{I}\cdot\text{H}_2\text{O}$   
(Distance along b-axis shown adjacent to atoms (Å)).

factor only gave a value of R equal to .392.

#### 4.4. DETERMINATION OF LIGHT ATOM POSITIONS

A difference Fourier synthesis phased on the model (I(20)+Co(20)) gave the positions of the atoms in the cobalt coordination octahedron (Table 4.5). These atoms were arbitrarily given the assignments O(10), O(20), N(10), N(20), N(30) and N(40). Individual isotropic temperature factors for these atoms were set equal to 3.5 Å. Two cycles of B.D.L.S. (scale factor and thermal parameters of I(20) and Co(20)) gave a residual of .351.

A difference Fourier synthesis phased on the model gave one of the aromatic rings and an attached carbon atom (C(10) to C(70)). Due to the position of the aromatic ring it was necessary to reassign the oxygen and nitrogen atoms. These changes were N(20) → O(120) (known) and O(10) → N(110) (arbitrary, to preserve the stoichiometry of the asymmetric unit). The carbon atoms were each given isotropic temperature factors equal to 3.5 Å.

One cycle of B.D.L.S. (scale factor only) gave a value for R equal to .335. Contouring of a difference Fourier phased on this model enabled the location of the second aromatic ring (C(110) to C(160)) (Table 4.5). It was again necessary to reassign the nitrogen and oxygen atoms: N(110) → O(10) and O(20) → N(120). Individual isotropic temperature factors of the new carbon atoms were set equal to 3.5 Å.

The scale factor was again updated by one cycle of B.D.L.S. and a difference Fourier synthesis, phased on the resulting data, was calculated, giving R = .300. From this synthesis the position of the remaining carbon atoms from both ligands were determined (Table 4.5). These carbon atoms were given individual isotropic temperature factors of 3.5 Å.



Table 4.5

Initial atom positions for  $\text{Co}(\text{sal en})_2\text{I}\cdot\text{H}_2\text{O}$  obtained from difference Fourier syntheses

Atom	X	Y	Z	Interatomic distances (Å)	
O(10)	.304	.500	.417	Co(20)-O(10)	2.08 cf 2.13 <sup>a</sup>
O(20) (N(120))	.112	.371	.221	Co(20)-O(20)	2.33
N(10)	.213	.350	.462	Co(20)-N(10)	1.95 cf 1.99 <sup>b</sup>
N(20) (O(120))	.263	.321	.266	Co-N(20)	1.81
N(30)	.202	.560	.179	Co-N(30)	2.14
N(40)	.160	.604	.394	Co-N(40)	2.01
C(10)	.305	.237	.327	C(10)-C(20)	1.50
C(20)	.302	.193	.444	C(20)-C(40)	1.36 cf 1.395 <sup>a</sup>
C(30)	.350	.192	.286	C(30)-C(10)	1.19
C(40)	.347	.090	.498	C(40)-C(60)	1.31
C(50)	.398	.060	.348	C(50)-C(30)	1.65
C(60)	.389	.018	.453		
C(70)	.254	.258	.494	C(70)-C(20)	1.40
				C(70)-N(10)	1.18
C(110)	.333	.645	.254	C(110)-C(120)	1.49
C(120)	.354	.601	.379	C(120)-C(130)	1.35
C(130)	.427	.630	.449	C(130)-C(140)	1.30
C(140)	.481	.685	.420	C(140)-C(150)	1.74
C(150)	.464	.745	.278	C(150)-C(160)	1.33
C(160)	.389	.718	.228	C(160)-C(110)	1.39
C(170)	.259	.634	.174	C(170)-C(110)	1.38
				C(170)-N(30)	1.31
C(80)	.834	.589	.473		
C(90)	.173	.557	.519		
C(180)	.095	.412	.101		
C(190)	.124	.559	.097		
OH(21)	.220	.851	.349	H bonds (?)	
				OH21-N30	3.67
				OH21-N40	2.79
					cf 2.73-3.22 <sup>a</sup>

<sup>a</sup> International Tables (1962)

<sup>b</sup> Saito (1968)

One cycle of B.D.L.S. (scale factor only) reduced the value of  $R$  to .286 and a difference Fourier synthesis phased on the model gave the position of the oxygen atom from the one molecule of water present in the asymmetric unit (Table 4.5). The isotropic temperature factor of this oxygen atom was set equal to  $4.5 \text{ \AA}^2$ .

#### 4.5 LEAST-SQUARES REFINEMENT

##### 4.5.1. Weighting scheme analysis

An empirical weighting scheme was used in this analysis because unobserved data were included in the refinement (Cruickshank, 1961; Cruickshank, 1965 and section 2.5). One cycle of B.D.L.S. (scale factor only), using unit weights and a sample width of 26 for  $|F_o|$  enabled a weighting analysis to be carried out. The equation  $(1/w) = 3.67 + 0.089|F_o|$  was deduced by the method of least-squares (Figure 4.2) and this weighting scheme was used for subsequent refinement.

##### 4.5.2. Isotropic refinement and absorption correction

Seven cycles of B.D.L.S. (109 parameters; scale factor, isotropic temperature factors and atom positional parameters) reduced the value of the residual from .280 to .229. On examination of the data it was found that one reflection  $(-1 \ 0 \ 2)$ , which was the most intense, calculated very much less than the observed value. Since no other reflection occupied the same  $|F_o|$  range in the weighting analysis it was thought justified to omit the reflection from the data.

The data were corrected for absorption (Busing & Levy, 1957b) using a linear absorption coefficient for  $\text{Cu-K}\alpha$  equal to  $180.5 \text{ cm}^{-1}$  obtained from available data (International Tables, 1962) and the following crystal dimensions

1	0	0	(.05 mm)	-1	0	0	(.05 mm)
0	1	0	(.12 mm)	0	-1	0	(.12 mm)
0	0	1	(.18 mm)	0	0	-1	(.18 mm)



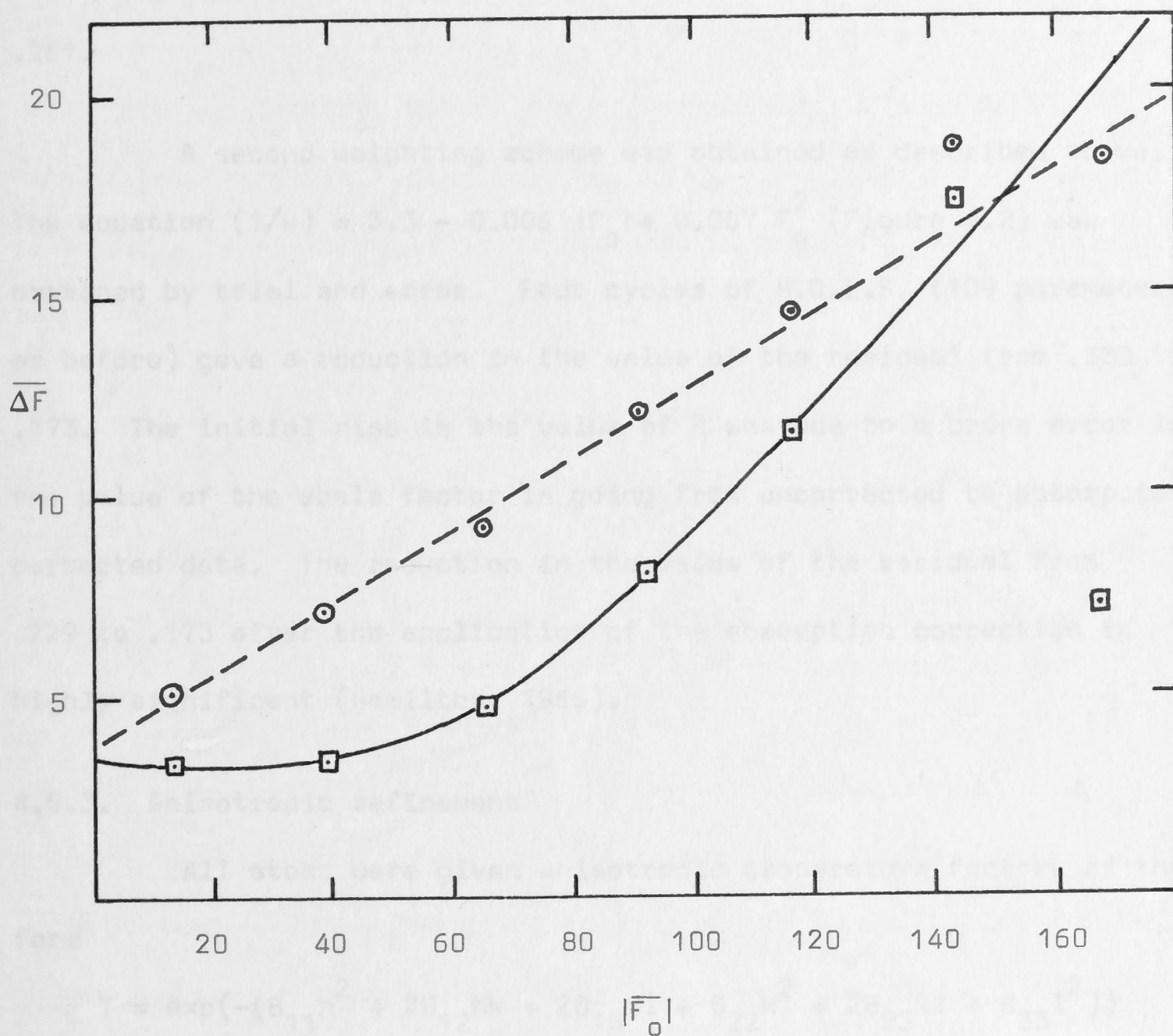


Figure 4.2 Empirical weighting schemes for  $\text{Co}(\text{sal en})_2 \text{I} \cdot \text{H}_2\text{O}$ .

Pre-absorption correction

⊙ experimental data; ---  $\Delta F = 3.67 + 0.89|F_0|$

Post-absorption correction

□ experimental data; —  $\Delta F = 3.3 - 0.006|F_0| + 0.0006F_0^2$

where the perpendicular to the face is measured relative to an arbitrary internal origin. Absorption corrections ranged from .063 to .261.

A second weighting scheme was obtained as described above. The equation  $(1/w) = 3.3 - 0.006 |F_o| + 0.007 F_o^2$  (Figure 4.2) was obtained by trial and error. Four cycles of B.D.L.S. (109 parameters as before) gave a reduction in the value of the residual from .330 to .173. The initial rise in the value of R was due to a cross error in the value of the scale factor in going from uncorrected to absorption corrected data. The reduction in the value of the residual from .229 to .173 after the application of the absorption correction is highly significant (Hamilton, 1965).

#### 4.5.3. Anisotropic refinement

All atoms were given anisotropic temperature factors of the form

$$T = \exp(-(B_{11}h^2 + 2B_{12}hk + 2B_{13}hl + B_{22}k^2 + 2B_{23}kl + B_{33}l^2))$$

Seven cycles of B.D.L.S. (144 parameters; positional and anisotropic thermal parameters for all non-hydrogen atoms and scale factor) gave, with no absorption correction, a reduction in the value of R from .228 to .151. However, using absorption corrected data, five cycles of B.D.L.S. (144 parameters as before) gave a final value for R of .098. Both the reduction in the value of R for absorption corrected data and with the introduction of anisotropic thermal motion are highly significant (Hamilton, 1965).

An electron density synthesis phased on the final parameters showed only the expected atoms and a difference Fourier synthesis showed no evidence of misplaced atoms. No positive peaks in the difference map were greater than  $1.7e \text{ \AA}^{-3}$ , less than a quarter of



typical carbon atom peaks in earlier difference syntheses (ca  $7\text{e } \text{\AA}^{-3}$ ).

On the final cycle of B.D.L.S. no individual parameter shift was greater than 0.1 of the parameter e.s.d. (derived from inversion of the block-diagonal matrices). The standard deviation of an observation of unit weight ( $m = 2850$ ,  $n = 144$ ; see section 2.6) was 1.995.

No hydrogen atoms were included in this analysis. A summary of the analysis is given in Table 4.6. The final positional and thermal parameters, together with their estimated standard deviations, are listed in Table 4.7. Structure factors are listed in Appendix C.

#### 4.6 DESCRIPTION OF THE STRUCTURE

The crystal structure consists of discrete ions. The cations have pseudo- $C_2$  symmetry and consist of two essentially planar tridentate N-(2-aminoethyl)salicylaldiminato ligands, which are approximately at right angles to one another, surrounding the central cobalt atom. A perspective view of the  $\text{Co}(\text{sal en})_2^+$  ion, together with the atom numbering scheme, is shown in Figure 4.3. Thermal ellipsoids have been drawn to include 50% of the probability distribution. The unit cell, showing molecular packing arrangement, is illustrated in Figure 4.4.

Least-squares planes for the two ligands are given in Table 4.8. The conformation of the two ligands was found to be essentially the same (Figure 7.6, Chapter 7).

The water oxygen atom, OH(21), is in such a position as to suggest hydrogen bonding with N(40);  $2.93 \text{ \AA}$ . It is also suggested that hydrogen bonding occurs between I(10) and both N(120) and N(40);

Table 4.6

Summary of crystal structure analysis for  $\text{Co}(\text{sal en})_2\text{I}\cdot\text{H}_2\text{O}$ 

Solution method	Heavy atom
Least-squares method	Block-diagonal
Atom scattering factors (neutral atoms)	Cromer & Waber, 1965
Absorption correction	Applied (Busing & Levy, 1957 )
Anomalous dispersion (source)	Included (International Tables, 1962)
Co	$\Delta F' = -2.2$ $\Delta F'' = 3.8$
I	$\Delta F' = -1.2$ $\Delta F'' = 6.9$
O	$\Delta F' = 0.0$ $\Delta F'' = 0.1$
Weighting scheme	Empirical
	pre-absorption correction:
	$w = 1.0 / (3.67 + 0.089  F_o )$
	post-absorption correction:
	$w = 1.0 / (3.3 - 0.006  F_o  + 0.0007 F_o^2)$
Range of transmission factors	0.061 to 0.261
Data for final refinement	All data used
Final model	All atoms anisotropic/no hydrogen atoms
Largest parameter shift on final cycle (average)	0.04 (0.02)
Summary of R' values:	
end of isotropic refinement	Pre-absorption correction 0.229
	Post-absorption correction 0.173
end of anisotropic refinement	Pre-absorption correction 0.151
	Post-absorption correction 0.098
Final difference Fourier peaks	$1.7e \text{ } \text{\AA}^{-3}$



Table 4.7

(a)

Fractional coordinates ( $\times 10^4$ ), with estimated standard deviations in parentheses

Atoms	x/a	y/b	z/c
I(10)	536(1)	498(1)	2456(1)
Co(20)	2110(1)	4595(2)	3239(1)
O(10)	3069(4)	5332(8)	4177(7)
O(120)	2635(4)	3288(8)	2659(6)
N(10)	2130(5)	3584(9)	4590(8)
N(30)	2030(5)	5613(9)	1866(8)
N(40)	1604(6)	5966(9)	3887(9)
N(120)	1127(5)	3843(9)	2259(8)
C(10)	3047(5)	2341(10)	3307(9)
C(20)	3005(6)	1925(10)	4415(9)
C(30)	3552(7)	1646(13)	2852(13)
C(40)	3458(6)	874(12)	5009(11)
C(50)	3990(7)	585(13)	3490(15)
C(60)	3941(8)	168(13)	4584(13)
C(70)	2516(6)	2554(12)	4985(10)
C(80)	1642(7)	4185(13)	5215(11)
C(90)	1761(9)	5638(13)	5181(12)
C(110)	3339(6)	6406(11)	2539(10)
C(120)	3544(6)	5948(12)	3754(11)
C(130)	4301(7)	6210(13)	4521(13)
C(140)	4834(7)	6861(15)	4121(18)
C(150)	4628(9)	7320(16)	2946(17)
C(160)	3905(8)	7085(11)	2177(15)
C(170)	2589(7)	6237(10)	1687(10)
C(180)	993(8)	4155(14)	1015(11)
C(190)	1267(7)	5554(13)	957(11)
OH(21)	2213(6)	8528(10)	3531(12)

Table 4.7 continued

(b)

Anisotropic temperature factors of the form

$$T = \exp(-(B_{11}h^2 + 2B_{12}hk + 2B_{13}hl + B_{22}k^2 + 2B_{23}kl + B_{33}l^2))$$

( $\times 10^4$ ), with estimated standard deviations in parentheses

Atom	$B_{11}$	$B_{22}$	$B_{33}$	$B_{12}$	$B_{13}$	$B_{23}$
I(10)	28(1)	120(1)	115(1)	-11(1)	29(1)	20(1)
Co(20)	15(1)	52(2)	37(1)	1(1)	13(1)	-1(1)
O(10)	26(3)	110(9)	58(6)	-10(4)	10(3)	-4(6)
O(120)	27(3)	106(9)	42(5)	18(4)	15(3)	15(5)
N(10)	27(3)	79(9)	65(7)	-10(4)	26(4)	-6(7)
N(30)	28(3)	91(10)	55(7)	10(4)	15(4)	10(7)
N(40)	36(4)	55(8)	85(8)	-1(4)	28(5)	-3(7)
N(120)	26(3)	84(10)	63(7)	4(4)	8(4)	-2(7)
C(10)	20(3)	67(10)	53(8)	2(4)	12(4)	1(7)
C(20)	25(3)	56(9)	55(8)	-1(4)	8(4)	3(7)
C(30)	34(5)	94(13)	105(13)	11(6)	29(6)	-3(10)
C(40)	25(4)	85(12)	78(10)	4(5)	7(5)	17(9)
C(50)	22(4)	103(14)	138(16)	14(6)	16(6)	-14(12)
C(60)	40(5)	76(12)	112(14)	15(6)	30(7)	37(10)
C(70)	25(4)	95(12)	64(9)	-2(5)	20(5)	-2(8)
C(80)	40(5)	111(14)	73(10)	-2(7)	41(6)	-2(9)
C(90)	52(6)	113(15)	71(10)	1(7)	41(7)	-9(10)
C(110)	25(4)	70(10)	82(10)	-7(5)	25(5)	-10(8)
C(120)	22(3)	79(11)	95(11)	3(5)	23(5)	-11(9)
C(130)	25(4)	85(13)	120(14)	-4(6)	12(6)	-9(11)
C(140)	24(4)	116(16)	201(23)	-4(7)	41(8)	-28(15)
C(150)	39(6)	114(16)	160(19)	-5(8)	47(9)	10(14)
C(160)	43(5)	47(10)	173(18)	-8(6)	54(8)	-3(11)
C(170)	35(4)	63(10)	73(9)	5(5)	28(5)	5(8)
C(180)	36(5)	116(15)	66(10)	5(7)	6(6)	-12(10)
C(190)	27(4)	113(14)	68(10)	14(6)	-3(5)	-4(9)
OH(21)	48(10)	89(10)	190(15)	-16(5)	31(7)	-20(10)



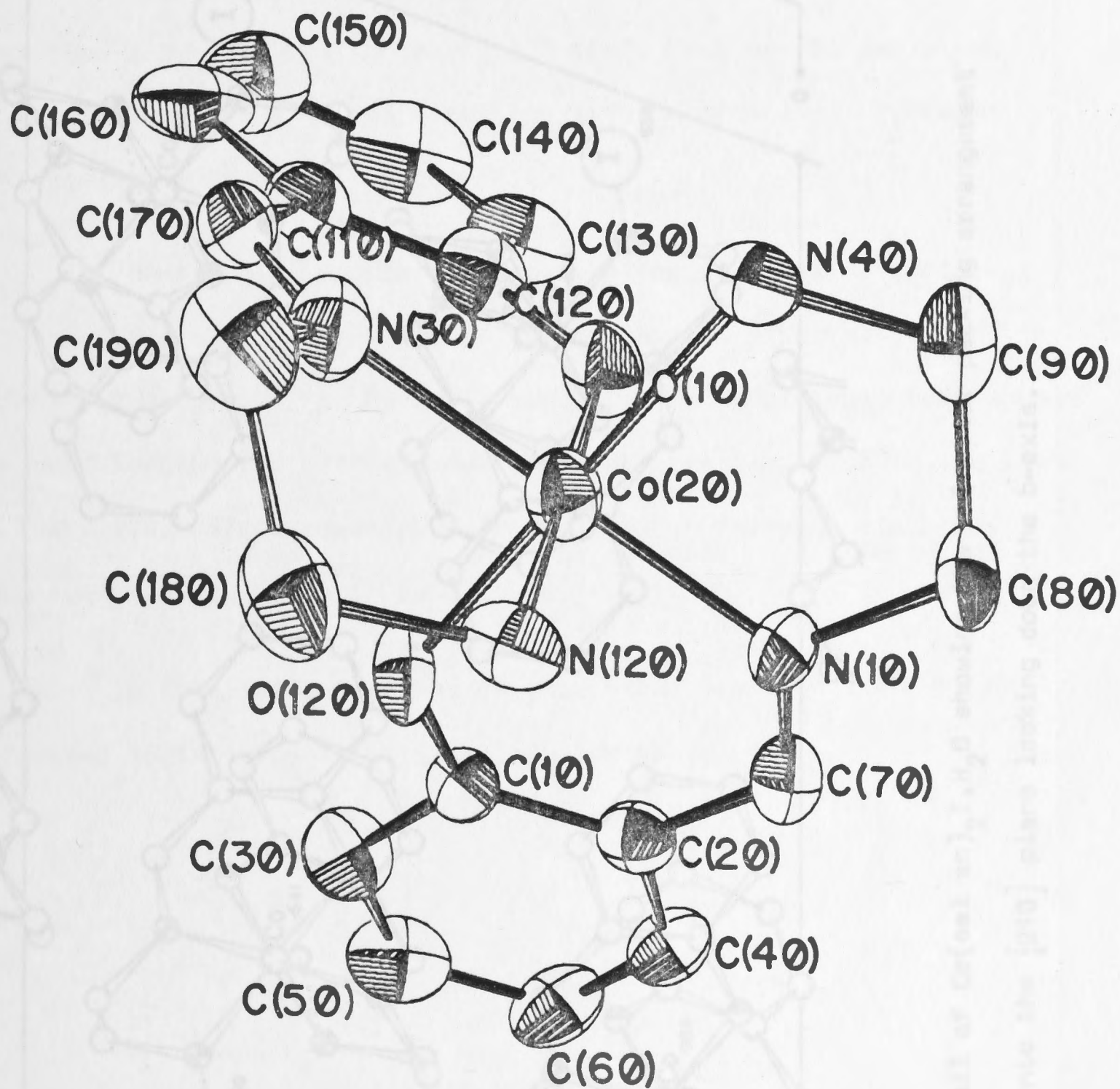


Figure 4.3 Overall stereochemistry of the  $\text{Co}(\text{sal en})_2^+$  ion and atom numbering scheme.





3.61 and 3.74 Å respectively. Similar iodine-nitrogen interactions occur in the chromium analogue (Gardner, Gatehouse & White, 1971).

The cobalt-nitrogen bonds for N(120) and N(40) differ by more than  $2.3 \sigma_{av}$ ; the longer Co(20)-N(40) bond may be explained by the interaction of N(40) with both I(10) and OH(21). Hydrogen bonding is illustrated in Figure 4.4.

Bond angles and bond lengths, given in Table 4.9, Figures 4.5 and 4.6, are in no way unusual when compared with those found in related structures. Furthermore, comparison of individual bond angles and bond lengths for both ligands shows no irregularities in the light of the e.s.d. values reported. Intermolecular approach distances less than 4 Å are given in Table 4.10.

A detailed comparison of this structure with those others discussed in this thesis is given in Chapter 7.

Table 4.8

Mean planes for the N-(2-aminoethyl)salicylaldiminato ligand in  
 $\text{Co}(\text{sal en})_2\text{I}\cdot\text{H}_2\text{O}$

Equations are of the form  $Ax + By + Cz + D = 0$  where  $x$ ,  $y$  and  $z$  refer to the unit cell axes. The coefficients for each plane are given, followed by the atoms defining the plane and their distances from that plane ( $\text{\AA} \times 10^4$ ).

				A	B	C	D
Plane (1)				-.6193	-.6257	-.4743	+5.9027
C(10)	C(20)	C(30)	C(40)	C(50)	C(60)		
10	37	-32	-100	-35	123		
Plane (2)				+.4187	-.8701	-.2600	+4.3032
C(110)	C(120)	C(130)	C(140)	C(150)	C(160)		
15	-3	-46	114	-94	9		
Plane (3)				-.6719	-.5479	-.4984	+6.0983
Co(20)	O(120)	N(10)	C(10)	C(20)	C(30)	C(40)	C(50)
-151	2345	1395	691	366	-369	-1081	-1674
C(60)	C(70)						
-1862	1244						
Plane (4)				+.4994	-.8148	-.2944	+3.6377
Co(20)	N(30)	O(10)	C(110)	C(120)	C(130)	C(140)	C(150)
136	-1721	-2200	108	-733	-54	1550	2139
C(160)	C(170)						
1587	-830						
Plane (5)				-.6907	-.5428	-.4778	+6.0579
Co(20)	N(10)	O(120)	C(10)	C(20)	C(30)	C(40)	C(50)
-45	1858	2023	378	389	-1034	-1086	-2349
C(60)	C(70)	N(40)	C(80)	C(90)			
-2202	1644	-2891	3077	-6408			
Plane (6)				+.5116	-.8156	-.2704	+3.5128
Co(20)	O(10)	N(30)	C(110)	C(120)	C(130)	C(140)	C(150)
43	-1878	-2143	123	-401	616	2245	2525
C(160)	C(170)	N(120)	C(180)	C(190)			
1644	-1172	2078	4618	-4158			



Table 4.8 continued

## Dihedral angles (degrees)

Plane (2) - Plane (1) 65.9	Plane (2) - Plane (3) 71.0
Plane (2) - Plane (4) 5.9	Plane (2) - Plane (6) 6.2
Plane (2) - Plane (5) 72.1	Plane (1) - Plane (3) 5.6
Plane (1) - Plane (4) 70.1	Plane (1) - Plane (6) 71.2
Plane (1) - Plane (5) 6.3	Plane (3) - Plane (4) 75.1
Plane (3) - Plane (6) 76.2	Plane (3) - Plane (5) 1.6
Plane (4) - Plane (6) 1.5	Plane (4) - Plane (5) 76.2
Plane (6) - Plane (5) 77.4	

Table 4.9

(a)

Bond lengths and angles about cobalt in  $\text{Co}(\text{sal en})_2\text{I}\cdot\text{H}_2\text{O}$  (e.s.d. values in parentheses)

Atoms	Bond lengths (Å)	Atoms	Bond angles (degrees)
Co(20)-O(10)	1.876(7)	O(10)-Co(20)-N(120)	179.3(4)
Co(20)-O(120)	1.912(8)	O(10)-Co(20)-O(120)	90.6(3)
Co(20)-N(10)	1.913(10)	O(10)-Co(20)-N(30)	94.6(4)
Co(20)-N(120)	1.949(8)	O(10)-Co(20)-N(10)	88.0(4)
Co(20)-N(30)	1.912(10)	O(10)-Co(20)-N(40)	87.3(4)
Co(20)-N(40)	1.982(11)	O(120)-Co(20)-N(30)	88.1(4)
		O(120)-Co(20)-N(40)	177.9(3)
		O(120)-Co(20)-N(10)	93.8(4)
		O(120)-Co(20)-N(120)	89.1(4)
		N(10)-Co(20)-N(120)	92.6(4)
		N(10)-Co(20)-N(40)	85.7(4)
		N(30)-Co(20)-N(40)	92.5(4)
		N(30)-Co(20)-N(120)	84.8(4)
		N(120)-Co(20)-N(40)	93.0(4)

Table 4.9 continued

(b)

Bond lengths and angles for sal en ligands in  $\text{Co}(\text{sal en})_2\text{I}\cdot\text{H}_2\text{O}$   
(e.s.d. values in parentheses)

Atoms	Bond lengths (Å)	Atoms	Bond angles (degrees)
Ligand A			
C(10)-C(20)	1.423(16)	C(20)-C(10)-C(30)	117.5(10)
C(10)-C(30)	1.417(19)	C(10)-C(30)-C(50)	120.3(14)
C(20)-C(40)	1.397(15)	C(30)-C(50)-C(60)	122.0(15)
C(40)-C(60)	1.370(22)	C(50)-C(60)-C(40)	116.2(12)
C(60)-C(50)	1.413(25)	C(60)-C(40)-C(20)	124.4(13)
C(50)-C(30)	1.411(18)	C(40)-C(20)-C(10)	119.6(11)
C(20)-C(70)	1.451(18)	C(70)-C(20)-C(10)	123.2(9)
C(10)-O(120)	1.310(12)	C(20)-C(10)-O(120)	124.8(10)
C(70)-N(10)	1.268(14)	C(20)-C(70)-N(10)	123.3(11)
C(80)-N(10)	1.484(18)	C(70)-N(10)-Co(20)	127.7(9)
C(80)-C(90)	1.504(20)	C(80)-N(10)-Co(20)	111.4(7)
C(90)-N(40)	1.517(17)	N(10)-C(80)-C(90)	106.0(12)
		C(80)-C(90)-N(40)	105.5(10)
		C(90)-N(40)-Co(20)	107.1(7)
Ligand B			
C(110)-C(120)	1.454(17)	C(110)-C(120)-C(130)	117.1(12)
C(120)-C(130)	1.409(15)	C(120)-C(130)-C(140)	121.2(14)
C(130)-C(140)	1.398(24)	C(130)-C(140)-C(150)	121.4(14)
C(140)-C(150)	1.398(24)	C(140)-C(150)-C(160)	119.3(17)
C(150)-C(160)	1.358(20)	C(150)-C(160)-C(110)	121.5(16)
C(160)-C(110)	1.435(21)	C(160)-C(110)-C(120)	119.5(10)
C(110)-C(170)	1.421(14)	C(170)-C(110)-C(120)	122.8(11)
C(170)-N(30)	1.290(17)	C(110)-C(120)-O(10)	124.3(9)
C(120)-O(10)	1.310(16)	C(120)-O(10)-Co(20)	124.9(7)
N(30)-C(190)	1.457(14)	C(110)-C(170)-N(30)	125.0(11)
C(190)-C(180)	1.525(20)	C(170)-N(30)-Co(20)	125.5(7)
C(180)-N(120)	1.464(17)	C(190)-N(30)-Co(20)	113.4(8)
		N(30)-C(190)-C(180)	104.7(9)
		C(190)-C(180)-N(120)	107.9(10)
		C(180)-N(120)-Co(20)	109.2(8)



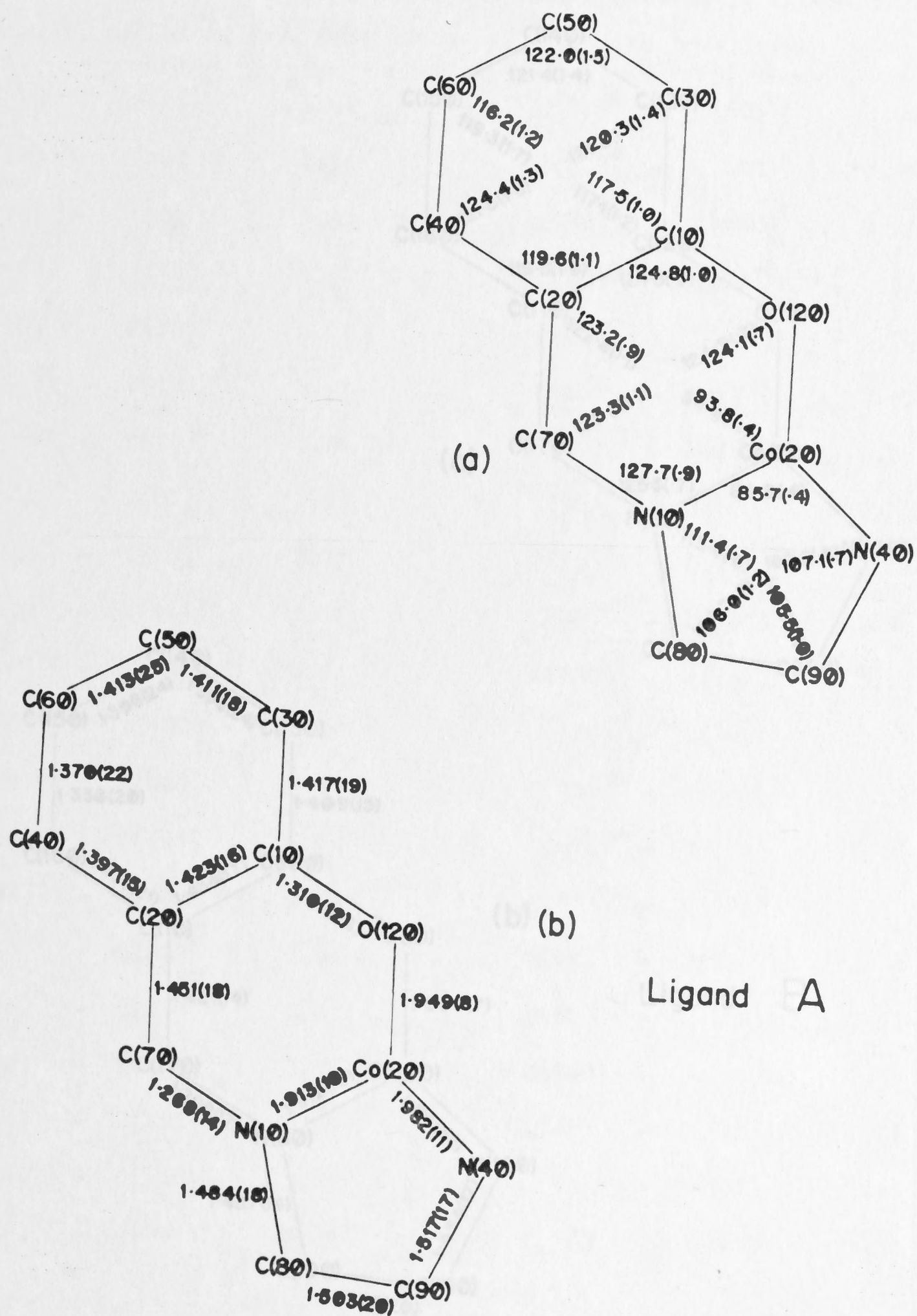


Figure 4.5 (a) Bond angles (degrees) and (b) bond lengths ( $\text{\AA}$ ) for  $\text{Co}(\text{sal en})_2\text{I}\cdot\text{H}_2\text{O}$  (estimated standard deviations in parentheses).

Table 4.6  
 Interatomic approach distances for  $\text{Co}(\text{sal en})_2\text{I}\cdot\text{H}_2\text{O}$  (3)  
 Transformations of the asymmetric unit are indicated by superscripts  
 as  $x, y, z$ ;  $b, \bar{x}, \bar{y}, \bar{z}$ ;  $c, \bar{x}, \bar{y}, \bar{z}$ ;  $d, \bar{x}, \bar{y}, \bar{z}$

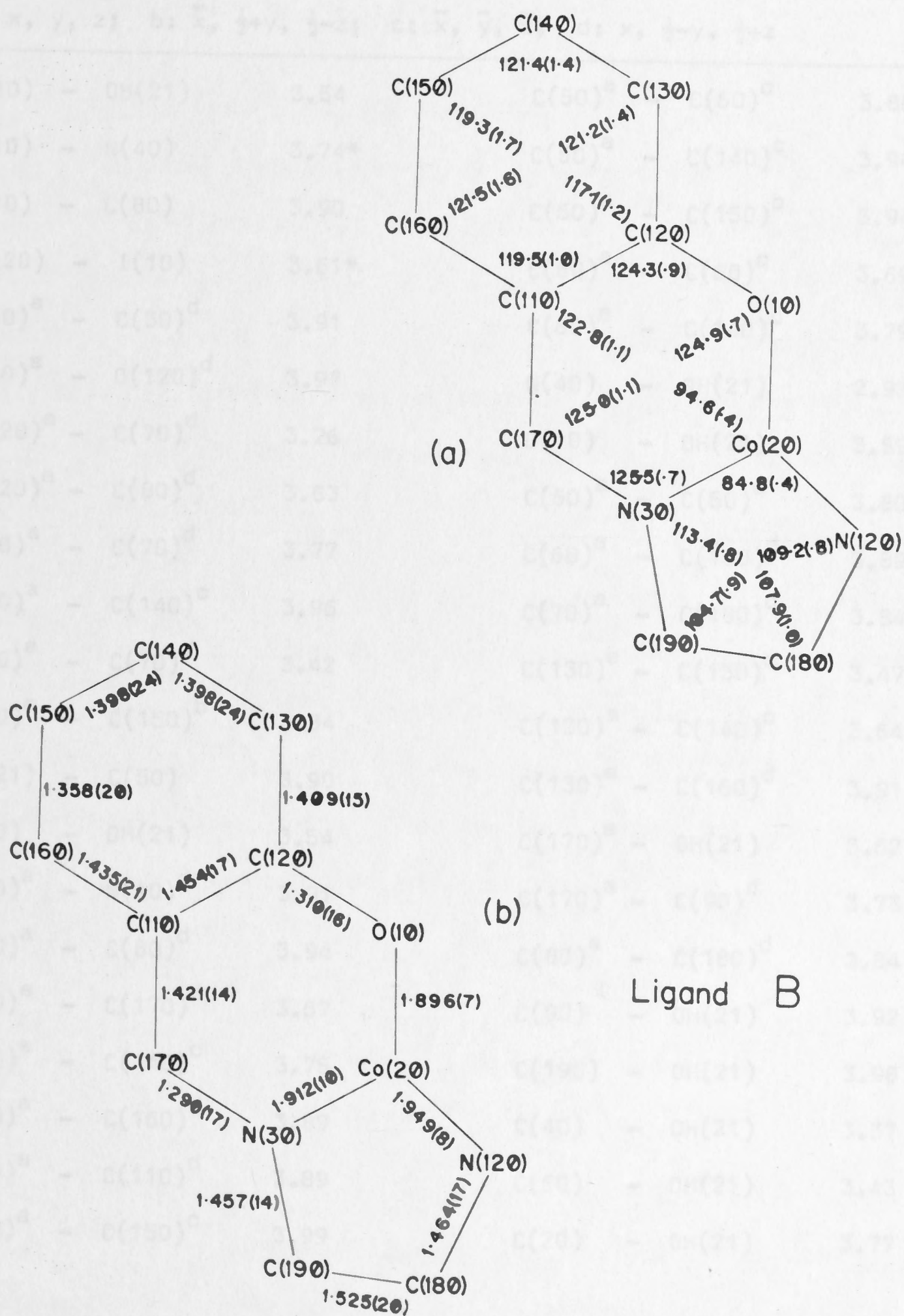


Figure 4.6 (a) Bond angles (degrees) and (b) bond lengths ( $\text{\AA}$ )  
 for  $\text{Co}(\text{sal en})_2\text{I}\cdot\text{H}_2\text{O}$  (estimated standard deviations  
 in parentheses).



Table 4.10

Intermolecular approach distances for  $\text{Co}(\text{sal en})_2\text{I}\cdot\text{H}_2\text{O}$  (Å)

Transformations of the asymmetric unit are indicated by superscripts

a:  $x, y, z$ ; b:  $\bar{x}, \frac{1}{2}+y, \frac{1}{2}-z$ ; c:  $\bar{x}, \bar{y}, \bar{z}$ ; d:  $x, \frac{1}{2}-y, \frac{1}{2}+z$ 

I(10) - OH(21)	3.54	C(50) <sup>a</sup> - C(60) <sup>c</sup>	3.80
I(10) - N(40)	3.74*	C(50) <sup>a</sup> - C(140) <sup>c</sup>	3.94
I(10) - C(80)	3.90	C(50) <sup>a</sup> - C(150) <sup>b</sup>	3.94
N(120) - I(10)	3.61*	C(60) <sup>a</sup> - C(60) <sup>c</sup>	3.69
N(10) <sup>a</sup> - C(30) <sup>d</sup>	3.91	C(60) <sup>a</sup> - C(140) <sup>c</sup>	3.79
N(10) <sup>a</sup> - O(120) <sup>d</sup>	3.97	N(40) - OH(21)	2.93*
O(120) <sup>a</sup> - C(70) <sup>d</sup>	3.26	O(10) - OH(21)	3.59
O(120) <sup>a</sup> - C(80) <sup>d</sup>	3.83	C(60) <sup>a</sup> - C(50) <sup>c</sup>	3.80
C(10) <sup>a</sup> - C(70) <sup>d</sup>	3.77	C(60) <sup>a</sup> - C(160) <sup>d</sup>	3.89
C(20) <sup>a</sup> - C(140) <sup>c</sup>	3.96	C(70) <sup>a</sup> - C(180) <sup>d</sup>	3.84
C(30) <sup>a</sup> - C(70) <sup>d</sup>	3.42	C(130) <sup>a</sup> - C(130) <sup>c</sup>	3.47
C(30) <sup>a</sup> - C(150) <sup>b</sup>	3.84	C(130) <sup>a</sup> - C(140) <sup>c</sup>	3.64
OH(21) - C(50)	3.90	C(130) <sup>a</sup> - C(160) <sup>d</sup>	3.91
N(30) - OH(21)	3.54	C(170) <sup>a</sup> - OH(21)	3.62
C(30) <sup>a</sup> - N(10) <sup>d</sup>	3.91	C(170) <sup>a</sup> - C(90) <sup>d</sup>	3.73
C(30) <sup>a</sup> - C(80) <sup>d</sup>	3.94	C(80) <sup>a</sup> - C(180) <sup>d</sup>	3.84
C(40) <sup>a</sup> - C(170) <sup>d</sup>	3.67	C(90) - OH(21)	3.92
C(40) <sup>a</sup> - C(140) <sup>c</sup>	3.75	C(190) - OH(21)	3.98
C(40) <sup>a</sup> - C(160) <sup>d</sup>	3.89	C(40) - OH(21)	3.37
C(40) <sup>a</sup> - C(110) <sup>d</sup>	3.89	C(60) - OH(21)	3.43
C(40) <sup>a</sup> - C(150) <sup>c</sup>	3.99	C(20) - OH(21)	3.77

\* hydrogen bonds illustrated in Figure 4.4 as broken lines

## CHAPTER 5

CRYSTAL AND MOLECULAR STRUCTURE OF  $(-)_409$ -R,S-[(R-N(2-AMINOPROPYL)SALICYLALDIMINATO)CHROMIUM(III)]PERCHLORATE\*

## 5.1 UNIT CELL AND DIFFRACTION SYMMETRY

Euhedral crystals were grown by slow evaporation of a solution of R,S-[Cr(sal (R)pn(2-Me))<sub>2</sub>]ClO<sub>4</sub>. Crystals were generally twinned as shown by re-entrant angles and appearance under crossed polarizers. One reasonably large hand picked specimen proved to be a single crystal. Initial photographic studies suggested that the crystal belonged to the triclinic system and examination of the crystal morphology supported this.

The crystal was mounted about a perpendicular to one of the two largest faces and a series of precession photographs were taken in order to determine the space group (Buerger, 1960). The crystal system was confirmed to be triclinic and the space group was P1 (No. 1) (International Tables, 1952). This was confirmed by the subsequent analysis. Unit cell dimensions were determined to be

$$\begin{aligned} a &= 8.65 \text{ \AA} & \alpha &= 113.2^\circ \\ b &= 12.61 \text{ \AA} & \beta &= 105.3^\circ \\ c &= 12.62 \text{ \AA} & \gamma &= 103.1^\circ \\ & & V &= 1133 \text{ \AA}^3 \end{aligned}$$

The density of the crystalline material was determined to be 1.45 g cm<sup>-3</sup>, by the method of flotation using a mixture of carbon tetrachloride and ethyl bromide. This value for D<sub>m</sub> gave Z = 2, corresponding to D<sub>c</sub> = 1.48 g cm<sup>-3</sup>.

\* R,S-[Cr(sal (R)pn(2-Me))<sub>2</sub>]ClO<sub>4</sub> for brevity



The photographically determined unit cell parameters were subjected to a Delaunay reduction (International Tables, 1952) and it was shown that the cell was indeed the reduced form.

## 5.2 DATA COLLECTION AND REDUCTION

### 5.2.1. Unit cell refinement

The crystal was mounted about the reciprocal  $a$ -axis (Araldite Fast Set; glass capillary) and placed on a Picker FACS-I automatic four-circle diffractometer. The crystal was oriented so that the  $a^*$ -axis was coincident with the  $\phi$ -axis of the diffractometer.

Unit cell parameters were refined using the method of least-squares (Busing, Ellison, Levy, King & Rosebury, 1968). Twelve prominent reflections were chosen to give a wide range of  $h$ ,  $k$  and  $l$  with large  $2\theta$  values using  $\text{Cu-K}\alpha_1$  radiation (Table 5.1).  $2\theta$ ,  $\chi$ ,  $\phi$  and  $\omega$  were each individually refined and the results used to calculate a better orientation matrix and the refined unit cell parameters given below

$$\begin{aligned} a &= 8.626(1) \text{ \AA} & \alpha &= 113.01(3)^\circ \\ b &= 12.729(2) \text{ \AA} & \beta &= 105.16(3)^\circ \\ c &= 12.580(2) \text{ \AA} & \gamma &= 103.15(3)^\circ \\ & & V &= 1158.61 \text{ \AA}^3 \end{aligned}$$

Table 5.1

Unit cell refinement data for  $\text{R}_2\text{S} \cdot [\text{Cr}(\text{sal}(\text{R})\text{pn}(2\text{-Me}))_2]\text{ClO}_4$

$h$	$k$	$l$	$2\theta$	$h$	$k$	$l$	$2\theta$
-8	0	0	105.72	1	2	8	89.84
0	0	10	92.59	-8	1	4	92.40
0	11	0	102.30	-8	1	2	94.48
-6	7	6	98.54	-3	-8	1	88.33
-1	2	10	99.65	-1	-10	2	87.17
-2	6	8	105.90	-1	4	-10	84.47

## 5.2.2. Data collection and reduction

$\bar{H}KL$  and  $H\bar{K}\bar{L}$  data were collected, at room temperature, using graphite monochromated  $Cu-K\alpha_1$  radiation to a maximum value of  $62.5^\circ$  for  $\theta$ . Intensities were measured in the bisecting  $\theta-2\theta$  mode as described in section 3.2.1.

Three standard reflections were each measured after every 97 reflections.

During data collection movement of the crystal was detected by a) noting a change in the standard reflection count for the standard  $-8,0,0$  which fell in value by 30% and b) checking the crystal orientation against the stored orientation matrix. The movement was thought to be due to either 'uncured' Araldite or slackness in the goniometer arcs.

The crystal was re-oriented and data collection resumed (machine time being limited) at a point corresponding to the 1847th reflection in the data set. This point was chosen because the difference between standard reflection counts up to this point was less than 10%.

A graph of intensity versus reflection sequence number for each of the three standard reflections, for each of the data sets, was plotted. To each of the six graphs a least-squares fit was calculated to give the slope which was then used to obtain anisotropic linear correction factors, these were

	Data set 1	Data set 2
0 0 10	$.42 \times 10^{-7}$	$.75 \times 10^{-7}$
0 11 0	$.18 \times 10^{-4}$	$.78 \times 10^{-5}$
-8 0 0	$.11 \times 10^{-3}$	$.48 \times 10^{-5}$

A single data set corrected for linear decay was obtained by combining the first 1847 reflections of the first data set with the



second data set. Observed intensities were calculated and those with  $I_o < 3.0 \sigma_1(I_o)$  were rejected as unobserved. Structure factors and their  $\sigma_1(F_o)$  and  $\sigma_2(F_o)$  were calculated as described in section 3.2.2. A total of 4466 observed reflections were collected (574 unobserved, 11.4%; 25 reflections had uneven backgrounds). Data collection conditions are summarised in Table 5.2.

Comparison of the most intense reflections with a powder pattern, obtained using a Philips PW 1050/25 recording diffractometer, showed that the single crystal was representative of the bulk material.

### 5.3 DETERMINATION OF CHROMIUM ATOM POSITIONS

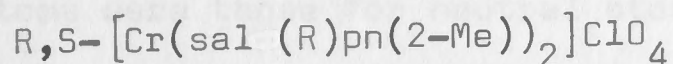
The ratio  $\sum Z_h^2 / \sum Z_l^2$ , using chromium as the only heavy atom, was 0.36, whilst with chromium and chlorine as the heavy atoms, the value was 0.65. Hence it was decided to use normal heavy atom methods to solve the structure.

Since the compound crystallizes in space group P1 (No. 1) there are no non-general vectors in the Patterson function. However, with  $Z = 2$  the highest peak in the Patterson function should correspond to a chromium-chromium vector. The cell origin must be defined by placing one of these chromium atoms at 0,0,0. The position of the second chromium atom may then be determined. Furthermore, the distance between these two chromium atoms should be in the range 6 to 8 Å (i.e. half the maximum diagonal of the unit cell).

Examination of a three-dimensional, unsharpened Patterson function showed one strong peak at .490, .272, .711 (Cr(20)), which was 7.69 Å from the unit cell origin. This was assumed to be a chromium position. The heavy atom model consisted of Cr(10) at the unit cell origin and Cr(20), both of which were given individual isotropic

Table 5.2

Summary of crystal data and data collection for



Chemical formula	$C_{20}H_{26}N_4O_2CrClO_4$
Formula weight	505.95
Space group	P1 (No. 1)
Boundary faces of crystal; (mm from internal origin in parentheses)	$\begin{array}{ccccccc} 1 & 0 & 0 & (.30) & 0 & 1 & 0 & (.22) \\ 0 & 0 & 1 & (.09) & 0 & -1 & 0 & (.22) \\ 0 & 0 & -1 & (.09) & 0 & 1 & 1 & (.17) \\ -1 & 1 & 0 & (.26) & -1 & -1 & 0 & (.26) \end{array}$
Unit cell parameters	$a = 8.626(1) \text{ \AA}$ $b = 12.729(2) \text{ \AA}$ $c = 12.580(2) \text{ \AA}$ $\alpha = 113.01(3)^\circ$ $\beta = 105.16(3)^\circ$ $\gamma = 103.15(3)^\circ$ $V = 1158.61 \text{ \AA}^3$
Radiation for unit cell refinement	$Cu-K\alpha_1 = 1.5405 \text{ \AA}$
Density	$1.45 \pm 0.04 \text{ g cm}^{-3}$
$D_m$	
$D_c$	$1.48 \text{ g cm}^{-3}$
Z	2
Linear absorption coefficients	$\mu(Cu-K\alpha) = 57.09 \text{ cm}^{-1}$ $\mu(Mo-K\alpha) = 6.76 \text{ cm}^{-1}$
Radiation used for data collection (monochromator; $2\theta$ )	$Cu-K\alpha_1$ (graphite; $26.50^\circ$ )
Scan width; speed; dispersion	$(1.25 + \Delta)^\circ$ ; $2^\circ \text{min}^{-1}$ ; $0.285$
Scan mode	$\theta - 2\theta$
Background times	10 sec
Standard reflections	0 0 10; 0 11 0; -8 0 0
Standard linear correction factors ( $\times 10^5$ )	Data 1: .0042; 1.8; 11.0; Data 2: .0075; .78; .45
Standard frequency	97
Data collected ( $2\theta$ limit)	$-H \pm K \pm L$ ( $125.0^\circ$ )
Number of observed data (%)	4466 (88.6)



temperature factors equal to  $2.5 \text{ \AA}^2$ . Scattering factors used for non-hydrogen atoms were those for neutral atoms (Cromer & Waber, 1965). Anomalous dispersion terms,  $\Delta F'$  and  $\Delta F''$ , were included (International Tables, 1962), although no allowance was made for their dependence upon  $\sin \theta$ .

The scale factor was set equal to unity and the heavy atom model was subjected to one cycle of B.D.L.S. (scale factor, atom positional and thermal parameters (the Cr(10) position is invariant and therefore never refined)), this gave a value for R equal to .448. A difference Fourier synthesis was then phased on the model.

#### 5.4 DETERMINATION OF LIGHT ATOM POSITIONS

Examination of the difference Fourier map gave the positions of the atoms in both chromium atom coordination octahedra. These atoms were given the designations N(10) to N(60) and N(110) to N(160) (Table 5.3), since, at this stage, differentiation between oxygen and nitrogen atoms was not necessary. The new atoms were given individual isotropic temperature factors equal to  $3.5 \text{ \AA}^2$ .

One cycle of B.D.L.S. (scale factor, atom positional and thermal parameters) gave a value for R equal to .447. A difference Fourier synthesis was phased on the model and this gave the position of one chlorine atom (Cl(10) Table 5.3), which was given an individual temperature factor equal to  $3.5 \text{ \AA}^2$ .

The model was subjected to one cycle of B.D.L.S. (scale factor, atom positional and thermal parameters) and the data were used to phase a difference Fourier synthesis, R was .355 at this point. The positions of the second chlorine atom (Cl(20) Table 5.3) and three perchlorate oxygen atoms (O(10) to O(30) Table 5.3) were determined from this map.

105.  
Table 5.3

Initial atom positions for R,S-[Cr(sal (R)pn(2-Me))<sub>2</sub>]ClO<sub>4</sub> obtained  
from difference Fourier syntheses

Atom	X	Y	Z	Interatomic distances (Å)	
Cr(20)	.490	.272	.711	Cr(20) - N(10)	2.06 cf Cr-O 1.92 <sup>a</sup>
N(10)	.229	.184	.629	Cr(20) - N(20)	1.91 (O(120)) Cr-N 2.15 <sup>a</sup>
N(20)	.739	.351	.794	Cr(20) - N(30)	1.93
N(30)	.482	.318	.877	Cr(20) - N(40)	1.98 (O(140))
N(30)	.508	.112	.676	Cr(20) - N(50)	2.14
N(50)	.510	.240	.245	Cr(20) - N(60)	2.05
N(60)	.457	.430	.726		
N(110)	.255	.088	.081	Cr(10) - N(110)	2.02 (O(210))
N(120)	-.255	.922	.919	Cr(10) - N(120)	1.94
N(130)	-.025	.163	.036	Cr(10) - N(130)	2.05
N(140)	.011	.956	.834	Cr(10) - N(140)	1.96 (O(240))
N(150)	.022	.032	.167	Cr(10) - N(150)	1.93
N(160)	.029	.844	.984	Cr(10) - N(160)	2.00
Cl(10)	.005	.294	.414		
Cl(20)	.494	.684	.005		
O(10)	-.077	.361	.316	Cl(10) - O(10)	1.67 cf 1.41 <sup>b</sup>
O(20)	.035	.354	.510	Cl(10) - O(20)	1.11
O(30)	.154	.263	.420	Cl(10) - O(20)	1.42
O(40)	.615	.684	.947	Cl(20) - O(40)	1.38
O(50)	.519	.816	.079	Cl(20) - O(50)	1.52
O(60)	.557	.671	.105	Cl(20) - O(60)	1.31
O(70)	.346	.605	.921	Cl(20) - O(70)	1.46
O(80)	-.154	.184	.334	Cl(10) - O(80)	1.45
C(10)	.462	.816	.474	C(10) - C(40)	1.25 cf 1.395 <sup>b</sup>
C(20)	.538	.026	.474	C(20) - C(30)	1.55
C(30)	.500	.026	.579		
C(40)	.562	.895	.553	C(40) - C(10)	1.25
C(50)	.556	.974	.395	C(50) - C(60)	1.75?
C(60)	.556	.828	.395	C(60) - C(10)	1.44
C(70)	.557	.144	.485	C(20) - C(70)	1.42
C(110)	-.018	-.136	-.256	C(110) - C(120)	1.43 C(110)-O(240) 1.23
C(120)	-.051	-.165	-.383	C(120) - C(110)	1.43
C(130)	-.038	-.263	-.474	C(130) - C(120)	1.29
C(140)	.038	-.344	-.447	C(140) - C(130)	1.56
C(150)	.000	-.342	-.342	C(150) - C(140)	1.40
C(160)	.033	-.241	-.231	C(160) - C(150)	1.35



Table 5.3 continued

Atom	X	Y	Z	Interatomic distances (Å)
C(170)	.038	-.211	-.105	C(170) - C(160) 1.32
C(80)	.538	.355	.513	C(80) - N(50) 1.58
C(90)	.615	.474	.658	C(90) - C(80) 1.76?
C(91)	.577	.579	.632	C(90) - N(60) 1.74?
C(180)	.096	-.158	.105	C(180) - N(160) 1.43
C(190)	.038	-.079	.303	C(191) - C(180) 1.69?
C(191)	-.019	-.100	.190	C(100) - N(20) 1.3 (O(120))
C(100)	.808	.421	.921	C(100) - C(200) 1.36
C(200)	.010	.484	.971	C(200) - C(300) 1.42
C(300)	.077	.553	.079	C(300) - C(400) 1.37
C(400)	.019	.579	.184	C(400) - C(500) 1.49
C(500)	.846	.526	.144	C(500) - C(600) 1.33
C(600)	.769	.447	.026	C(600) - C(700) 1.49
C(700)	.577	.394	.000	C(800) - C(900) 1.32
				C(800) - N(30) 1.56
C(800)	.289	.276	.855	C(900) - N(10) 1.45
C(900)	.192	.198	.737	C(900) - C(910) 1.68
C(910)	-.019	.144	.698	C(310) - C(360) 1.52
C(310)	.231	.289	.158	C(310) - C(320) 1.44
C(320)	.346	.421	.234	C(320) - C(330) 1.30
C(330)	.500	.447	.289	C(330) - C(340) 1.40
C(340)	.596	.381	.276	C(340) - C(350) 1.33
C(350)	.500	.263	.211	C(350) - C(360) 1.45
C(360)	.237	.200	.145	C(360) - N(110) 1.19 (O(210))
C(370)	.057	.263	.105	C(370) - N(130) 1.23
C(380)	.773	.140	.983	C(380) - C(390) 1.60?
C(390)	.663	.026	.982	C(390) - C(391) 1.56
C(391)	.462	.976	.902	C(380) - N(130) 1.47
				C(390) - N(120) 1.45

a Gardner, Gatehouse &amp; White (1971)

b International Tables (1962)

The oxygen atoms were given individual isotropic temperature factors equal to  $5.0 \text{ \AA}^2$  and that for the chlorine atom was set equal to  $3.5 \text{ \AA}^2$ .

One cycle of B.D.L.S. (scale factor, atom thermal and positional parameters) was calculated giving an R value of .326. A difference Fourier map phased on this model gave the positions of the atoms in two aromatic rings (C(10) to C(70) and C(110) to C(160), Table 5.3) and also four perchlorate oxygen atoms (O(40) to O(70), Table 5.3). At this stage the atom re-designations  $N(40) \rightarrow O(140)$  and  $N(140) \rightarrow O(240)$  were made. All new atoms were given individual isotropic temperature factors equal to  $5.0 \text{ \AA}^2$ .

The model was subjected to one cycle of B.D.L.S. (scale factor, atom positional and thermal parameters) which gave a value for R equal to .300. A difference Fourier synthesis gave the positions of the remaining carbon atoms associated with the known sal pn ligands (C(80), C(90), C(91), C(180), C(190) and C(191), Table 5.3) and also the last perchlorate oxygen atom (O(80)). The new atoms were given individual isotropic temperature factors equal to  $5.0 \text{ \AA}^2$ .

One cycle of B.D.L.S. (scale factor, atom positional and thermal parameters) was followed by a difference Fourier synthesis, which gave the positions of the atoms in the third ligand (C(100) to C(900) and C(910), Table 5.3). The value of R at this stage was equal to .291. The atom re-designation  $N(20) \rightarrow O(120)$  was now made and the new carbon atoms were given individual temperature factors equal to  $5.0 \text{ \AA}^2$ .

The model was subjected to one cycle of B.D.L.S. (scale factor, atom positional and thermal parameters), which gave an R value equal to .246. A difference Fourier synthesis phased on the model gave the positions of the atoms of the fourth and final aromatic ring (C(310)



to C(370), Table 5.3). These atoms were given individual isotropic temperature factors equal to  $5.0 \text{ \AA}^2$  and the atom re-designation  $N(110) \rightarrow O(210)$  was now made.

One cycle of B.D.L.S. (scale factor, atom positional and thermal parameters) gave a value for R equal to .220 and a difference Fourier synthesis phased on the model gave the positions of the last three carbon atoms (C(380), C(390) and C(391), Table 5.3). These carbon atoms were given individual isotropic temperature factors equal to  $5.0 \text{ \AA}^2$ . One cycle of B.D.L.S. (scale factor, atom positional and thermal parameters) gave a value for R equal to .200.

## 5.5 LEAST-SQUARES REFINEMENT AND ABSORPTION CORRECTION

### 5.5.1 Initial least-squares refinement

The model was subjected to eight cycles of B.D.L.S. (254 parameters; scale factor, atom positional and thermal parameters), at which point the value of R was .109. All B.D.L.S. calculations included  $\sigma_2(F_o)$  weights.

Temperature factors were now converted to the anisotropic form

$$T = \exp(-(B_{11}h^2 + 2B_{12}hk + 2B_{13}hl + B_{22}k^2 + 2B_{23}kl + B_{33}l^2)),$$

and ten cycles of B.D.L.S. were calculated (574 parameters; scale factor, atom positional and thermal parameters) giving an R value of 0.082. This drop in the value of R is highly significant (Hamilton, 1965).

Hydrogen atom positions were calculated (Churchill, 1973), with the exception of those hydrogens attached to the methyl carbon atoms, using a bond length of  $1.0 \text{ \AA}$ . The isotropic temperature factors of the hydrogen atoms were set equal to 1.1 of the equivalent isotropic B for the attached non-hydrogen atom. Hydrogen scattering factors were those of Stewart, Davidson & Simpson (1965). The new model was

subjected to five cycles of B.D.L.S. (574 parameters; scale factor, atom positional and thermal parameters). The hydrogen atom parameters were not refined. The resulting value of R was .077. A difference Fourier synthesis phased on this model did not show the positions of the methyl hydrogen atoms.

#### 5.5.2. Absorption correction and final anisotropic refinement

The data were corrected for absorption (de Meulenaer & Tompa, 1965) using a linear absorption coefficient for Cu-K $\alpha_1$  equal to  $57.09 \text{ cm}^{-1}$ , obtained from data available (International Tables, 1962), and the following crystal dimensions

1	0	0	(.030)	0	0	-1	(.009)
0	1	0	(.022)	-1	1	0	(.026)
0	-1	0	(.022)	-1	-1	0	(.026)
0	0	1	(.009)	0	1	1	(.017)

where the perpendicular to the face is measured relative to an arbitrary internal origin (cm). Absorption corrections ranged from .3477 to .6546.  $\sigma_2(F_o)$  was recalculated for the 4473 observed data.

The model, without calculated hydrogen positions and with absorption corrected data, was subjected to eleven cycles of B.D.L.S. (574 parameters; scale factor, non-hydrogen atom positional and thermal parameters) and the value for R dropped from .472 to .054. The initial rise in the value of R was due to a gross error in the value of the scale factor, which changed from 6.684 to 12.766 in the first cycle.

The positions of the hydrogen atoms were recalculated as before and added to the model. Twelve cycles of B.D.L.S. (574 parameters; scale factor, non-hydrogen atom positional and thermal parameters) gave a final R value equal to .044.



Comparison of the final R value for absorption corrected data with that obtained for the uncorrected data, showed that the former model is the more correct (Hamilton, 1965).

On the final cycle of B.D.L.S. no parameter shift was greater than 0.1 of the e.s.d. (e.s.d.'s were obtained by inversion of the B.D.L.S. matrices). The standard deviation of an observation of unit weight ( $m = 4473$ ,  $n = 574$ ; see section 2.6) was 2.349. An electron density synthesis phased on the final parameters showed only the expected atoms and a difference Fourier synthesis showed no evidence of misplaced atoms. No positive peak in the difference map was greater than  $0.66e \text{ \AA}^{-3}$ , less than a tenth of the average carbon peak height in earlier difference maps (ca  $7e \text{ \AA}^{-3}$ ).

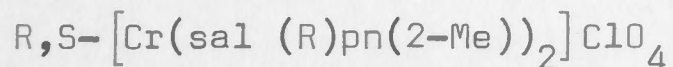
A summary of the analysis is given in Table 5.4. Final positional and thermal parameters, together with their estimated standard deviations, where appropriate, are listed in Table 5.5. Structure factors are listed in Appendix D.

## 5.6 DETERMINATION OF THE ABSOLUTE CONFIGURATION

The sign of the x, y and z-coordinates of all atoms was reversed and the enantiomorphic structure subjected to six cycles of B.D.L.S. (574 parameters; scale factor, atom positional and thermal parameters; calculated hydrogen atom parameters not refined) which gave a final R value equal to .102. This value is highly significant (Ibers & Hamilton, 1964; Hamilton, 1965) when compared to .044 for the original model. Examination of individual sal pn ligands showed that in the original configuration ( $R = .044$ ) the R-pn moiety was present; this confirms the R-ratio test.

Table 5.4

Summary of crystal structure analysis for



Solution method	Heavy atom
Least-squares method	Block-diagonal
Atom scattering factors (neutral atoms)	Non-hydrogen: Cromer & Waber, 1965 Hydrogen: Stewart, Davidson & Simpson, 1965
Absorption correction	Applied (de Meulenaer & Tompa, 1965)
Anomalous dispersion (source)	Included (International Tables, 1962)
Cr	$\Delta F' = -0.1$ $\Delta F'' = 2.60$
Cl	$\Delta F' = 0.3$ $\Delta F'' = 0.7$
O	$\Delta F' = 0.0$ $\Delta F'' = 0.1$
Weighting scheme	$w = 1/\sigma^2$
Range of transmission factors	0.3477 to 0.6546
Data for final refinement	All 'observed' data used
Final model	All non-hydrogen atoms anisotropic; calculated hydrogen atoms isotropic and not refined
Largest parameter shift on final cycle (average)	0.1 (0.05)
Summary of R values:	
end of isotropic refinement;	Pre-absorption correction 0.109
end of anisotropic refinement;	Pre-absorption correction 0.082
	Post-absorption correction 0.054
	model plus calculated hydrogen atoms 0.044
Final difference Fourier peaks	0.66e $\text{\AA}^{-3}$
Disorder	Possible for methyl hydrogens



Table 5.5

(A)

Atom fractional coordinates, with estimated standard deviations in parentheses.

ATOM	x/A	y/B	z/C	ATOM	x/A	y/B	z/C
CR(10)	0.0	0.0	0.0	C(120)	-0.0463(8)	-0.1640(5)	-0.3742(5)
CR(20)	0.4919(1)	0.2706(1)	0.7127(1)	C(130)	-0.0284(9)	-0.2618(5)	-0.4625(5)
N(10)	0.2201(5)	0.1965(4)	0.6379(4)	C(140)	0.0228(9)	-0.3462(5)	-0.4347(6)
O(120)	0.7359(4)	0.3470(3)	0.8082(3)	C(150)	0.0498(8)	-0.3347(5)	-0.3179(6)
N(30)	0.4495(5)	0.3142(3)	0.8721(3)	C(160)	0.0340(6)	-0.2353(4)	-0.2241(5)
O(140)	0.4809(5)	0.1063(3)	0.6749(3)	C(170)	0.0638(7)	-0.2323(4)	-0.1053(5)
N(50)	0.5372(5)	0.2508(4)	0.5570(3)	C(180)	0.5637(7)	0.3588(5)	0.5372(5)
N(60)	0.4865(6)	0.4345(4)	0.7165(4)	C(190)	0.6019(7)	0.4713(5)	0.6553(5)
O(210)	0.2445(4)	0.0946(3)	0.0758(3)	C(191)	0.5793(8)	0.5778(5)	0.6320(6)
N(120)	-0.2714(5)	-0.0756(3)	-0.0706(4)	C(180)	0.0949(9)	-0.1544(5)	0.1079(5)
N(130)	-0.0508(5)	0.1540(3)	0.0298(3)	C(190)	0.0476(9)	-0.0825(6)	0.3095(5)
O(240)	-0.0229(5)	-0.0488(3)	-0.1706(3)	C(191)	-0.0082(8)	-0.0973(5)	0.1778(5)
N(150)	0.0126(5)	0.0211(4)	0.1760(4)	C(1100)	0.8254(6)	0.4217(4)	0.9301(4)
N(160)	0.0505(5)	-0.1499(3)	-0.0117(4)	C(1200)	1.0015(6)	0.4812(5)	0.9725(5)
CL(10)	0.0051(2)	0.2935(1)	0.4158(1)	C(1300)	1.1032(6)	0.5604(4)	1.0985(5)
CL(20)	0.4976(2)	0.6831(1)	0.0067(1)	C(1400)	1.0287(7)	0.5804(4)	1.1860(5)
O(10)	0.0123(8)	0.3699(6)	0.3613(5)	C(1500)	0.8523(7)	0.5230(4)	1.1466(4)
O(20)	0.0043(10)	0.3510(5)	0.5365(5)	C(1600)	0.7466(6)	0.4421(4)	1.0184(4)
O(30)	0.1522(6)	0.2562(4)	0.4228(4)	C(1700)	0.5657(6)	0.3858(4)	0.9860(4)
O(40)	0.6223(5)	0.6790(4)	-0.0485(4)	C(1800)	0.2703(7)	0.2781(5)	0.8582(5)
O(50)	0.4987(8)	0.8029(4)	0.0562(5)	C(1900)	0.1572(6)	0.1695(4)	0.7267(5)
O(60)	0.5388(8)	0.6506(6)	0.1012(5)	C(1910)	-0.0337(6)	0.1444(5)	0.6938(6)
O(70)	0.3336(6)	0.5954(5)	-0.0887(6)	C(110)	0.2442(6)	0.3002(4)	0.1640(4)
O(80)	-0.1468(6)	0.1848(5)	0.3365(5)	C(120)	0.3424(7)	0.4259(4)	0.2426(4)
C(10)	0.4831(9)	-0.1856(6)	0.4740(6)	C(130)	0.5232(7)	0.4671(4)	0.3004(4)
C(20)	0.5369(6)	0.0436(5)	0.4883(4)	C(140)	0.6010(6)	0.3833(5)	0.2815(4)
C(30)	0.4959(7)	0.0227(5)	0.5812(4)	C(150)	0.5071(6)	0.2604(4)	0.2058(4)
C(40)	0.4663(8)	-0.0935(5)	0.5689(5)	C(160)	0.3265(6)	0.2151(4)	0.1462(4)
C(50)	0.5568(8)	-0.0509(6)	0.3902(5)	C(170)	0.0603(6)	0.2652(4)	0.1038(4)
C(60)	0.5286(9)	-0.1635(6)	0.3860(6)	C(180)	-0.2360(6)	0.1336(4)	-0.0276(5)
C(70)	0.5612(6)	0.1569(5)	0.4830(4)	C(190)	-0.3422(6)	0.0237(4)	-0.0228(5)
C(110)	-0.0109(6)	-0.1461(4)	-0.2516(4)	C(191)	-0.5344(7)	-0.0188(6)	-0.0959(6)

Table 5.5 continued

(B)

Anisotropic temperature factors of the form

$$T = \exp(-B_{11}h^2 + 2B_{12}hk + 2B_{13}hl + B_{22}k^2 + 2B_{23}kl + B_{33}l^2)$$

(estimated standard deviations in parentheses)

ATOM	BETA11	BETA22	BETA33	BETA12	BETA13	BETA23
CR110)	0.0117(1)	0.0053(1)	0.0080(1)	0.0038(1)	0.0042(1)	0.0028(1)
CR120)	0.0123(1)	0.0091(1)	0.0057(1)	0.0044(1)	0.0042(1)	0.0032(1)
N110)	0.0121(8)	0.0103(4)	0.0071(4)	0.0025(5)	0.0029(4)	0.0043(3)
O1120)	0.0114(6)	0.0153(4)	0.0064(3)	0.0055(4)	0.0041(4)	0.0041(3)
N130)	0.0094(7)	0.0090(4)	0.0063(3)	0.0040(4)	0.0027(4)	0.0029(3)
O1140)	0.0277(10)	0.0112(4)	0.0090(3)	0.0097(5)	0.0093(4)	0.0052(3)
N150)	0.0118(8)	0.0109(4)	0.0070(4)	0.0044(5)	0.0038(4)	0.0034(3)
N160)	0.0186(9)	0.0091(4)	0.0075(4)	0.0032(5)	0.0041(5)	0.0036(3)
O1210)	0.0121(6)	0.0060(3)	0.0121(4)	0.0041(3)	0.0045(4)	0.0026(3)
N1120)	0.0137(8)	0.0067(4)	0.0100(4)	0.0032(4)	0.0050(5)	0.0037(3)
N1130)	0.0115(7)	0.0061(3)	0.0080(4)	0.0032(4)	0.0033(4)	0.0031(3)
O1240)	0.0206(8)	0.0072(3)	0.0080(3)	0.0063(4)	0.0040(4)	0.0032(3)
N1150)	0.0159(9)	0.0078(4)	0.0092(4)	0.0057(5)	0.0040(5)	0.0038(3)
N1160)	0.0154(8)	0.0055(3)	0.0096(4)	0.0047(4)	0.0044(5)	0.0026(3)
CL110)	0.0223(3)	0.0104(1)	0.0092(1)	0.0087(2)	0.0061(2)	0.0047(1)
CL120)	0.0199(3)	0.0095(1)	0.0119(1)	0.0059(2)	0.0090(2)	0.0056(1)
O110)	0.0066(2)	0.0263(8)	0.0222(7)	0.0290(11)	0.0251(11)	0.0190(7)
O120)	0.0095(29)	0.0191(7)	0.0151(6)	0.0215(12)	0.0274(11)	0.0083(5)
O130)	0.0173(9)	0.0170(6)	0.0172(6)	0.0104(6)	0.0022(6)	0.0070(5)
O140)	0.0200(9)	0.0122(4)	0.0122(4)	-0.0008(5)	0.0097(5)	0.0018(3)
O150)	0.0592(20)	0.0146(6)	0.0233(7)	0.0204(9)	0.0233(10)	0.0109(6)
O160)	0.0612(21)	0.0258(8)	0.0198(7)	0.0285(11)	0.0240(10)	0.0169(7)
O170)	0.0166(10)	0.0216(7)	0.0244(8)	0.0023(7)	0.0093(8)	0.0061(6)
O180)	0.0188(11)	0.0189(7)	0.0226(8)	0.0059(7)	0.0072(7)	0.0005(6)
C110)	0.0301(18)	0.0111(7)	0.0117(7)	0.0077(9)	0.0048(9)	0.0027(5)
C120)	0.0109(9)	0.0110(5)	0.0071(4)	0.0047(6)	0.0030(5)	0.0017(4)
C130)	0.0136(10)	0.0099(5)	0.0072(4)	0.0059(6)	0.0022(5)	0.0020(4)
C140)	0.0270(15)	0.0109(6)	0.0103(6)	0.0090(8)	0.0062(8)	0.0046(5)
C150)	0.0181(13)	0.0139(7)	0.0080(5)	0.0064(7)	0.0035(6)	0.0019(5)
C160)	0.0272(17)	0.0145(8)	0.0106(6)	0.0091(9)	0.0052(8)	0.0013(6)
C170)	0.0112(10)	0.0124(6)	0.0058(4)	0.0028(6)	0.0031(5)	0.0025(4)
C110)	0.0116(9)	0.0057(4)	0.0096(5)	0.0022(5)	0.0045(5)	0.0026(4)
C120)	0.0212(13)	0.0079(5)	0.0090(5)	0.0015(6)	0.0065(7)	0.0022(4)
C130)	0.0302(17)	0.0098(6)	0.0091(6)	0.0028(8)	0.0079(8)	0.0014(5)
C140)	0.0310(18)	0.0093(6)	0.0118(7)	0.0073(8)	0.0091(9)	0.0000(5)
C150)	0.0196(13)	0.0075(5)	0.0127(6)	0.0057(6)	0.0057(7)	0.0017(5)
C160)	0.0126(10)	0.0057(4)	0.0091(5)	0.0021(5)	0.0034(5)	0.0009(4)
C170)	0.0161(11)	0.0054(4)	0.0109(5)	0.0047(6)	0.0032(6)	0.0030(4)
C180)	0.0178(12)	0.0137(6)	0.0082(5)	0.0050(7)	0.0064(6)	0.0069(5)
C190)	0.0141(11)	0.0111(6)	0.0087(5)	0.0012(6)	0.0044(6)	0.0047(4)
C191)	0.0270(16)	0.0105(6)	0.0121(6)	0.0029(8)	0.0068(8)	0.0065(5)
C1100)	0.0326(17)	0.0093(5)	0.0099(6)	0.0111(8)	0.0061(8)	0.0049(5)
C1190)	0.0353(19)	0.0123(7)	0.0095(6)	0.0084(9)	0.0065(9)	0.0070(5)
C1191)	0.0229(13)	0.0075(5)	0.0087(6)	0.0030(6)	0.0038(7)	0.0041(4)
C1100)	0.0129(9)	0.0087(5)	0.0086(5)	0.0052(5)	0.0047(5)	0.0052(4)
C1200)	0.0116(9)	0.0099(5)	0.0099(5)	0.0048(5)	0.0049(6)	0.0061(4)
C1300)	0.0135(10)	0.0081(5)	0.0113(6)	0.0036(6)	0.0037(6)	0.0057(4)
C1400)	0.0172(11)	0.0065(4)	0.0087(5)	0.0021(6)	0.0017(6)	0.0034(4)
C1500)	0.0160(10)	0.0069(4)	0.0071(4)	0.0035(5)	0.0034(5)	0.0032(4)
C1600)	0.0111(9)	0.0071(4)	0.0068(4)	0.0038(5)	0.0032(5)	0.0037(3)
C1700)	0.0125(9)	0.0090(5)	0.0063(4)	0.0046(5)	0.0043(5)	0.0042(4)
C1800)	0.0116(10)	0.0140(7)	0.0076(5)	0.0046(7)	0.0039(6)	0.0038(5)
C1900)	0.0125(10)	0.0077(5)	0.0097(5)	0.0032(5)	0.0043(6)	0.0041(4)
C1910)	0.0087(10)	0.0121(6)	0.0147(7)	0.0025(6)	0.0024(7)	0.0068(6)
C1310)	0.0127(9)	0.0057(4)	0.0082(4)	0.0029(5)	0.0033(5)	0.0029(3)
C1320)	0.0165(10)	0.0068(4)	0.0078(5)	0.0035(5)	0.0037(6)	0.0039(4)
C1330)	0.0164(11)	0.0073(5)	0.0071(4)	0.0011(6)	0.0019(6)	0.0036(4)
C1340)	0.0122(9)	0.0105(5)	0.0075(4)	0.0022(6)	0.0029(5)	0.0055(4)
C1350)	0.0106(9)	0.0095(5)	0.0081(4)	0.0047(5)	0.0038(5)	0.0052(4)
C1360)	0.0124(9)	0.0074(4)	0.0069(4)	0.0035(5)	0.0042(5)	0.0041(4)
C1370)	0.0130(9)	0.0062(4)	0.0079(4)	0.0045(5)	0.0046(5)	0.0038(3)
C1380)	0.0108(9)	0.0084(5)	0.0103(5)	0.0049(5)	0.0037(6)	0.0044(4)
C1390)	0.0122(9)	0.0082(4)	0.0089(5)	0.0040(5)	0.0047(5)	0.0041(4)
C1391)	0.0101(10)	0.0138(7)	0.0121(6)	0.0045(6)	0.0034(6)	0.0051(5)



Table 5.5 continued

(c)

Calculated hydrogen positional and isotropic thermal parameters.

Isotropic temperature factors of the form  $T = \exp(-4B_{\text{iso}}(\sin\theta/\lambda)^2)$ 

ATOM	X/A	Y/B	Z/C	B(A <sup>2</sup> )
H(200)	1.057	0.468	0.909	3.6
H(300)	1.232	0.604	1.128	4.2
H(400)	1.104	0.634	1.278	4.1
H(500)	0.800	0.541	1.212	3.6
H(700)	0.525	0.403	1.057	3.3
H(120)	-0.081	-0.100	-0.396	4.8
H(130)	-0.052	-0.272	-0.551	6.2
H(140)	0.029	-0.421	-0.499	6.3
H(150)	0.088	-0.396	-0.295	5.3
H(170)	0.095	-0.299	-0.094	3.9
H(350)	0.568	0.201	0.192	3.4
H(340)	0.731	0.412	0.324	3.8
H(330)	0.594	0.558	0.356	3.9
H(320)	0.283	0.488	0.259	3.8
H(370)	0.015	0.333	0.120	3.1
H(40)	0.435	-0.110	0.638	5.4
H(10)	0.460	-0.271	0.468	7.1
H(60)	0.549	-0.227	0.315	7.3
H(50)	0.588	-0.033	0.323	5.6
H(70)	0.601	0.164	0.417	4.3
H(80)	0.457	0.347	0.471	4.4
H(81)	0.663	0.371	0.510	4.4
HN(60)	0.526	0.501	0.805	4.2
HN(61)	0.365	0.424	0.668	4.2
H(380)	-0.266	0.117	-0.117	3.8
H(381)	-0.257	0.210	0.020	3.8
HN(12)	-0.310	-0.139	-0.045	3.8
HN(13)	-0.320	-0.116	-0.165	3.8
H(180)	0.224	-0.108	0.160	5.4
H(181)	0.068	-0.242	0.091	5.4
HN(15)	-0.079	0.050	0.196	3.8
HN(16)	0.129	0.084	0.242	3.8
H(800)	0.231	0.350	0.869	4.6
H(801)	0.258	0.256	0.925	4.6
HN(10)	0.176	0.119	0.555	4.0
HN(11)	0.173	0.257	0.621	4.0
H(191)	-0.134	-0.151	0.135	4.6
H(390)	-0.325	0.048	0.068	3.5
H(90)	0.728	0.500	0.712	4.3
H(900)	0.171	0.092	0.725	3.6

All diagrams are presented with respect to a right-handed set of crystal axes and show the correct absolute configurations for the cations in  $R,S-[Cr(sal(R)pn(2-Me))_2]ClO_4$ .

## 5.7 DESCRIPTION OF THE STRUCTURE

The crystal structure consists of discrete ions. Each cation has  $C_1$  symmetry and consists of two essentially planar tridentate sal pn ligands, which are approximately at right angles to one another, surrounding the central chromium atom. The structure is of particular interest since the absolute configuration of the immediate environment of the two chromium atoms is opposite, i.e. both S and R configurations are present. Since the ligands attached to both chromium atoms are of identical configuration, R-N(2-amino-propyl)salicylalimine, the structure may be described as a pseudo-racemate. Perspective views of both cations, together with atom numbering schemes, are given in Figures 5.1 and 5.2. Thermal ellipsoids are drawn to include 50% of the probability distribution. The unit cell, showing molecular packing arrangement, is illustrated in Figure 5.3.

The conformation of the ligands in both cations is such that the methyl groups are equatorial to their respective diamine-cobalt rings; thus steric hindrance is minimised (Corey & Bailer, 1959). The conformation of the R-N(2-amino-propyl) moieties is  $\lambda$ . However, the overall conformation of each ligand is different, possibly due to solid state interactions (see Chapter 7 ; Figure 7.6). Least-squares planes for the ligands are given in Table 5.6.

The perchlorate ions are illustrated in Figure 5.4, where thermal ellipsoids are drawn to include 50% of the probability distribution. Both ions show excellent tetrahedral geometry. Hydrogen



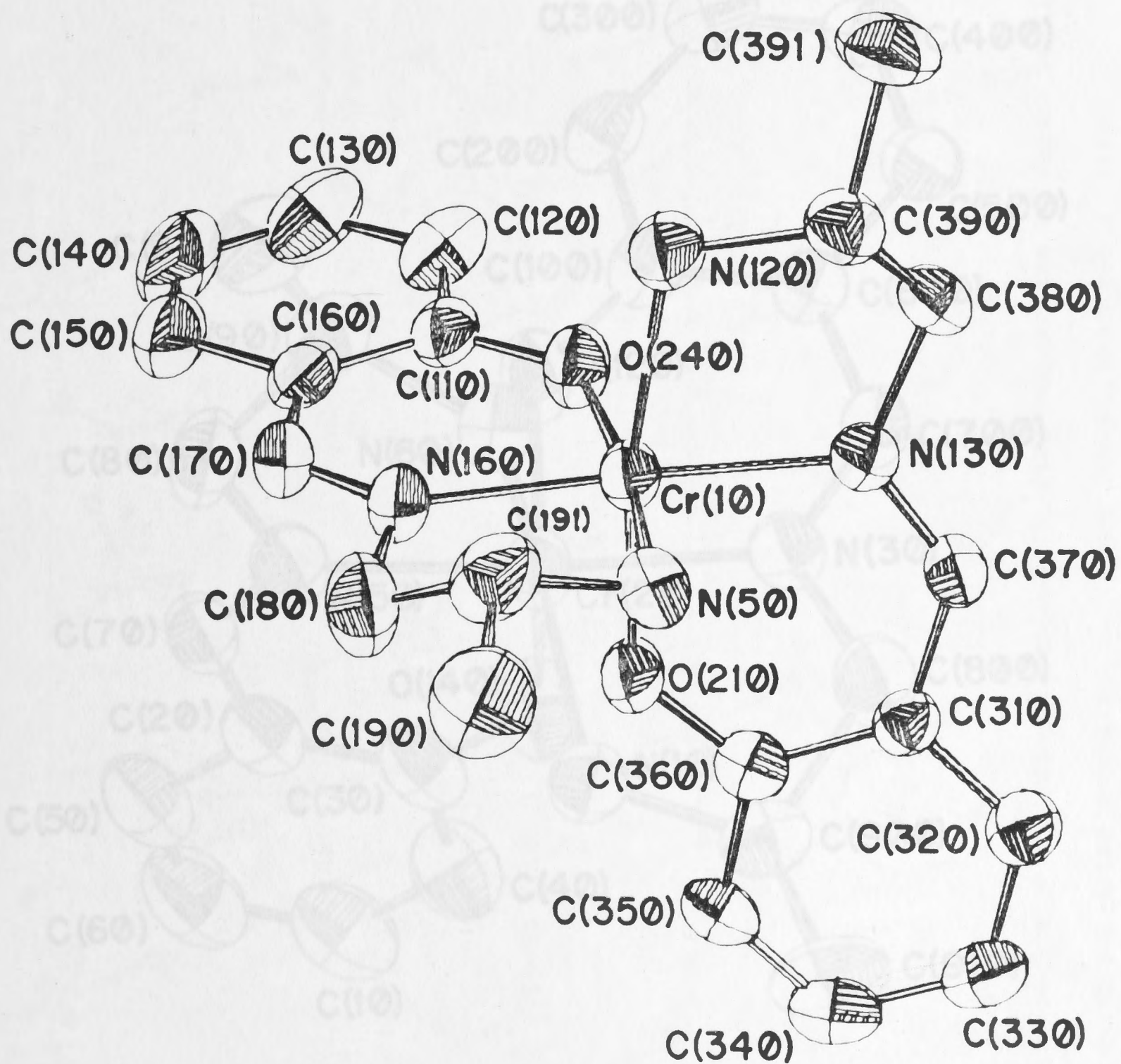


Figure 5.1 Overall stereochemistry of the  $R-[Cr(sal(R)pn(2-Me))_2]^+$  ion in  $R,S-[Cr(sal(R)pn(2-Me))_2]ClO_4$  and atom numbering scheme.

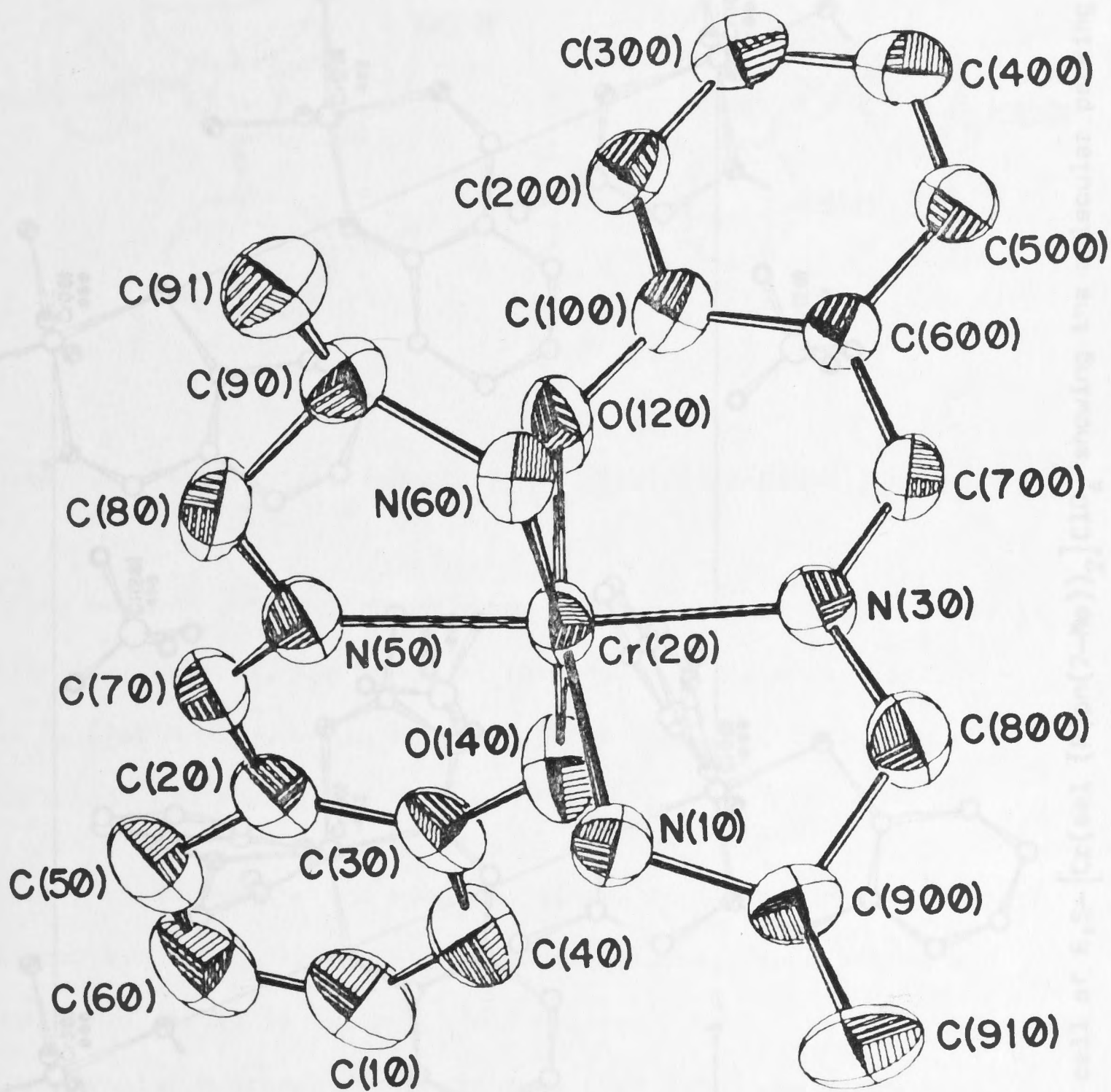


Figure 5.2 Overall stereochemistry of the  $S\text{-}[\text{Cr}(\text{sal}(\text{R})\text{pn}(2\text{-Me}))_2]^+$  ion in  $R,S\text{-}[\text{Cr}(\text{sal}(\text{R})\text{pn}(2\text{-Me}))_2]\text{ClO}_4$  and atom numbering scheme.



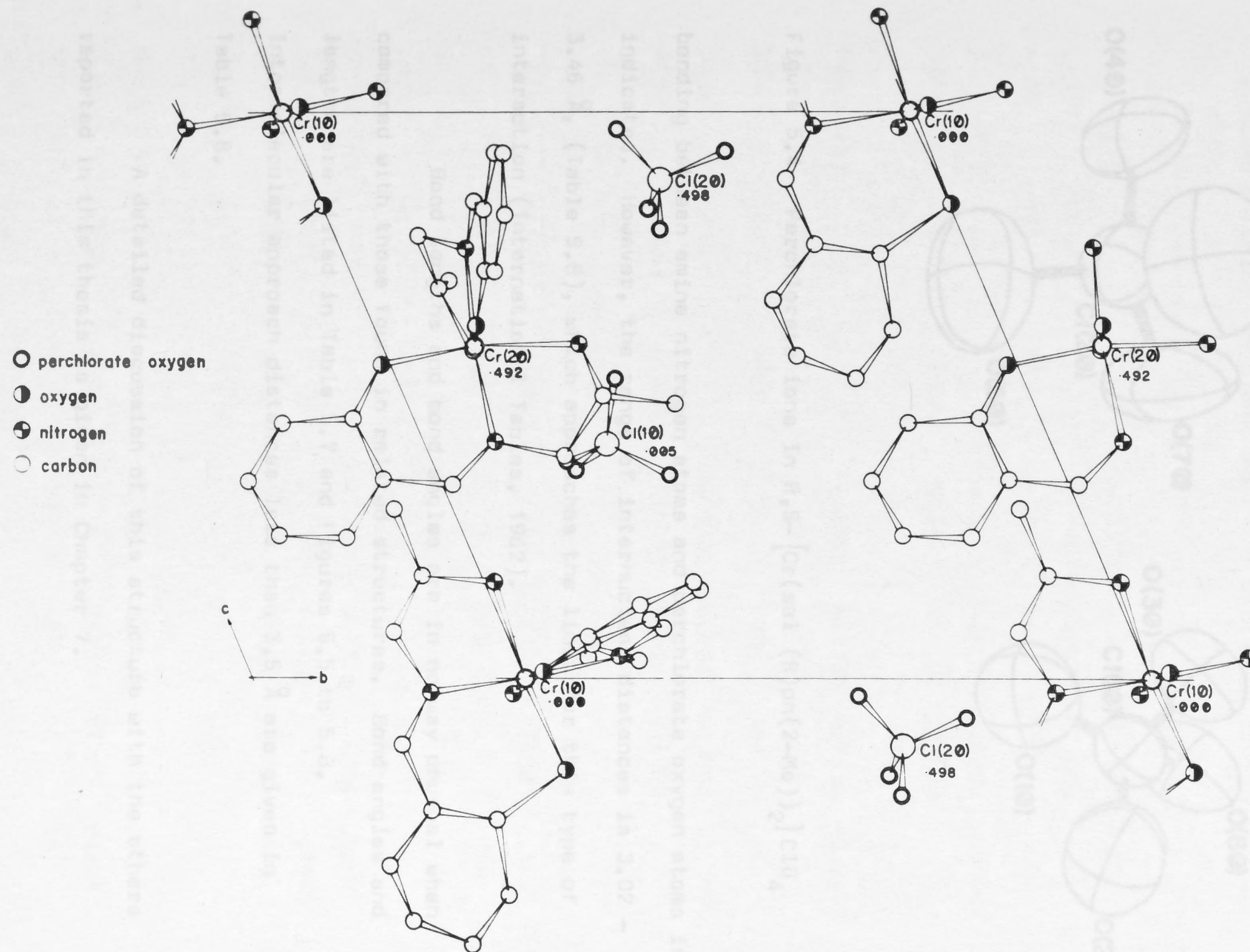


Figure 5.3 The unit cell of  $R,S-[Cr(sal(R)pn(2-Me))_2]ClO_4$  showing the molecular packing arrangement projected onto the  $[100]$  plane looking down the  $a^*$  axis.

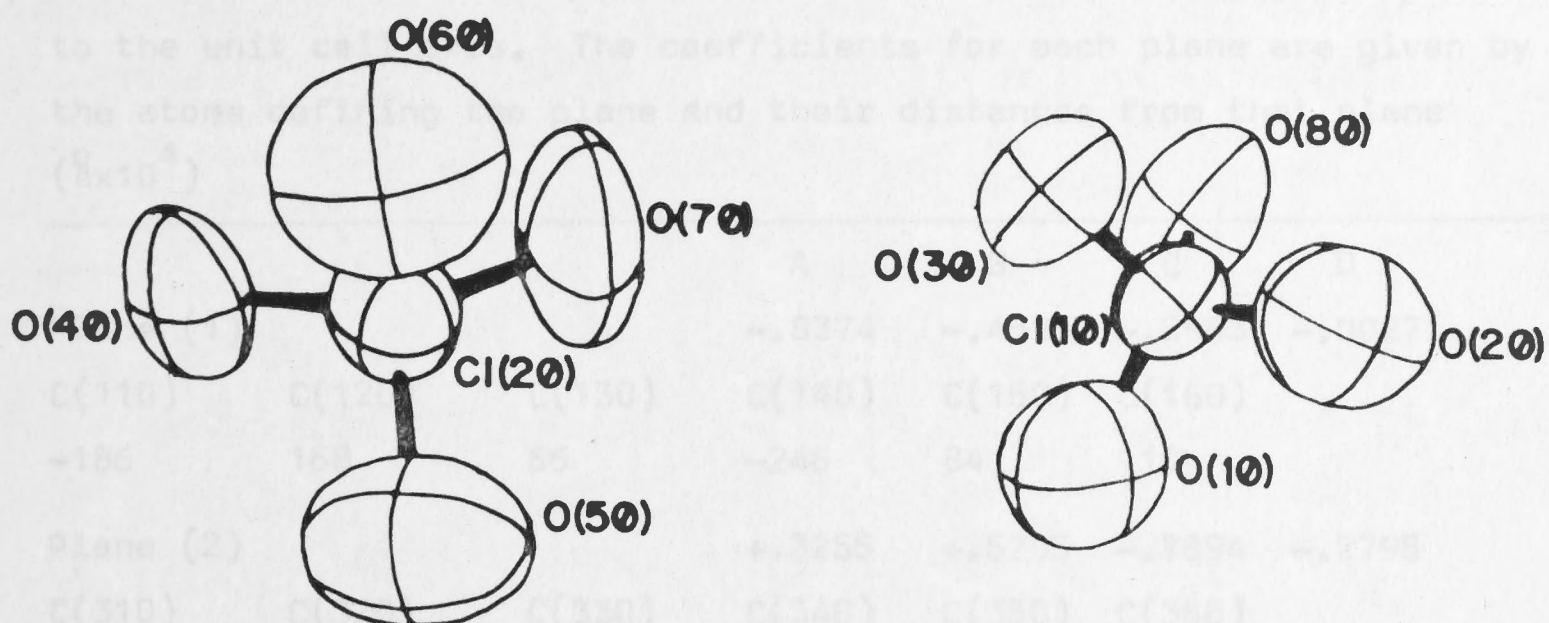


Figure 5.4 Perchlorate ions in  $R,S-[Cr(sal(R)pn(2-Me))_2]ClO_4$

bonding between amine nitrogen atoms and perchlorate oxygen atoms is indicated. However, the range of internuclear distances is 3.02 – 3.46 Å, (Table 5.8), which approaches the limit for this type of interaction (International Tables, 1962).

Bond lengths and bond angles are in no way unusual when compared with those found in related structures. Bond angles and lengths are listed in Table 5.7 and Figures 5.5 to 5.8.

Intermolecular approach distances less than 3.5 Å are given in Table 5.8.

A detailed discussion of this structure with the others reported in this thesis is given in Chapter 7.



Table 5.6

Mean planes for the ligands in  $R,S-[Cr(sal(R)pn(2-Me))_2]ClO_4$

Equations are of the form  $Ax + By + Cz + D = 0$  where  $x$ ,  $y$  and  $z$  refer to the unit cell axes. The coefficients for each plane are given by the atoms defining the plane and their distances from that plane ( $\text{\AA} \times 10^4$ )

			A	B	C	D
Plane (1)			-.8374	-.4594	-.2963	-.0027
C(110)	C(120)	C(130)	C(140)	C(150)	C(160)	
-186	168	66	-246	84	110	
Plane (2)			+.3255	+.5205	-.7894	-.2795
C(310)	C(320)	C(330)	C(340)	C(350)	C(360)	
77	-77	38	-24	43	-72	
Plane (3)			-.8256	-.0393	-.5630	+5.2461
C(10)	C(20)	C(30)	C(40)	C(50)	C(60)	
51	149	-160	108	-70	-81	
Plane (4)			-.3383	+.9347	-.1094	+2.2170
C(100)	C(200)	C(300)	C(400)	C(500)	C(600)	
-14	-14	55	-63	32	3	
Plane (5)			-.8478	-.4298	-.3107	.0000
Cr(10)	O(240)	N(160)	C(110)	C(120)	C(130)	C(140)
00	-304	376	5	678	429	-345
C(150)	C(160)	C(170)				
-334	-173	-83				
Plane (6)			+.3307	+.4429	-.8334	.0000
Cr(10)	O(210)	N(130)	C(310)	C(320)	C(330)	C(340)
00	2030	1863	75	-1490	-1480	-678
C(350)	C(360)	C(370)				
770	792	775				
Plane (7)			-.8299	-.0840	-.5515	+5.0452
Cr(20)	O(140)	N(50)	C(10)	C(20)	C(30)	C(40)
4	44	44	77	55	56	71
C(50)	C(60)	C(70)				
66	79	53				

Table 5.6 continued

			A	B	C	D		
Plane (8)			-.3267	+.9442	-.0422	+1.4462		
Cr(20)	O(120)	N(30)	C(100)	C(200)	C(300)	C(400)		
125	-1735	-934	-748	-254	764	1132		
C(500)	C(600)	C(700)						
758	-243	-692						
Plane (9)			-.8513	-.4137	-.3226	.0000		
Cr(10)	O(240)	N(150)	N(160)	C(110)	C(120)	C(130)	C(140)	
00	-42	1636	71	229	1133	859	-166	
C(150)	C(160)	C(170)	C(180)	C(190)	C(191)			
-385	-207	-370	-949	4188	6344			
Plane (10)			+.3151	+.4518	-.8346	.0000		
Cr(10)	O(210)	N(120)	N(130)	C(310)	C(320)	C(330)	C(340)	
00	1558	-2049	2094	109	-1203	-1616	-1051	
C(350)	C(360)	C(370)	C(380)	C(390)	C(391)			
146	594	1032	3314	-5326	-3361			
Plane (11)			-.8339	-.1095	-.5409	+4.9403		
Cr(20)	O(140)	N(50)	N(60)	C(10)	C(20)	C(30)	C(40)	
-85	-140	149	1946	1394	-389	131	1321	
C(50)	C(60)	C(70)	C(80)	C(90)	C(91)			
-482	452	-810	-143	-4510	-1199			
Plane (12)			-.3085	+.9501	-.0461	+1.4525		
Cr(20)	O(120)	N(10)	N(30)	C(100)	C(200)	C(300)	C(400)	
48	-1542	1633	-1284	-565	156	1184	1320	
C(500)	C(600)	C(700)	C(800)	C(900)	C(910)			
710	-300	-999	-397	-4561	-1019			



Table 5.6 continued

Dihedral angles (degrees)

Plane (1) - Plane (2) 73.8	Plane (4) - Plane (12) 4.1
Plane (1) - Plane (5) 2.0	Plane (5) - Plane (6) 77.9
Plane (1) - Plane (9) 3.1	Plane (5) - Plane (9) 1.2
Plane (2) - Plane (6) 5.4	Plane (6) - Plane (10) 1.1
Plane (2) - Plane (10) 4.7	Plane (7) - Plane (8) 77.6
Plane (3) - Plane (4) 72.2	Plane (7) - Plane (11) 1.6
Plane (3) - Plane (7) 2.6	Plane (8) - Plane (12) 1.1
Plane (3) - Plane (11) 4.2	Plane (9) - Plane (10) 79.2
Plane (4) - Plane (8) 3.9	Plane (11) - Plane (12) 79.7

Table 5.7

(a)

Bond lengths and angles for the perchlorate ions in  
 $R,S-[Cr(sal(R)pn(2-Me))_2]ClO_4$  (e.s.d. values in parentheses)

Atoms	Bond length (Å)	Atoms	Bond angles (degrees)
Cl(10)-O(10)	1.392(8)	O(30)-Cl(10)-O(20)	109.6(4)
Cl(10)-O(20)	1.406(7)	O(30)-Cl(10)-O(10)	108.9(4)
Cl(10)-O(30)	1.446(6)	O(30)-Cl(10)-O(80)	107.2(3)
Cl(10)-O(80)	1.428(4)	O(20)-Cl(10)-O(10)	112.4(4)
		O(20)-Cl(10)-O(80)	109.7(4)
		O(10)-Cl(10)-O(80)	108.9(4)
Cl(20)-O(40)	1.426(5)	O(40)-Cl(10)-O(50)	108.2(4)
Cl(20)-O(50)	1.401(6)	O(40)-Cl(10)-O(60)	109.8(4)
Cl(20)-O(60)	1.394(8)	O(40)-Cl(10)-O(70)	107.8(3)
Cl(20)-O(70)	1.426(4)	O(50)-Cl(10)-O(60)	110.4(4)
		O(50)-Cl(10)-O(70)	112.0(4)
		O(60)-Cl(10)-O(70)	108.6(4)

Table 5.7 continued

(b)

Bond lengths and bond angles about chromium in

 $R,S-[Cr(sal(R)pn(2-Me))_2]ClO_4$  (e.s.d. values in parentheses)

Atoms	Bond lengths (Å)	Atoms	Bond angles (degrees)
R-cation:			
Cr(10)-N(120)	2.101(4)	N(120)-Cr(10)-N(130)	80.4(2)
Cr(10)-N(150)	2.094(5)	N(130)-Cr(10)-O(210)	90.5(2)
Cr(10)-N(130)	2.019(4)	O(210)-Cr(10)-N(160)	89.5(2)
Cr(10)-N(160)	2.011(5)	N(160)-Cr(10)-N(120)	99.3(2)
Cr(10)-O(210)	1.924(3)	N(120)-Cr(10)-O(240)	87.0(2)
Cr(10)-O(240)	1.926(4)	O(240)-Cr(10)-O(210)	95.9(2)
		O(210)-Cr(10)-N(150)	88.4(2)
		N(150)-Cr(10)-N(120)	90.1(2)
		N(150)-Cr(10)-N(130)	92.8(2)
		N(130)-Cr(10)-O(240)	95.9(2)
		O(240)-Cr(10)-N(160)	90.1(2)
		N(160)-Cr(10)-N(150)	81.1(2)
S-cation:			
Cr(20)-N(10)	2.101(4)	N(60)-Cr(20)-N(30)	92.3(2)
Cr(20)-N(60)	2.079(5)	N(30)-Cr(20)-O(140)	97.3(2)
Cr(20)-N(30)	2.018(4)	O(140)-Cr(20)-N(50)	90.7(2)
Cr(20)-N(50)	2.027(5)	N(50)-Cr(20)-N(60)	79.8(2)
Cr(20)-O(120)	1.911(3)	N(60)-Cr(20)-O(120)	90.1(2)
Cr(20)-O(140)	1.928(4)	O(120)-Cr(20)-O(140)	95.1(2)
		O(140)-Cr(20)-N(10)	86.5(2)
		N(10)-Cr(20)-N(60)	90.0(2)
		N(10)-Cr(20)-N(50)	100.9(2)
		N(50)-Cr(20)-O(120)	88.8(2)
		O(120)-Cr(20)-N(30)	90.3(2)
		N(30)-Cr(20)-N(10)	79.8(2)



(c)

Bond lengths and bond angles for ligands in  $R,S-[Cr(sal(R)pn(2-Me))_2]ClO_4$   
(e.s.d. values in parentheses)

Atoms	Bond lengths (Å)	Atoms	Bond angles (degrees)
C(110)-C(120)	1.404(9)	C(110)-C(120)-C(130)	120.9(6)
C(120)-C(130)	1.379(9)	C(120)-C(130)-C(140)	121.7(7)
C(130)-C(140)	1.379(11)	C(130)-C(140)-C(150)	118.7(6)
C(140)-C(150)	1.368(11)	C(140)-C(150)-C(160)	121.4(7)
C(150)-C(160)	1.417(8)	C(150)-C(160)-C(110)	119.4(6)
C(160)-C(110)	1.411(9)	C(160)-C(110)-C(120)	117.7(5)
C(160)-C(170)	1.433(9)	C(110)-O(240)-Cr(10)	129.8(4)
C(170)-N(160)	1.288(7)	O(240)-C(110)-C(160)	124.2(5)
C(110)-O(240)	1.308(6)	C(110)-C(160)-C(170)	123.6(5)
C(180)-N(160)	1.480(9)	C(160)-C(170)-N(160)	124.5(6)
C(180)-C(191)	1.516(10)	C(170)-N(160)-Cr(10)	127.6(4)
C(191)-C(190)	1.520(9)	Cr(10)-N(160)-C(180)	113.6(3)
C(191)-N(150)	1.485(8)	N(160)-C(180)-C(191)	108.7(6)
		C(180)-C(191)-N(150)	106.4(5)
		C(180)-C(191)-C(190)	112.0(6)
		C(190)-C(191)-N(150)	113.2(4)
		C(191)-N(150)-Cr(10)	110.3(3)
C(310)-C(320)	1.401(3)	C(310)-C(320)-C(330)	120.1(5)
C(320)-C(330)	1.405(7)	C(320)-C(330)-C(340)	119.3(4)
C(330)-C(340)	1.362(9)	C(330)-C(340)-C(350)	121.3(5)
C(340)-C(350)	1.366(2)	C(340)-C(350)-C(360)	121.4(5)
C(350)-C(360)	1.402(6)	C(350)-C(360)-C(310)	118.0(4)
C(360)-C(310)	1.404(8)	C(360)-C(310)-C(320)	119.9(4)
C(310)-C(370)	1.441(6)	Cr(10)-O(210)-C(360)	128.9(3)
C(370)-N(130)	1.294(5)	O(210)-C(360)-C(310)	124.2(4)
C(360)-O(210)	1.324(5)	C(360)-C(310)-C(370)	123.1(3)
C(380)-N(30)	1.484(7)	C(310)-C(370)-N(130)	125.8(5)
C(380)-C(390)	1.520(8)	C(370)-N(30)-Cr(10)	125.3(4)
C(390)-C(391)	1.514(7)	Cr(10)-N(30)-C(380)	115.1(3)
C(390)-N(120)	1.510(8)	N(30)-C(380)-C(390)	107.7(5)
		C(380)-C(390)-N(120)	106.4(5)
		C(380)-C(390)-C(391)	112.9(6)
		C(391)-C(390)-N(120)	112.5(4)
		C(390)-N(120)-Cr(10)	110.5(2)

125.  
Table 5.7 continued

(c) continued

Atoms	Bond length (Å)	Atoms	Bond angles (degrees)
C(10)-C(60)	1.371(12)	C(10)-C(60)-C(50)	121.2(7)
C(20)-C(30)	1.407(9)	C(20)-C(30)-C(40)	117.3(5)
C(30)-C(40)	1.381(9)	C(30)-C(40)-C(10)	122.7(7)
C(40)-C(10)	1.377(10)	C(40)-C(10)-C(60)	119.6(7)
C(50)-C(20)	1.428(8)	C(50)-C(20)-C(30)	120.3(6)
C(60)-C(50)	1.375(12)	C(60)-C(50)-C(20)	118.8(7)
C(70)-C(20)	1.440(9)	Cr(20)-O(140)-C(30)	130.7(4)
C(70)-N(50)	1.297(7)	O(140)-C(30)-C(20)	123.2(6)
C(30)-O(140)	1.304(7)	C(30)-C(20)-C(70)	124.3(5)
C(80)-N(50)	1.470(9)	C(20)-C(70)-N(50)	125.4(6)
C(80)-C(90)	1.494(7)	C(70)-N(50)-Cr(20)	125.3(5)
C(90)-C(91)	1.537(11)	Cr(20)-N(50)-C(80)	115.7(3)
C(90)-N(60)	1.508(9)	N(50)-C(80)-C(90)	110.5(5)
		C(80)-C(90)-N(60)	107.2(4)
		C(90)-N(60)-Cr(20)	109.4(4)
		C(80)-C(90)-C(91)	112.5(5)
		C(91)-C(90)-N(60)	112.3(5)
C(100)-C(200)	1.379(7)	C(100)-C(200)-C(300)	122.0(6)
C(200)-C(300)	1.385(6)	C(200)-C(300)-C(400)	119.9(5)
C(300)-C(400)	1.384(9)	C(300)-C(400)-C(500)	119.7(4)
C(400)-C(500)	1.383(7)	C(400)-C(500)-C(600)	121.1(5)
C(500)-C(600)	1.414(5)	C(500)-C(600)-C(100)	118.5(4)
C(600)-C(100)	1.419(8)	C(600)-C(100)-C(200)	118.9(4)
C(100)-O(120)	1.326(5)	Cr(20)-O(120)-C(100)	130.6(4)
C(600)-C(700)	1.429(7)	O(120)-C(100)-C(600)	122.3(4)
C(700)-N(30)	1.303(5)	C(100)-C(600)-C(700)	124.1(4)
N(30)-C(800)	1.451(7)	C(600)-C(700)-N(30)	125.3(4)
C(800)-C(900)	1.533(6)	C(700)-N(30)-Cr(20)	126.0(4)
C(900)-C(910)	1.512(8)	Cr(20)-N(30)-C(800)	116.6(3)
C(900)-N(10)	1.481(5)	N(30)-C(800)-C(900)	109.4(5)
		C(800)-C(900)-N(10)	106.9(4)
		C(900)-N(10)-Cr(20)	110.4(3)
		C(800)-C(900)-C(910)	112.7(5)
		C(910)-C(900)-N(10)	113.2(5)



Table 5.7 continued  
(d)

Bond lengths involving calculated hydrogen atoms (e.s.d. values in parentheses)

Atoms	Bond lengths (Å)	Atoms	Bond length (Å)
N(10)-HN(11)	1.009(5)	N(10)-HN(10)	1.011(3)
N(60)-HN(60)	1.003(4)	N(60)-HN(61)	1.013(5)
N(120)-HN(12)	1.002(5)	N(120)-HN(13)	1.010(5)
N(150)-HN(15)	0.998(5)	N(150)-HN(16)	1.013(3)
C(40)-H(40)	1.057(8)	C(10)-H(10)	1.026(8)
C(50)-H(50)	1.037(8)	C(60)-H(60)	1.028(8)
C(70)-H(70)	1.008(6)	C(120)-H(120)	1.030(7)
C(130)-H(130)	1.026(7)	C(140)-H(140)	1.003(7)
C(150)-H(150)	1.016(7)	C(170)-H(170)	0.999(6)
C(80)-H(80)	0.999(6)	C(80)-H(81)	1.007(7)
C(90)-H(90)	1.020(5)	C(180)-H(181)	1.010(7)
C(180)-H(180)	1.015(6)	C(191)-H(191)	1.004(5)
C(200)-H(200)	1.010(6)	C(300)-H(300)	1.009(5)
C(400)-H(400)	1.006(4)	C(500)-H(500)	1.010(6)
C(700)-H(700)	1.012(6)	C(800)-H(801)	1.006(7)
C(800)-H(800)	1.018(7)	C(900)-H(900)	1.017(6)
C(320)-H(320)	1.016(6)	C(330)-H(330)	1.014(4)
C(340)-H(340)	1.011(5)	C(350)-H(350)	1.006(6)
C(370)-H(370)	1.003(6)	C(380)-H(381)	1.009(6)
C(380)-H(380)	1.010(6)	C(390)-H(390)	1.018(6)



Figure 5.5 (a) Bond angles (degrees) and (b) bond lengths (Å) for  $R,S\text{-Cr}(\text{sal}(R)\text{pn}(2\text{-Me}))_2\text{ClO}_4$  (estimated standard deviations in parentheses).



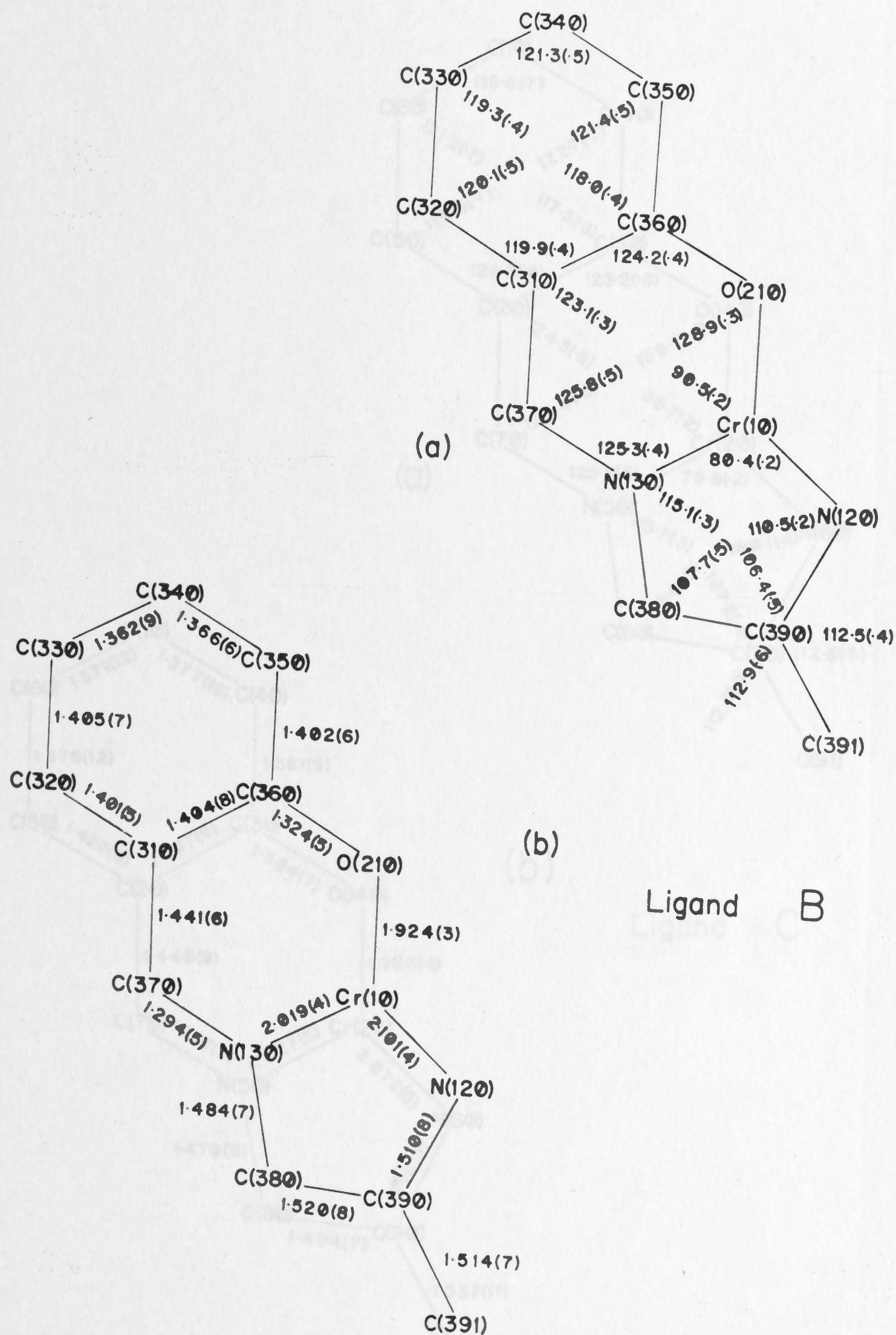


Figure 5.6 (a) Bond angles (degrees) and (b) bond lengths ( $\text{\AA}$ ) for  $R,S\text{-Cr}(\text{sal}(R)\text{pn}(2\text{-Me}))_2\text{ClO}_4$  (estimated standard deviations in parentheses).

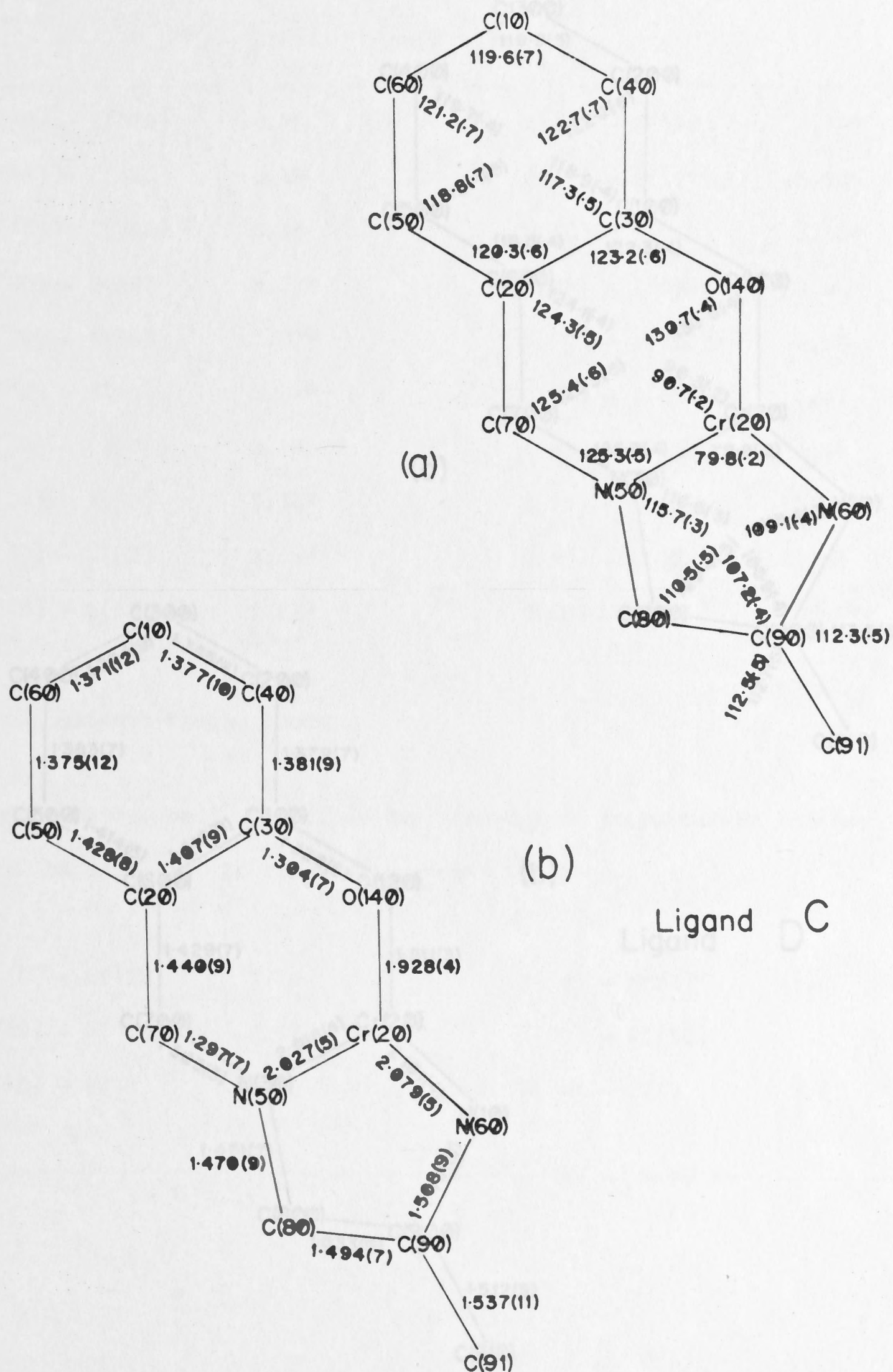
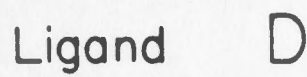


Figure 5.7 (a) Bond angles (degrees) and (b) bond lengths (Å) for  $R,S\text{-Cr}(\text{sal}(R)\text{pn}(2\text{-Me}))_2\text{ClO}_4$  (estimated standard deviations in parentheses).

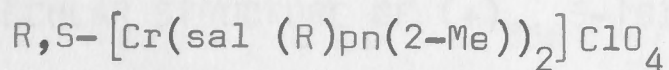



$$\text{R}_5\text{S}-\text{Cr}(\text{sal}(\text{R})\text{pn}(2\text{-Me}))_2\text{ClO}_4 \text{ (estimated standard)}$$

deviations in parentheses).

Table 5.8

Intermolecular approach distances less than 3.5 Å for



O(10) - C(370)	3.16	O(40) - N(120)	3.19*
O(10) - C(140)	3.48	O(40) - C(191)	3.34
O(10) - C(340)	3.49	O(50) - N(120)	3.33*
O(20) - N(10)	3.37*	O(50) - C(390)	3.45
O(30) - N(150)	3.03*	O(60) - C(700)	3.20
O(30) - N(10)	3.04*	O(60) - C(60)	3.47
O(30) - C(380)	3.18	O(60) - C(500)	3.49
O(30) - N(50)	3.34*	O(70) - N(60)	3.31*
O(30) - N(60)	3.46*	O(70) - C(200)	3.32
O(40) - N(60)	3.02*	O(80) - N(150)	3.13*

\* suggested hydrogen bonds

The distances below are given for the sake of completeness and may also be important in terms of hydrogen bonding

O(10) - N(130)	3.79	O(20) - N(60)	3.83
O(40) - N(160)	3.64	O(50) - N(160)	3.97
O(60) - N(30)	3.86	O(70) - N(30)	3.82



## CHAPTER 6

CRYSTAL AND MOLECULAR STRUCTURE OF  $(+)_366$ S-[BIS(N-(2-AMINOETHYL)SALICYLALDIMINATO)CHROMIUM(III)] HYDROGEN-O-DIBENZOYL-(R,R)-TARTRATE TRIHYDRATE\*

## 6.1 UNIT CELL AND DIFFRACTION SYMMETRY

Euhedral, acicular crystals were grown by evaporation of an aqueous solution of  $S-[Cr(sal en)_2]bz_2-(R,R)-Htart, 3H_2O$ . Suitable lengths of crystal were cut from several long, single crystals, and were separately mounted about their needle axes. Initial photographic studies showed that the needle axis was coincident with the crystallographic b-axis.

Unit cell parameters and diffraction symmetry were determined from equi-inclination Weissenberg and precession photographs. The crystals were found to belong to the monoclinic system, with the following unit cell dimensions

$$\begin{array}{ll} a = 14.68 \text{ \AA} & \alpha = \gamma = 90^\circ \\ b = 7.75 \text{ \AA} & \beta = 109^\circ \\ c = 17.48 \text{ \AA} & V = 1881 \text{ \AA}^3 \end{array}$$

Systematic absences were determined to be

$$hkl; \text{ no conditions} \quad Ok0; \quad k = 2n + 1$$

These absences and the conditions for an optically active compound, established the space group as  $P2_1$  (No. 4) (International Tables, 1952), which was confirmed by the subsequent analysis.

Re-examination of the crystals showed that the crystal morphology was due to the presence of the pinacoid forms (001), (010) and (001).

\*  $S-[Cr(sal en)_2]bz_2-(R,R)-Htart, 3H_2O$  for brevity

The density of the crystals was determined to be  $1.39 \text{ g cm}^{-3}$  by the method of flotation using a mixture of carbon tetrachloride and ethyl bromide, giving  $Z = 2$  and  $D_c = 1.39 \text{ g cm}^{-3}$ .

## 6.2 DATA COLLECTION AND REDUCTION

### 6.2.1. Refinement of unit cell dimensions

A suitable crystal for data collection was selected from several crystals used for photographic experiments. The crystal was mounted about the b-axis (Araldite Fast Set; glass capillary) and placed on a <sup>Picker</sup>FACS-I four circle diffractometer. The crystal was oriented so that the b-axis was coincident with the  $\phi$ -axis.

Unit cell parameters were refined using the method of least-squares (Busing, Ellison, Levy, King & Rosebury, 1968). Twelve prominent reflections (with  $2\theta$  greater than  $89^\circ$ ) were chosen to give a wide range of h, k and l using  $\text{Cu-K}\alpha_1$  radiation (Table 6.1). Values of  $2\theta$  were refined as described in section 3.2.1. Final unit cell parameters are listed below

$$\begin{aligned} a &= 14.552(1) \text{ \AA} & \alpha &= \gamma = 90.0^\circ \\ b &= 7.791(1) \text{ \AA} & \beta &= 109.30(1)^\circ \\ c &= 17.445(1) \text{ \AA} & V &= 1866.7 \text{ \AA}^3 \end{aligned}$$

Table 6.1

Unit cell refinement data for  $\text{S-[Cr(sal en)}_2\text{]bz}_2\text{-(R,R)-Htart, 3H}_2\text{O}$

h	k	l	$2\theta$	h	k	l	$2\theta$
0	0	15	89.16	9	2	10	109.74
0	0	17	105.36	7	2	-17	103.80
0	8	0	104.55	0	3	-17	116.14
15	0	0	114.53	12	3	-14	110.91
10	1	10	115.68	-3	8	-3	112.24
11	1	8	111.48	3	8	-3	108.36



### 6.2.2. Data collection and reduction

HKL and  $\overline{\text{HKL}}$  data were collected using graphite monochromated  $\text{Cu-K}\alpha_1$  radiation and a maximum value of  $\theta = 63^\circ$ . Intensities were measured at room temperature by the bisecting  $\theta - 2\theta$  scan mode. Ni-foil attenuators were introduced when the count rate exceeded 5000 counts per second. Three standard reflections were monitored every 97 reflections and a graph of intensity versus reflection sequence was plotted in each case. The following linear correction factors (see section 3.2.2.) were applied to the data

4	0	0	$0.1507 \times 10^{-5}$
0	2	0	$0.2993 \times 10^{-5}$
0	0	4	$0.3805 \times 10^{-5}$

A total of 5843 reflections were measured, of which 4735 (81%) were considered to be observed using the criterion  $I \gg 3\sigma_1$  (22 reflections had uneven background counts). Structure factors and their  $\sigma_1(F_o)$  and  $\sigma_2(F_o)$  were calculated as described in section 3.2.2.

A comparison of the most intense reflections with a powder pattern, obtained using a Philips PW1050/25 recording diffractometer, showed that the single crystal used for data collection was representative of the bulk sample.

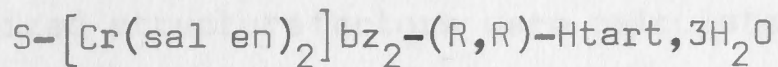
Linear absorption coefficients for both  $\text{Cu-K}\alpha$  and  $\text{Mo-K}\alpha$  radiations were calculated from available data (International Tables, 1962) as  $31.5 \text{ cm}^{-1}$  and  $3.8 \text{ cm}^{-1}$  respectively. Data collection conditions are summarised in Table 6.2.

### 6.3 INITIAL ANALYSIS BY DIRECT METHODS

Since the ratio  $\sum Z_h^2 / \sum Z_l^2$  was calculated as 0.32 with chromium as the only heavy atom, and in order to gain experience, it was

Table 6.2

Summary of crystal data and data collection for



Chemical formula	$C_{36}H_{41}O_{13}N_4Cr$
Formula weight	790.82
Space group	$P2_1$ (No. 4)
Boundary faces of crystal; (mm from internal origin in parentheses)	$\begin{array}{cccccc} 1 & 0 & 0 & (.041) & -1 & 0 & 0 & (.041) \\ 0 & 0 & 1 & (.052) & 0 & 0 & -1 & (.052) \\ 0 & 1 & 0 & (.268) & 0 & -1 & 0 & (.268) \end{array}$
Unit cell parameters	$a = 14.552(1) \text{ \AA}$ $b = 7.791(1) \text{ \AA}$ $c = 17.445(1) \text{ \AA}$ $\alpha = \gamma = 90.0^\circ$ $\beta = 109.30(1)^\circ$ $V = 1866.7 \text{ \AA}^3$
Radiation used for unit cell refinement	$Cu-K\alpha_1 = 1.5405 \text{ \AA}$
Density	$D_m = 1.39 \pm 0.04 \text{ g cm}^{-3}$ $D_c = 1.39 \text{ g cm}^{-3}$
Z	2
Linear absorption coefficients	$\mu(Cu-K\alpha) = 31.5 \text{ cm}^{-1}$ $\mu(Mo-K\alpha) = 3.8 \text{ cm}^{-1}$
Radiation used for data collection (monochromator; $2\theta$ )	$Cu-K\alpha_1$ (graphite; $26.50^\circ$ )
Scan width; speed; dispersion	$(1.8 + \Delta)^\circ$ ; $2^\circ \text{ min}^{-1}$ ; 0.285
Scan mode	$\theta - 2\theta$
Background times	10 secs
Standard reflections	4 0 0; 0 2 0; 0 0 4
Standard linear correction factors ( $\times 10^5$ )	0.1507; 0.2993; 0.3805
Standard frequency	97
Data collected ( $2\theta$ limit)	HKL and $\overline{HKL}$ ( $126^\circ$ )
Number of observed data (%)	4735 (81)

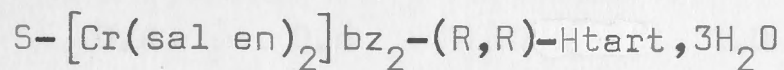


decided to utilize direct methods.

Normalized structure factors were calculated with the inclusion of spherical scattering factors for benzene groups. Scale factors were calculated for each of the 8 parity groups of reflections and an overall isotropic temperature factor was estimated from a Wilson plot (Wilson, 1942). The experimental cumulative probability distribution of the intensity data was in excellent agreement with theoretical non-centrosymmetric statistics (Howells, Phillips & Rogers, 1950) (Figure 6.1). The distribution of the normalized structure factors (Karle, Dragonette & Brenner, 1965) (Table 6.3) suggested that the presence of the chromium atom had not caused serious deviations due to pseudo-symmetry or rational dependence (Karle & Karle, 1965).

Table 6.3

Distribution of normalized structure factors for



Type	experimental	centrosymmetric	non-centrosymmetric
$\langle  E ^2 \rangle$	1.0	1.0	1.0
$\langle  E  \rangle$	0.882	0.7980	0.8860
$\langle  E ^2 - 1  \rangle$	0.7394	0.9680	0.7360
$ E  > 1.0$ (%)	37.8	31.7	36.8
$ E  > 1.5$	10.1	13.4	10.5
$ E  > 2.0$	1.5	4.6	1.8
$ E  > 2.5$	0.1	1.2	0.2
$ E  > 3.0$	<0.02	0.3	0.01

Initial phase relationships were calculated by means of the MULTAN phase-permutation program described by Germain, Main & Woolfson (1968, 1970, 1971). A brief outline is given below.

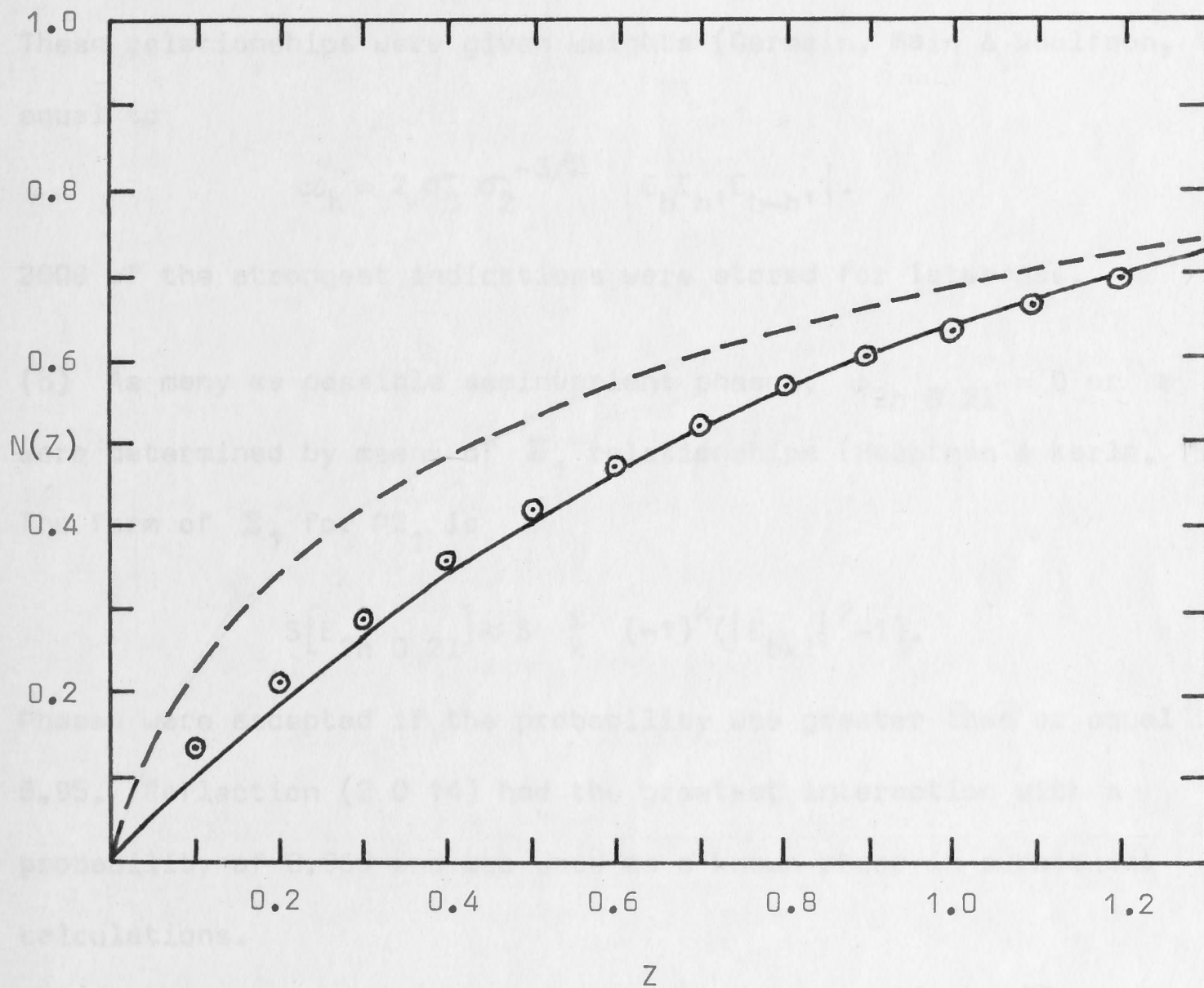


Figure 6.1 Cumulative probability distribution of intensities

for  $S-[Cr(salen)_2]DB-(R)-Htart, 3H_2O$ .

- centrosymmetric (Howells, Phillips & Rogers, 1950)
- non-centrosymmetric
- ⊙ experimental



(a)  $\Sigma_2$  relationships (Karle & Karle, 1966) of the form

$$\phi_h = \phi_{h'} + \phi_{h-h'}$$

were found using 500 of the largest normalized structure factors.

These relationships were given weights (Germain, Main & Woolfson, 1970) equal to

$$\alpha_h = 2 \sigma_3 \sigma_2^{-3/2} |E_h E_{h'} E_{h-h'}|.$$

2000 of the strongest indications were stored for later use.

(b) As many as possible seminvariant phases,  $\phi_{2h \ 0 \ 2l} = 0$  or  $\pi$ , were determined by means of  $\Sigma_1$  relationships (Hauptman & Karle, 1953).

The form of  $\Sigma_1$  for  $P2_1$  is

$$S[E_{2h \ 0 \ 2l}] \approx S \sum_k (-1)^k (|E_{hk1}|^2 - 1).$$

Phases were accepted if the probability was greater than or equal to 0.95. Reflection (2 0 14) had the greatest interaction with a probability of 0.969 and was used as a known phase in subsequent calculations.

(c) Four linearly independent phases were specified (i.e. 0 or  $\pi$ ), thus uniquely defining the origin and enantiomorph. These reflections were selected to give the maximum weighted interaction and hence largest  $\Sigma \psi_h$ . Two other reflections with next largest  $\Sigma \psi_h$  were included in the starting set of reflections. This selection process was carried out using the convergence method of Germain, Main & Woolfson (1970).

(d) Starting sets of phases were generated by assigning a phase, ( $\pm \pi/4$  or  $\pm 3\pi/4$ ) to the two extra reflections obtained by the convergence process. The weighted tangent formula (Germain, Main & Woolfson, 1971) and the  $\Sigma_2$  relationships were then used to develop the starting phases into a complete set. Phases were accepted when the

probabilities were  $\gg 0.95$ .

A total of 32 sets of phase data were so generated and the following four figures of merit were used to select the most probable set:

- (1) The absolute figure of merit,  $M_{\text{abs}}$  (Germain, Main & Woolfson, 1971).

This should be of the order of unity for the correct set of phases and zero for random phases.

- (2) The  $\psi_0$  figure of merit (Cochran & Douglas, 1957).

This is sensitive to molecular position, and independent of the tangent formula, and has proven to be a good indication of the correctness of sets of phases, particularly those associated with small or zero E-values.  $\psi_0$  should be as small as possible.

- (3) The ordinary crystallographic residual,  $R$ , (Cochran & Douglas, 1957).

This was calculated for the equations

$$E_h = S \langle E_h, E_{h-h} \rangle$$

where  $S$  was calculated so as to minimize the residual.

- (4) The combined figure of merit,  $C$ , calculated using

$$C = w_1 \frac{M_{\text{abs}} - M_{\text{abs}}(\text{min})}{M_{\text{abs}}(\text{max}) - M_{\text{abs}}(\text{min})} + w_2 \frac{\psi_0(\text{max}) - \psi_0}{\psi_0(\text{max}) - \psi_0(\text{min})} \\ + w_3 \frac{R(\text{max}) - R}{R(\text{max}) - R(\text{min})}$$

where  $w_1$ ,  $w_2$  and  $w_3$  are weights which are generally unity.  $C$  has a maximum value of  $(w_1 + w_2 + w_3)$  and should be a maximum for the best set of phases.

The set of phases with the highest value of  $C$  was used to calculate an E-map from which the positions of the chromium atom, the six donor atoms and the atoms of one benzene ring were found (Table 6.4).



Table 6.4

Initial atom positions for  $S-[Cr(sal\ en)_2]bz_2-(R,R)\text{-Htart}, 3H_2O$ 

Atom	X	Y	Z	Interatomic distance (Å)	
a) E-map derived:					
Cr(10)	.730	.197	.038	Cr(10) - N(10)	2.05 cf 2.15 <sup>a</sup>
N(10)	.596	.314	-.036	- N(20)	2.01
N(20)	.871	.113	.093	- N(30)	2.13
N(30)	.746	.415	.121	- N(40)	1.99 (0(140))
N(40)	.689	.019	-.054	- N(50)	1.88 (0(150))
N(50)	.692	.098	.122	- N(60)	2.17
N(60)	.802	.329	-.033		
C(1)	.155	.844	-.360	C(1) - C(2)	1.51 cf 1.395 <sup>b</sup>
C(2)	.059	.921	-.362	C(2) - C(3)	1.36
C(3)	.005	.988	-.445	C(3) - C(4)	1.47
C(4)	.041	.992	-.514	C(4) - C(5)	1.41
C(5)	.138	.938	-.505	C(5) - C(6)	1.40
C(6)	.200	.896	-.411	C(6) - C(1)	1.36
b) ΔF-map derived:					
C(100)	.622	.990	.894	C(100) - C(200)	1.42
C(200)	.604	.841	.856	C(200) - C(300)	1.38
C(300)	.530	.804	-.308	C(300) - C(400)	1.39
C(400)	.455	-.080	-.225	C(400) - C(500)	1.33
C(500)	.466	.109	-.200	C(500) - C(600)	1.41
C(600)	.554	.120	.885	C(700) - C(600)	1.44
C(700)	.547	.291	-.086	C(700) - N(10)	1.21 cf 1.33 <sup>a</sup>
C(800)	.580	.460	.000	C(800) - C(900)	1.57 cf 1.541 <sup>b</sup>
C(900)	.690	.580	.100	C(900) - N(30)	1.50 cf 1.46-1.58 <sup>a</sup>
C(7)	.000	.913	.679	C(7) - O(2)	1.30 cf 1.36 <sup>b</sup>
C(8)	.880	.921	.738	C(8) - O(1)	1.40
C(9)	.800	.043	.720	C(8) - C(9)	1.51
OH(10)	.805	.694	.783		
O(1)	.063	.833	.758	C(7) - O(1)	1.30
O(2)	.927	.941	.670	O(2) - C(8)	1.34
C(110)	.725	.011	.185	C(110) - C(120)	1.40
C(120)	.823	-.045	.215	C(120) - C(130)	1.43
C(130)	.876	-.130	.268	C(130) - C(140)	1.39

Table 6.4 continued

Atom	X	Y	Z	Interatomic distance (Å)		
C(140)	.820	-.145	.322	C(140) - C(150)	1.39	
C(150)	.731	-.078	.318	C(150) - C(160)	1.39	
C(160)	.678	-.009	.241	C(160) - C(110)	1.40	
C(170)	.894	.017	.155	C(170) - C(120)	1.41	C(170) - N(20) 1.32
C(180)	.938	.143	.061	C(180) - C(190)	1.50	C(180) - N(20) 1.49
C(190)	.915	.347	.028	C(190) - N(60)	1.48	
C(11)	.572	.092	.561	C(11) - C(12)	1.36	
C(12)	.470	.134	.547	C(12) - C(13)	1.41	
C(13)	.398	.091	.460	C(13) - C(14)	1.34	
C(14)	.442	.085	.395	C(14) - C(15)	1.35	
C(15)	.545	.108	.415	C(15) - C(16)	1.39	
C(16)	.597	.044	.490	C(16) - C(11)	1.43	
C(17)	.642	.097	.644	C(17) - C(11)	1.46	C(17) - O(30) 1.34
O(30)	.728	.024	.649	O(30) - C(9)	1.43	
O(40)	.624	.169	.696	O(40) - C(17)	1.22	
O(50)	.800	.334	.676	O(50) - C(91)	1.26	
O(60)	.920	.261	.792	O(60) - C(91)	1.22	
C(81)	.850	.739	.733	C(80) - C(81)	1.50	
C(91)	.846	.227	.741	C(90) - C(91)	1.56	
O(7)	.803	.697	.784	O(7) - C(81)	1.24	
O(8)	.856	.627	.680	O(8) - C(81)	1.25	
OH(20)	.684	.436	.810			
OH(30)	.843	.790	.950			

<sup>a</sup> Gardner, Gatehouse & White (1971)

<sup>b</sup> International Tables (1962)



Examination of the position of the benzene ring in relation to the chromium atom showed that the ring belonged to the anion. A summary of the results of the direct methods analysis is given in Table 6.5.

#### 6.4 DIFFERENCE FOURIER ANALYSIS

Due to the symmetry of the space group,  $P2_1$ , all atoms occupy general positions and one atom may have an arbitrary y-coordinate of any value. The obvious choice would have been to set the y-coordinate of Cr(10) equal to 0,  $\frac{1}{4}$  or  $\frac{1}{2}$  (see Co(10) Chapter 3). However, since the positions of 13 atoms were available for the initial difference Fourier synthesis it was decided to use the atom coordinates obtained directly from the E-map. This avoided any rational dependence which might introduce pseudo-symmetry if the space group origin was defined by setting the y-coordinate of Cr(10) equal to 0,  $\frac{1}{4}$  or  $\frac{1}{2}$ .

The six atoms in the coordination octahedron of the chromium atom were all designated as nitrogen (N(10) to N(60)), since, at this stage, differentiation between oxygen and nitrogen was not necessary. A structure factor calculation, using individual isotropic temperature factors of  $3 \text{ \AA}^2$  for all atoms and a scale factor of 2.5 (determined by a Wilson analysis, 1942), gave an R value of 0.428. Scattering factors for neutral atoms, as given by Cromer & Waber, (1965), were used for all non-hydrogen atoms. Anomalous dispersion terms,  $\Delta F'$  and  $\Delta F''$ , were included (International Tables, 1962), although no allowance was made for their dependence upon  $\sin \theta$ . The resulting phases were used to calculate a difference Fourier synthesis.

Examination of the difference map gave the positions of 12 carbon atoms (C(100) to C(900)), a complete sal en moiety, and C(7) to C(9)) and 3 oxygen atoms (OH(10), O(1) and O(2)) (Table 6.4). The

Table 6.5

Summary of direct methods data for  $S-[Cr(salen)_2]bz_2-(R,R)-Htart, 3H_2O$ 

Atoms in asymmetric unit	95 (including hydrogen atoms)
Number of reflections used	500
$E_{max}; E_{min}$	3.00; 1.54
$\Sigma_2$ relationships:	
number	2000
minimum value of $ E_h E_h, E_{h-h} $	7.16 ( $\alpha_h = 2.05$ )
$\Sigma_1$ relationships:	
number; $P_{max}; P_{min}$	15; 0.969; 0.5
Total estimated $Z (= \sum_h \sigma_h)$	$1255.10^5$ ( $3852.10^4$ for random phases)
Tangent formula results:	

	$h$	$k$	$l$	$E$	$\phi^0$	$P$	$\psi_h$	$(\phi I)_h^0$	$\langle \sigma_h \rangle_e$
seminvariant	2	0	14	2.8	360	0.93	116.8	360	141.3
origin fixing	15	0	0	3.0	360	1.0	190.6	360	222.1
	2	0	-13	2.62	360	1.0	114.0	360	133.8
	3	1	-13	1.67	360	1.0	28.0	360	34.0
enantiomorph fixing	9	3	4	2.93	135	1.0	294.6	126	355.0
other starting refs	2	1	-15	2.95	225	1.0	153.0	291	158.0
	9	2	4	2.28	315	1.0	87.8	300	95.4
undetermined phases	55								

Summary of figures of merit:

	set used	max	min	weights used
$M_{abs}$	1.296	1.317	0.981	$w_1 = 0.80$
$\phi_0$	714	774	315	$w_2 = 1.20$
$R$	22.14	34.1	21.7	$w_3 = 1.0$
$C$	1.86	1.86	1.09	



"new" atoms were given individual isotropic temperature factors of  $3 \text{ \AA}^2$ .

A second structure factor calculation was carried out which gave an R value equal to 0.380. A difference Fourier synthesis phased on the data gave the positions of the carbon atoms C(110) to C(190) (Table 6.4), which constitute the second sal en ligand. The re-assignments N(40)  $\rightarrow$  O(140) and N(50)  $\rightarrow$  O(150) were made at this stage.

The model was subjected to a structure factor calculation, with individual isotropic temperature factors of  $3 \text{ \AA}^2$  for all atoms, followed by a difference Fourier synthesis;  $R = 0.354$ . The positions of atoms C(11) to C(17), O(30) and O(40) (Table 6.4) were determined from this synthesis and given individual isotropic temperature factors equal to  $3 \text{ \AA}^2$  for the next structure factor calculation, which gave  $R = 0.326$ . The subsequent difference Fourier synthesis gave the positions of the atoms O(50), O(60) and C(81) (Table 6.4), which were also given individual isotropic temperature factors equal to  $3 \text{ \AA}^2$ .

The model was subjected to two cycles of B.D.L.S. (scale factor, positional and thermal parameters of all non-hydrogen atoms), which gave an R value equal to 0.256. A difference Fourier synthesis phased on the resulting model gave the positions of atoms C(91), O(7) and O(8) (Table 6.4). These atoms were given individual isotropic temperature factors of  $3 \text{ \AA}^2$ .

Two cycles of B.D.L.S. (scale factor, atom positional and thermal parameters) gave an R value of 0.228. The sixth and final difference Fourier synthesis yielded the positions of the last two water oxygen atoms, OH(20) and OH(30) (Table 6.4) which were given individual isotropic temperature factors equal to  $3 \text{ \AA}^2$ .

## 6.5 LEAST-SQUARES REFINEMENT AND DETERMINATION OF THE ABSOLUTE CONFIGURATION

### 6.5.1. Isotropic refinement and determination of absolute configuration

The model was subjected to ten cycles of B.D.L.S. (216 parameters; scale factor, positional and thermal parameters of all non-hydrogen atoms), which reduced the value of  $R$  from 0.201 to 0.122. All B.D.L.S. calculations were carried out using  $\sigma_2(F_o)$  weights. Examination of the chiral carbon atoms of the (R,R)-dibenzoyl-hydrogen-tartrate anion showed that the wrong absolute configuration had been proposed for the model. The  $y$ -coordinates of all atoms were changed to  $-y$  in order to obtain the enantiomorph and this model was then refined (Stout & Jensen, 1968). After six cycles of B.D.L.S. (216 parameters; scale factor, atom positional and thermal parameters) the value of  $R$  was 0.098. This decrease in the value of  $R$  is highly significant (Hamilton, 1965). The average value of  $\Delta_i/\sigma_i$ , where  $\Delta_i$  is the shift in parameter  $i$  and  $\sigma_i$  is the estimated standard deviation, was compared for both enantiomorphous models since the refinement was not yet complete. This comparison showed that the  $R$  ratio test could be accepted ( $R = 0.122$ ,  $\Delta_i/\sigma_i = 0.21$ ;  $R = 0.098$ ,  $\Delta_i/\sigma_i = 0.24$ ; i.e. both models were at approximately the same stage of refinement). Examination of the second model ( $R = 0.098$ ) showed that the absolute configuration about the chromium atom was  $S$  (Figure 6.2).

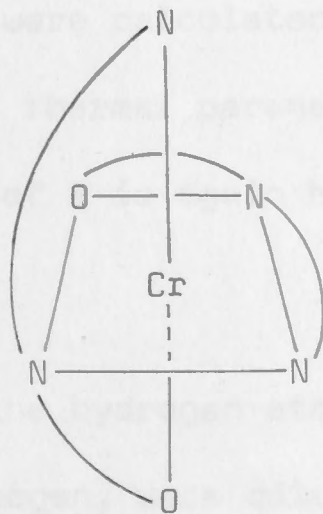


Figure 6.2 The Absolute Configuration of the Cation in  $S-[Cr(salen)_2]bz_2-(R,R)-Htart, 3H_2O$



## 6.5.2. Absorption correction and anisotropic refinement

The data were corrected for absorption (de Meulenaer & Tompa, 1965) using a linear absorption coefficient of  $31.5 \text{ cm}^{-1}$  for  $\text{Cu-K}\alpha$ , obtained from data available (International Tables, 1962), and the following crystal dimensions

1	0	0	(.0041)	0	0	-1	(.0052)
-1	0	0	(.0041)	0	-1	0	(.0268)
0	0	1	(.0052)	0	1	0	(.0268)

where the perpendicular to the face is measured relative to an arbitrary internal origin (cm). Absorption corrections ranged from 0.7813 to 0.8937. The weights,  $\sigma_2(F_o)$ , were recalculated for the 4735 observed data.

The model was subjected to nine cycles of B.D.L.S. (216 parameters; scale factor, atom positional and thermal parameters) and the value of R decreased from 0.161 to 0.077. The initial increase in the value of R was due to a large error in the scale factor. The decrease in the R value when absorption corrected data are used is highly significant (Hamilton, 1965),

Temperature factors were now converted to the anisotropic form

$$T = \exp(-(B_{11}h^2 + 2B_{12}hk + 2B_{13}hl + B_{22}k^2 + 2B_{23}kl + B_{33}l^2))$$

and six cycles of B.D.L.S. were calculated (486 parameters, scale factor, atom positional and thermal parameters) and this gave  $R = 0.052$ . This decrease in the value of R is again highly significant (Hamilton, 1965).

The positions of the hydrogen atoms, with the exception of water and the carboxyl hydrogen, were calculated (Churchill, 1973) using a fixed bond length equal to 0.95 Å. The isotropic temperature

factors of the hydrogen atoms were set equal to 1.1 times that of the equivalent B for the atom to which the hydrogen atom is attached. Scattering factors for hydrogen atoms were those given by Stewart, Davidson & Simpson (1965). Examination of a difference Fourier synthesis phased on the model with only non-hydrogen atoms showed the presence of all the calculated hydrogen atoms as diffuse peaks with heights in the range 0.47 to 0.86e  $\text{\AA}^{-3}$ .

Nine cycles of B.D.L.S. (486 parameters; scale factor, non-hydrogen atom positional and thermal parameters) reduced the value of R to .038, a highly significant drop (Hamilton, 1965).

On the final cycle of B.D.L.S. no parameter shift was greater than 0.15 of the e.s.d. (e.s.d.'s were obtained by inversion of the B.D.L.S. matrices). The standard deviation of an observation of unit weight ( $m = 4735$ ,  $n = 486$ ; see section 2.6) was 1.548. An electron density synthesis phased on the final parameters showed only the expected atoms and a difference Fourier synthesis showed no evidence of misplaced atoms. No positive peak in the difference map was greater than 0.63e  $\text{\AA}^{-3}$ , which was less than one tenth of the average carbon peaks height in earlier difference maps (ca 7e  $\text{\AA}^{-3}$ ).

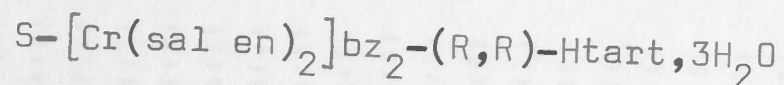
Refinement of the R-enantiomorph (the original model) converged to a final R value of .102 and an R ratio test confirmed that the S-enantiomorph was indeed the correct model (Hamilton, 1965). All diagrams are therefore referred to a left-handed set of crystallographic axes.

A summary of the analysis is given in Table 6.6. Final positional and thermal parameters, together with their estimated standard deviations, where appropriate, are listed in Table 6.7.



Table 6.6

Summary of crystal structure analysis for



Solution method	Direct methods (Tangent formula); Difference Fourier synthesis
Least-squares method	Block diagonal
Atom scattering factors (neutral atoms)	Non-hydrogen: Cromer & Waber, 1965 Hydrogen: Stewart, Davidson & Simpson, 1965
Absorption correction	Applied (de Meulenaer & Tompa, 1965)
Anomalous dispersion (source)	Included (International Tables, 1962)
Cr	$\Delta F' = -0.1$ $\Delta F'' = 2.60$
O	$\Delta F' = 0.0$ $\Delta F'' = 0.1$
Weighting scheme	$w = 1/\sigma^2$
Range of transmission factors	0.7813 to 0.8937
Data for final refinement	All 'observed' data
Final model	All non-hydrogen atoms anisotropic; calculated hydrogen atoms isotropic and not refined.
Largest parameter shift on final cycle (average)	0.15 (0.15) (0.04)
Summary of R values:	
end of isotropic refinement	Pre-absorption correction      0.098 Post-absorption correction      0.077
end of anisotropic refinement	Post-absorption correction non hydrogen atom only      0.052 Post-absorption correction including calculated hydrogen atoms      0.038
Final difference Fourier peaks	0.63e $\text{\AA}^{-3}$

Table 6.7

(A)

Atom fractional coordinates, with estimated standard deviations in parentheses.

ATOM	X/A	Y/B	Z/C	ATOM	X/A	Y/B	Z/C
CR(10)	0.7303(1)	-0.1970	1.0369(1)	C(3)	1.0028(3)	-0.9891(6)	0.5503(2)
N(10)	0.6041(2)	-0.3154(5)	0.9757(2)	C(4)	1.0427(4)	-0.10051(7)	0.4890(3)
N(20)	0.8632(2)	-0.0984(4)	1.0939(2)	C(5)	1.1341(3)	-0.9349(8)	0.4991(3)
N(30)	0.7494(2)	-0.4208(4)	1.1077(2)	C(6)	1.1860(3)	-0.8558(8)	0.5704(3)
N(60)	0.8066(2)	-0.3176(5)	0.9697(2)	C(7)	1.0176(2)	-0.8903(5)	0.6908(2)
O(140)	0.6966(2)	-0.0085(4)	0.9592(1)	C(8)	0.8813(2)	-0.9086(5)	0.7347(2)
O(150)	0.6795(2)	-0.0904(4)	1.1139(1)	C(9)	0.8027(2)	-0.10427(4)	0.7251(2)
C(100)	0.6181(2)	0.0132(5)	0.8949(2)	C(11)	0.5694(3)	-0.10743(5)	0.5591(2)
C(200)	0.6078(3)	0.1698(6)	0.8527(2)	C(12)	0.4731(3)	-0.10930(8)	0.5476(3)
C(300)	0.5278(3)	0.2013(7)	0.7852(3)	C(13)	0.4056(4)	-0.10888(9)	0.4705(3)
C(400)	0.4555(3)	0.0792(8)	0.7573(3)	C(14)	0.4334(4)	-0.10703(8)	0.4063(3)
C(500)	0.4627(3)	-0.0735(7)	0.7973(2)	C(15)	0.5295(5)	-0.10510(10)	0.4167(3)
C(600)	0.5441(2)	-0.1097(5)	0.8667(2)	C(16)	0.5983(4)	-0.10527(8)	0.4926(3)
C(700)	0.5415(2)	-0.2675(5)	0.9081(2)	C(17)	0.6401(2)	-0.10850(5)	0.6427(2)
C(800)	0.5846(3)	-0.4723(6)	1.0152(3)	C(81)	0.8435(2)	-0.7250(5)	0.7340(2)
C(900)	0.6788(3)	-0.5525(6)	1.0610(3)	C(91)	0.8457(2)	-0.12244(5)	0.7330(2)
C(110)	0.7266(2)	-0.0123(5)	1.1827(2)	O(1)	1.0650(2)	-0.8395(4)	0.7574(2)
C(120)	0.8252(3)	0.0402(5)	1.2037(2)	O(2)	0.9237(2)	-0.9373(3)	0.6722(1)
C(130)	0.8680(3)	0.1293(6)	1.2767(3)	O(30)	0.7280(2)	-0.10169(3)	0.6486(1)
C(140)	0.8181(4)	0.1642(7)	1.3291(3)	O(40)	0.6228(2)	-0.11464(4)	0.6993(2)
C(150)	0.7245(3)	0.1061(7)	1.3105(3)	O(50)	0.8001(2)	-0.13296(3)	0.6773(1)
C(160)	0.6799(3)	0.0199(6)	1.2391(2)	O(60)	0.9183(2)	-0.12567(3)	0.7911(2)
C(170)	0.8876(2)	-0.0052(5)	1.1585(2)	O(7)	0.8058(2)	-0.6915(4)	0.7857(1)
C(180)	0.9388(3)	-0.1548(6)	1.0599(3)	O(8)	0.8569(2)	-0.6251(3)	0.6828(2)
C(190)	0.8917(3)	-0.2111(7)	0.9750(2)	OH(10)	1.0791(2)	-0.11014(4)	0.9085(2)
C(1)	1.1474(3)	-0.8434(6)	0.6321(2)	OH(20)	0.6831(2)	-0.4276(4)	0.8090(2)
C(2)	1.0551(3)	-0.9092(5)	0.6220(2)	OH(30)	0.8437(2)	-0.7792(4)	0.9507(2)



Table 6.7 continued

(B)

Anisotropic temperature factors of the form

$$T = \exp(-B_{11}h^2 + 2B_{12}hk + 2B_{13}hl + B_{22}k^2 + 2B_{23}kl + B_{33}l^2)$$

(estimated standard deviations in parentheses)

ATOM	BETA11	BETA22	BETA33	BETA12	BETA13	BETA23
CR(10)	0.0034(1)	0.0133(1)	0.0027(1)	-0.0008(1)	0.0008(1)	0.0004(1)
N(10)	0.0043(2)	0.0163(7)	0.0030(1)	-0.0014(3)	0.0010(1)	0.0001(2)
N(20)	0.0033(1)	0.0150(7)	0.0033(1)	-0.0006(2)	0.0009(1)	0.0011(2)
N(30)	0.0057(2)	0.0152(7)	0.0035(1)	-0.0002(3)	0.0013(1)	0.0014(2)
N(60)	0.0048(2)	0.0184(7)	0.0037(1)	0.0006(3)	0.0018(1)	0.0004(3)
O(140)	0.0042(1)	0.0155(6)	0.0036(1)	-0.0009(2)	0.0005(1)	0.0016(2)
O(150)	0.0038(1)	0.0191(6)	0.0033(1)	-0.0008(2)	0.0008(1)	-0.0010(2)
C(100)	0.0038(2)	0.0173(9)	0.0029(1)	0.0012(3)	0.0012(1)	0.0002(3)
C(200)	0.0057(2)	0.0182(10)	0.0041(2)	0.0015(4)	0.0016(2)	0.0020(3)
C(300)	0.0065(3)	0.0238(11)	0.0045(2)	0.0028(4)	0.0012(2)	0.0027(4)
C(400)	0.0073(3)	0.0285(13)	0.0039(2)	0.0035(5)	-0.0001(2)	0.0020(4)
C(500)	0.0056(3)	0.0241(11)	0.0035(2)	0.0008(4)	0.0004(2)	-0.0004(4)
C(600)	0.0039(2)	0.0181(9)	0.0026(1)	0.0003(3)	0.0009(1)	-0.0009(3)
C(700)	0.0038(2)	0.0179(9)	0.0034(2)	-0.0015(3)	0.0011(1)	-0.0019(3)
C(800)	0.0063(3)	0.0207(11)	0.0050(2)	-0.0038(4)	0.0014(2)	0.0012(4)
C(900)	0.0062(3)	0.0175(10)	0.0066(2)	-0.0014(4)	0.0019(2)	0.0027(4)
C(110)	0.0046(2)	0.0103(7)	0.0033(1)	0.0011(3)	0.0009(1)	0.0006(3)
C(120)	0.0047(2)	0.0110(8)	0.0036(2)	-0.0009(3)	0.0007(1)	0.0004(3)
C(130)	0.0069(3)	0.0202(12)	0.0048(2)	-0.0020(4)	0.0003(2)	-0.0017(4)
C(140)	0.0087(3)	0.0250(12)	0.0043(2)	-0.0018(5)	0.0018(2)	-0.0034(4)
C(150)	0.0083(3)	0.0216(11)	0.0041(2)	0.0030(5)	0.0023(2)	-0.0003(4)
C(160)	0.0056(2)	0.0171(9)	0.0036(2)	0.0014(4)	0.0015(2)	0.0003(3)
C(170)	0.0040(2)	0.0142(8)	0.0036(2)	-0.0010(3)	0.0004(1)	0.0011(3)
C(180)	0.0039(2)	0.0234(12)	0.0048(2)	0.0000(3)	0.0020(2)	0.0009(3)
C(190)	0.0056(2)	0.0215(10)	0.0051(2)	0.0002(5)	0.0031(2)	0.0011(4)
C(1)	0.0056(2)	0.0228(11)	0.0040(2)	-0.0017(4)	0.0018(2)	-0.0002(3)
C(2)	0.0049(2)	0.0116(7)	0.0030(1)	0.0006(3)	0.0011(1)	0.0002(3)
C(3)	0.0063(2)	0.0157(9)	0.0036(2)	-0.0004(4)	0.0013(2)	-0.0012(3)
C(4)	0.0093(3)	0.0221(11)	0.0039(2)	0.0015(5)	0.0019(2)	-0.0023(4)
C(5)	0.0089(3)	0.0327(15)	0.0041(2)	0.0034(6)	0.0034(2)	0.0014(4)
C(6)	0.0072(3)	0.0326(15)	0.0047(2)	-0.0007(5)	0.0027(2)	0.0006(4)
C(7)	0.0047(2)	0.0084(7)	0.0031(1)	0.0001(3)	0.0009(1)	0.0000(2)
C(8)	0.0048(2)	0.0079(7)	0.0027(1)	0.0001(3)	0.0010(1)	-0.0004(2)
C(9)	0.0045(2)	0.0063(7)	0.0028(1)	0.0001(3)	0.0007(1)	0.0002(2)
C(11)	0.0054(2)	0.0105(8)	0.0040(2)	0.0006(3)	0.0007(2)	0.0003(3)
C(12)	0.0044(2)	0.0389(16)	0.0055(2)	0.0019(5)	0.0003(2)	0.0000(5)
C(13)	0.0066(3)	0.0434(18)	0.0057(3)	0.0033(6)	-0.0008(2)	0.0004(6)
C(14)	0.0099(4)	0.0263(13)	0.0059(3)	-0.0023(6)	-0.0025(3)	0.0015(5)
C(15)	0.0123(5)	0.0452(20)	0.0039(2)	-0.0008(8)	0.0006(3)	0.0007(5)
C(16)	0.0082(3)	0.0338(15)	0.0038(2)	-0.0050(6)	0.0005(2)	0.0002(4)
C(17)	0.0043(2)	0.0101(7)	0.0035(1)	0.0019(3)	0.0012(1)	0.0004(3)
C(18)	0.0048(2)	0.0091(8)	0.0029(1)	0.0004(3)	0.0011(1)	-0.0002(2)
C(19)	0.0043(2)	0.0090(7)	0.0029(1)	0.0007(3)	0.0010(1)	0.0008(2)
O(1)	0.0056(2)	0.0271(18)	0.0032(1)	-0.0034(3)	0.0010(1)	-0.0025(2)
O(2)	0.0043(1)	0.0093(5)	0.0031(1)	-0.0002(2)	0.0012(1)	-0.0010(2)
O(30)	0.0043(1)	0.0080(5)	0.0031(1)	0.0001(2)	0.0006(1)	0.0006(2)
O(40)	0.0050(1)	0.0231(8)	0.0042(1)	0.0005(2)	0.0017(1)	0.0013(2)
O(50)	0.0059(2)	0.0075(4)	0.0036(1)	0.0005(2)	0.0008(1)	-0.0006(2)
O(60)	0.0060(2)	0.0103(5)	0.0049(1)	0.0016(2)	-0.0007(1)	0.0005(2)
O(7)	0.0084(2)	0.0110(5)	0.0043(1)	0.0024(3)	0.0034(1)	0.0006(2)
O(8)	0.0081(2)	0.0081(5)	0.0043(1)	0.0015(2)	0.0031(1)	0.0006(2)
OH(10)	0.0071(2)	0.0183(7)	0.0059(1)	-0.0031(3)	0.0017(1)	0.0004(3)
OH(20)	0.0088(2)	0.0169(6)	0.0040(1)	0.0016(3)	0.0023(1)	0.0002(2)
OH(30)	0.0062(2)	0.0275(8)	0.0046(1)	-0.0040(3)	0.0007(1)	0.0010(3)

Table 6.7 continued

(C)

Calculated hydrogen positional and isotropic thermal parameters.  
 Isotropic temperature factors of the form  $T = \exp(-4B_{\text{iso}}(\sin\theta/\lambda)^2)$

ATOM	X/A	Y/B	Z/C	B (Å <sup>2</sup> )
H(1)	1.184	-0.789	0.682	5.1
H(3)	0.938	-0.1032	0.542	4.8
H(4)	1.007	-0.1064	0.439	5.9
H(5)	1.160	-0.938	0.456	6.8
H(6)	1.250	-0.810	0.577	6.4
H(8)	0.931	-0.923	0.786	3.2
H(9)	0.776	-0.1028	0.769	3.2
H(12)	0.451	-0.1107	0.595	6.9
H(13)	0.337	-0.1098	0.463	8.6
H(14)	0.374	-0.1075	0.361	8.2
H(15)	0.549	-0.1035	0.369	8.8
H(16)	0.667	-0.1040	0.498	7.0
H(130)	0.935	0.164	1.291	6.0
H(140)	0.849	0.231	1.378	6.2
H(150)	0.689	0.126	1.349	6.1
H(160)	0.614	-0.023	1.228	4.6
H(170)	0.953	0.035	1.179	4.0
H(180)	0.974	-0.250	1.091	5.1
H(181)	0.983	-0.064	1.062	5.1
H(190)	0.937	-0.271	0.957	5.2
H(191)	0.871	-0.110	0.942	5.2
H(200)	0.657	0.259	0.874	4.9
H(300)	0.522	0.309	0.754	5.9
H(400)	0.401	0.101	0.709	6.6
H(500)	0.411	-0.155	0.779	5.2
H(700)	0.488	-0.345	0.883	4.0
H(800)	0.544	-0.549	0.975	5.5
H(810)	0.549	-0.443	1.052	5.5
H(900)	0.704	-0.608	1.023	6.0
H(910)	0.669	-0.639	1.097	6.0
HN(30)	0.814	-0.461	1.121	4.4
HN(31)	0.737	-0.396	1.157	4.4
HN(60)	0.828	-0.430	0.991	4.4
HN(61)	0.766	-0.331	0.914	4.4



Structure factors are listed in Appendix E.

## 6.6 DESCRIPTION OF THE STRUCTURE

The crystal structure consists of discrete ions. The cation has  $C_1$  symmetry and consists of two essentially planar tridentate sal en ligands, which are approximately at right angles to one another, about the central chromium atom. A perspective view of the  $S-[Cr(sal\ en)_2]^+$  ion, together with the atom numbering scheme, is shown in Figure 6.3. Thermal ellipsoids have been drawn to include 50% of the probability distribution. The absolute configuration of the chromium atom was S (Figure 6.2) and the conformations of the two en rings were opposite (N(20) - N(60),  $\lambda$ ; N(10) - N(30),  $\delta$ ). The unit cell, showing the molecular packing arrangement, is illustrated in Figure 6.4.

Least-squares planes for the ligands are given in Table 6.8. The conformation of the ligands is discussed in Chapter 7.

The dibenzoyl-(R,R)-hydrogen tartrate ion, together with the atom numbering scheme, is shown in Figure 6.5; where thermal ellipsoids have been drawn to include 50% of the probability distribution.

Statistical analysis (Stout & Jensen, 1968; Deming, 1943; Ractliffe, 1967) of the bond lengths and bond angles for the benzene ring present in the anion gave the following results

$$C(1) - C(6) \quad \bar{l}_w = 1.382 \pm 0.010 \text{ \AA}; \quad \bar{\theta}_w = 119.9 \pm 0.4^\circ$$

$$C(11) - C(16) \quad \bar{l}_w = 1.366 \pm 0.012 \text{ \AA}; \quad \bar{\theta}_w = 119.8 \pm 1.0^\circ$$

where the subscript, w, denotes weighted average. Both F and t tests indicated that the two groups of bond lengths could be combined and

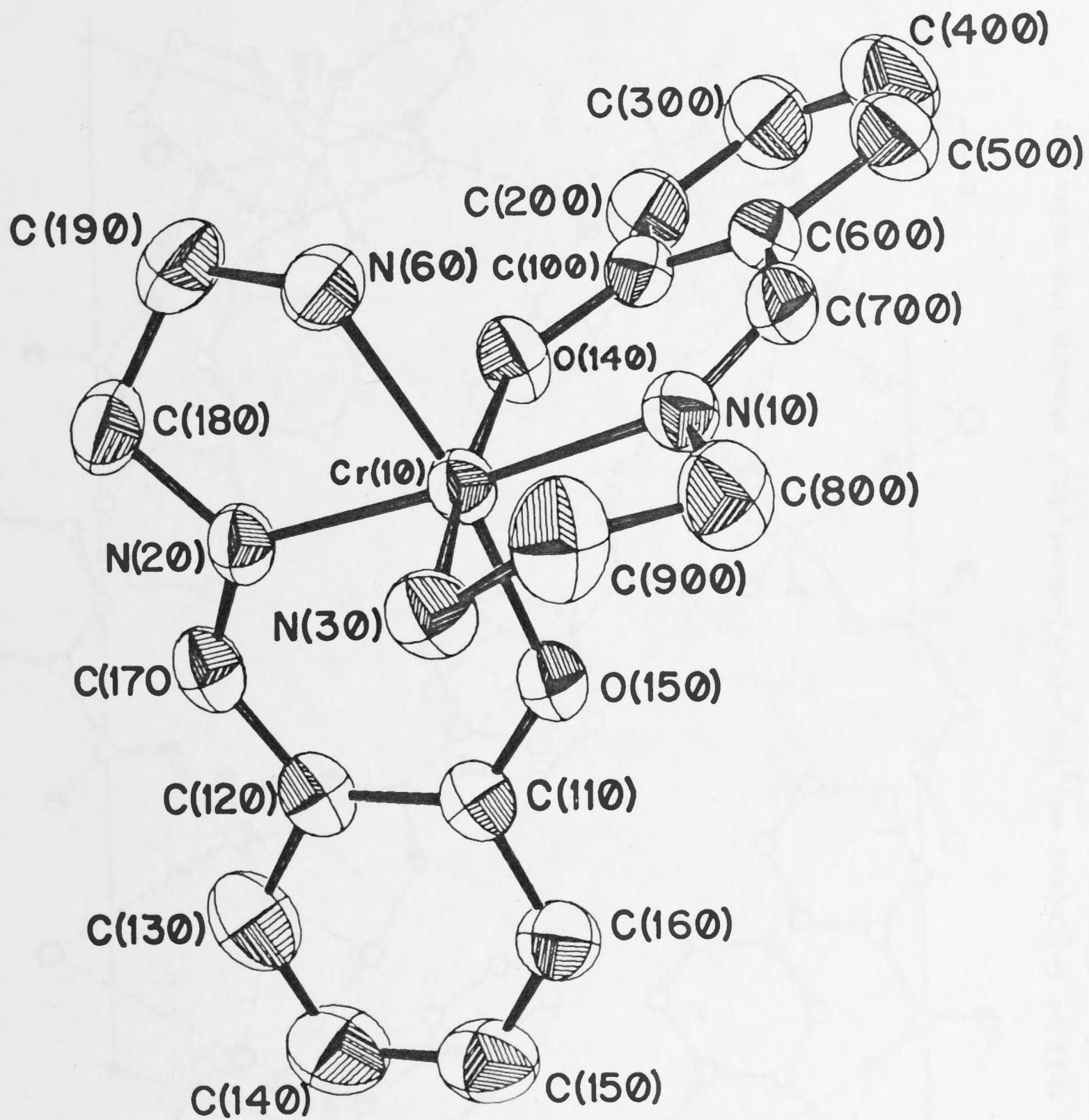


Figure 6.3 Overall stereochemistry of the  $S\text{-}[\text{Cr}(\text{sal en})_2]^+$  ion in  $S\text{-}[\text{Cr}(\text{sal en})_2]\text{bz}_2\text{-(R,R)-Htart, 3H}_2\text{O}$  and atom numbering scheme.



- oxygen
- ⊕ nitrogen
- carbon
- ⊙ water oxygen

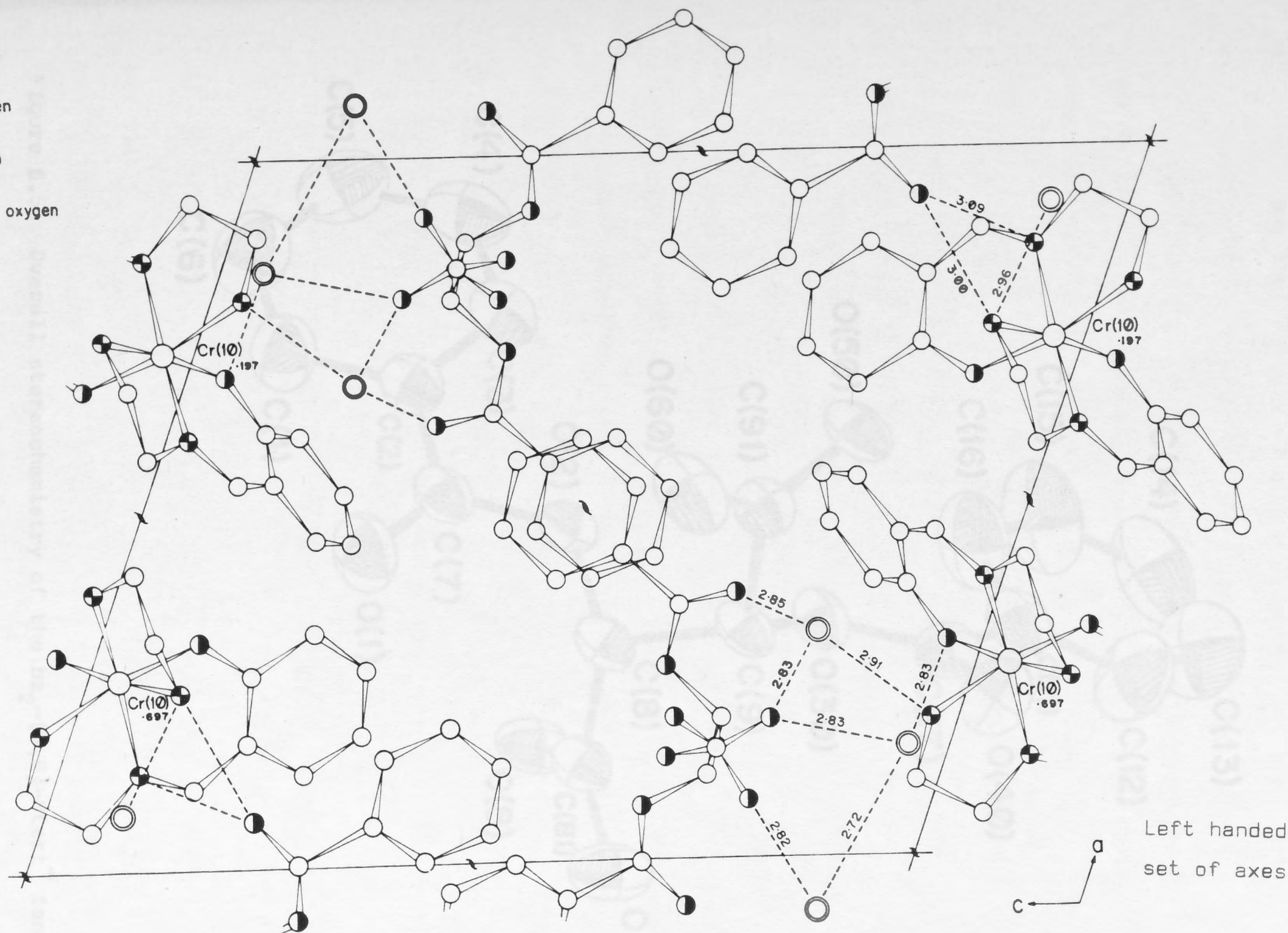


Figure 6.4 The unit cell of  $S-[Cr(salen)_2]bz_2-(R,R)\text{-Htart}, 3H_2O$  showing the molecular packing arrangement projected onto the  $[010]$  plane looking down the  $b$ -axis.

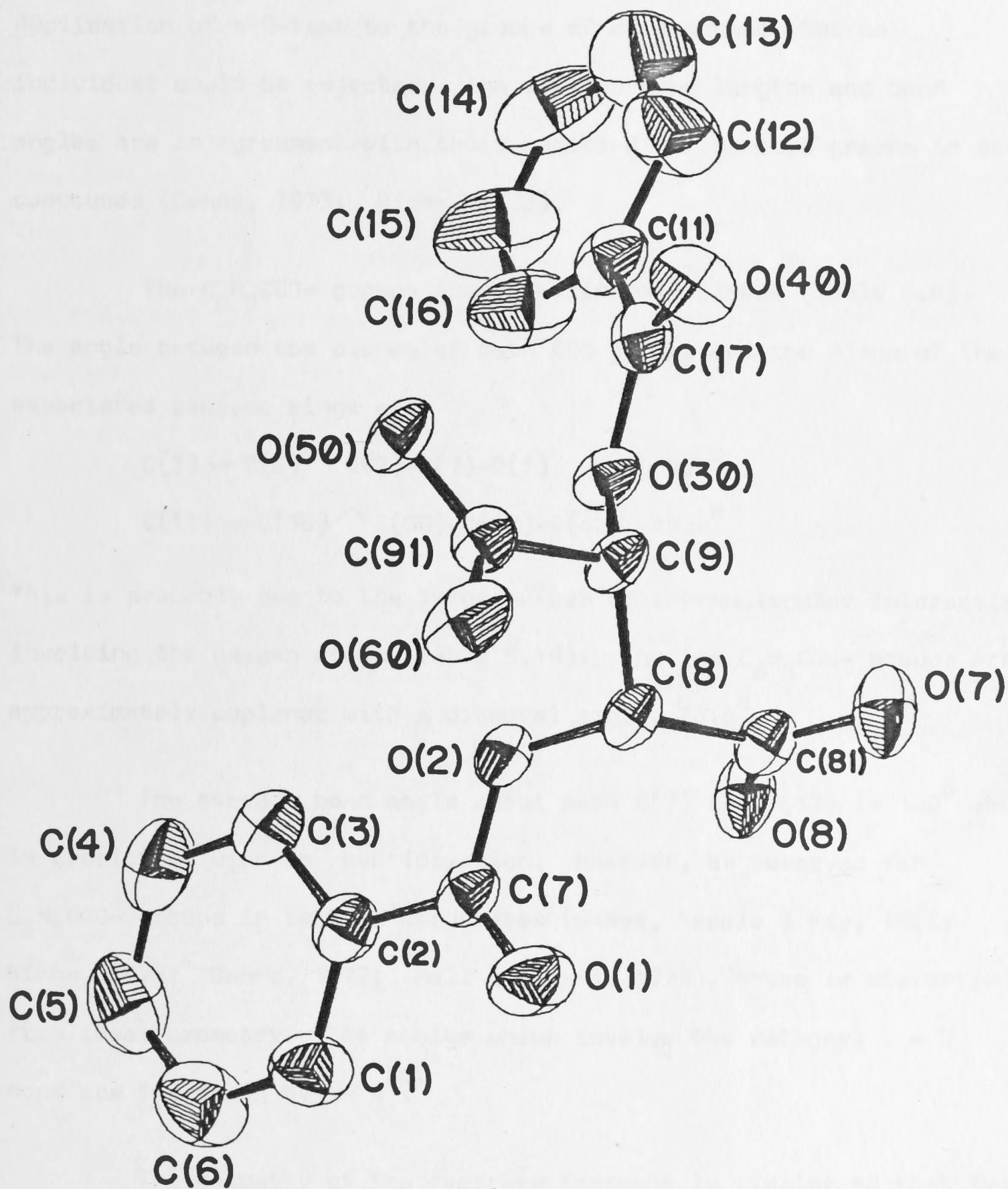


Figure 6.5 Overall stereochemistry of the  $\text{bz}_2\text{-(R,R)-Htart}^-$  ion in  $\text{S-[Cr(sal en)}_2\text{]bz}_2\text{-(R,R)-Htart}\cdot 3\text{H}_2\text{O}$  and atom numbering scheme.



this gave a mean bond length of  $1.374 \pm 0.007 \text{ \AA}$ . However, the same tests showed that the two groups of bond angles could not be combined. Application of a Q-test to the groups of data showed that no individual could be rejected. The average bond lengths and bond angles are in agreement with those reported for benzoyl groups in other compounds (Denne, 1973; Riche, 1973).

The  $\text{C}_6\text{H}_5\text{COO}^-$  groups are approximately planar (Table 6.8). The angle between the planes of both COO groups and the planes of the associated benzene rings are

$$\text{C}(1) \rightarrow \text{C}(6) \wedge \text{O}(2)-\text{C}(7)-\text{O}(1) \quad 8.8^\circ$$

$$\text{C}(11) \rightarrow \text{C}(16) \wedge \text{O}(30)-\text{C}(17)-\text{O}(40) \quad 19.2^\circ$$

This is probably due to the large number of intramolecular interactions involving the oxygen atoms (Table 6.10). The two  $\text{C}_6\text{H}_5\text{COO}^-$  groups are approximately coplanar with a dihedral angle,  $28.6^\circ$ .

The average bond angle about both C(7) and C(17) is  $120^\circ$  which is consistent with  $\text{sp}^2$  hybridization. However, as observed for  $\text{C}_6\text{H}_5\text{COO}^-$  groups in related structures (Okaya, Semple & Kay, 1966; Riche, 1973; Denne, 1973; Hall & Masaki, 1973), there is distortion from ideal geometry. The angles which involve the carbonyl  $\text{C}=\text{O}$  bond are increased by  $\sim 4^\circ$ .

The geometry of the tartrate fragment is similar to that found in simple tartrates (Okaya, Semple & Kay, 1966; van Bommel & Bijvoet, 1958; Prout, Carruthers & Rossotti, 1971; Tapscott, Belford & Paul, 1968; Stern & Beevers, 1950). The carboxyl groups are trans relative to the C(8) - C(9) bond and the mean planes (Table 6.8) of the two CO<sub>2</sub> groupings include an angle of  $72.2^\circ$ , which is  $\sim 12^\circ$  larger than that in R,R-tartaric acid (Stern & Beevers, 1950; Okaya, Semple & Kay, 1966). The angle included by the two C - O bonds of each carboxyl group

is  $\langle 126.6^\circ \rangle$  reducing both of the other angles to ( $\langle 116.7^\circ \rangle$ ). This suggests that both groups are ionized to approximately the same extent. This is supported by the C - O bond lengths, statistical analysis of which suggests that both C(81) - O(8), 1.248 Å and C(91) - O(50), 1.276 Å are significantly ( $>2.5\sigma_1$ ) longer than the associated C - O bond. A longer C - O bond is associated with an unionized group (van Bommel & Bijvoet, 1958; Okaya, Semple & Kay, 1966) for which the average value is  $\sim 1.31$  Å. Examination of the final difference Fourier synthesis gave no indication of the presence of hydrogen atoms associated with the carbonyl groups.

The chiral carbon atoms C(8) and C(9) have average bond angles,  $110 \pm 0.9^\circ$  and  $110.5 \pm 0.9^\circ$ , respectively.

The positions of the water oxygen atoms indicate that there is hydrogen bonding between these atoms and between them and the cation and anion (Figure 6.4). Hydrogen bonding probably lengthens the Cr(10) - N(30) bond compared to the Cr(10) - N(60) bond. Inter-cell interactions are present between the anion oxygen atoms (Table 6.10) and these are responsible, at least in part, for the geometry of the tartrate moiety.

The bond lengths and bond angles for  $S-[Cr(salen)_2]bz_2-(R,R)\text{-Htart}, 3H_2O$ , given in Table 6.9 and Figures 6.6, 6.7 and 6.8, are in no way unusual when compared to those found in related structures. Intermolecular approach distances less than 4 Å are given in Table 6.10.

A detailed discussion of this structure together with the others reported in this thesis is given in Chapter 7.



Table 6.8

Mean planes for  $S-[Cr(sal en)_2]bz_2-(R,R)-Htart, 3H_2O$

Equations are of the form  $Ax + By + Cz + D = 0$  where  $x$ ,  $y$  and  $z$  refer to the unit cell axes. The coefficients for each plane are given by the atoms defining the plane and their distances from that plane ( $\text{\AA} \times 10^4$ )

(a) Mean planes for  $S-[Cr(sal en)_2]^{3+}$  ion

			A	B	C	D
Plane (1)			-.1784	+.8693	-.4610	+9.7531
C(110)	C(120)	C(130)	C(140)	C(150)	C(160)	
214	-167	-34	-191	-96	-85	
Plane (2)			+.7116	-.3915	-.5834	+5.9113
C(100)	C(200)	C(300)	C(400)	C(500)	C(600)	
33	-19	-2	45	-31	-10	
Plane (3)			-.1246	+.8674	-.4993	+10.3356
Cr(10)	N(20)	O(150)	C(110)	C(120)	C(130)	C(140)
-844	-942	1427	620	765	465	-225
C(150)	C(160)	C(170)				
-1017	-605	0				
Plane (4)			+.7011	-.4348	-.5651	+5.7230
Cr(10)	N(10)	O(140)	C(100)	C(200)	C(300)	C(400)
5	-687	555	391	-326	-545	-69
C(500)	C(600)	C(700)				
504	781	-687				
Plane (5)			-.1445	+.8229	-.5495	+11.452
Cr(10)	N(20)	N(60)	O(150)	C(110)	C(120)	C(130)
991	-162	-2818	2574	932	501	-681
C(140)	C(150)	C(160)	C(170)	C(180)	C(190)	
-1694	-1927	-646	0	-2570	1781	
Plane (6)			+.7008	-.4344	-.5658	-5.7337
Cr(10)	N(10)	N(30)	O(140)	C(100)	C(200)	C(300)
-26	-710	48	539	385	323	-530
C(400)	C(500)	C(600)	C(700)	C(800)	C(900)	
-52	512	777	311	-2656	3538	

Table 6.8 continued

(b) Mean planes for $bz_2-(R,R)-H_{\text{tart}}$					
		A		B	
		C		D	
Plane (7)		-.3072		+.8748	
		-.3747		+13.6504	
C(1)	C(2)	C(3)	C(4)	C(5)	C(6)
-75	4	55	-125	128	65
Plane (8)		-.1153		-.9912	
		-.0646		-8.2858	
C(11)	C(12)	C(13)	C(14)	C(15)	C(16)
0	33	-94	-49	-8	-31
Plane (9)		-.2040		+.9377	
		-.2814		+11.9132	
O(7)	O(1)	O(2)			
Plane (10)		+.3971		-.8931	
		-.2115		-7.5386	
O(17)	O(30)	O(40)			
Plane (11)		-.7239		-.2429	
		-.6457		+12.2538	
C(8)	C(81)	O(2)	O(7)	O(8)	
-549	0	-438	0	0	
Plane (12)		+.8267		+.1951	
		-.5278		+1.5194	
C(9)	C(91)	O(30)	O(50)	O(60)	
-1668	-318	28	84	90	
Plane (13)		-.3072		+.8748	
		-.3747		+13.6504	
C(1)	C(2)	C(3)	C(4)	C(5)	C(6)
-75	4	55	-125	128	65
Plane (14)		+.1153		-.9912	
		-.0646		-8.2858	
C(11)	C(12)	C(13)	C(14)	C(15)	C(16)
0	33	-94	49	-8	-31
Plane (15)		-.7239		-.2429	
		-.6457		+12.2538	
C(8)	C(81)	O(2)	O(7)	O(8)	
-549	0	-438	0	0	
(Plane (16)		+.8267		.1951	
		-.5278		+1.5194	
C(9)	C(91)	O(30)	O(50)	O(60)	
-1668	-318	28	84	90	



Table 6.8 continued

Dihedral angles (degrees)

Plane (1) - Plane (2)	78.6	Plane (3) - Plane (4)	79.7
Plane (1) - Plane (3)	3.8	Plane (9) - Plane (10)	62.2
Plane (1) - Plane (5)	6.1	Plane (3) - Plane (6)	78.8
Plane (7) - Plane (8)	24.6	Plane (4) - Plane (6)	0.1
Plane (2) - Plane (4)	2.8	Plane (5) - Plane (6)	81.5
Plane (2) - Plane (6)	2.7		

Table 6.9

(a)

Bond lengths and angles about cobalt in

S-[Cr(salen)<sub>2</sub>]bz<sub>2</sub>-(R,R)-Htart, 3H<sub>2</sub>O (e.s.d. values in parentheses)

Atoms	Bond lengths (Å)	Atoms	Bond angles (degrees)
Cr(10)-N(10)	2.017(3)	N(10)-Cr(10)-N(30)	81.5(1)
Cr(10)-N(20)	2.012(3)	N(10)-Cr(10)-N(60)	93.3(1)
Cr(10)-N(30)	2.101(3)	N(10)-Cr(10)-O(140)	90.0(1)
Cr(10)-N(60)	2.087(4)	N(10)-Cr(10)-O(150)	94.3(1)
Cr(10)-O(140)	1.922(3)	N(20)-Cr(10)-N(30)	96.2(1)
Cr(10)-O(150)	1.948(3)	N(20)-Cr(10)-N(60)	81.2(1)
		N(20)-Cr(10)-O(140)	92.0(1)
		N(20)-Cr(10)-O(150)	91.0(1)
		N(30)-Cr(10)-N(60)	88.0(1)
		N(30)-Cr(10)-O(150)	87.4(1)
		O(140)-Cr(10)-N(60)	90.4(1)
		O(140)-Cr(10)-O(150)	95.4(1)

161.  
Table 6.9 continued

(b)

Bond lengths and angles for ligands in

S-[Cr(sal en)<sub>2</sub>]bz<sub>2</sub>-(R,R)-Htart, 3H<sub>2</sub>O (e.s.d. values in parentheses)

Atoms	Bond lengths (Å)	Atoms	Bond angles (degrees)
C(110)-C(120)	1.419(5)	C(110)-C(120)-C(130)	119.0(4)
C(120)-C(130)	1.403(6)	C(120)-C(130)-C(140)	122.0(4)
C(130)-C(140)	1.369(8)	C(130)-C(140)-C(150)	118.8(4)
C(140)-C(150)	1.369(7)	C(140)-C(150)-C(160)	120.7(5)
C(150)-C(160)	1.375(6)	C(150)-C(160)-C(110)	122.3(4)
C(160)-C(110)	1.390(6)	C(160)-C(110)-C(120)	117.0(3)
C(170)-C(120)	1.431(6)	C(170)-C(120)-C(110)	124.0(3)
C(170)-N(20)	1.287(5)	C(170)-C(120)-C(130)	116.8(3)
C(180)-N(20)	1.481(6)	C(120)-C(170)-N(20)	125.4(3)
C(180)-C(190)	1.478(6)	C(160)-C(110)-O(150)	120.0(3)
C(190)-N(60)	1.468(6)	C(120)-C(110)-O(150)	123.0(4)
O(150)-C(110)	1.318(4)	C(110)-O(150)-Cr(10)	129.2(2)
		C(170)-N(20)-Cr(10)	126.2(3)
		C(180)-N(20)-Cr(10)	114.1(2)
		C(190)-C(180)-N(20)	109.3(3)
		C(180)-C(190)-N(60)	109.5(4)
		C(190)-N(60)-Cr(10)	107.7(3)
C(100)-C(200)	1.408(6)	C(100)-C(200)-C(300)	121.0(4)
C(200)-C(300)	1.377(5)	C(200)-C(300)-C(400)	120.5(5)
C(300)-C(400)	1.383(7)	C(300)-C(400)-C(500)	119.9(4)
C(400)-C(500)	1.365(8)	C(400)-C(500)-C(600)	120.8(4)
C(500)-C(600)	1.414(5)	C(500)-C(600)-C(100)	119.5(4)
C(600)-C(100)	1.402(5)	C(600)-C(100)-C(200)	118.1(3)
C(700)-C(600)	1.434(6)	C(100)-C(600)-C(700)	123.6(3)
C(700)-N(10)	1.284(4)	C(500)-C(600)-C(700)	116.6(3)
C(800)-N(10)	1.476(6)	C(600)-C(700)-N(10)	125.6(3)
C(800)-C(900)	1.478(6)	C(700)-N(10)-Cr(10)	126.8(3)
C(900)-N(30)	1.491(5)	C(800)-N(10)-Cr(10)	114.4(2)
O(140)-C(100)	1.321(4)	N(10)-C(800)-C(900)	108.5(4)
		C(800)-C(900)-N(30)	110.7(4)
		C(900)-N(30)-Cr(10)	108.5(2)
		C(100)-O(140)-Cr(10)	129.4(2)
		C(200)-C(100)-O(140)	117.9(3)
		C(600)-C(100)-O(140)	124.0(4)



162.  
Table 6.9 continued

(c)

Bond lengths and bond angles for  $\text{bz}_2-(R,R)\text{-Htart}^+$  ion in  
 $\text{S-}[\text{Cr}(\text{sal en})_2]\text{bz}_2-(R,R)\text{-Htart}\cdot 3\text{H}_2\text{O}$  (e.s.d. values in parentheses)

Atoms	Bond lengths (Å)	Atoms	Bond lengths (Å)
C(1)-C(2)	1.393(6)	C(11)-C(12)	1.355(6)
C(2)-C(3)	1.380(5)	C(12)-C(13)	1.379(6)
C(3)-C(4)	1.381(7)	C(13)-C(14)	1.349(9)
C(4)-C(5)	1.395(7)	C(14)-C(15)	1.359(9)
C(5)-C(6)	1.369(7)	C(15)-C(16)	1.372(6)
C(6)-C(1)	1.374(7)	C(16)-C(11)	1.368(7)
C(7)-C(2)	1.482(6)	C(17)-C(11)	1.483(5)
C(7)-O(1)	1.205(4)	C(17)-O(30)	1.357(4)
C(7)-O(2)	1.346(4)	C(17)-O(40)	1.197(5)
C(8)-C(81)	1.531(5)	C(9)-C(91)	1.535(5)
C(8)-O(2)	1.437(5)	C(9)-O(30)	1.431(3)
C(81)-O(7)	1.230(5)	C(91)-O(50)	1.276(4)
C(81)-O(8)	1.248(5)	C(91)-O(60)	1.225(4)
C(8)-C(9)	1.516(5)		
Atoms	Bond angle (degrees)	Atoms	Bond angle (degrees)
C(1)-C(2)-C(3)	120.0(4)	C(11)-C(12)-C(13)	120.7(5)
C(2)-C(3)-C(4)	119.7(4)	C(12)-C(13)-C(14)	120.7(5)
C(3)-C(4)-C(5)	119.6(4)	C(13)-C(14)-C(15)	119.4(5)
C(4)-C(5)-C(6)	120.6(5)	C(14)-C(15)-C(16)	121.2(6)
C(5)-C(6)-C(1)	119.7(5)	C(15)-C(16)-C(11)	119.3(5)
C(6)-C(1)-C(2)	120.2(4)	C(16)-C(11)-C(12)	118.7(4)
C(7)-C(2)-C(1)	117.3(3)	C(17)-C(11)-C(12)	119.1(4)
C(7)-C(2)-C(3)	122.6(4)	C(17)-C(11)-C(16)	122.1(4)
O(1)-C(7)-C(2)	124.5(3)	O(30)-C(17)-C(11)	112.4(3)
O(2)-C(7)-C(2)	113.2(3)	O(40)-C(17)-C(11)	124.6(3)
O(2)-C(7)-O(1)	122.3(4)	O(40)-C(17)-O(30)	122.9(3)
C(7)-O(2)-C(8)	115.5(2)	C(17)-O(30)-C(9)	115.0(3)
O(2)-C(8)-C(81)	112.4(3)	O(30)-C(9)-C(91)	112.0(3)
O(2)-C(8)-C(9)	107.8(3)	O(30)-C(9)-C(8)	108.6(3)
C(9)-C(8)-C(81)	112.8(3)	C(8)-C(9)-C(91)	110.8(3)
C(8)-C(81)-O(7)	116.0(3)	C(9)-C(91)-O(50)	115.5(2)
C(8)-C(81)-O(8)	116.6(3)	C(9)-C(91)-O(60)	118.6(3)
O(7)-C(81)-O(8)	127.3(4)	O(50)-C(91)-O(60)	125.9(3)

Table 6.9 continued  
(d)

Bond lengths involving calculated hydrogen atoms (e.s.d. values in parentheses)

Atoms	Bond lengths (Å)	Atoms	Bond lengths (Å)
H(1)-C(1)	.962(4)	H(180)-C(180)	.959(4)
H(3)-C(3)	.960(4)	H(181)-C(180)	.954(4)
H(4)-C(4)	.969(4)	H(190)-C(190)	.949(5)
H(5)-C(5)	.947(5)	H(191)-C(190)	.967(5)
H(6)-C(6)	.965(5)	H(200)-C(200)	.984(4)
H(8)-C(8)	.957(3)	H(300)-C(300)	.931(5)
H(9)-C(9)	.978(4)	H(400)-C(400)	.959(4)
H(12)-C(12)	.979(6)	H(500)-C(500)	.958(4)
H(13)-C(13)	.968(5)	H(700)-C(700)	.974(4)
H(14)-C(14)	.965(5)	H(800)-C(800)	.958(4)
H(15)-C(15)	.974(7)	H(810)-C(800)	.974(5)
H(16)-C(16)	.975(5)	H(900)-C(900)	.964(6)
H(130)-C(130)	.964(5)	H(910)-C(900)	.960(5)
H(140)-C(140)	.969(5)	HN(30)-N(30)	.947(3)
H(150)-C(150)	.977(5)	HN(31)-N(30)	.965(4)
H(160)-C(160)	.968(4)	HN(60)-N(60)	.961(4)
H(170)-C(170)	.952(4)	HN(61)-N(60)	.956(3)



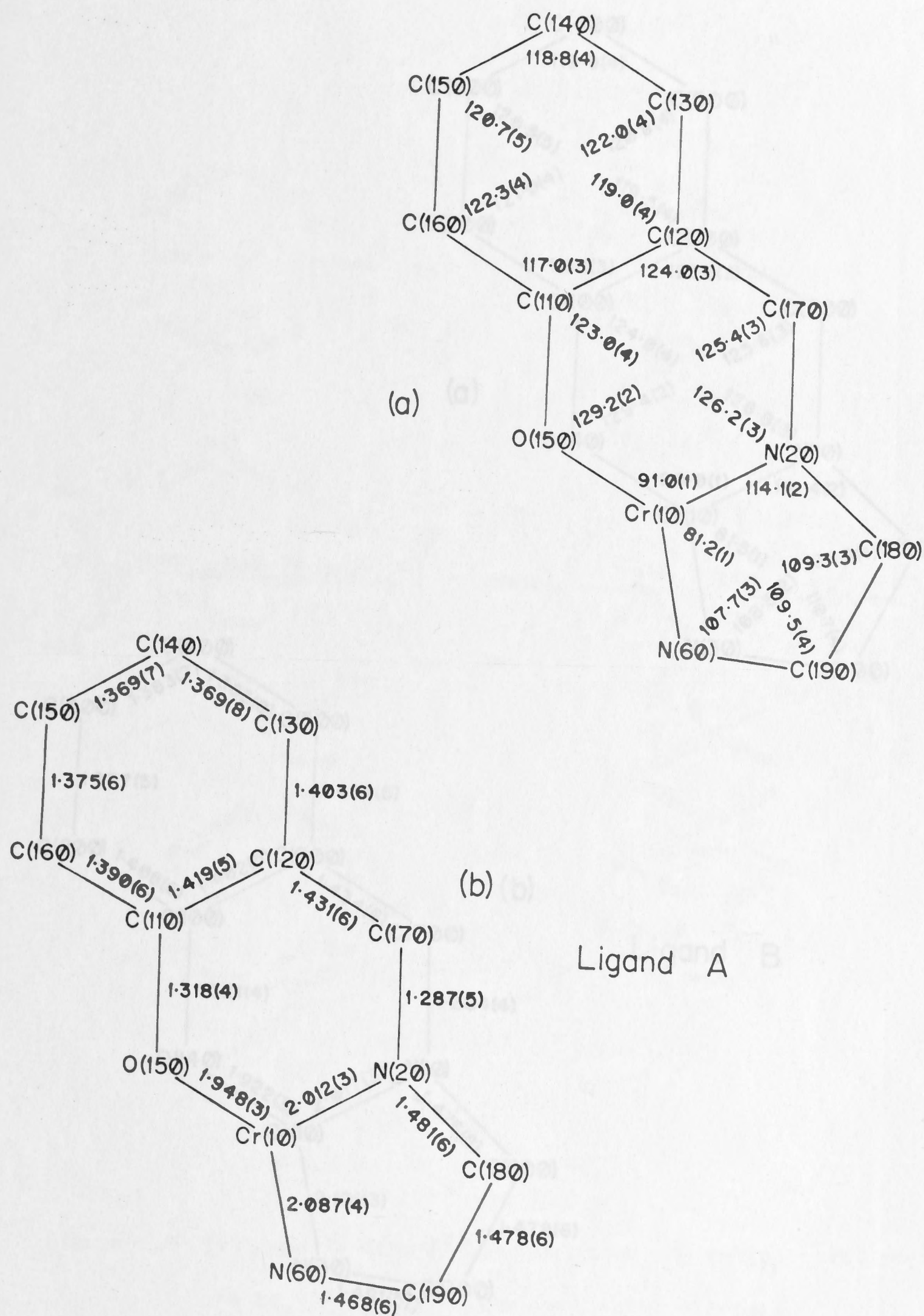


Figure 6.6 (a) Bond angles (degrees) and (b) bond lengths ( $\text{\AA}$ ) for the  $\text{S-}[\text{Cr}(\text{sal en})_2]^+$  ion (estimated standard deviations in parentheses).



Figure 6.7 (a) Bond angles (degrees) and (b) bond lengths (Å) for the  $S-[Cr(salen)_2]^+$  ion (estimated standard deviations in parentheses).



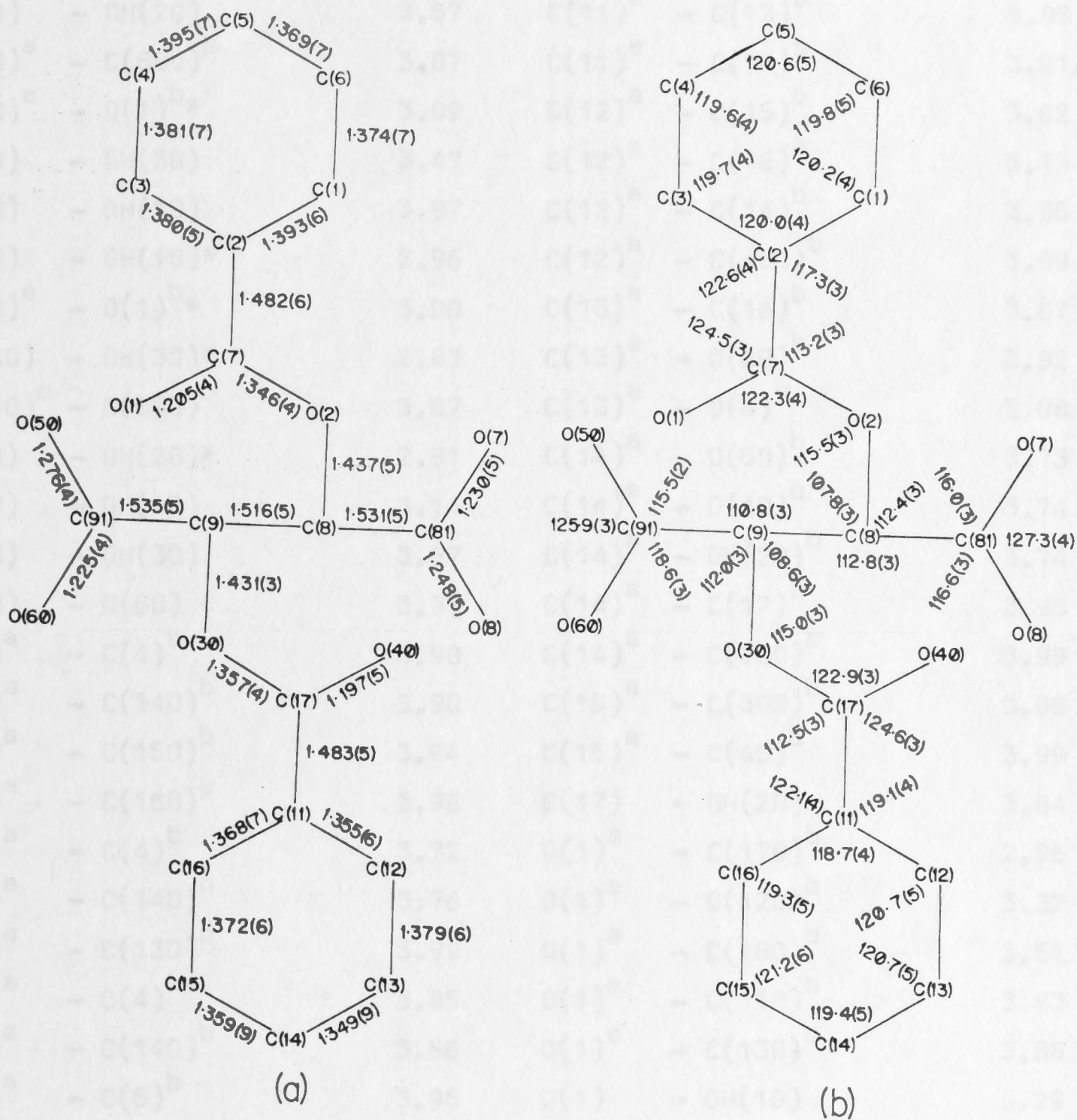


Figure 6.8 (a) Bond lengths (Å) and (b) bond angles (degrees) for the  $\text{bz}_2\text{-(R,R)-Htart}^-$  ion (estimated standard deviations in parentheses).

167.  
Table 6.10

Intermolecular approach distances for  $S-[Cr(sal\ en)_2]bz_2-(R,R)-Htart, 3H_2O$

Transformations of the asymmetric unit are indicated by superscripts

a:  $x, y, z$ ; b:  $\bar{x}, \frac{1}{2}+y, \bar{z}$

N(10)	- OH(20)	3.57	C(11) <sup>a</sup>	- C(13) <sup>b</sup>	3.85
N(10) <sup>a</sup>	- C(800) <sup>b</sup>	3.87	C(11) <sup>a</sup>	- C(14) <sup>b</sup>	3.91/3.97
N(20) <sup>a</sup>	- O(1) <sup>b*</sup>	3.09	C(12) <sup>a</sup>	- C(15) <sup>b</sup>	3.62
N(20)	- OH(30)	3.47	C(12) <sup>a</sup>	- C(16) <sup>b</sup>	3.73
N(20)	- OH(10)	3.97	C(12) <sup>a</sup>	- C(14) <sup>b</sup>	3.95
N(30)	- OH(10)*	2.96	C(12) <sup>a</sup>	- C(400) <sup>b</sup>	3.99
N(30) <sup>a</sup>	- O(1) <sup>b*</sup>	3.00	C(13) <sup>a</sup>	- C(16) <sup>b</sup>	3.67
O(140)	- OH(30)*	2.83	C(13) <sup>a</sup>	- O(50) <sup>b</sup>	3.82
O(150) <sup>a</sup>	- C(800) <sup>b</sup>	3.87	C(13) <sup>a</sup>	- O(8) <sup>b</sup>	3.88
N(60)	- OH(20)*	2.91	C(14) <sup>a</sup>	- O(50) <sup>b</sup>	3.73
N(60)	- OH(10)	3.14	C(14) <sup>a</sup>	- O(40) <sup>b</sup>	3.74
N(60)	- OH(30)	3.67	C(14) <sup>a</sup>	- OH(20) <sup>b</sup>	3.74
N(60)	- O(60)	3.97	C(14) <sup>a</sup>	- C(17) <sup>b</sup>	3.95
C(1) <sup>a</sup>	- C(4) <sup>b</sup>	3.90	C(14) <sup>a</sup>	- C(300) <sup>b</sup>	3.99
C(1) <sup>a</sup>	- C(140) <sup>b</sup>	3.90	C(15) <sup>a</sup>	- C(300) <sup>b</sup>	3.86
C(1) <sup>a</sup>	- C(150) <sup>b</sup>	3.94	C(15) <sup>a</sup>	- O(40) <sup>b</sup>	3.99
C(1) <sup>a</sup>	- C(160) <sup>b</sup>	3.96	C(17)	- OH(20)	3.84
C(2) <sup>a</sup>	- C(4) <sup>b</sup>	3.72	O(1) <sup>a</sup>	- C(170) <sup>b</sup>	2.96
C(2) <sup>a</sup>	- C(140) <sup>b</sup>	3.76	O(1) <sup>a</sup>	- C(120) <sup>b</sup>	3.32
C(2) <sup>a</sup>	- C(130) <sup>b</sup>	3.99	O(1) <sup>a</sup>	- C(180) <sup>b</sup>	3.51
C(3) <sup>a</sup>	- C(4) <sup>b</sup>	3.85	O(1) <sup>a</sup>	- C(110) <sup>b</sup>	3.83
C(3) <sup>a</sup>	- C(140) <sup>b</sup>	3.86	O(1) <sup>a</sup>	- C(130) <sup>b</sup>	3.88
C(3) <sup>a</sup>	- C(5) <sup>b</sup>	3.95	O(1)	- OH(10)	3.29
C(4) <sup>a</sup>	- C(140) <sup>b</sup>	3.76	O(1) <sup>a</sup>	- O(8) <sup>a</sup>	3.32 A
C(4) <sup>a</sup>	- O(8) <sup>b</sup>	3.86	O(2) <sup>a</sup>	- O(8) <sup>a</sup>	2.65 A
C(4)	- C(130)	3.88	O(2) <sup>a</sup>	- O(30) <sup>a</sup>	2.81 A
C(5) <sup>a</sup>	- O(8) <sup>b</sup>	3.54	O(2) <sup>a</sup>	- O(60) <sup>a</sup>	3.26 A
C(5) <sup>a</sup>	- O(50) <sup>b</sup>	3.61	O(2) <sup>a</sup>	- O(50) <sup>a</sup>	3.56 A
C(7) <sup>a</sup>	- C(170) <sup>b</sup>	3.93	O(30) <sup>a</sup>	- O(50) <sup>a</sup>	2.63 A
C(7)	- OH(10)	3.96	O(30) <sup>a</sup>	- O(7) <sup>a</sup>	3.41 A
C(8)	- OH(10)	3.74	O(30) <sup>a</sup>	- O(8) <sup>a</sup>	3.53 A
C(81)	- OH(30)	3.80	O(40)	- OH(20)*	2.85
C(81)	- OH(20)	3.82	O(40) <sup>a</sup>	- O(50) <sup>a</sup>	3.08 A
C(9)	- OH(20)	3.98	O(40)	- C(500)	3.36
C(91)	- OH(20)	3.46	O(40)	- C(400)	3.42
C(91)	- OH(10)	3.87	O(40)	- C(600)	3.48



Table 6.10 continued

O(40) - C(300)	3.59	C(180) - OH(30)	3.37/3.52
O(40) - C(100)	3.65	C(180) - OH(10)	3.55/3.57
O(40) - C(200)	3.70	C(190) - OH(10)	3.41/3.60
O(50) <sup>a</sup> - O(8) <sup>a</sup>	2.44 B	C(190) - OH(30)	3.43/3.67
O(50) - OH(20)	3.37	C(190) - OH(20)	3.83
O(50) <sup>a</sup> - O(7) <sup>a</sup>	3.38 B	C(100) - OH(30)	3.50
O(60) - OH(10)*	2.82	C(100) <sup>a</sup> - C(800) <sup>b</sup>	3.77
O(60) <sup>a</sup> - O(8) <sup>a</sup>	3.39 B	C(100) - OH(20)	3.98
O(60) <sup>a</sup> - O(7) <sup>a</sup>	3.75 B	C(200) - OH(30)	3.31
O(60) - OH(20)	3.78	C(200) - OH(20)	3.49
O(60) <sup>a</sup> - C(130) <sup>b</sup>	3.78	C(300) <sup>a</sup> - C(800) <sup>b</sup>	3.39
O(7) - OH(30)*	2.83	C(300) - OH(20)	3.55
O(7) - OH(20)*	2.84	C(300) - C(900)	3.87
O(7) - C(200)	3.61	C(500) <sup>a</sup> - C(800) <sup>b</sup>	3.65
O(7) - C(180)	3.81	C(500) <sup>a</sup> - C(900) <sup>b</sup>	3.71
O(8) - C(170)	3.94	C(600) <sup>a</sup> - C(800) <sup>b</sup>	3.39
C(120) - OH(10)	3.92	C(600) <sup>a</sup> - C(900) <sup>b</sup>	3.87
C(150) <sup>a</sup> - C(500) <sup>b</sup>	3.72	C(700) - OH(20)	3.34
C(160) <sup>a</sup> - C(500) <sup>b</sup>	3.73	C(700) <sup>a</sup> - C(800) <sup>b</sup>	3.47
C(160) <sup>a</sup> - C(700) <sup>b</sup>	3.77	C(700) <sup>a</sup> - C(900) <sup>b</sup>	3.81
C(160) <sup>a</sup> - C(300) <sup>b</sup>	3.83	C(900) - OH(10)	3.41
C(160) <sup>a</sup> - C(400) <sup>b</sup>	3.97	C(900) - OH(30)	3.96
C(170) - OH(20)	3.45	OH(10) - OH(30)*	2.72
C(170) - OH(30)	3.89	OH(20) - OH(30)	3.91

\* Hydrogen bonds shown as dashed lines in Figure 6.4

A Intramolecular interactions which are important in determining the conformation of the (R) tartrate moiety

B Intercell interactions of the anion

## CHAPTER 7

THE STRUCTURAL AND CONFORMATIONAL ASPECTS OF COMPLEXES OF COBALT(III)  
AND CHROMIUM(III) WITH TRIDENTATE SCHIFF-BASE LIGANDS

The aim of this chapter is to inter-relate what may be termed the "chemically unique" bond lengths and angles, distortions and conformations of these complexes. "Statistically unique" parameters are mathematically invariable quantities which have their place when dealing with an ideal universe of data. However, strict adherence to this ideal in interpreting the statistics is considered by the author to be of less value than using these statistics as a guide to chemically "real" conclusions. Indeed, rigorous acceptance of statistical results may be detrimental when these results are discussed in a chemical sense (Raymond, Corfield & Ibers, 1968a).

## 7.1 STATISTICAL PARAMETERS

The weighted average of a parameter,  $\bar{p}_w$ , is given by (Deming, 1943; Ractliffe, 1967)

$$\bar{p}_w = \frac{\sum_{i=1}^n (p_i / \sigma_i^2)}{\sum_{i=1}^n (1 / \sigma_i^2)}$$

where  $p_i$  is the parameter,  $\sigma_i$ , the estimated standard deviation and  $n$  is the sample size.

The estimated variance,  $\text{var}(\bar{p}_w)$ , of the mean was calculated as (Deming, 1943; International Tables, 1962)

$$\text{var}(\bar{p}_w) = \sigma_w^2 = \frac{\sum_{i=1}^n (1 / \sigma_i^2) (p_i - \bar{p}_w)^2}{\sum_{i=1}^n (1 / \sigma_i^2)} \cdot (n-1)^{-1}$$

where  $\sigma_w$  is the estimated standard deviation of the weighted mean.



In order to simplify calculation of the correlation coefficients the estimated variance of an individual parameter,  $\text{var}(p)$ , was calculated as (Deming, 1943; Ractliffe, 1967)

$$\text{var}(p) = \sigma_I^2 = \left[ \sum_i^n p_i^2 - \left( \sum_i^n p_i \right)^2 / n \right] (n - 1)^{-1}$$

where  $\sigma_I$  is the estimated standard deviation of an individual.

The estimated covariance of two parameters,  $\text{cov}(p,q)$ , is given by (Ractliffe, 1967)

$$\text{cov}(p,q) = \left[ \sum_i^n p_i q_i - \left( \sum_i^n p_i \right) \left( \sum_i^n q_i \right) / n \right] (n - 1)^{-1}$$

and the correlation coefficient,  $r$ , was calculated as (Ractliffe, 1967)

$$r_{pq} = \frac{\text{cov}(p,q)}{(\text{var}(p) \cdot \text{var}(q))^{\frac{1}{2}}}$$

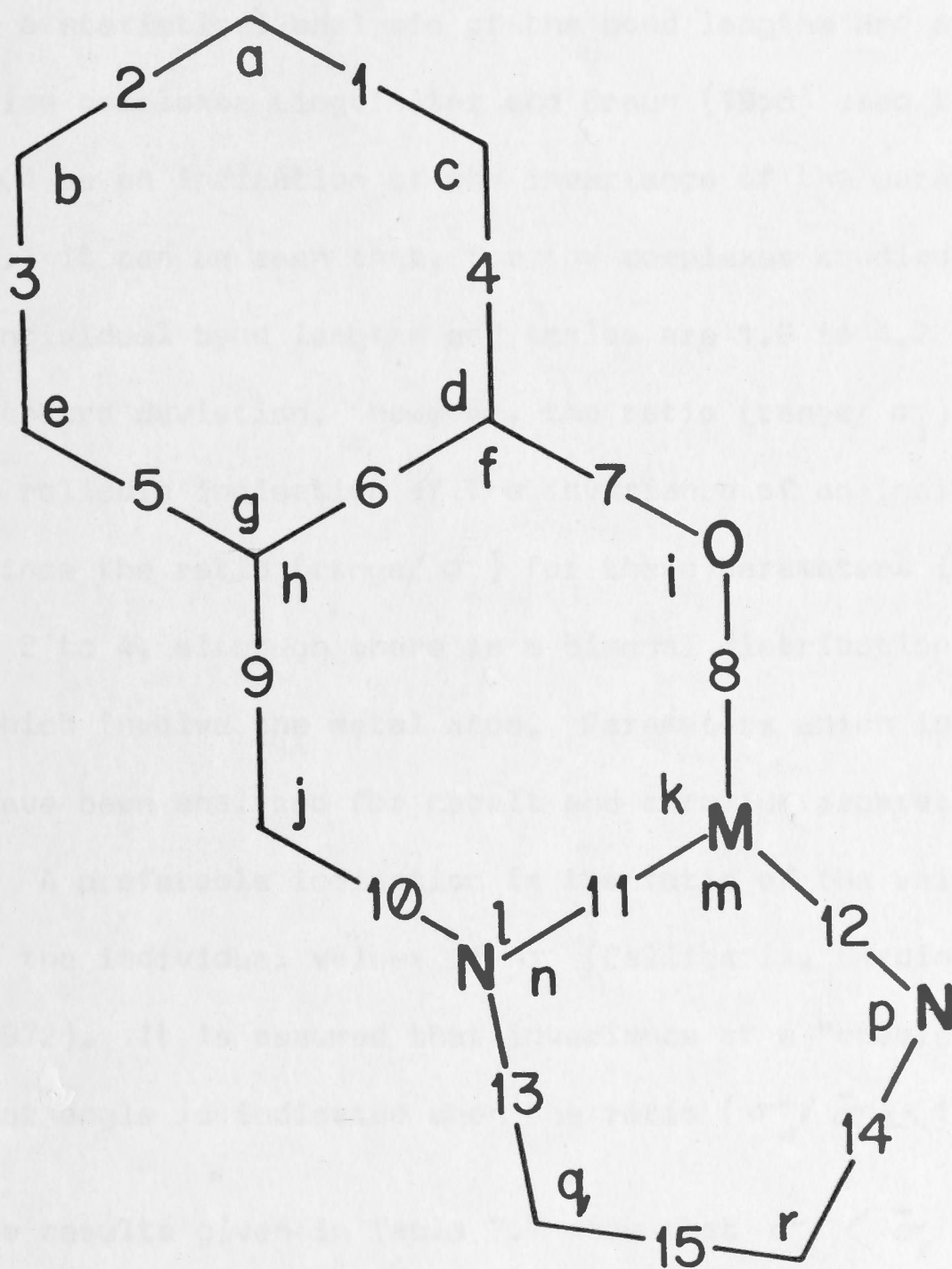
The correlation coefficient,  $r$ , is distributed as  $t$  with  $(n - 2)$  degrees of freedom (Ractliffe, 1967), where  $t$  is given by

$$t = r(n - 2)^{\frac{1}{2}} / (1 - r^2)^{\frac{1}{2}}.$$

## 7.2 BOND LENGTHS AND ANGLES

Statistical analysis was carried out for each bond length and bond angle, in order to determine the constancy of the measured parameters reported for sal en and sal (R)pn ligands. The correlations which exist between various geometrical parameters were also determined.

The coding scheme for bonds and angles used in the statistical analysis is shown in Figure 7.1. The range of each parameter, together with calculated weighted average values and their estimated standard



Numbers - bond lengths

Lower case letters - bond angles

Figure 7.1 Bond and angle coding used in statistical analyses



deviations are given in Table 7.1.

#### 7.2.1. Bond lengths and bond angles of the ligands

In a statistical analysis of the bond lengths and angles of salicylaldehyde complexes Lingafelter and Braun (1966) used the ratio,  $(\text{range}/\sigma_I) < 4$ , as an indication of the invariance of the parameters. From Table 7.1 it can be seen that, for the complexes studied, the ranges for individual bond lengths and angles are 1.8 to 4.2 times the estimated standard deviation. However, the ratio  $(\text{range}/\sigma_I)$  does not seem to be a reliable indication of the invariance of an individual parameter, since the ratio  $(\text{range}/\sigma_I)$  for these parameters is still of the order of 2 to 4, although there is a bimodal distribution of the parameters which involve the metal atom. Parameters which involve the metal atom have been analysed for cobalt and chromium separately (Table 7.1). A preferable indication is the ratio of the value of  $\sigma_w$  and  $\bar{\sigma}_r$ , and the individual values of  $\sigma_r$  (Calligaris, Nardin & Randaccio, 1972). It is assumed that invariance of a "chemically unique" bond length or angle is indicated when the ratio  $(\sigma_w/\bar{\sigma}_r) < 1$ .

The results given in Table 7.1 show that  $\sigma_w < \bar{\sigma}_r$  for the parameters which do not involve the metal atom, and it is concluded that these bond lengths and angles are characteristic of the ligand and independent of the metal. The mean values of bond lengths and angles given in Table 7.1 are consistent with those reported for related ligands (Lingafelter & Braun, 1966; Calligaris, Nardin & Randaccio, 1972; Gardner, Gatehouse & White, 1971; Table 7.2).

The difference in the C - C bond length between "near" and "far" sides (with respect to the metal atom) of the benzene ring is similar to that previously observed for both salicylaldehyde and bis(salicylaldehyde) ethylenediimine ligands (Lingafelter & Braun,

Table 7.1

Statistical analysis of bond lengths and bond angles  
(a)

Bonds ( $\text{\AA}$ )					
Bond*	$\bar{d}_w$	$\sigma_w(\bar{d}_w)$	$\bar{\sigma}_r(d)$	Range	Range/ $\sigma_i$
1	1.376	.004	.019	.112	4.2
2	1.374	.004	.021	.081	3.5
3	1.378	.004	.018	.090	3.4
4	1.398	.004	.016	.119	3.6
5	1.409	.005	.016	.118	3.9
6	1.411	.004	.018	.154	4.2
7	1.320	.003	.015	.096	1.7
8	Co 1.902	.012	.011	.069	2.4
	Cr 1.926	.005	.003	.037	3.0
9	1.432	.003	.030	.047	3.5
10	1.287	.005	.015	.086	3.7
11	Co 1.897	.006	.012	.028	2.1
	Cr 2.017	.002	.004	.016	3.3
12	Co 1.971	.006	.014	.040	2.2
	Cr 2.093	.004	.004	.022	2.2
13	1.476	.004	.016	.047	2.8
14	1.489	.005	.016	.068	2.9
15	1.502	.007	.017	.132	3.6

\* See Figure 7.1



Table 7.1 continued

(b)

Angles (degrees)

Angle <sup>e*</sup>	$\bar{\theta}_w$	$\sigma_w(\bar{\theta}_w)$	$\bar{\sigma}_r(\theta)$	Range	Range/ $\sigma_i$	
a	120.7	0.3	1.0	3.4	2.6	
b	119.3	0.4	0.9	3.8	2.3	
c	121.5	0.2	0.9	2.9	2.9	
d	117.9	0.2	0.7	2.2	2.2	
e	121.4	0.4	0.9	5.6	3.4	
f	123.6	0.3	0.7	1.8	1.8	
g	119.2	0.2	0.7	3.3	3.3	
h	123.6	0.1	0.7	1.5	2.3	
i	128.9	0.6	0.8	8.7	2.6	
j	125.3	0.2	0.7	2.5	2.5	
k	Co	94.5	0.2	0.4	1.0	2.2
	Cr	90.5	0.2	0.2	1.0	2.0
l	126.4	0.3	0.8	2.6	2.6	
m	Co	85.7	0.3	0.4	1.5	2.2
	Cr	81.0	0.3	0.2	1.7	2.3
n	114.6	0.4	0.7	5.2	3.9	
p	109.4	0.3	0.6	3.4	3.4	
q	108.5	0.4	0.7	4.7	2.4	
r	108.0	0.5	0.7	5.2	2.6	

\* See Figure 7.1

Table 7.2

Comparison of bond lengths for the ligands sal en, sal (R)pn, salim  
and salen. ( $\text{\AA}$ )

Bond*	This work	salim	salen	Cr(sal en) <sub>2</sub> I	Theoretical
1	1.376(4)	1.388(3)	1.389(4)	1.42(2)	1.38
2	1.374(4)	1.384(5)	1.395(4)	1.43(2)	1.39
3	1.378(4)	1.367(3)	1.372(3)	1.41(2)	1.38
4	1.398(4)	1.415(6)	1.412(3)	1.44(2)	1.40
5	1.409(5)	1.423(4)	1.422(3)	1.45(3)	1.40
6	1.411(4)	1.415(6)	1.416(3)	1.42(3)	1.42
7	1.320(3)	1.312(3)	1.321(3)	1.35(3)	1.31
9	1.432(3)	1.430(6)	1.434(3)	1.45(3)	1.42
10	1.287(5)	1.295(5)	1.291(3)	1.32(2)	1.29
13	1.476(4)	—	1.481(3)	1.55(2)	—
14	1.489(5)	—	1.481(3)	1.49(2)	—
15	1.502(7)	—	1.510(11)	1.54(3)	—

This work: Combined values for sal en and sal (R)pn.

salim: Lingafelter & Braun (1966).

salen: Calligaris, Nardin & Randaccio (1972).

Cr(sal en)<sub>2</sub>I: Gardner, Gatehouse & White (1971).

Theoretical: Lingafelter & Braun (1966).

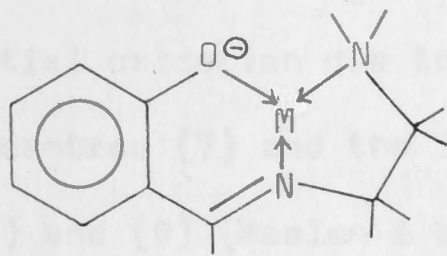
\* See Figure 7.1



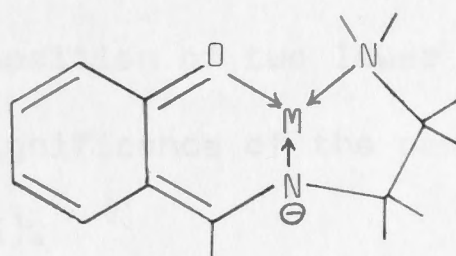
1966; Calligaris, Nardin & Randaccio, 1972). These differences are significant in that  $(\bar{d}_{1,2,3} - \bar{d}_{4,5,6}) > 4\sigma_1$ , where  $d_{x,y,z}$  is the average of the bond lengths  $x$ ,  $y$  and  $z$  and  $\sigma_1 = (\bar{\sigma}_{1,2,3}^2 + \bar{\sigma}_{4,5,6}^2)^{\frac{1}{2}}$ . This phenomenon has been explained by Lingafelter and Braun (1966) on the basis of calculations using a simple Huckel MO method applied to the  $\pi$ -electron system of the salicylaldiminate ion. The excellent agreement between the measured and calculated bond lengths showed that there is a real difference in the C - C bond lengths on the "near" and "far" sides of the benzene ring, which is unrelated to the chelation of a metal atom (Lingafelter & Braun, 1966).

The average C - O and C - C (code 9, Figure 7.1) bond lengths, 1.320 Å and 1.432 Å, respectively, are intermediate between the typical single and double bond lengths. This is consistent with a  $\pi$ -electron system, which includes the carbon and oxygen atoms of the chelate ring.

The main canonical form of  $M(\text{sal en})_2^+$  may be written as (1) and consideration of the bond lengths in the six membered chelate ring shows that (2) is also significant.

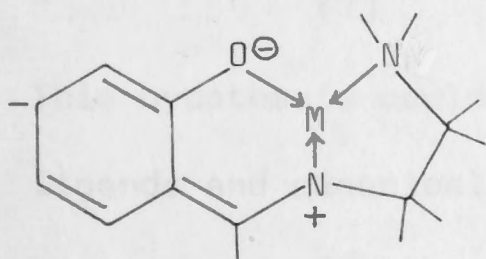


(1)

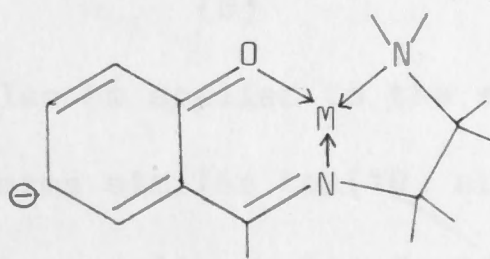


(2)

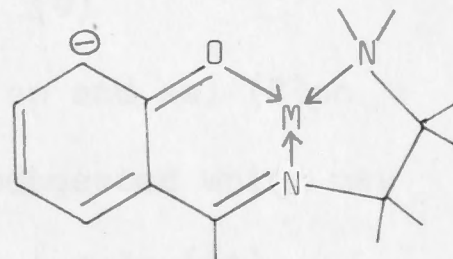
However, the situation must be more complex than these two structures imply since the benzene ring has three consecutive short bonds. The canonical forms (3), (4) and (5) may also contribute.



(3)

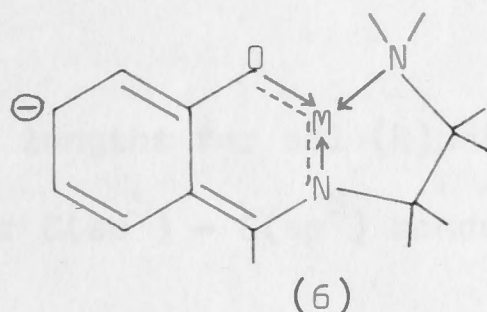


(4)

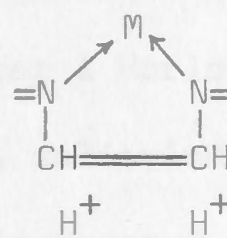
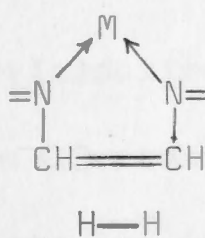
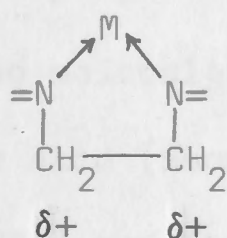


(5)

$\pi$ -bonding with the metal atom, which is consistent with the idea that the salim moiety may be regarded as a modified naphthalene system, allows the following electron transfer to occur and leads to the form (6).

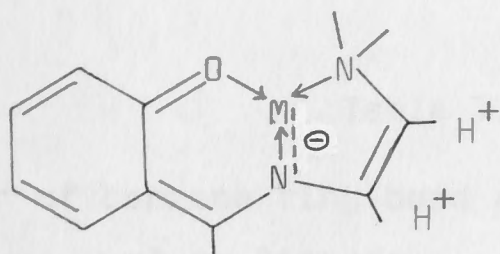


The average lengths of the C - N bond of the diamine moiety are typical of a C - N single bond (International Tables, 1962). The average length of the azomethine C - N bond (code 10 Figure 7.1) is shorter than a typical C = N bond (1.337 Å, International Tables, 1962). Also, the CH<sub>2</sub> - CH<sub>2</sub> bond length (code 15 Figure 7.1) is shorter than the value expected for a C(sp<sup>3</sup>) - C(sp<sup>3</sup>) bond (International Tables, 1962). These effects are also characteristic of complexes of salen (Calligaris, Nardin & Randaccio, 1972) and other tridentate Schiff-base ligands (Gardner, Gatehouse & White, 1971; Fallon & Gatehouse, 1975; Kistenmacher, Szalda & Marzilli, 1975; Orioli, Vaira & Sacconi, 1966). The shortening of the CH<sub>2</sub> - CH<sub>2</sub> bond in salen ligands has been regarded as a partial oxidation due to the juxtaposition of two lower electron density centres (7) and the increased significance of the canonical forms (8) and (9) (Maslen & Waters, 1975).

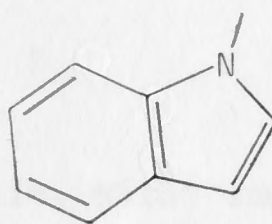


This hypothesis could also be applied to the sal en and sal (R)pn ligands and canonical forms similar to (10) are suggested which may be compared with the heterocyclic system found in indole (11).





(10)



(11)

The C - C(methyl) bond lengths for sal (R)pn(1-Me) and sal (R)pn(2-Me) ligands are typical for C(sp<sup>3</sup>) - C(sp<sup>3</sup>) bonds (International Tables, 1962).

The average values of the individual angles in the benzene ring are close to the ideal 120° with the exception of angle 'd' (Figure 7.1), which is significantly smaller than the other bond angles. However, the statistics suggest that the angles for the benzene ring may be divided into three groups; (a,c,e), (b,g) and (d) (Figure 7.1). In order to assess the reality of this distribution of the bond angles, the average values for 28 comparable structures (40 measurements) were calculated (Table 7.3). From these data (intended to be a representative not an exhaustive compilation) two conclusions may be reached. First, the variability of the bond angles, as measured by the value of (range/ $\sigma_i$ ) and the range, appears to be the same for all six angles. Secondly, the features noted above for the bond angles in the benzene ring, in sal en and sal (R)pn complexes are probably real. Comparison of this grouping of bond angles with the angles reported for the uncomplexed molecules salicylaldehyde (Pfluger & Harlow, 1973), salicyclic acid (Sundaralingam & Jensen, 1965), salicylamide (Hsu & Craven, 1974) and the salicylate ion (Klug, Alexander & Sumner, 1958), shows that the values for the angles (a,c,e) are generally > 120° and those for (b,d,g) < 120°, with g the smallest.

The presence of steric strain in the salim chelate rings is demonstrated by the magnitude of the ring angles (Table 7.1). Average angles within the salim chelate ring are in no way unusual when

Table 7.3

Comparison of benzene ring bond angles in salim, salen and  
N-substituted sal en ligands

(degrees)

Angle*	This work	Sample average	$\sigma_i$	$\sigma_A$	Range	Range/ $\sigma_i$
a	120.7(3)	120.8	1.6	0.3	7.0	4.4
b	119.3(4)	120.0	2.1	0.3	9.3	4.4
c	121.5(2)	120.4	1.7	0.3	7.5	4.4
d	117.9(2)	118.5	1.7	0.3	7.1	4.2
e	121.4(4)	120.7	2.0	0.3	9.3	4.7
g	119.2(2)	119.5	1.3	0.2	6.2	4.8

Averages are unweighted due to the inconsistency in reporting  
estimated standard deviations which were generally  $0.3^\circ$  to  $2.6^\circ$ .

Data source:

Bailey, Higson & McKenzie (1972)	Gardner, Gatehouse & White (1971)
Bailey, Higson & McKenzie (1975)	Gerloch & Mabbs (1967)
Baker, Hall & Waters (1970a, b)	Jarski & Lingafelter (1964)
Braun & Lingafelter (1966)	Kistenmacher, Szalda & Marzilli
Braun & Lingafelter (1967a, b)	(1975)
Bruckner, Calligaris, Nardin &	Klug, Alexander & Sumner (1958)
Randaccio (1969)	Lingafelter, Simmons & Morosin
Calligaris, Nardin, Randaccio &	(1961)
Minichelli (1971)	Orioli, Lingafelter & Brown (1964)
Calligaris, Manzini, Nardin &	Orioli, Vaira & Sacconi (1966)
Randaccio (1972)	Schaeffer & Marsh (1969)
Coggan, McPhail, Mabbs, Richards	Shkol'nikova, Obodovskaya &
& Thornley (1970)	Shugum (1973)
Coggan, McPhail, Mabbs, &	Vaira & Orioli (1967)
McLachlan (1971)	Wei, Stogsdill & Lingafelter (1964)
Chieh & Palenik (1972)	
Davies & Gatehouse (1972)	
Fallon & Gatehouse (1975)	
Fox, Orioli, Lingafelter &	
Sacconi (1964)	
Frasson & Panattoni (1964)	

\* See Figure 7.1



compared with those reported for similar structures (see references in Table 7.3) and are consistent with  $C(sp^2) - N, O(sp^2)$  bonding in a  $\pi$ -system. The largest angle is C-O-M (code i, Figure 7.1) which has both the largest range and  $\sigma_w(\bar{\theta})$ . Examination of the correlation coefficients for both bond lengths and angles (Table 7.4) shows that a strong correlation exists between the angles C-O-M and O-M-N (code k, Figure 7.1). The angle C-O-M is also correlated to a small extent with the C - O and O - M bond lengths (codes 7 and 8, Figure 7.1).

The bond angles about the azomethine nitrogen atom indicate the presence of steric strain in that the angle M-N-C (code n, Figure 7.1) is intermediate between that expected for  $sp^2$  and  $sp^3$  hybridized nitrogen atoms. The average bond angles at the other nitrogen atom and carbon atoms within the diamine chelate ring are characteristic of  $sp^3$  hybridized atoms and for both sal (R)pn(1-Me) and sal (R)pn(2-Me) ligands, the carbon atom to which the methyl group is attached shows excellent tetrahedral geometry. Strong correlation exists between the N-M-N angle (code m, Figure 7.1) and the other angles in the chelate ring, with the exception of angle 'r' (Figure 7.1). Correlations between bonds and angles are of less importance, the largest is between the bond length N - M and the angle M-N-C (codes 11 and n respectively, Figure 7.1).

Examination of the more important correlation coefficients (Table 7.4) shows that distortions of the chelate rings can be explained mainly in terms of angle adjustments. Theoretical calculations (Hawkins, 1971; Buckingham, Maxwell, Sargeson & Snow, 1970) have shown that unfavourable non-bonded interactions can be relieved with a smaller increase in energy by the distortions of bond angles rather than by the distortion of bond lengths.

Table 7.4

Correlation coefficients for Co/Cr sal en and sal (R)pn complexes

Parameters*		r	t <sub>c</sub>	N.H.	Parameters*		r	t <sub>c</sub>	N.H.
i	k	-0.95	9.1	D	m	p	-0.61	2.3	D
i	7	-0.47	1.6	N	m	q	-0.82	4.3	D
i	8	+0.42	1.4	N	m	r	-0.16	0.5	N
j	1	-0.77	3.6	D	m	11	-0.94	7.7	D
k	m	+0.95	9.1	D	m	12	-0.92	7.0	D
k	8	-0.38	1.2	N	n	11	+0.62	2.4	D
k	11	-0.93	7.6	D	p	12	+0.56	2.0	N
l	10	-0.49	1.7	N	8	11	+0.40	1.3	N
l	11	-0.38	1.2	N	8	12	+0.42	1.4	N
m	n	-0.74	3.3	D	9	10	+0.53	1.9	N
					10	11	+0.55	2.0	N

D indicates that the null hypothesis - "the parameters are NOT correlated," is disproved at the 95% confidence level.

N indicates that the null hypothesis has not been disproved.

$$t_{(9,0.05)} = 2.26$$

$$t_{(9,0.02)} = 2.82$$

\* See Figure 7.1



### 7.2.2 Metal-ligand bond lengths and angles

Comparison of the  $\sigma_A$  values for the metal-ligand bond distances (ignoring the identity of the metal) with the values for individual determinations shows a large variation of these distances, as expected. The influence of the metal is clearly illustrated by the weighted mean values for bond lengths given in Table 7.1. Significant differences in the value of metal-ligand bond lengths can occur in a single cation due to differences in the extent of hydrogen bonding of the two ligands, particularly when this involves the amine nitrogen atom (Gardner, Gatehouse & White, 1971; this study). However, the average values given in Table 7.1 are consistent with those reported for salen complexes (Calligaris, Nardin & Randaccio, 1972). The M - O distances show least variation. The combined sample has  $\sigma_A = 0.007 \text{ \AA}$ , which is of the same order as that for the other bond lengths not involving the metal atom. This difference between the variation of M - O and M - N bond lengths is in accord with previously published data (Calligaris, Nardin & Randaccio, 1972), and has been attributed to differences in the extent of hydrogen bonding involving the oxygen and nitrogen atoms.

The bond angles about the metal atom are very dependent upon the metal type, which is to be expected. In common with other related complexes (references in Table 7.3, Lingafelter & Braun, 1966) the distance between the two donor atoms of each chelate ring (i.e. the 'bite') seems to be independent of the metal ion. This implies that, as the M - O and M - N bond lengths increase, the angles at the metal atom decrease. This is supported by the large negative correlation coefficients listed in Table 7.4.

### 7.3 ANALYSIS OF ASYMMETRY IN THE COMPLEXES

Optical activity has been attributed to four main sources of asymmetry in metal complexes (Bosnich & Harrowfield, 1972):

- (1) The configurational asymmetry, due to the helical arrangement of chelate rings around the metal atom.
- (2) The conformational contribution arising from the dissymmetric<sup>m</sup> ~~er~~ puckling of the chelate rings.
- (3) A vicinal effect which arises from the presence of an asymmetric centre in the ligand.
- (4) Dissymmetric distortion of donor atoms, which define a helical system about the metal atom.

These features, with the exception of (3), will now be discussed for the complexes studied.

#### 7.3.1. Absolute configuration

All complexes studied were meridional isomers. The absolute configurations of the optically active complexes are listed in Table 7.5. The R,S convention is that of Cahn, Ingold and Prelog (1966) (Figure 7.2).

The angle between the mean planes of the ligands in a single cation is in the range 77.4 to 81.5° for these complexes. This is of the same order as 87° reported for the angle between the salicylaldiminato groups in  $\text{Cr}(\text{sal en})_2\text{I}$  (Gardner, Gatehouse & White, 1971).

Table 7.5

Absolute configuration of complexes

---

$(+)_486$	-S-	$[\text{Co}(\text{sal (R)pn(2-Me)})_2]\text{I}, 3\text{H}_2\text{O}$
$(+)_489$	-S-	$[\text{Co}(\text{sal (R)pn(1-Me)})(\text{sal (R)pn(2-Me)})]\text{ClO}_4, 0.75\text{EtOH}$
$(+)_366$	-S-	$[\text{Cr}(\text{sal en})_2]\text{bz}_2-(\text{R,R})\text{-Htart}, 3\text{H}_2\text{O}$

---



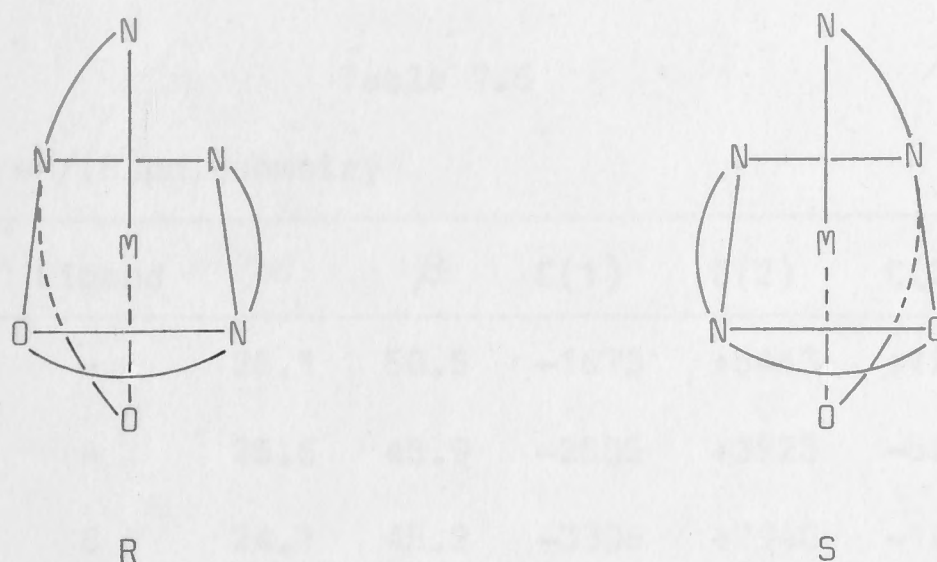


Figure 7.2 Assignment of the Cahn, Ingold and Prelog (1966) notation

### 7.3.2 Conformation of the ligands

#### 7.3.2.a Five-membered chelate rings

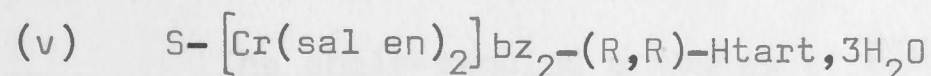
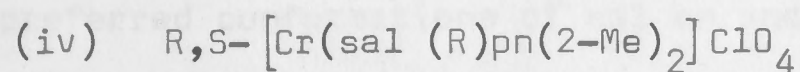
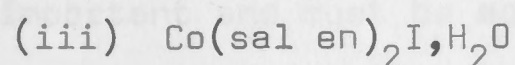
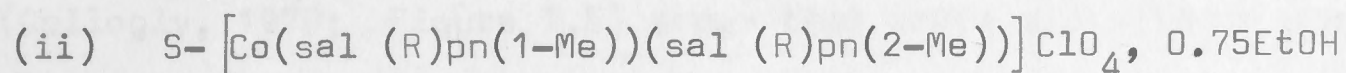
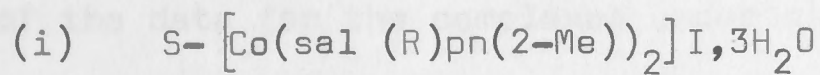
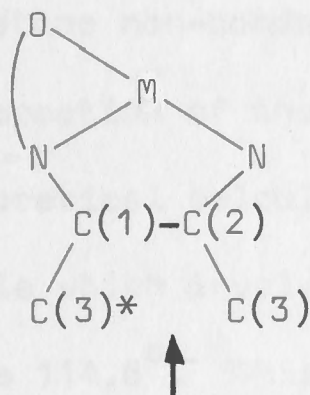
The conformation of the five-membered chelate rings may be described in terms of the parameters  $\alpha$ ,  $\beta$  and the distances of the ring carbon atoms above and/or below the N-M-N plane (Raymond, Corfield & Ibers, 1968b). The skew angle,  $\alpha$ , of the chelate ring is the angle between the planes N(1)-M-N(2) and C(1)-M-C(2). The dihedral angle,  $\beta$ , is the angle between the planes N(1)-C(1)-C(2) and C(1)-C(2)-N(2). The data for the complexes (Table 7.6) are similar to those found for five-membered diamine rings in compounds previously studied (Raymond, Corfield & Ibers, 1968b; Buckingham, Maxwell, Sargeson & Freeman, 1970; Gollogly & Hawkins, 1969).

Theoretical calculations for both en and (R)pn chelate rings (Gollogly, 1970; Gollogly & Hawkins, 1969; Corey & Bailer, 1959) suggest that the total torsional energy of the chelate ring depends almost exclusively upon the value of  $\beta$  and not the actual ring conformation. Gollogly & Hawkins (1969) also showed that the torsional energies of symmetric and unsymmetric skew conformations (Figure 7.3) are very similar provided that the dihedral angle,  $\beta$ , remains

Table 7.6

Summary of en/(R)pn geometry

Structure	Ligand	$\alpha$	$\beta$	C(1)	C(2)	C(3)	Comments
(i)	-	28.1	50.5	-1673	+5443	+1268	$\lambda$ S
(ii)	A	25.6	45.9	-2505	+3923	-508	$\lambda$ S
	B	24.1	45.2	-3306	+2940	-1864*	$\lambda$ S
(iii)	A	28.9	52.6	$\bar{+}2820$	$\bar{+}4444$	-	$\lambda/\delta$ (S/R)
	B	25.8	48.8	$\bar{+}2914$	$\bar{+}3722$	-	$\lambda/\delta$ (S/R)
(iv)	A	25.6	48.1	-2100	+4433	+2100	$\lambda$ R
	B	25.8	47.5	-2137	+4436	+1229	$\lambda$ R
	C	22.7	39.6	+1651	+6898	+5042	$\lambda$ S
	D	22.8	42.3	-168	+5593	+2979	$\lambda$ S
(v)	A	23.4	43.9	+319	+5893	-	$\lambda$ S
	B	23.3	44.6	+1854	-3949	-	$\delta$ S

All distances from the N-M-N plane ( $\text{\AA} \times 10^4$ )



approximately constant. The (R)pn chelate ring in the complexes has the complete range of conformations available to it that are available to the en chelate ring (Hawkins, 1971).

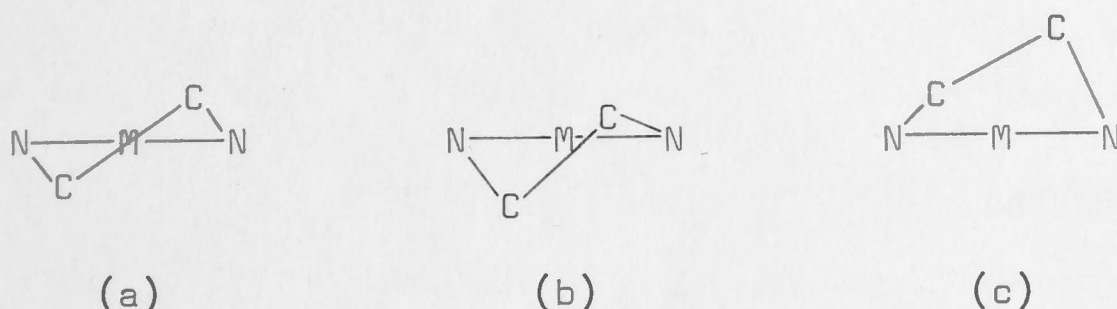
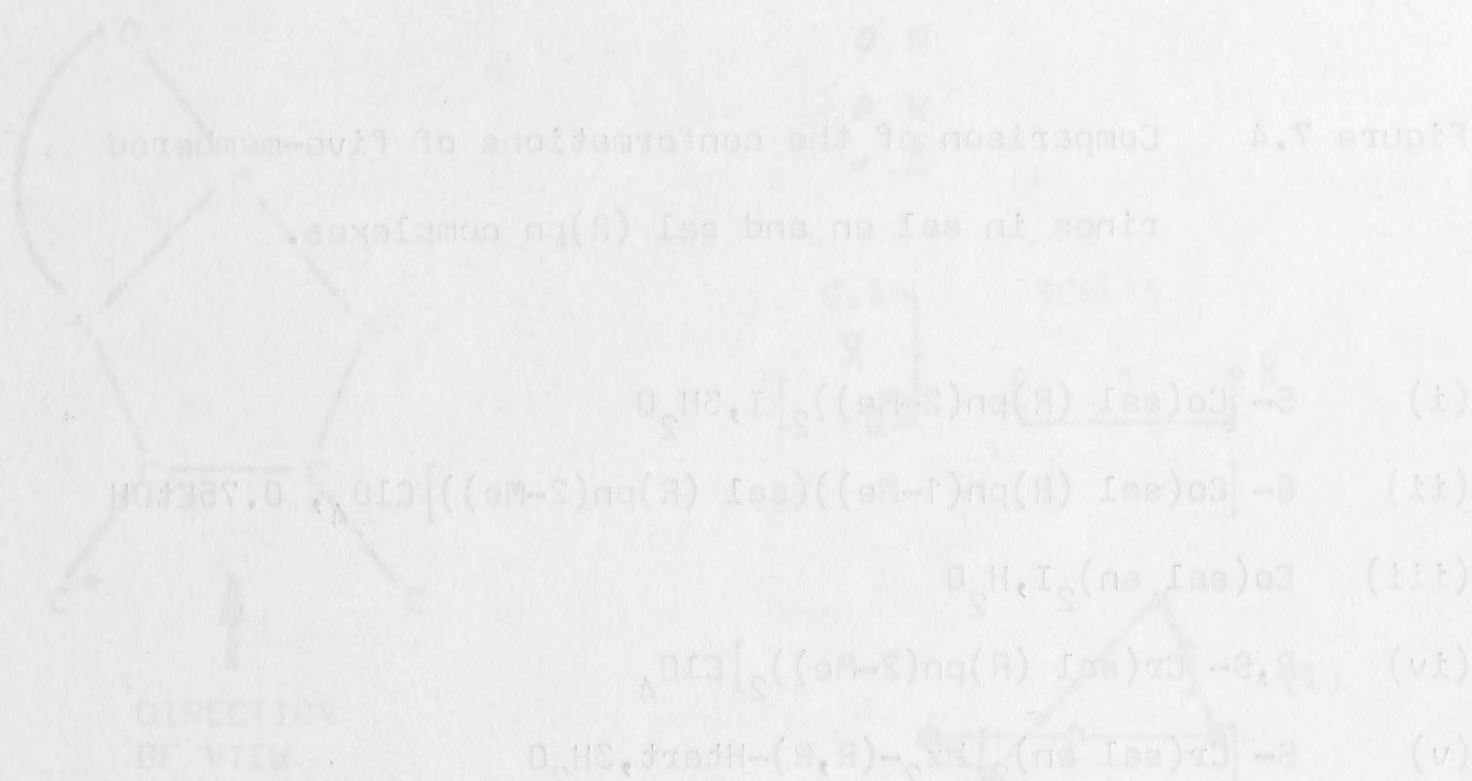


Figure 7.3 (a) symmetric skew  $\lambda$ , (b) unsymmetric skew  $\lambda$  and (c) asymmetric envelope  $\lambda$  conformations of a five-membered chelate ring (after Hawkins, 1971).

Examination of Figure 7.4 and Table 7.6 shows that, for the complexes under discussion, a wide range of skew conformations are present. These have approximately the same dihedral and skew angles, in agreement with theoretical conclusions. However, it must be remembered that all the complexes studied have varying degrees of hydrogen bonding (and other non-bonded interactions), which cause deviations of the conformation of the five-membered rings from any ideal situation used for theoretical calculations. Also, the average value for the M-N-C bond angle which involves the azomethine nitrogen atom (code n, Figure 7.1) is  $114.6^\circ$ . This introduces a distortion from the tetrahedral model used for nitrogen in en and (R)pn ligands. Comparison of the data for the complexes under discussion with published data (Gollogly, 1970; Figure 7.5) shows that these distortions are important and must be accounted for in any future calculations of the preferred conformations of sal en and sal (R)pn ligands.

The angle-bending energies of en and (R)pn chelate rings have been found to depend upon the angle at the metal atom (code m, Figure 7.1), the angles at the nitrogen atoms (codes n and p, Figure 7.1) and



Figures 7.4, 7.5, and 7.6 refer to the individual ligands in the cations.

FIGURE 7.4



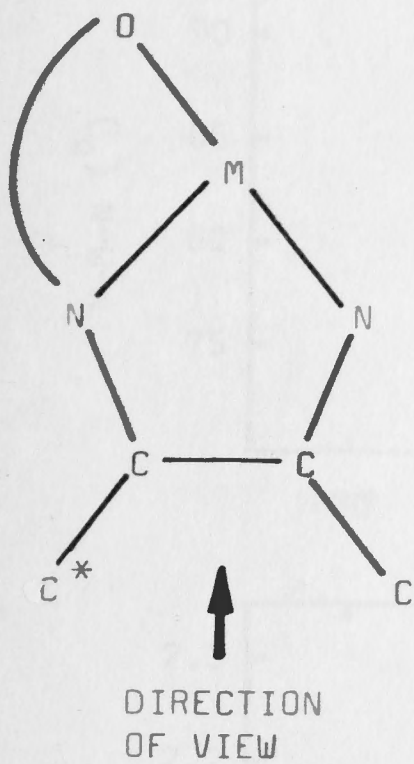


Figure 7.4 Comparison of the conformations of five-membered rings in sal en and sal (R)pn complexes.

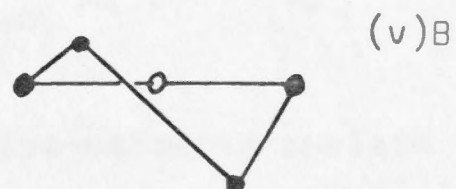
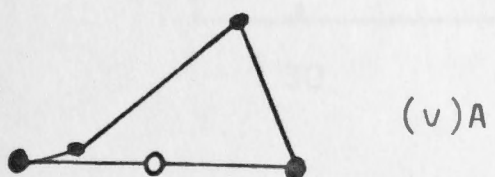
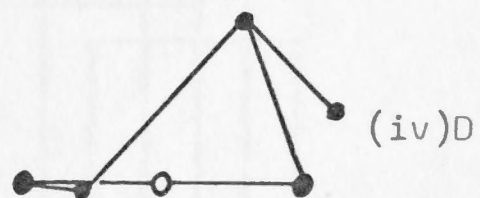
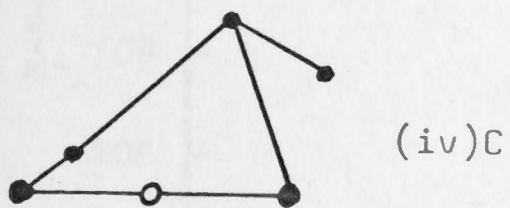
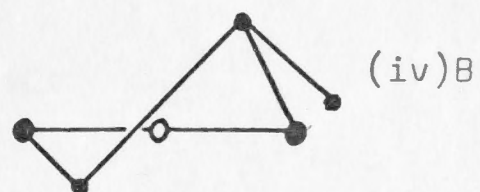
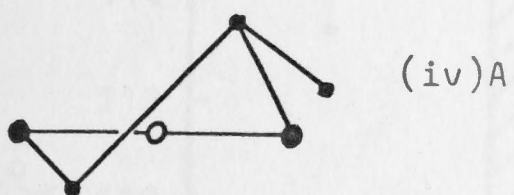
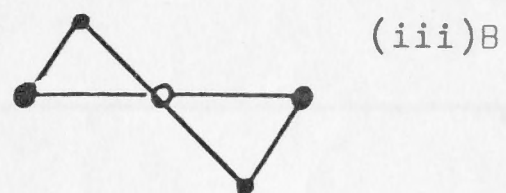
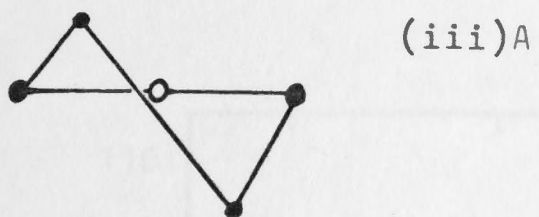
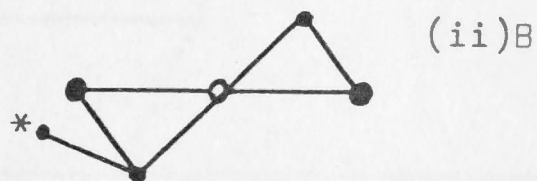
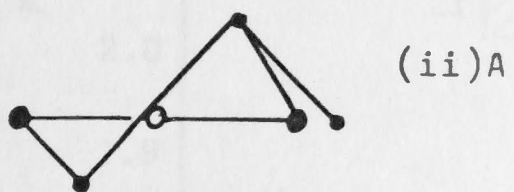
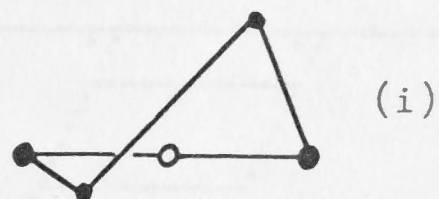
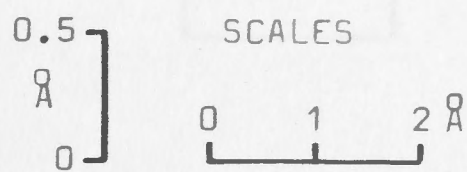
- (i)  $S-[Co(sal(R)pn(2-Me))_2]I, 3H_2O$
- (ii)  $S-[Co(sal(R)pn(1-Me))(sal(R)pn(2-Me))]ClO_4, 0.75EtOH$
- (iii)  $Co(sal en)_2I, H_2O$
- (iv)  $R,S-[Cr(sal(R)pn(2-Me))_2]ClO_4$
- (v)  $S-[Cr(sal en)_2]bz_2-(R,R)-Htart, 3H_2O$

A,B,C,D refers to the individual ligands in the cations.

NB vertical scale exaggerated (X 4)



○ M  
● N  
• C





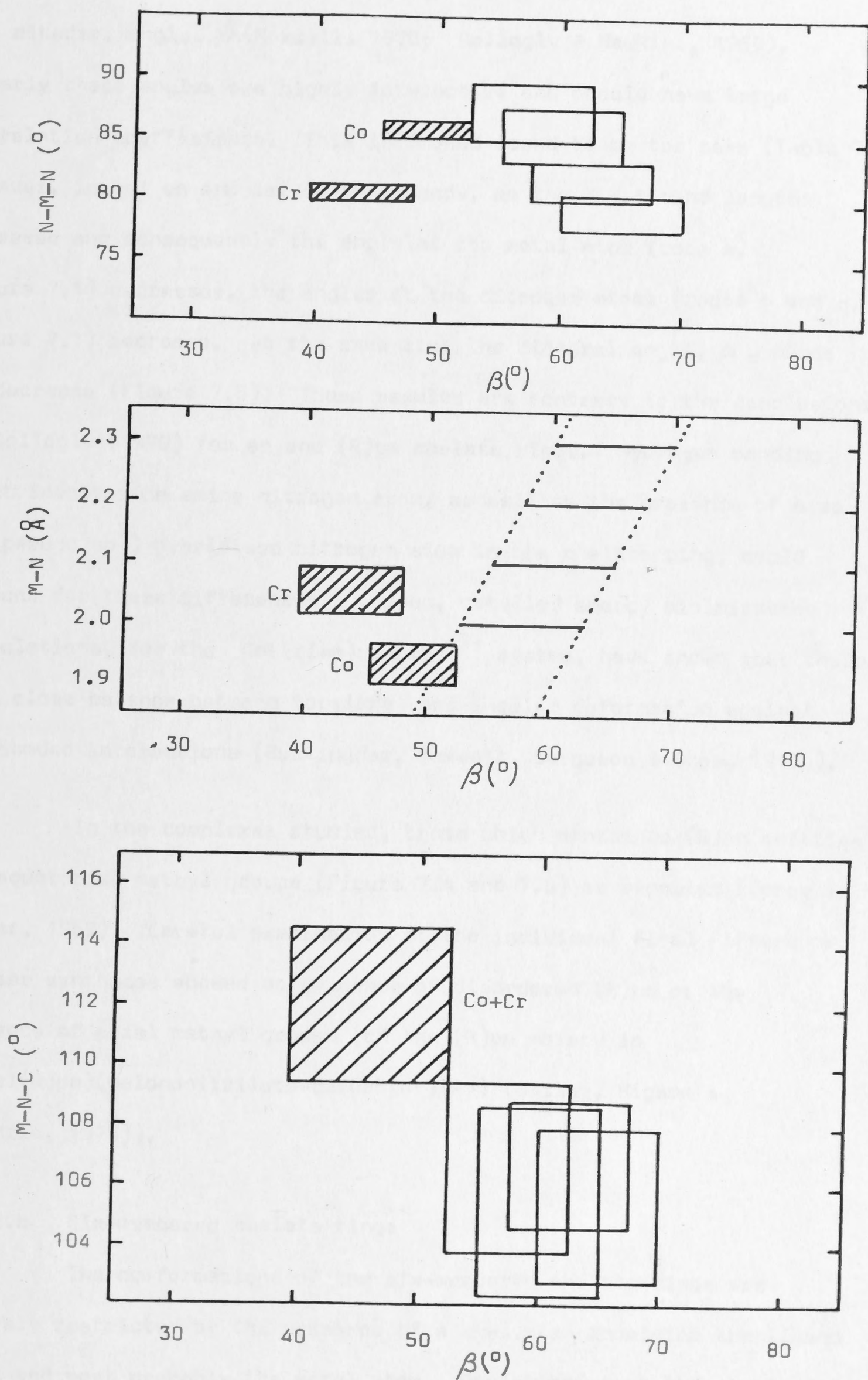


Figure 7.5 Comparison of data for five-membered chelate rings.  
 Unshaded; theoretical data after Gollogly (1970)  
 shaded; data from this work

the dihedral angle,  $\beta$  (Maxwell, 1970; Gollogly & Hawkins, 1969). Clearly these angles are highly interactive and should have large correlation coefficients. This is indeed found to be the case (Table 7.4). However, in sal en and sal (R)pn ligands, as the M - N bond lengths increase and consequently the angle at the metal atom (code m, Figure 7.1) decreases, the angles at the nitrogen atoms (codes p and q, Figure 7.1) increase. At the same time the dihedral angle,  $\beta$ , tends to decrease (Figure 7.5). These results are contrary to the conclusions of Gollogly (1970) for en and (R)pn chelate rings. Hydrogen bonding which involves the amine nitrogen atom, as well as the presence of a  $sp^2$  (or pseudo  $sp^2$ ) hybridised nitrogen atom in the chelate ring, could account for these differences. Indeed, detailed energy minimization calculations, for the  $Co(trien)(S-pro)^{2+}$  system, have shown that there is a close balance between torsional and angular deformation against non-bonded interactions (Buckingham, Maxwell, Sargeson & Snow, 1970).

In the complexes studied, those which contained (R)pn moieties had equatorial methyl groups (Figure 7.4 and 7.6) as expected (Corey & Bailer, 1959). Careful examination of the individual final difference Fourier syntheses showed no evidence of disordered (R)pn or the presence of axial methyl groups (cf the (R)pn moiety in  $Co(sal(R)pn)(malononitrilate-carbanion)(Py)$  (Bailey, Higson & McKenzie, 1975)).

#### 7.3.2.b Six-membered chelate rings

The conformations of the six-membered chelate rings are severely restricted by the presence of a  $\pi$ -system involving the ligand atoms and most probably the metal atom. Deviations from the plane of the ring are greatest for the metal and oxygen atoms (Figure 7.6). It must be remembered that in Figure 7.6 the vertical scale is exaggerated



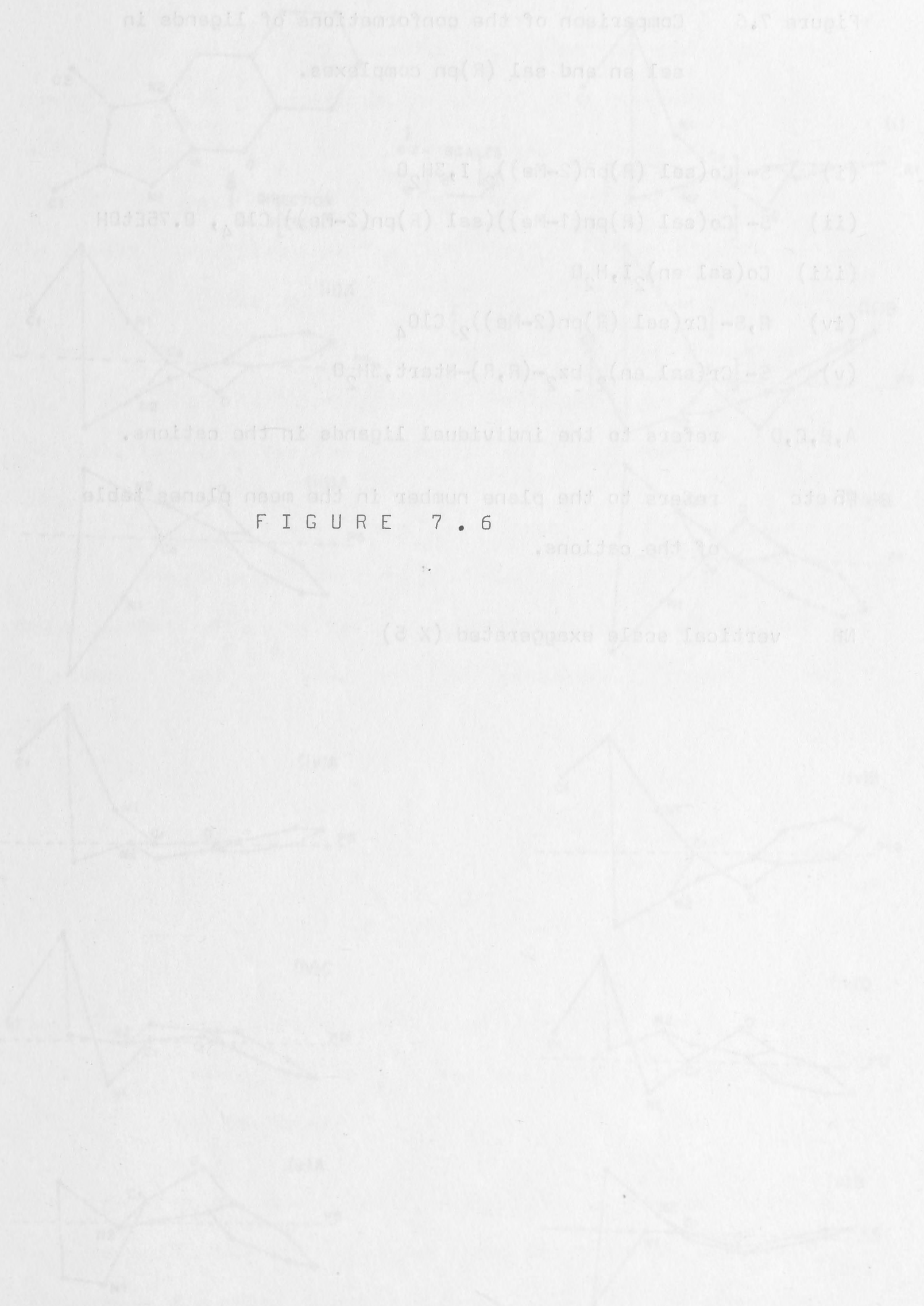


Figure 7.6 Comparison of the conformations of ligands in  
sal en and sal (R)pn complexes.

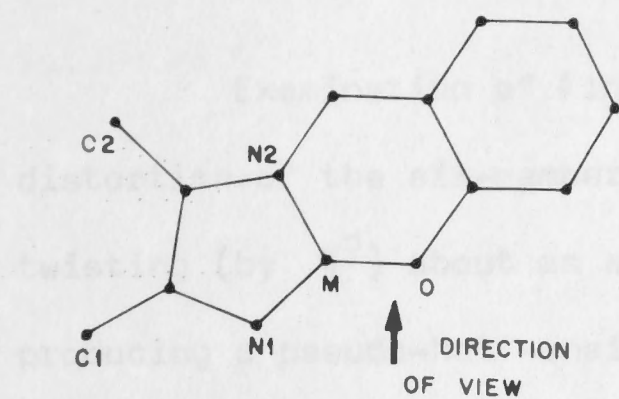
- (i)  $S-[Co(sal(R)pn(2-Me))_2]I, 3H_2O$
- (ii)  $S-[Co(sal(R)pn(1-Me))(sal(R)pn(2-Me))]ClO_4, 0.75EtOH$
- (iii)  $Co(sal en)_2I, H_2O$
- (iv)  $R,S-[Cr(sal(R)pn(2-Me))_2]ClO_4$
- (v)  $S-[Cr(sal en)_2]bz_2-(R,R)-Htart, 3H_2O$

A,B,C,D refers to the individual ligands in the cations.

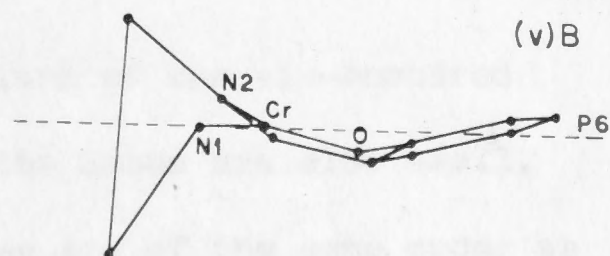
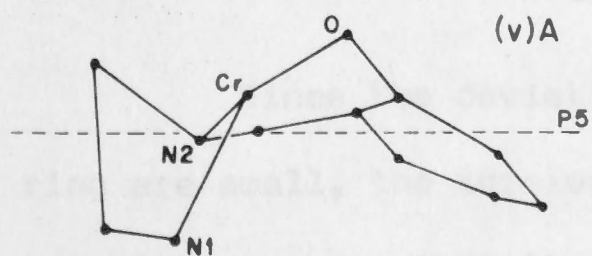
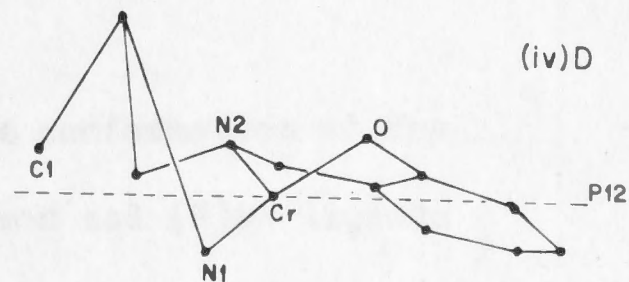
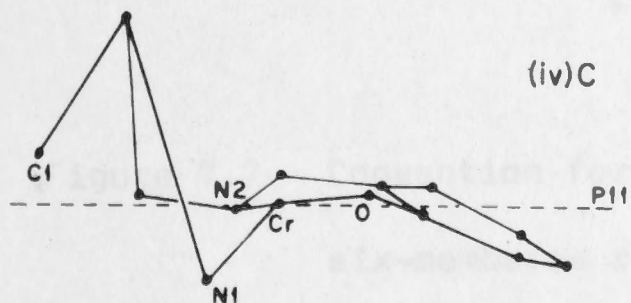
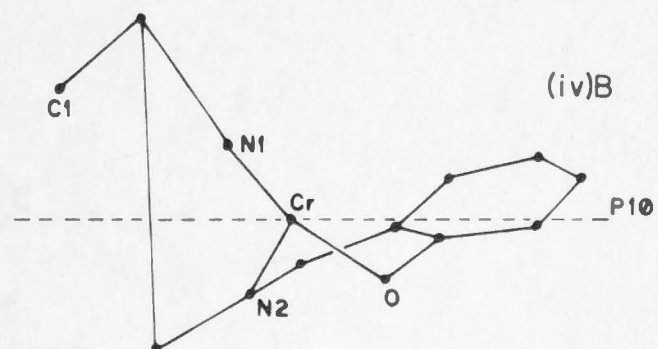
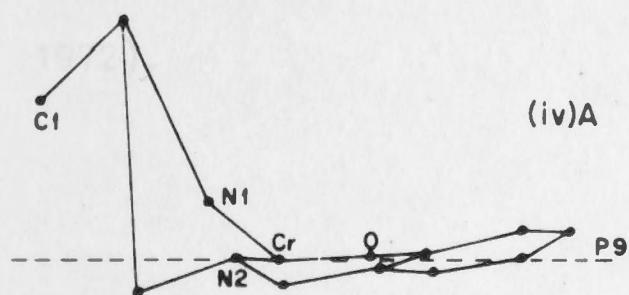
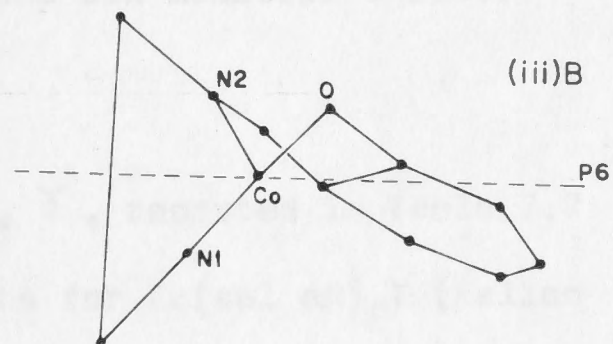
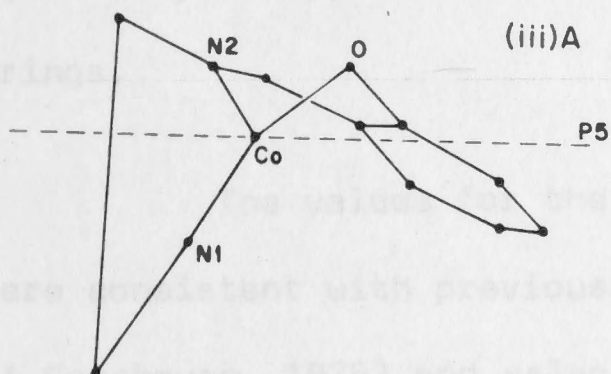
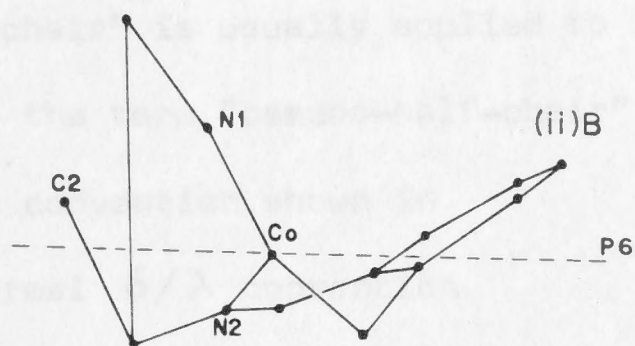
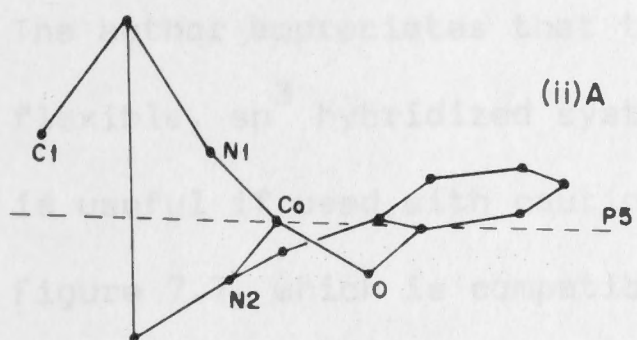
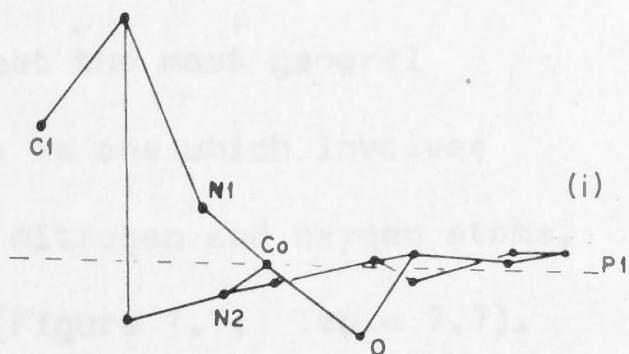
P5 etc refers to the plane number in the mean planes table  
of the cations.

NB vertical scale exaggerated (X 5)





Å  
0.2  
0 1 Å  
SCALES



(X 5) in order to emphasize the small ( $<0.25 \text{ \AA}$ ) deviations found in the salim moiety.

Examination of Figure 7.6 shows that the most general distortion of the six-membered chelate rings is one which involves twisting (by  $\gamma^\circ$ ) about an axis through the nitrogen and oxygen atoms, producing a pseudo-half-chair conformation (Figure 7.7; Table 7.7). The author appreciates that the term "half-chair" is usually applied to flexible,  $sp^3$  hybridized systems. However, the term "pseudo-half-chair" is useful if used with caution. Use of the convention shown in Figure 7.7, which is compatible with the normal  $\delta/\lambda$  convention (Hawkins, 1971), allows the description of the six-membered chelate rings.

The values for the angle of twist,  $\gamma$ , reported in Table 7.7 are consistent with previously published data for  $\text{Cr}(\text{sal en})_2\text{I}$  (Fallon & Gatehouse, 1975) and salen complexes (Calligaris, Nardin & Randaccio, 1972).

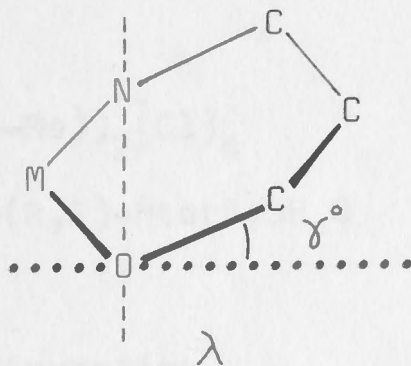


Figure 7.7 Convention for describing the conformation of the six-membered ring in sal en and sal (R)pn ligands (cf Hawkins, 1971)

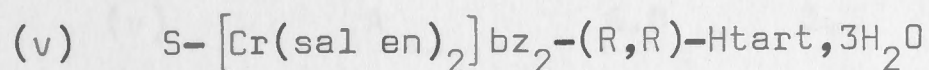
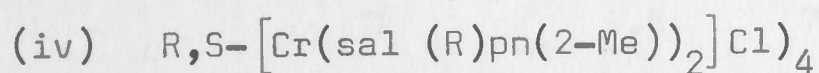
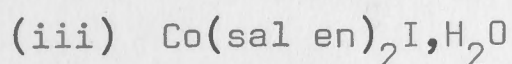
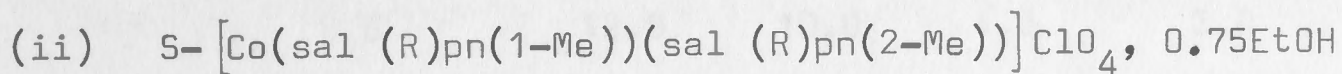
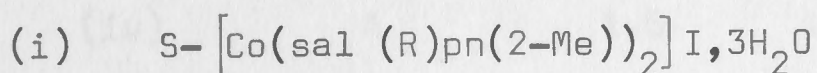
Since the deviations from the plane of the six-membered ring are small, the torsion angles about the bonds are also small. Calculation shows that these torsion angles are of the same order as the twist angle,  $\gamma$ , and often greater than the distortions of the



Table 7.7

Summary of the chirality of the chelate rings

Structure	Abs. Conf.*	Ligand	salim moiety	$\chi(^{\circ})$	en/(R)pn moiety
(i)	S	-	$\lambda$	10.0	$\lambda$
(ii)	S	A	$\lambda$	11.0	$\lambda$
		B	$\lambda$	11.0	$\lambda$
(iii)	R/S	A	$\delta/\lambda$	11.5	$\delta/\lambda$
		B	$\delta/\lambda$	13.5	$\delta/\lambda$
(iv)	R	A	$\lambda$	0.5	$\lambda$
		B	$\lambda$	13.0	$\lambda$
(v)	S	C	$\delta$	2.0	$\lambda$
		D	$\delta$	9.0	$\lambda$
(vi)	S	A	$\lambda$	10.5	$\lambda$
		B	$\lambda$	5.0	$\delta$



\*Abs. Conf. Absolute configuration

bond angles from the ideal,  $120^{\circ}$ . Torsion angles of interest are given in Table 7.8 and these show that the metal and oxygen atoms have the greatest deviations from the plane of the chelate ring.

### 7.3.2.c The overall conformation of the ligands.

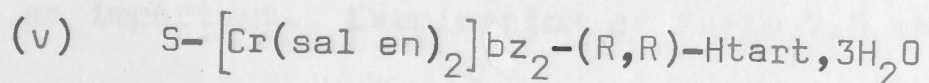
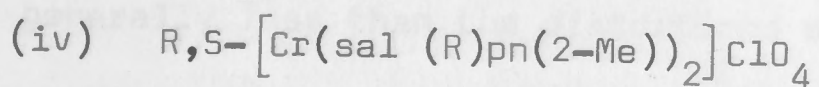
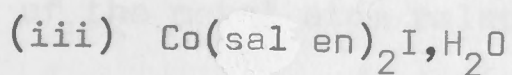
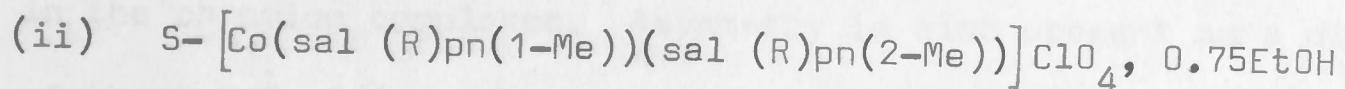
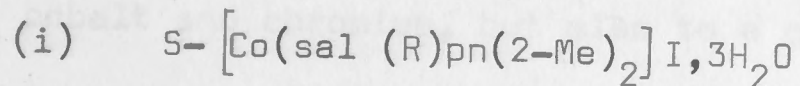
Examination of Figure 7.6 shows that the general shape of the ligands is that of a "curved plane". The ligand plane tends to bend

away from the oxygen atom so that the latter falls on the outside, and the metal atom on the inside, of the "curved plane". The plane of the benzene ring of each ligand is "angled" away from the mean plane of the ligand. These angles are in the range 2 to 7°. Twisting of the ligands in this manner results in an overall bending of the salim groups away from the pseudo-twofold axis of the cation.

Table 7.8

Torsion angles about selected bonds in the six-membered chelate ring (°)

Structure	Ligand	M-O	M-N	O-C	N-C
(i)	-	15.5	7.5	6.0	<0.25
(ii)	A	11.5	7.0	4.0	1.5
	B	15.0	6.5	7.5	1.5
(iii)	A	14.5	7.5	7.0	<0.25
	B	14.0	10.5	4.5	1.5
(iv)	A	1.5	4.0	3.0	<0.25
	B	12.0	10.0	4.0	3.0
	C	1.0	4.0	2.5	3.0
	D	9.5	7.0	5.5	2.5
(v)	A	6.0	3.5	4.5	6.5
	B	0.25	4.0	4.0	2.0





## 7.3.3 Distortions of the donor atoms

Because of the tridentate nature of the ligands, the amine nitrogen and salim oxygen atoms are 'pinched' towards the azomethine nitrogen atom. This should produce deviations from the ONNO plane, which alternate in sign (+ - + -). The orientation shown in Figure 7.8, where the perpendicular distance from the plane to N(3) is greater than the equivalent distance to N(4), is used to define the sign of the distortions listed in Table 7.9 for the S (and the enantiomer) absolute configuration. The angle N(3) - M - N(4) is in the range 175 to  $< 180^\circ$  for the complexes under discussion.

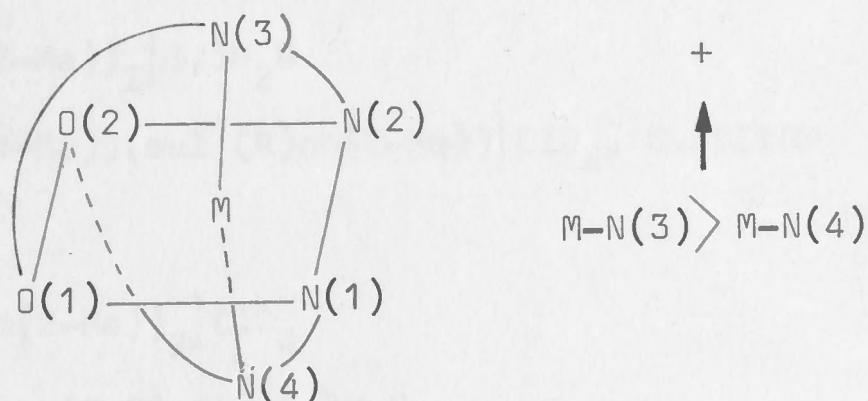


Figure 7.8 Orientation of the cation used to define donor atom distortions

The data in Table 7.9 show that distortions of the donor atoms from the ONNO plane are larger for chromium complexes. This is probably due not only to differences in the M - N bond lengths for cobalt and chromium, but also to a greater degree of hydrogen bonding in the chromium complexes. Asymmetry is also present as a displacement of the metal atom relative to the ONNO plane. These distortions are generally less than the distortions of the donor atoms, but are probably as important. Examination of Table 7.9 shows that the chromium atom in the S-cation of  $R,S-[Cr(sal(R)pn(2-Me))_2]ClO_4$  has the greatest displacement from the ONNO plane. This is attributed to hydrogen

Table 7.9

Donor atom distortions for the complexes studied

Structure	Abs. Conf.*	M	(X 10 <sup>4</sup> Å)				(Å)	
			O(1)	O(2)	N(1)	N(2)	N(3)	N(4)
(i)	S	C <sub>2</sub> symmetry						
(ii)	S	+53	+123	-136	-130	+101	+1.886	-1.884
(iii)	R/S	+6	+90	-94	-89	+87	+1.907	-1.903
(iv)	R	-2	+1641	-1604	-1560	+1546	+1.997	-2.010
	S	+1119	-16	-581	-528	+6	+2.125	-1.857
(v)	S	+43	+1680	-1507	-1187	+1368	+2.014	-1.996

(i) S-[Co(sal (R)pn(2-Me))<sub>2</sub>]I, 3H<sub>2</sub>O(ii) S-[Co(sal (R)pn(1-Me))(sal (R)pn(2-Me))]ClO<sub>4</sub>, 0.75EtOH(iii) Co(sal en)<sub>2</sub>I, H<sub>2</sub>O(iv) R,S-[Cr(sal (R)pn(2-Me))<sub>2</sub>]ClO<sub>4</sub>(v) S-[Cr(sal en)<sub>2</sub>]bz<sub>2</sub>-(R,R)-Htart, 3H<sub>2</sub>O

\*Abs. Conf. Absolute configuration

bonding between a perchlorate ion and the amine nitrogen atoms of this cation, which has induced larger distortions of the nitrogen atoms from the ideal coordination octahedron, resulting in a twist of the ONNO plane away from the chromium atom.

#### 7.4 THE CIRCULAR DICHROISM OF THE CRYSTALLINE COMPLEXES

Benson (1976) has reported the circular dichroism of the optically active complexes in solution. The C.D. of the crystalline complexes in KBr discs is presented in Figure 7.9. KBr discs were prepared according to the method of Bosnich and Harrowfield (1972) and



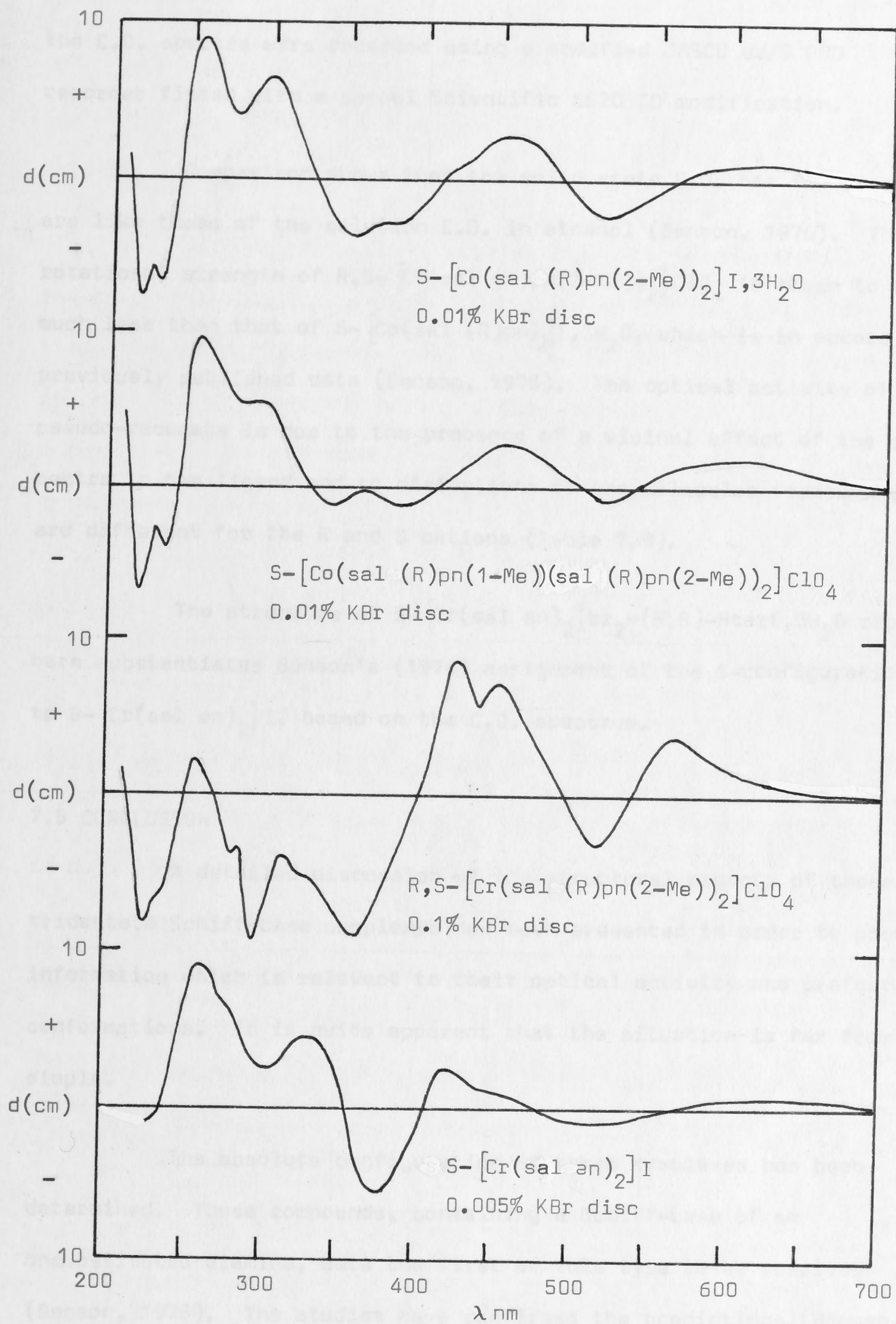


Figure 7.9 Solid state CD spectra.

The KBr disc spectra were recorded at a sensitivity of 5 mdeg cm<sup>-1</sup> at 23°C.

the C.D. spectra were recorded using a modified JASCO UV/5 ORD recorder fitted with a sproul Scientific SS20 CD modification.

Comparison shows that the solid state C.D. has features which are like those of the solution C.D. in ethanol (Benson, 1976). The rotational strength of  $R,S-[Cr(sal(R)pn(2-Me))_2]ClO_4$  is shown to be much less than that of  $S-[Co(sal(R)pn)_2]I, 3H_2O$ , which is in accord with previously published data (Benson, 1976). The optical activity of the pseudo-racemate is due to the presence of a vicinal effect of the chiral centre in the ligand and to distortions of the molecular framework, which are different for the R and S cations (Table 7.9).

The structure of  $S-[Cr(sal en)_2]bz_2-(R,R)-Htart, 3H_2O$  reported here substantiates Benson's (1976) assignment of the S-configuration to  $S-[Cr(sal en)_2]I$ , based on the C.D. spectrum.

## 7.5 CONCLUSION

A detailed discussion of the structural aspects of these tridentate Schiff-base complexes has been presented in order to provide information which is relevant to their optical activity and preferred conformations. It is quite apparent that the situation is far from simple.

The absolute configuration of three complexes has been determined. These compounds, containing a Schiff-base of an unsubstituted diamine, were the first of this type to be resolved (Benson, 1976). The studies have confirmed the predictions (Benson, 1976) concerning both the positions of the methyl groups in  $sal(R)pn$  ligands in the cobalt complexes, and the absolute configuration of the optical isomers of  $M(sal en)_2^+$  ions. The compound  $Cr(sal(R)pn)_2ClO_4$  was shown to be  $R,S-[Cr(sal(R)pn(2-Me))_2]ClO_4$ .



## CHAPTER 8

## SEPARATION OF THE ISOMERS OF BIS-(N-AMINO(R)PROPYLSALICYLALDIMINATO) CHROMIUM(III)

The fact that  $\text{Cr}(\text{sal}(\text{R})\text{pn}(2\text{-Me}))_2\text{ClO}_4$  was found to be a racemate naturally led to attempts to resolve the compound. Benson (1976) isolated two isomers from the reaction mixture (the pseudo-racemate and a second isomer (ii)) and suggested that separation of the mixture and resolution might be possible by the use of carboxymethyl cellulose column chromatography.

8.1 PREPARATION OF  $\text{Cr}(\text{sal}(\text{R})\text{pn})_2\text{ClO}_4$ 

$\text{Cr}(\text{sal}(\text{R})\text{pn})_2\text{ClO}_4$  was prepared by the method described by Benson (1976). However, the ratio of tris-(salicylaldehydato) chromium(III) to (R)pn was reduced to 1:7 and the mixture refluxed for 4 hours. Rotary evaporation of the solvent produced several crops of well-formed crystals. A three fold increase in product yield was obtained by this method. The circular dichroism of these crystals in ethanolic solution was in agreement with that reported by Benson (1976) for R,S- $[\text{Cr}(\text{sal}(\text{R})\text{pn}(2\text{-Me}))_2]\text{ClO}_4$ . Also the powder x-ray diffraction pattern of the crystals was characteristic of the pseudo-racemate.

Further evaporation of the solvent produced a gum which could not be induced to crystallize. Addition of 5 cm<sup>3</sup> of methanol and 15 cm<sup>3</sup> of diethyl ether to the gum produced a dark brown powder, which was shown by optical rotatory dispersion to be impure pseudo-racemate.

8.2 COLUMN CHROMATOGRAPHY OF R,S- $[\text{Cr}(\text{sal}(\text{R})\text{pn}))_2]\text{ClO}_4$ 

## 8.2.1. Carboxymethyl cellulose chromatography

Approximately 10 mg of the pseudo-racemate was dissolved in

5 cm<sup>3</sup> of distilled water and then loaded onto a 2.5 x 25 cm column of Whatman CM 11 carboxymethyl cellulose. The column was eluted with 600 cm<sup>3</sup> of distilled water (5 bed volumes) at a flow rate of 0.6 cm<sup>3</sup> min<sup>-1</sup>. This was carried out in order to stabilize the column and to establish the size of the absorption band. The column was then eluted with 0.1 M acetic acid, using the same flow rate, and 10 cm<sup>3</sup> fractions were collected. At the beginning of the experiment the absorption band was approximately 3 mm broad, this increased to 9 cm at the point where the first fractions were collected. The elution profile is shown in Figure 8.1. All chromatographic separations were carried out using equipment which measured the optical density of the eluant and plotted the elution profile automatically.

Examination of the O.R.D. of the fractions at points A and B on the profile (Figure 8.1) showed that some separation had occurred. This was also indicated by the shoulder on the profile, but the broadness of the profile limited the usefulness of this method. The O.R.D. of fractions at A in the region 300 - 450 nm showed a qualitative correspondence with the O.R.D. of isomer (ii) (Benson, 1976). The optical rotation of fractions at A and B was of opposite sign in this region. Examination of the fractions between A and B showed that there was a gradual change in the O.R.D. from A to B.

Repeated C.M.C. was carried out and the first and later fractions were separately combined (the two groups of fractions were arbitrarily divided at the centre of the elution profile). The O.R.D. of the first fractions were similar to that of isomer (ii) Benson, 1976) and the O.R.D. of later fractions were similar to that of the pseudo-racemate.



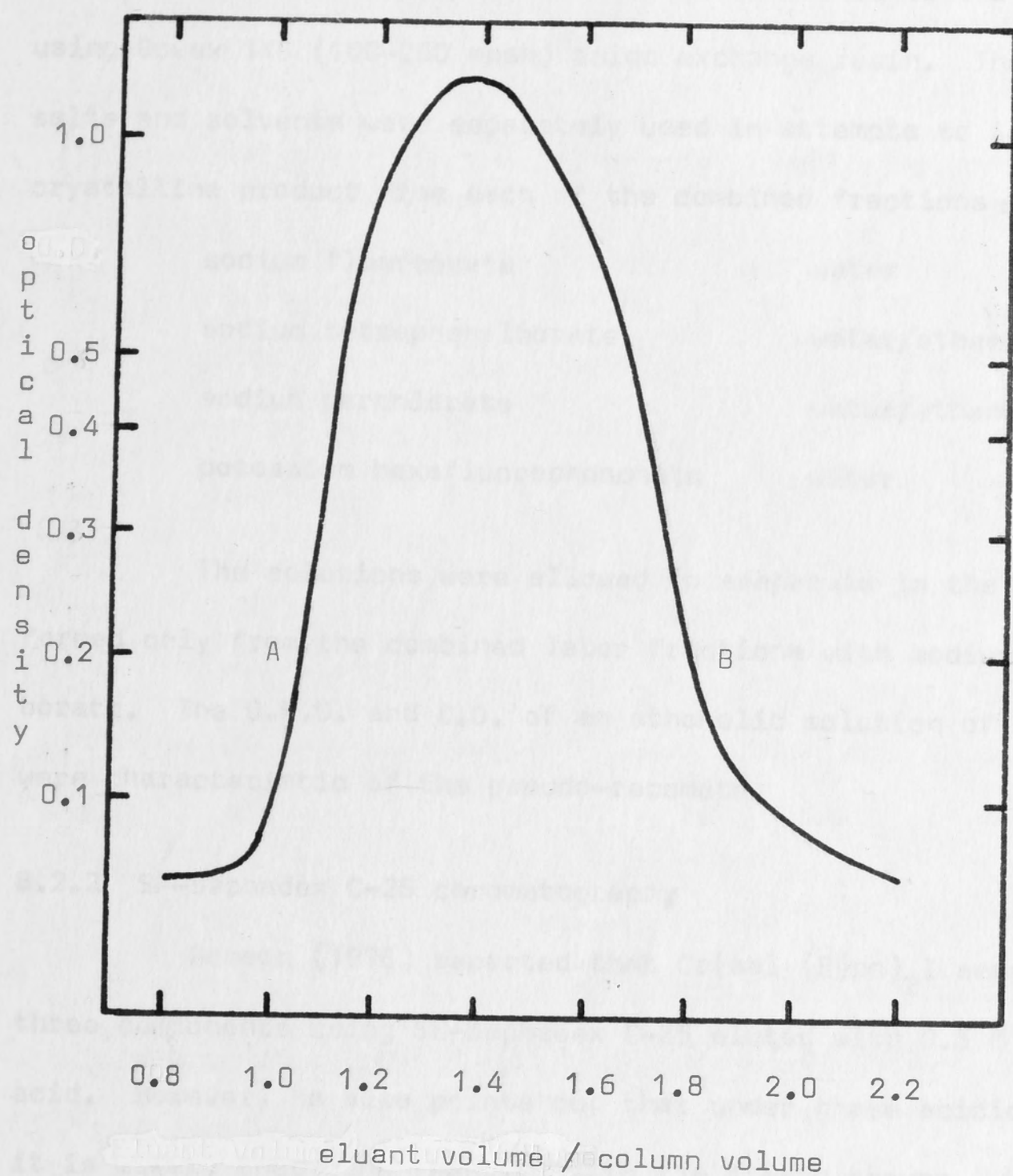


Figure 8.1 Elution profile for  $R,S-[Cr(sal(R)pn(2-Me))_2]ClO_4$  using carboxymethyl cellulose and 0.1M acetic acid.

These combined fractions were converted to the chloride by using Dowex 1X8 (100–200 mesh) anion exchange resin. The following salts and solvents were separately used in attempts to isolate a solid crystalline product from each of the combined fractions :

sodium fluoroborate	water
sodium tetraphenylborate	water/ethanol
sodium perchlorate	water/ethanol
potassium hexafluorophosphate	water

The solutions were allowed to evaporate in the air. Crystals formed only from the combined later fractions with sodium tetraphenylborate. The O.R.D. and C.D. of an ethanolic solution of these crystals were characteristic of the pseudo-racemate.

#### 8.2.2 SP-Sephadex C-25 chromatography

Benson (1976) reported that  $\text{Cr}(\text{sal}(\text{R})\text{pn})_2\text{I}$  separated into three components using SE-Sephadex C-25 eluted with 0.5 M hydrochloric acid. However, he also points out that under these acidic conditions it is likely that some reaction with the ligand occurs. Separation of the optical isomers of  $\text{tris}(2\text{-Me-1,2-propanediamine})\text{Co}(\text{III})$  has been successfully carried out using SP-Sephadex C-25 eluted with 0.15 M sodium (+)<sub>589</sub>tartrate (Kojima, Yoshikama & Yamasaki, 1973).

Approximately 30 mg of the pseudo-racemate were adsorbed onto the top of a column of SP-Sephadex C-25 (2.5 x 27 cm). The column was eluted with 500 cm<sup>3</sup> of distilled water followed by 0.14 M sodium (+)<sub>589</sub>tartrate. The flow rate was adjusted to 2 cm<sup>3</sup> min<sup>-1</sup> and 10 cm<sup>3</sup> fractions were collected. The elution profile was similar to that shown in Figure 8.2.

Examination of the O.R.D. of the eluant, in the region



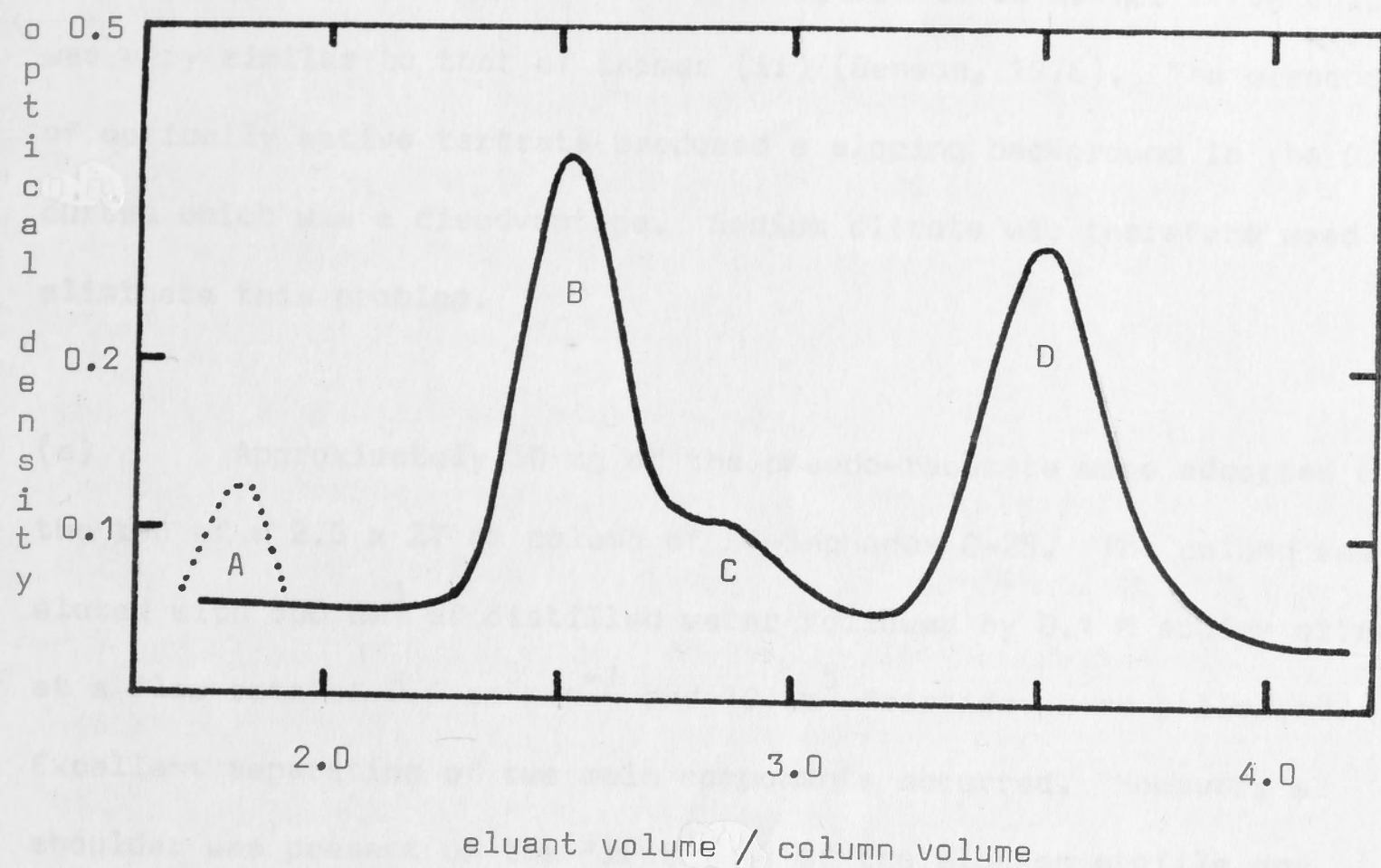


Figure 8.2 Elution profile for  $R,S-[Cr(sal(R)pn(2-Me))_2]ClO_4$   
using SP- SEPHEDEX C-25 and 0.1M sodium citrate.

- A - present only in last fractions of crystalline material isolated from preparation, not optically active.
- B,D - enantiomorphic fractions in approximately equal amounts.
- C - present in small amounts only, not characterised.

300 - 450 nm, showed that the components associated with the two principal peaks (B, D) on the elution profile had optical rotations of opposite sign. The second component, D, had an O.R.D. curve which was very similar to that of isomer (ii) (Benson, 1976). The presence of optically active tartrate produced a sloping background in the O.R.D. curves which was a disadvantage. Sodium citrate was therefore used to eliminate this problem.

(a) Approximately 30 mg of the pseudo-racemate were adsorbed onto the top of a 2.5 x 27 cm column of SP-Sephadex C-25. The column was eluted with 500 cm<sup>3</sup> of distilled water followed by 0.1 M sodium citrate at a flow rate of 0.6 cm<sup>3</sup> min<sup>-1</sup> and 10 cm<sup>3</sup> fractions were collected. Excellent separation of two main components occurred. However, a shoulder was present on the first peak of the elution profile and therefore the experiment was repeated using a column 2.5 x 80 cm in size. The elution profile is shown in Figure 8.2. Fractions collected at the peaks B and D (Figure 8.2) have O.R.D. curves of similar shape but of opposite rotation, in the region 250 - 500 nm. The O.R.D. of the component at D corresponds to that of isomer (ii) (Benson, 1976). Furthermore, since the areas under B and D were approximately equal it was thought that resolution of the pseudo-racemate had been achieved. The fractions collected at the shoulder C (Figure 8.2) showed the same O.R.D. as those at peak B, probably due either to swamping by the B component or to C being optically inactive. While it was thought possible to compare the optical densities of the eluant at peaks B and D, assuming that the materials were optical isomers of the same species and therefore had the same extinction coefficient for the monitored wavelength, no comparison of peak area could be made with the shoulder C since the component at C remained undetermined.



Repeated separations did not provide a sufficient amount of the component C, to allow further characterization.

SP.S.C. of several batches of the pseudo-racemate was carried out with the object of obtaining sufficient material for crystallization. The combined fractions corresponding to B and D (Figure 8.2) were rotary evaporated. The chromium complex in each case was extracted from the mass of sodium citrate with chloroform under reflux. The chloroform extracts were rotary evaporated and the resulting solids dissolved separately in 5 cm<sup>3</sup> distilled water. Each fraction was converted to the chloride by using Dowex 1X8 (100-200 mesh) anion exchange resin. The combined fractions were then treated with a saturated ethanolic solution of sodium tetraphenylborate. The two solutions were allowed to evaporate slowly in the air.

Microscopic crystals (total amount < 20 mg) which formed from the B fraction had an O.R.D. curve in ethanolic solution of similar shape, in the region 250 - 500 nm, but with opposite sign of rotation to that of isomer (ii) (Benson, 1976). The O.R.D. was also different to that of the pseudo-racemate (Figure 8.3). Micro-analysis of the crystals gave the single result:  $C_{48}H_{44}N_4O_2CrB \cdot 3H_2O$  requires C 69.6, H 6.3, N 6.8; found C 69.8, H 6.8, N 7.2. A powder x-ray diffraction pattern did not have the distinct peaks characteristic of sodium tetraphenylborate.

(b) A small amount of the gum (< 30 mg) from the preparation of  $Cr(sal(R)pn)_2ClO_4$  was loaded onto a 2.5 x 90 cm column of SP-Sephadex C-25 and eluted with 0.1 M sodium citrate as described above. A slight increase in the proportion of C occurred and a fourth peak, A (Figure 8.2), was present on the elution profile. The fraction A, was too dilute to allow O.R.D. measurements - assuming the species present was optically

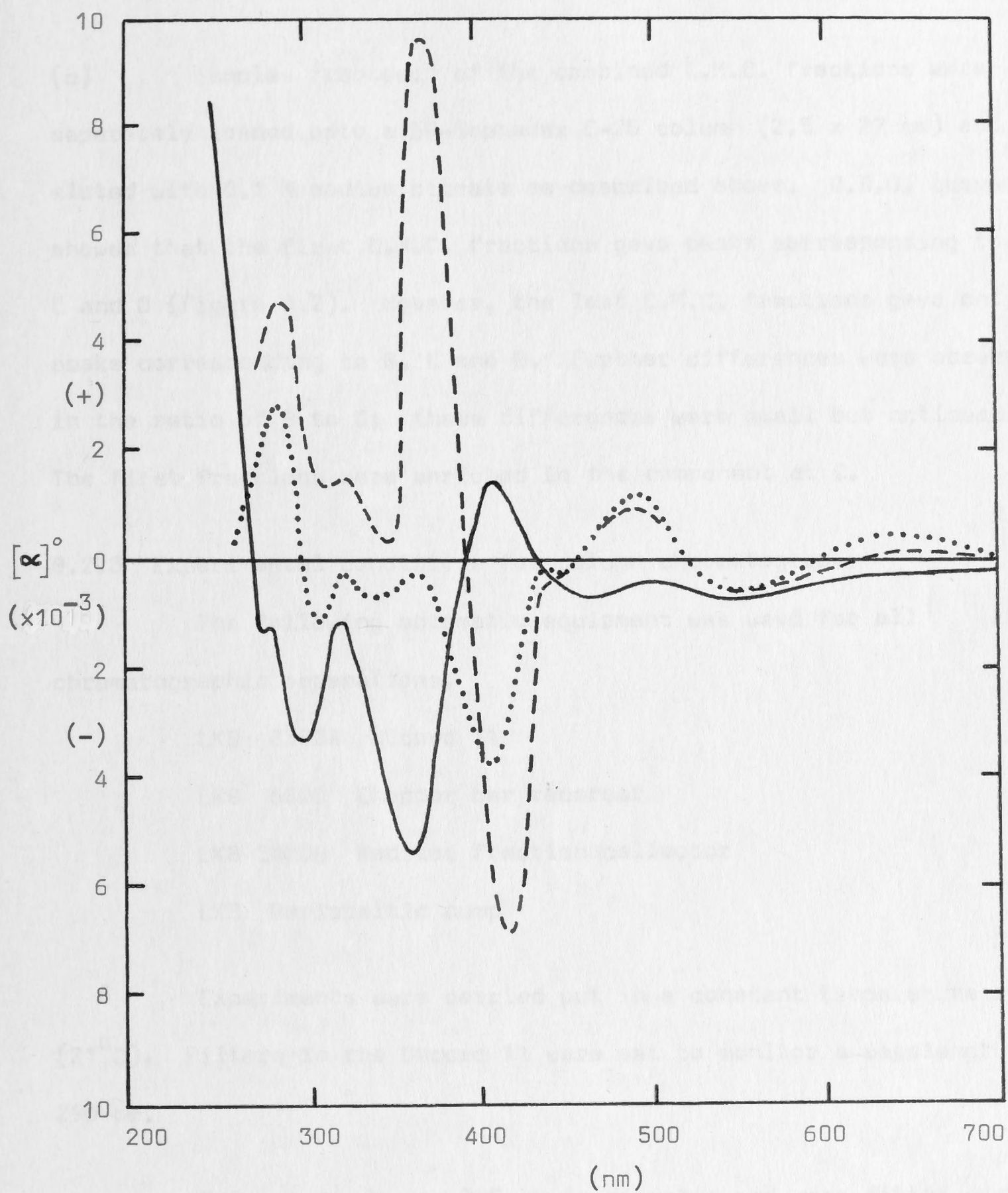


Figure 8.3 Optical rotary dispersion of  $\text{Cr}(\text{sal}(\text{R})\text{pn})_2^{3+}$  isomers in ethanol.

.....  $\text{R,S-}[\text{Cr}(\text{sal}(\text{R})\text{pn}(2\text{-Me}))_2]\text{ClO}_4$

----- isomer (ii) (Benson, 1976)

———— B fraction tetraphenylborate



active.

(c) Samples from each of the combined C.M.C. fractions were separately loaded onto a SP-Sephadex C-25 column (2.5 x 27 cm) and eluted with 0.1 M sodium citrate as described above. O.R.D. curves showed that the first C.M.C. fractions gave peaks corresponding to A, B, C and D (Figure 8.2). However, the last C.M.C. fractions gave only peaks corresponding to B, C and D. Further differences were observed in the ratio of B to C; these differences were small but noticeable. The first fractions were enriched in the component at C.

### 8.2.3 Experimental conditions for column chromatography

The following automatic equipment was used for all chromatographic separations.

LKB 8300A UVcord 11

LKB 6520 Chopper bar recorder

LKB 3400B Radirac fraction collector

LKB Peristaltic pump

Experiments were carried out in a constant temperature room (21°C). Filters in the UVcord 11 were set to monitor a wavelength of 290 nm.

Columns used were 2.5 cm in diameter and were fitted with Sephadex flow adaptors, thus minimizing the dead volume and mixing of eluant fractions.

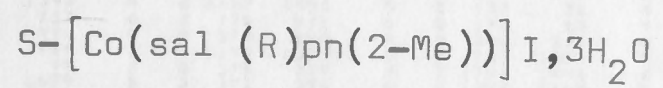
### 8.3 CONCLUSIONS

The experiments above show that it seems possible that the pseudo-racemate could be resolved by using SP-Sephadex C-25 column chromatography. Large scale preparation of  $\text{Cr}(\text{sal}(\text{R})\text{pn})_2\text{ClO}_4$

followed by batch separations using SP.S.C. would give workable amounts of components B and D. Component C is most probably a minor product which could be removed by first crystallizing the pseudo-racemate to constant rotation. This was not done for the above experiments, as their aim was rather to test the method than obtain pure components.



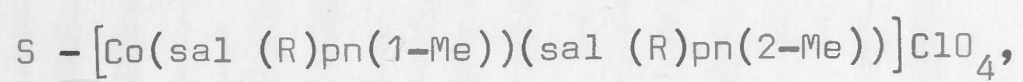
## APPENDIX A

STRUCTURE AMPLITUDES ( $\times 10$ ) FOR





## APPENDIX B

STRUCTURE AMPLITUDES ( $\times 10$ ) FOR

0.75EtOH

[illegible]

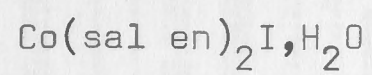


[illegible]





## APPENDIX C

STRUCTURE AMPLITUDES ( $\times 10$ ) FOR



[illegible]



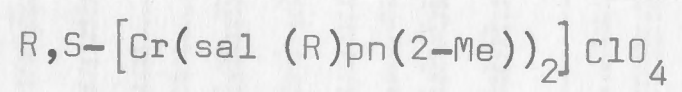


APC

3

STRUCTURE FACTORS FOR  $\text{Co}(\text{sal en})_2\text{I} \cdot \text{H}_2\text{O}$

## APPENDIX D

STRUCTURE AMPLITUDES ( $\times 10$ ) FOR



[illegible]

AP. D . |

STRUCTURE FACTORS FOR  $R,S-[Cr(sal(R)m(2-Me))]ClO_4$



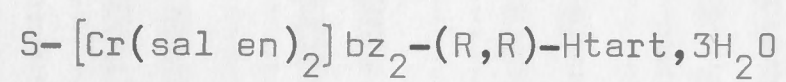


[illegible]





## APPENDIX E

STRUCTURE AMPLITUDES ( $\times 10$ ) FOR





APE

STRUCTURE FACTORS FOR  $S-[Cr(salen)_2]$

$b_{22} = (R, R) + H_{\text{ant}}, 3H_2O$









## REFERENCES

- Bailey, N.A., Higson, B.M., & McKenzie, E.D. (1972)  
J.Chem.Soc., Dalton, 503.
- Bailey, N.A., Higson, B.M., & McKenzie, E.D. (1975)  
J.Chem.Soc., Dalton, 1105.
- Baker, E.N., Hall, D., Waters, T.N. (1970a) J.Chem.Soc., (A), 400.
- Baker, E.N., Hall, D., Waters, T.N. (1970b) J.Chem.Soc., (A), 406.
- Benson, T.H. (1976) M.Sc. Thesis, Aust. Nat. Univ.
- Bijvoet, J.M. (1955) Endeavor 14, 71.
- Black, D. St. C., & Hartshorn, A.J. (1972) Coord.Chem.Revs. 9, 219.
- van Bommel, A.J., & Bijvoet, J.M. (1958) Acta.Cryst. 11, 61.
- Bosnich, B., & Harrowfield, J.M. (1972) J.Amer.Chem.Soc. 94, 3425.
- Braun, R.L., & Lingafelter, E.C. (1966) Acta.Cryst. 21, 546.
- Braun, R.L., & Lingafelter, E.C. (1967a) Acta.Cryst. 22, 780.
- Braun, R.L., & Lingafelter, E.C. (1967b) Acta.Cryst. 22, 787.
- Bruckner, S., Calligaris, M., Nardin, G., & Randaccio, L. (1969)  
Acta.Cryst. B25, 1671.
- Buckingham, D.A., Maxwell, I.E., Sargeson, A.M., & Freeman, H.C. (1970)  
Inorg.Chem. 9, 1921.
- Buckingham, D.A., Maxwell, I.E., Sargeson, A.M., & Snow, M.R. (1970)  
J.Amer.Chem.Soc. 92, 3617.
- Budzikiewicz, H., Djerassi, I.C., Williams, D.H. (1967)  
"Mass Spectrometry of Organic Compounds," Holden Day, London.
- Buerger, M.J. (1960) "Crystal Structure Analysis," Wiley, New York.
- Busing, W.R., & Levy, H.A. (1957a) J. Chem. Phys. 26, 563.
- Busing, W.R., & Levy, H.A. (1957b) Acta. Cryst. 10, 180.
- Busing, W.R., Ellison, R.D., Levy, H.A., King, S.P., & Rosebury, R.T.  
(1968) Report ORNL-4143, Oak Ridge National Laboratory, Oak Ridge,  
Tennessee.
- Cahn, R.S., Ingold, C.K., & Prelog, V. (1966)  
Angew.Chem., Internat.Ed., 5, 385.
- Calligaris, M., Nardin, G., Randaccio, L., & Minichelli, D. (1971)  
J.Chem.Soc., (A), 2720.



- Calligaris, M., Nardin, G., & Randaccio, L. (1972)  
Coord.Chem.Revs. 7, 385.
- Calligaris, M., Manzini, G., Nardin, G., & Randaccio, L. (1972)  
J.Chem.Soc., Dalton, 543.
- Chieh, P.C., & Palenik, G.J. (1972) Inorg.Chem. 11, 816.
- Churchill, M.R. (1973) Inorg.Chem. 12, 1213.
- Churchill, M.R., & Kalra, K.L. (1974) Inorg.Chem. 13, 1427.
- Ciardelli, F., & Salvadori, P. (1973) "Fundamental Aspects and Recent Developments in Optical Rotatory Dispersion and Circular Dichroism," Heydon & Son, London.
- Cochran, W., & Douglas, A.S. (1957) Proc.Roy.Soc. A227, 486.
- Coggan, P., McPhail, A.T., Mabbs, F.E., Richards, A., & Thornley, A.S. (1970) J.Chem.Soc., (A), 3296.
- Coggan, P., McPhail, A.T., Mabbs, F.E., & McLachlan, V.N. (1971) J.Chem.Soc., (A), 1014.
- Corfield, P.W.R., Doedens, R.J., & Ibers, J.A. (1967) Inorg.Chem. 6, 197.
- Corey, E.J., & Bailer, J.C. (1959) J.Amer.Chem.Soc. 81, 2620.
- Cozens, R.J. & Murray, K.S. (1972) Aust.J.Chem. 25, 911.
- Cromer, D.T., & Waber, J.T. (1965) Acta.Cryst. 18, 104.
- Cruickshank, D.W.J., & Pilling, D.E. (1961) "Computing Methods and the Phase Problem in X-ray Crystal Analysis," ch.6, pp.32-78, (Eds. Pepinsky, R., Robertson, J.M., & Speakman, J.C.), Pergamon Press, London.
- Cruickshank, D.W.J. (1965) "Computing Methods in Crystallography," ch.14, pp.112-116, (Ed. Rollett, J.S.), Pergamon Press, London.
- Davies, J.E., & Gatehouse, B.M. (1972) Acta.Cryst. B28, 3641.
- Deming, W.E. (1943) "Statistical Adjustment of Data," Wiley, New York.
- Denne, W.A. (1973) Cryst.Mol.Struct. 3, 367.
- Dey, K. (1974) J.Sci. and Ind.Res. 33, 76.
- Dey, K., & Ray, K.C. (1974) Inorg.Chim.Acta. 10, 139.
- Fallon, G.D., & Gatehouse, B.M. (1975) J.Chem.Soc., Dalton, 1344.



- Finney, K.A. & Everett, G.W. Jr. (1974) *Inorg.Chim.Acta.* 11, 185.
- Fox, M.R., Orioli, P.L., Lingafelter, E.C., & Sacconi, L. (1964) *Acta.Cryst.* 17, 1159.
- Frasson, E., Panattoni, C., & Sacconi, L. (1964) *Acta.Cryst.* 17, 477.
- Gardner, A.P., Gatehouse, B.M., & White, J.C.B. (1971) *Acta.Cryst.* B27, 1505.
- Gerloch, M., & Mabbs, F.E. (1967) *J.Chem.Soc.*, (A), 1900.
- Germain, G., & Woolfson, M.M. (1968) *Acta.Cryst.* B24, 91.
- Germain, G., Main, P., & Woolfson, M.M. (1970) *Acta.Cryst.* B26, 274.
- Germain, G., Main, P., & Woolfson, M.M. (1971) *Acta.Cryst.* A27, 368.
- Gillard, R.D. (1971) *J.Inorg.Nucl.Chem.* 33, 997.
- Gollogly, J.R., & Hawkins, C.J. (1969) *Inorg.Chem.* 8, 1168.
- Gollogly, J.R. (1970) Ph.D. thesis, Univ. of Queensland, data in Hawkins, C.J. (1971) "Absolute Configuration of Metal Complexes," ch.3, p.67, Wiley-Interscience, New York.
- Hall, D., & Masaki, N. (1973) *Cryst.Struct.Comm.* 2, 271.
- Hamilton, W.C. (1965) *Acta.Cryst.* 18, 502.
- Hauptman, H., & Karle, J. (1953) "Solution of the Phase Problem. I. The Centrosymmetric Crystal," A.C.A. Monograph No.3, Polycrystal Book Service, Pittsburgh.
- Hawkins, C.J. (1971) "Absolute Configuration of Metal Complexes," Wiley-Interscience, New York.
- Hawkins, C.J., & Larsen, E. (1965) *Acta.Chem.Scand.* 19, 1969.
- Hobday, M.D., & Smith, T.D. (1972) *Coord.Chem.Revs.* 9, 311.
- Holm, R.H., Everett, G.W. Jr., & Chakrovorty, A. (1966) *Prog.Inorg.Chem.* 7, 83.
- Hoppe, W. (1965) *Angew.Chem., Internat.Ed.*, 4, 508.
- Howells, E.R., Phillips, D.C., & Rogers, D. (1950) *Acta.Cryst.* 3, 210.
- Hsu, I-Nan, & Craven, B.M. (1974) *Acta.Cryst.* B30, 843.
- Hughes, E.W. (1941) *J.Amer.Chem.Soc.* 63, 1737.
- Ibers, J.A., Hamilton, W.C. (1964) *Acta.Cryst.* 17, 781.

- International Tables for X-ray Crystallography (1952) Vol.I;  
(1959) Vol.II; (1962) Vol.III, Knock Press, Birmingham.
- Jarski, M.A., & Lingafelter, E.C. (1964) *Acta.Cryst.* 17, 1109.
- Karle, I.L., Dragonette, K.S., & Brenner, S.A. (1965) *Acta.Cryst.* 19, 713.
- Karle, J., & Karle, I.L. (1965) "Computing Methods in Crystallography,"  
ch.17, pp.151-165, (Ed. Rollett, J.S.), Pergamon Press, London.
- Karle, J., & Karle, I.L. (1966) *Acta.Cryst.* 21, 849.
- Kistenmacher, T.J., Szalda, D.J., & Marzilli, L.G. (1975)  
*Inorg.Chem.* 14, 1686.
- Klug, H.P., Alexander, L.E., & Sumner, G.G. (1958) *Acta.Cryst.* 11, 41.
- Kojima, M., Yoshikama, Y., & Yamasaki, K. (1973) *Bull.Chem.Soc. Japan*  
46, 1687.
- Levey, M.A. (1956) *Acta.Cryst.* 9, 679.
- Lingafelter, E.C., Simmons, G.L., & Morosin, B. (1961)  
*Acta.Cryst.* 14, 1222.
- Lingafelter, E.C., & Braun, R.L. (1966) *J.Amer.Chem.Soc.* 88, 2951.
- Lipson, H., & Cochran, W. (1966) Vol.III "The Crystalline State,"  
(Ed. Bragg, L.), Bell & Son, London.
- Mangia, A., Nardelli, M., Pelizzi, G., & Plelizzi, G. (1973)  
*J.Chem.Soc., Dalton*, 1141.
- Maslen, H.S., & Waters, T.N. (1975) *Coord.Chem.Revs.* 17, 137.
- Mason, S.F. (1971) *J.Chem.Soc., (A)*, 667.
- Maxwell, I.E. (1970) Ph.D. thesis, Aust. Nat. Univ.
- de Meulenaer, J., & Tompa, H. (1965) *Acta.Cryst.* 19, 1014.
- O'Connor, M.J., & West, B.O. (1968) *Aust.J.Chem.* 21, 369.
- Okaya, Y., Semple, N.R., & Kay, M.I. (1966) *Acta.Cryst.* 21, 237.
- Orioli, P.L., Lingafelter, E.C., & Brown, B.W. (1964) *Acta.Cryst.*  
17, 1113.
- Orioli, P.L., Vaira, M.D., & Sacconi, L. (1966) *J.Amer.Chem.Soc.*  
88, 4383.

- Peerdeman, A.F., van Bommel, A.J., & Bijvoet, J.M. (1951)  
Nature, 168, 271.
- Peerdeman, A.F., & Bijvoet, J.M. (1956) Acta.Cryst. 9, 1012.
- Peterse, W.J.A.M., & Palm, J.H. (1966) Acta.Cryst. 20, 147.
- Pflugger, C.E., & Harlow, R.L. (1973) Acta.Cryst. B29, 2608.
- Prout, C.K., Carruthers, J.R., & Rossotti, F.J.C. (1971)  
J.Chem.Soc., (A), 3336.
- Ractliffe, J.F. (1967) "Elements of Mathematical Statistics,"  
2nd Ed., Oxford Univ. Press.
- Ramachandran, G.N., & Srinivasan, R. (1970) "Fourier Methods in  
Crystallography," ch.11, pp.166-200, Wiley-Interscience, London.
- Ramaseshan, S. (1964) "Advanced Methods of Crystallography," pp.67-96,  
(Ed. Ramaseshan, S.), Academic Press, London.
- Raymond, K.N., Corfield, P.W.R., & Ibers, J.A. (1968a)  
Inorg.Chem. 7, 1362.
- Raymond, K.N., Corfield, P.W.R., & Ibers, J.A. (1968b)  
Inorg.Chem. 7, 842.
- Richardson, F.S. (1972) Inorg.Chem. 11, 2366.
- Riche, C. (1973) Acta.Cryst. B29, 2154.
- Sacconi, L. (1966) Coord.Chem.Revs. 1, 192.
- Sacconi, L., Nardin, N., & Zanobini, F. (1966) Inorg.Chem., 5, 1872.
- Saito, Y. (1968) Pure and Applied Chem. 17, 21.
- Saito, Y. (1974) Coord.Chem.Revs. 13, 305.
- Schaeffer, W.P., & Marsh, R.E. (1969) Acta.Cryst. B25, 1675.
- Shkol'nikova, L.M., Obodovskaya, A.E., & Shugum, E.A. (1973)  
Zh.Struct.Khim. 14, 286.
- Sim, G.A. (1961) "Computing Methods and the Phase Problem in X-ray  
Crystal Analysis," ch.24, pp.227-236, (Eds. Pepinsky, R.,  
Robertson, J.M., & Speakman, J.C.), Pergamon Press, London.
- Stern, F., & Beevers, C.A. (1950) Acta.Cryst. 3, 341.



- Stewart, R.F., Davidson, E.R., & Simpson, W.T. (1965)  
J.Chem.Phys. 42, 3175.
- Stout, G.H., & Jensen, L.H. (1968) "X-ray Structure Determination -  
A Practical Guide," MacMillan & Co, London.
- Strickland, R.W., & Richardson, F.S. (1973) Inorg.Chem. 12, 1025.
- Srinivasan, R. (1961) Acta.Cryst. 14, 1163.
- Sundaralingam, M., & Jensen, L.H. (1965) Acta.Cryst. 18, 1053.
- Tapscott, R.E., Belford, R.C. & Paul, I.C. (1968) Inorg.Chem. 7, 357.
- Vaira, M.D., & Orioli, P.L. (1967) Inorg.Chem. 6, 490.
- Wei, L., Stogsdill, R.M., & Lingafelter, E.C. (1964) Acta.Cryst.  
17, 1058.
- West, B.O. (1968) New Pathways in Inorg.Chem. 303.
- Wilson, A.J.C. (1942) Nature, 150, 151.
- Yamada, S. (1966) Coord.Chem.Revs. 1, 415.